

UNITED STATES DEPARTMENT OF THE INTERIOR
GEOLOGICAL SURVEY

Middle Tertiary sedimentation and tectonics
of the La Honda basin, central California

by

Richard G. Stanley¹

Open-File Report 85-596

This report is preliminary and has not been reviewed for conformity with U.S. Geological Survey editorial standards and stratigraphic nomenclature.

¹. Menlo Park, California

TABLE OF CONTENTS

	<u>Page</u>
TABLE OF CONTENTS	ii
LIST OF ILLUSTRATIONS	v
LIST OF TABLES	viii
ABSTRACT	1
PREFACE AND ACKNOWLEDGEMENTS	1
INTRODUCTION	2
REGIONAL SETTING	3
Introduction	
The Salinian Block	
Restoration of Neogene Deformation	
Early Tertiary Paleogeographic Setting	
Plate Motions	
Climate and Eustasy	
METHODS	11
Research Strategy	
Depositional Systems	
Paleocurrents	
Subsurface Investigations	
Thickness Maps	
Paleobathymetry	
General Principles	
Application to the La Honda Basin	
Biostratigraphy and Time Scale	
GENERAL GEOLOGY OF THE LA HONDA BASIN.	30
Limits of Study	
Structural Geology	
Structural Blocks and Basement	
Patterns of Folding and Faulting	
Faults	
Zayante-Vergeles Fault	
Summary of Structural Geology	
NATURE OF THE STRATIGRAPHIC FILL	36
Introduction	
Stratigraphic Packaging and Nomenclature	
Stratigraphy and Sedimentation	
PALEOCENE SEQUENCE	41

	<u>Page</u>
Locatelli Formation	41
EOCENE TO LOWER MIOCENE SEQUENCE	42
Butano Sandstone	42
Twobar Shale.	45
Rices Mudstone	54
Introduction	
Age and Stratigraphic Relations	
Thickness	
Lithology	
Depositional Systems and Provenance	
Vaqueros Sandstone	75
Introduction	
Castle Rock Unit of the Vaqueros Sandstone	78
Introduction	
Age	
Stratigraphic Relations	
Lithology	
Paleocurrents	
Large-scale Variations in Lithology	
Depositional Systems and Provenance	
Laurel Unit of the Vaqueros Sandstone	102
Introduction	
Age	
Stratigraphic Relations	
Middle Oligocene Unconformity	
Lithology	
Paleocurrents	
Depositional Systems and Provenance	
Vaqueros Sandstone of the Woodside Area	112
Zayante Sandstone	114
Introduction	
Thickness, Stratigraphic Relations, and Age	
Lithology	
Paleocurrents	
Depositional Systems and Provenance	
Zayante(?) Sandstone of the Majors Creek Area	125
Stratigraphic Relationships	
Lithology	
Depositional Systems and Provenance	
Mindego Basalt	128
Introduction	
Stratigraphic Relations	
Age	
Thickness	
Lithology	
Summary	
Lambert Shale	140
Introduction	
Age	
Stratigraphic Relations	
Thickness	
Lithology	
Depositional Systems	
LOWER TO MIDDLE MIOCENE SEQUENCE	151

	<u>Page</u>
Lonipico Sandstone	151
Monterey Formation.	153
MIDDLE TO UPPER MIOCENE SEQUENCE.	156
Santa Margarita Sandstone.	156
Santa Cruz Mudstone	158
UPPER MIOCENE TO PLIOCENE SEQUENCE.	160
Purisima Formation	
LOWER TO MIDDLE TERTIARY STRATA OF THE	
NORTHERN GABILAN RANGE	162
Introduction	
San Juan Bautista Formation	
Pinecate Formation	
Redbeds	
Volcanic Rocks	
Summary and Comparison with the Santa	
Cruz Mountains	
PALEOGEOGRAPHY, GEOLOGIC HISTORY, AND PALEOTECTONICS	166
Introduction	
Paleogeography and Geologic History.	166
Paleocene	
Early to Middle Eocene	
Middle to Late Eocene	
Late Eocene to Early Oligocene	
Late Oligocene to Early Miocene	
Early to Middle Miocene	
Middle Miocene and Younger	
Middle Tertiary Paleotectonics of the La Honda Basin.	181
Introduction	
Early to Middle Eocene Rapid Subsidence	
Late Eocene to Early Oligocene Slow Subsidence	
Middle Oligocene Regression and Uplift	
Late Oligocene to Early Miocene Extension	
Early Miocene Uplift	
New Estimates of Offset Along the San Andreas Fault.	192
Speculations on Offset Along the San Gregorio-Hosgri Fault	194
SUMMARY OF MAJOR CONCLUSIONS	195
APPENDIX 1: PALEONTOLOGIC DATA FROM THE	
SANTA CRUZ MOUNTAINS	197
APPENDIX 2: PALEONTOLOGIC DATA FROM THE	
NORTHERN GABILAN RANGE	214
APPENDIX 3: THICKNESS ESTIMATES FROM OUTCROPS	
AND CROSS-SECTIONS	215
APPENDIX 4: DATA FROM EXPLORATORY WELLS.	229
APPENDIX 5: PALEOCURRENT DATA	239
REFERENCES CITED	246

LIST OF ILLUSTRATIONS

	<u>Page</u>
1. Map showing inferred disruption of the La Honda-San Joaquin basin by movements along the San Andreas and San Gregorio-Hosgri faults.	5
2. Generalized paleogeographic map of early Tertiary California.	7
3. Schematic model of plate interactions along the west coast of North America.	8
4. Schematic illustration of three-stage history of plate interactions and the San Andreas fault in central California.	9
5. Location map of important physical and cultural features in the La Honda basin area.	13
6. Location map of important outcrop sections and wells in the La Honda basin.	14
7. Index to U.S. Geological Survey 7.5 minute quadrangles in the La Honda basin area.	16
8. Classification of marine benthic environments.	21
9. Time scale used in this thesis.	25
10. Simplified geologic map of the La Honda basin area.	27
11. Generalized map of folds and faults in the La Honda basin area.	29
12. Fault-bounded blocks and representative stratigraphic columns in the La Honda basin area.	32
13. Depositional sequences and formations of the La Honda basin.	37
14. Tentative middle Tertiary chronostratigraphic correlation chart of the La Honda basin.	39
15. Stratigraphic correlation of wells and outcrop sections in the La Honda basin.	43
16. Geographic distribution of the Twobar shale.	46
17. Thickness of the Twobar shale.	47
18. Lithologic symbols for stratigraphic columns.	49
19. San Lorenzo River section at Riverside Grove.	50
20. Photographs: outcrops of the Twobar Shale.	52
21. Kings Creek section.	55

	<u>Page</u>
22. Geographic distribution of the Rices Mudstone.	56
23. Soquel Creek-Hinckley Creek section.	57
24. Thickness of the Rices Mudstone.	60
25. Thickness of the Refugian Stage.	61
26. Western Gulf Wells Fargo #1 well.	63
27. Humble Santa Cruz Lumber #1 well.	64
28. Photographs: bioturbated mudrocks of the Rices Mudstone.	65
29. Photographs: outcrops of the Blooms Creek sandstone.	68
30. Photographs: turbidite sandstones in the Rices Mudstone.	70
31. Photographs: glauconitic sandstones in the Rices Mudstone.	72
32. Geographic distribution of the Zayante Sandstone and the Vaqueros Sandstone.	76
33. Thickness of the Zayante and Vaqueros sandstones.	77
34. Twobar Creek section.	81
35. Upper Zayante Creek section.	83
36. Photographs: outcrops of the Castle Rock unit.	87
37. Photographs: sedimentary structures in the Castle Rock unit.	88
38. Corralitos Creek section.	90
39. Photographs: more outcrops of the Castle Rock unit.	91
40. Photographs: bioturbated rocks of the Castle Rock unit.	92
41. Paleocurrents in the Castle Rock unit.	95
42. Lithologic variations in the Vaqueros Sandstone.	98
43. QFL plots of middle Tertiary sandstones.	100
44. Lower Zayante Creek section.	103
45. Geologic sketch map of the contact between the Zayante Sandstone and the Laurel unit of the Vaqueros Sandstone.	106
46. Photographs: outcrops of the Laurel unit.	110
47. Photographs: bioturbated sandstones in the Laurel unit.	111

	<u>Page</u>
48. Paleocurrents in the Laurel unit.	113
49. Photographs: outcrops of the Zayante Sandstone.	117
50. Photographs: sandstone and conglomerate in the Zayante Sandstone.	118
51. Idealized fining-upward sequence in the Zayante Sandstone.	119
52. Photographs: sandstones in the Zayante Sandstone.	120
53. Paleocurrents in the Zayante Sandstone.	123
54. Majors Creek section.	126
55. Geographic distribution of the Mindego Basalt.	129
56. Thickness of the Mindego Basalt.	131
57. Sketch map of an idealized pull-apart basin.	132
58. Photographs: outcrops of middle Tertiary volcanic rocks.	134
59. Photographs: sawn slabs of fossiliferous limestones from the Mindego Basalt.	137
60. Slate Creek section.	139
61. Geographic distribution of the Lambert Shale.	141
62. Photographs: laminated mudrocks from the Lambert Shale.	144
63. Photographs: laminated and bioturbated mudrocks from the Lambert Shale.	145
64. Photographs: more rocks from the Lambert Shale.	147
65. Photographs: laminated and bioturbated mudrocks from the Monterey Formation.	155
66. Paleobathymetric maps of the La Honda basin.	169
67. Late Oligocene-early Miocene paleogeography of the La Honda basin.	178
68. Qualitative geohistory diagrams.	182
69. Approximate relative accumulation rates for selected rock units.	186
70. Zemorrian and Saucian paleobathymetry of the San Joaquin basin.	193

LIST OF TABLES

	<u>Page</u>
1. La Honda basin oil fields.	17
2. Formation symbols used in this report.	38
3. Comparison of Zemorrian sandstones in the La Honda basin.	79
4. Depositional systems of the central La Honda basin.	167
5. Raw data for qualitative geohistory diagrams.	183
6. Approximate relative rates of accumulation for selected rock units in the La Honda basin (uncorrected for compaction).	188

MIDDLE TERTIARY SEDIMENTATION AND TECTONICS OF THE LA HONDA BASIN, CENTRAL CALIFORNIA

Richard G. Stanley

ABSTRACT

Middle Tertiary sedimentary and volcanic rocks in the Santa Cruz Mountains and northern Gabilan Range were deposited in the La Honda basin. These rocks record the change from convergent to transform tectonics accompanying collision of the Farallon-Pacific spreading ridge with the California coast about 30 m.y. ago. The upper Eocene (Refugian) to lower Miocene (Saucesian) section is 2-3 km thick, exhibits rapid lateral facies changes and several unconformities, and includes shelf and turbidite sandstones, nonmarine redbeds, anoxic shales, basin-plain mudstones, and volcanic rocks.

Depositional systems were identified in the field using sedimentary structures and vertical sequences. Paleogeographic maps were constructed using benthic foraminiferal paleobathymetry, paleocurrents, and inferred depositional systems and provenance.

Normal convergence along the continental margin during the late Eocene and early Oligocene was associated with low rates of subsidence in the La Honda basin, and slow hemipelagic deposition of the Narizian Twobar Shale and the Refugian to lower Zemorrian Rices Mudstone in lower bathyal basin-plain environments.

Major restructuring of the basin during the middle Oligocene—including uplift and erosion of the basin margins, movement along the Zayante-Vergeles fault, and marine regression—apparently resulted from the approach and collision of the Farallon-Pacific ridge with the California margin. A fan-delta and submarine fan complex represented by the Vaqueros and Zayante Sandstones was fed by braided streams flowing northward from a nearby granitic highland.

An episode of extension marked by volcanism, marine transgression, rapid subsidence, and formation of a pull-apart occurred near the Oligocene-Miocene boundary. The extension may have been related to passage of the Mendocino triple junction or to regional transtension along the San Andreas fault.

Basin-wide uplift and erosion near the Saucesian-Relizian boundary about 18 m.y. ago may have been a response to northward subcrustal migration of the subducted Mendocino fracture zone or to regional transpression along the San Andreas fault.

Paleobathymetric evidence suggests that the La Honda and San Joaquin basins were once contiguous but have been separated by right-slip along the San Andreas fault amounting to 330 km since the late Zemorrian and 320 km since the Saucesian.

PREFACE AND ACKNOWLEDGEMENTS

This report is slightly modified from a Ph.D. thesis that was submitted to the University of California, Santa Cruz, in July, 1984. I'm grateful to the members of my thesis committee—Leo Laporte, Bob Garrison, and Casey Moore—for their considerable help and encouragement, and for providing an environment of freedom in which I could pursue answers to questions that were important to me. Helen Gibbons helped with the field work, did nearly all of the final drafting, and gave up a lot of evenings and weekends while this thesis was being prepared. Jim Ingle and Kris McDougall gave generously of their time and considerable knowledge in helping me with the benthic foraminiferal biostratigraphy and paleobathymetry. Harry Batlin of the California Department of Parks and Recreation helped secure a scientific collecting permit for Big Basin and the other State Parks in the area. Bill Odegard and Arlene Douglass typed preliminary versions of the manuscript, and Dotty Hollinger expertly prepared the final

draft.

Financial assistance was generously given by the U.S. Geological Survey, Exxon Production Research Co., Sohio Petroleum Co., Union Oil Co. of California, the U.C. Santa Cruz Patent Fund, a Grant-in-aid of Research from Sigma Xi, and a Harold T. Stearns Fellowship from the Geological Society of America.

Well logs and other subsurface information were provided by E. C. Bowen and John Randall of Gulf Oil Co., R. D. Diem and M. C. Steele of Texaco USA, Joe Newhart of Exxon USA, Magi Nielsen of OXY Petroleum Inc., Vic Rosato of Union Oil Co. of California, and Gerald E. Weber of Cordilleran Exploration.

Thin-section manufacture, x-ray diffraction, and other laboratory duties were performed by Dennis Davie and Bill Odegard under the supervision of Gene Gonzales.

Many other people provided additional assistance, including Al Almgren, Alan Allwardt, Sally Barrow, Kevin Biddle, Gregg Blake, Earl Brabb, Jim Broadwell, Carl Burger, Joe Clark, Jim Crouch, Mike Dempsey, Allen Glazner, Steve Graham, Cortez Hoskins, David Lindberg, Linda Long, A. W. Marianos, Dave McCulloch, Ken Morris, Tor Nilsen, Larry Phillips, Dick Poore, Eli Silver, Roberta Smith-Evernden, Miles Standish, Sean Stone, Bob Stuart, Connie Throckmorton, Peter Twight, and Peter Whelan.

INTRODUCTION

The La Honda basin of central California persisted through most of the Tertiary Period as a marine embayment on the western margin of the North American continent. The marine history of the basin has ended--although perhaps only temporarily--and is recorded by a pile of sedimentary and volcanic rocks more than 8 km thick that has been folded, faulted, and uplifted to form the modern Santa Cruz Mountains and northern Gabilan Range.

The geology and geologic history of the La Honda basin are extremely complex. This complexity reflects the fact that, throughout its history, the La Honda basin has been located on or near the tectonically active boundary between the North American continent and various oceanic plates of the Pacific Basin. The history of this plate boundary is still poorly understood; it apparently was a convergent boundary at some times, a translational boundary at others, and often a combination of the two. The changing modes of plate interactions had local tectonic effects that were recorded by patterns of sedimentation in basins, like the La Honda basin, that occur along the plate boundary. A detailed knowledge of the histories of such basins is potentially valuable in deciphering the history of plate interactions along the California margin, in refining hypotheses of the plate tectonic evolution of the northeastern Pacific, and in understanding the relationships between plate motions and sedimentary basin evolution.

This report focuses on the history of the La Honda basin during the middle Tertiary, a time of substantial tectonic activity associated with the end of subduction in central California and the birth of the modern San Andreas transform. The upper Eocene to lower Miocene rock record of the basin is 2 to 3 km thick and exhibits rapid lateral variations in sedimentary facies and stratigraphic thickness, several local and regional unconformities, and locally thick accumulations of volcanic rocks. Stratigraphic units deposited during this interval comprise a wide variety of different lithologies that interfinger with each other in complex ways and include shelf and turbidite sandstones, nonmarine redbeds, laminated anoxic shales, bioturbated basinal mudstones, and volcanic rocks. The general stratigraphy and structure of these rocks are fairly well known as a result of many years of study by earth scientists and students of Stanford University, the University of California, and the U.S. Geological Survey. The middle Tertiary of the La Honda basin is therefore ripe for re-evaluation in the light of recent advances in biostratigraphy,

paleoecology, sedimentology, and tectonics.

The goals of this report are to reconstruct the middle Tertiary history and paleogeography of the La Honda basin and to interpret these in terms of plate interactions as well as paleoceanographic events such as worldwide changes in sea level. My research strategy, described in detail in the section on "Methods," consisted of (1) recognition of major depositional systems, their ages, and relationships to each other, and (2) construction of paleobathymetric and paleogeographic maps for several time horizons by integrating information on foraminiferal paleobathymetry, depositional systems, paleocurrents, and provenance.

The results of this study shed additional light on the birth and history of the San Andreas transform during the Oligocene. Over much of central California, rocks of Oligocene age are either missing or consist mainly of nonmarine facies. Therefore, the thick Oligocene marine record in the La Honda basin offers an uncommon opportunity to understand the important events that occurred along the California continental margin at this time. In addition, the paleobathymetric and paleogeographic maps presented in this report may provide a framework for future detailed studies of sedimentology, paleoecology, and diagenesis, and may be applicable to exploration for oil and gas.

REGIONAL SETTING

Introduction

The name "La Honda basin" was first proposed by Cummings and others (1962, p. 236) to describe a Tertiary depositional basin that occurred in the area of the modern Santa Cruz Mountains. The name La Honda is preferred over the alternative "Santa Cruz basin" (Gribi, 1957; Beaulieu, 1970) because the latter is also the name of an offshore basin in the modern southern California continental borderland.

Lower and middle Tertiary rocks of the La Honda basin are now preserved in outcrop and in the subsurface in an area about 110 km long and 25 km wide, stretched out parallel to the San Andreas fault and extending from near San Juan Bautista in the southeast to Montara Mountain in the northwest. Originally the depositional basin was much larger, but exactly how much larger we cannot say because much of the lower and middle Tertiary rock record has been removed by erosion. In addition, major parts of the original basin have been truncated and carried away by strike-slip movement on the San Andreas and San Gregorio-Hosgri faults, as discussed below.

The Salinian Block

The La Honda basin is located west of the San Andreas fault on the Salinian block, an allochthonous tectonostratigraphic terrane whose structure, origin, and history are the subjects of much debate (J. G. Vedder and others, unpublished report, 1981). The Salinian block is traditionally regarded as a sliver of crust underlain primarily by granitic and metamorphic basement rocks that probably represent the roots of a late Mesozoic Andean-type volcanic arc. The Salinian block is clearly out of place in California, for it is bounded on either side by major faults, the San Andreas on the east and the Sur-Nacimiento on the west. In addition, the Salinian block is completely surrounded by rocks of the Franciscan Complex that probably represent one or more accretionary wedges that developed in one or more late Mesozoic-early Cenozoic subduction zones (Page, 1981, 1982). The site of origin and mode of emplacement of the Salinian block are unknown. The Salinian block may represent a former, southward continuation of the Sierra Nevada granitic belt that has been transported to its present position by strike-slip motion on faults of the San Andreas and proto-San Andreas systems (Dickinson, 1983). Alternatively, limited paleomagnetic evidence suggests that the Salinian block originated at the latitude of Mexico or Central America, traveled northward about 2500 km by unknown tectonic processes, and collided with southern California during early Tertiary time (Champion and others, 1981; J. G. Vedder and others, unpublished report, 1981). Whatever its origin and early history, the Salinian block must have been present in California prior to deposition of the early to middle Eocene Butano-Point of Rocks submarine fan, which consists of coarse sediment that was derived from a Salinian granitic source area and was deposited by

northward-flowing turbidity currents in a basin that straddled the future trace of the Neogene San Andreas fault (Clarke and Nilsen, 1973; J. G. Vedder and others, unpublished report, 1981).

Restoration of Neogene Deformation

In order to understand the early and middle Tertiary paleogeographic setting of the La Honda basin, one must first recognize and palinspastically restore the effects of Neogene strike-slip faulting. Large right-lateral displacements along the San Andreas, the San Gregorio-Hosgri, and other strike-slip faults have resulted in slicing and northwest-southeast elongation of the Salinian block, as well as transport of the block—together with the superjacent La Honda basin—several hundred kilometers to the northwest relative to the adjacent North American continent (Graham, 1976, 1978).

Detailed studies of offset geologic features such as ancient shorelines, submarine fans, and volcanic fields show that about 305 to 330 km of right-lateral displacement has occurred along the San Andreas fault since early Miocene time (Dickinson, 1983; Graham, 1976, 1978, and references therein). An early to middle Eocene submarine fan system—the Butano-Point of Rocks fan mentioned earlier—is offset by this amount, as is the lower Miocene Pinnacles-Neenach volcanic field, suggesting that little or no strike-slip movement took place along the San Andreas fault between middle Eocene and early Miocene time (Clarke and Nilsen, 1973; Nilsen and Link, 1975). Palinspastic restoration of 305 to 330 km of right-lateral displacement along the San Andreas fault suggests, therefore, that from middle Eocene to early Miocene time the La Honda basin west of the fault and the San Joaquin basin east of the fault were joined together as a single large basin (Figure 1). This interpretation is confirmed by similarities between the two sub-basins in late Eocene to early Miocene molluscan faunas and paleogeographies (Addicott, 1968), and also by evidence from benthic foraminiferal paleobathymetry presented later in this report. Several authors have argued for an earlier, pre-middle Eocene period of movement along the San Andreas, and the possible significance of this "proto-San Andreas" fault is discussed in the section on "Early Tertiary Paleogeographic Setting."

Studies of offset geologic features along the San Gregorio-Hosgri fault suggest that about 105 to 160 km of right-lateral displacement has occurred along this fault since the late middle Miocene (Graham and Dickinson, 1978a, 1978b; Graham and Peabody, 1981; Nagel and Mullins, 1983; Clark and others, 1984). Therefore, the western part of the early to middle Tertiary La Honda basin may have been carried away by right-lateral movement on the San Gregorio-Hosgri fault and may now lie along the coast or in the area offshore between Point Reyes and Point Arena (Figure 1). However, this basin fragment has not yet been identified.

Early Tertiary Paleogeographic Setting

The early Tertiary (Paleocene and Eocene) paleogeography and history of central California are poorly understood and controversial because much of the rock record has been eroded away, and also because much of the record that remains has been dramatically altered by Neogene deformation as noted above. However, studies based on geologic field work and on plate reconstructions from geophysical evidence suggest that during Late Cretaceous and early Tertiary time the central California coast was a convergent margin, with oceanic crust of the Farallon plate being consumed in an east-dipping subduction zone beneath the North American continent (Dickinson and others, 1979). The main paleogeographic features of this margin were largely inherited from the older and more vigorous Mesozoic convergent margin and included (1) an ancestral Sierra Nevada, a mountainous area consisting of the uplifted and exposed granitic roots of the Mesozoic magmatic arc; (2) a large and deep trough-shaped marine basin, a remnant of the Jurassic and Cretaceous Great Valley forearc basin; and (3) a trench and accretionary complex, represented by the Franciscan Complex, along the continent-ocean interface (Dickinson and others, 1979; Nilsen and McKee, 1979). This simple three-part paleogeography was disrupted in late Paleocene to early Eocene time by the emplacement of the Salinian block into the old arc-trench gap along the western margin of the old forearc basin (J. G. Vedder and others, unpublished report, 1981).

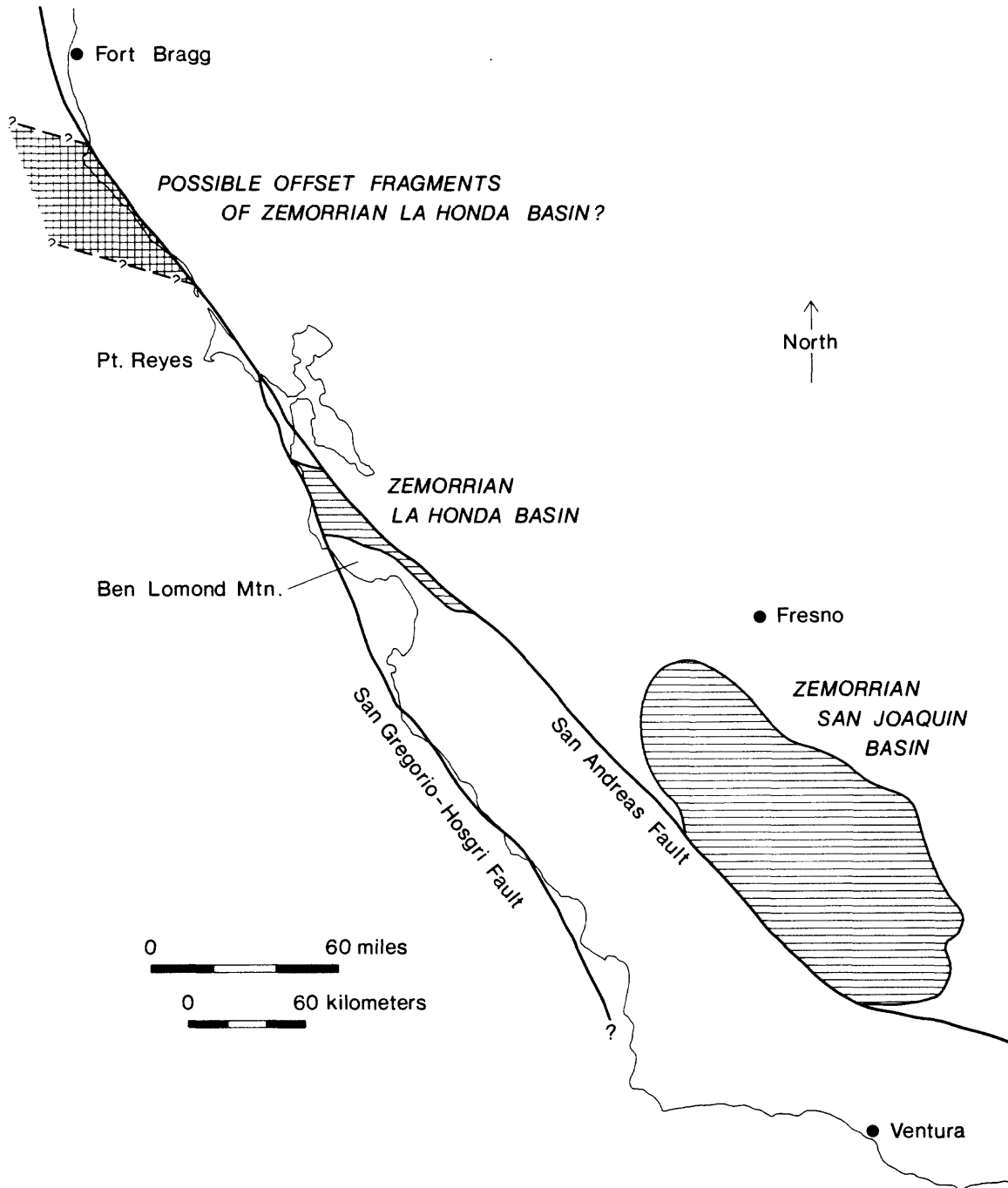


Figure 1. Map showing inferred disruption of the Oligocene La Honda-San Joaquin basin by Neogene right-lateral strike-slip motion along the San Andreas and San Gregorio-Hosgri faults, modified from Addicott (1968). The approximate areas of known Zemorrian marine strata in the La Honda and San Joaquin basins are shown by horizontal lines. Speculatively, fault-bounded fragments and erosional remnants of a hypothetical western extension of the La Honda basin may occur in the area between Fort Bragg and Point Reyes shown by crosshatching.

Although the exact mode of emplacement of the Salinian block is unknown, the final stages of its arrival were apparently accomplished by movement along an inferred right-lateral strike-slip fault termed the proto-San Andreas fault. Little is known about the offset history or even the location of the proto-San Andreas fault. It may have consisted of a braided system of fractures analogous to the modern San Andreas system. One of these fractures, for a time at least, may have followed the same pathway as the modern San Andreas fault proper, but proto-San Andreas activity on this trace must have ceased prior to deposition of the early to middle Eocene Butano-Point of Rocks submarine fan (Nilsen and Clarke, 1975). Speculatively, right-lateral movement on the proto-San Andreas system may have continued into the late Eocene along the Pilarcitos, Zayante-Vergeles, Sur-Nacimiento, or unidentified offshore faults, as suggested later in this report. Right-lateral motion along the proto-San Andreas system was probably driven by oblique subduction (Graham, 1978; Dickinson and others, 1979; Dickinson, 1983). The proto-San Andreas may therefore have been broadly analogous to the modern Semangko fault of Sumatra (Garfunkel, 1973; Carlson, 1982).

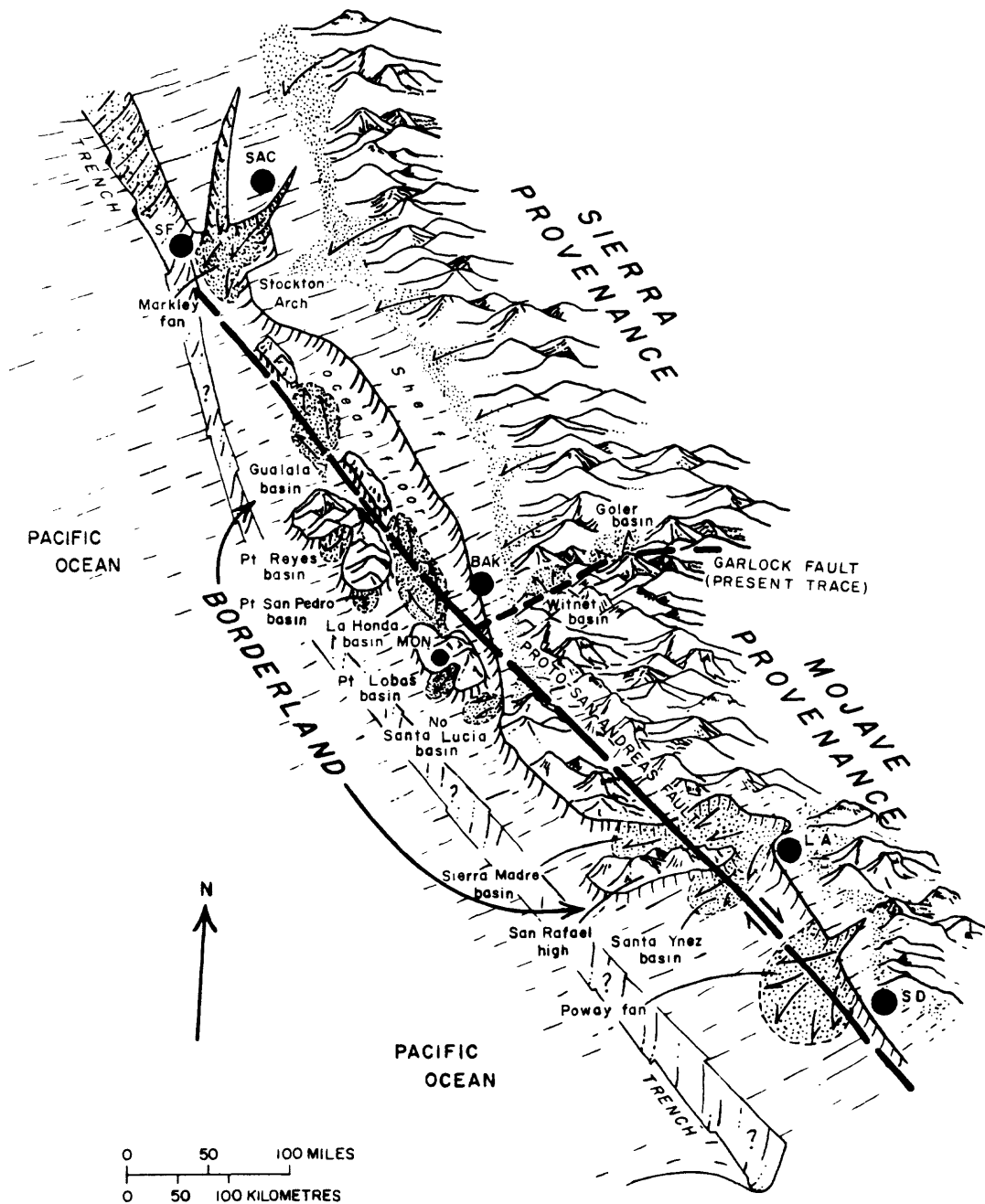
Wrench tectonism along the proto-San Andreas is believed to have caused extensive faulting and fragmentation of the Salinian block, resulting in a borderland topography of basins and ridges broadly analogous to the modern southern California continental borderland (Figure 2; Nilsen and Clarke, 1975). The early Tertiary borderland was characterized by small, deep, fault-bounded basins—including the La Honda basin—that were separated from each other by uplifted blocks of granitic basement. These borderland basins subsided rapidly and were filled mainly by coarse-grained deep-sea fan deposits derived from the vigorous erosion of the adjacent granitic highlands. Wrenching and the formation of these basins may have begun as early as Late Cretaceous (Howell and Vedder, 1978; Howell and others, 1980) but the La Honda basin apparently did not form until the late Paleocene or early Eocene when the Locatelli Formation and Butano Sandstone were deposited. Some of the early Tertiary borderland basins were very short-lived; examples are the small Paleocene basins recorded by the Carmelo Formation at Point Lobos, and the unnamed turbidites at Point San Pedro on the northern flank of Montara Mountain (Nilsen and Yount, 1981). However, other borderland basins—including the La Honda and Salinas basins—persisted as deep-water marine basins through much of the Tertiary and accumulated sedimentary sections that are many kilometers thick.

Plate Motions

A number of models based on studies of magnetic stripes on the ocean floor have been proposed to explain the Cenozoic plate tectonic evolution of the northeastern Pacific. Such models, including those of McKenzie and Morgan (1969), Atwater (1970), Atwater and Molnar (1973), Carlson (1982), and Engebretson (1982), have had an enormous impact on our understanding of California geology because they provide a framework in which to understand the relationships between plate motions and the rock record. Most significantly to this thesis, these studies imply that the western margin of the North American continent was a convergent plate boundary from at least the Late Cretaceous until about 30 m.y. ago during the Oligocene, when the Farallon-Pacific spreading center collided with the continent to create a complex transform fault boundary, the modern San Andreas fault system (Figure 3).

While this basic story is widely accepted, there is still much disagreement over important details such as the rates and directions of convergence and the timing of important changes in plate motions. Reconstructions of plate motions prior to 30 m.y. ago are hampered by a lack of knowledge of the displacement between the continent and the Farallon plate, which has been largely consumed by subduction. However, a recent study by Carlson (1982) uses indirect evidence from hot spot traces and other data to infer the following three-part history of Cenozoic plate interactions along the California coast (Figure 4).

(1) From at least 60 m.y. ago to about 42 m.y. ago, relative motion between the Farallon and North American plates was oblique convergence, which resulted in an unknown but possibly very large amount of right-lateral displacement along the inferred proto-San Andreas fault system. As previously noted, wrench tectonism along this fault system produced a continental borderland of ridges and basins,



—Generalized paleogeographic map of early Tertiary California, based on reversal of 190 miles (305 km) of post-Eocene right-lateral offset along the present San Andreas fault. The prominent paleogeographic features of both Paleocene and Eocene age are shown on the map; paleogeographic changes between the early Paleocene, when the proto-San Andreas fault may have been active, and the end of the Eocene are not shown. The present locations of several cities and the Garlock fault are included for orientation purposes. Abbreviations: SAC—Sacramento; SF—San Francisco; BAK—Bakersfield; MON—Monterey; LA—Los Angeles; SD—San Diego.

Figure 2. Generalized paleogeographic map of early Tertiary California, from Nilsen and Clarke (1975).

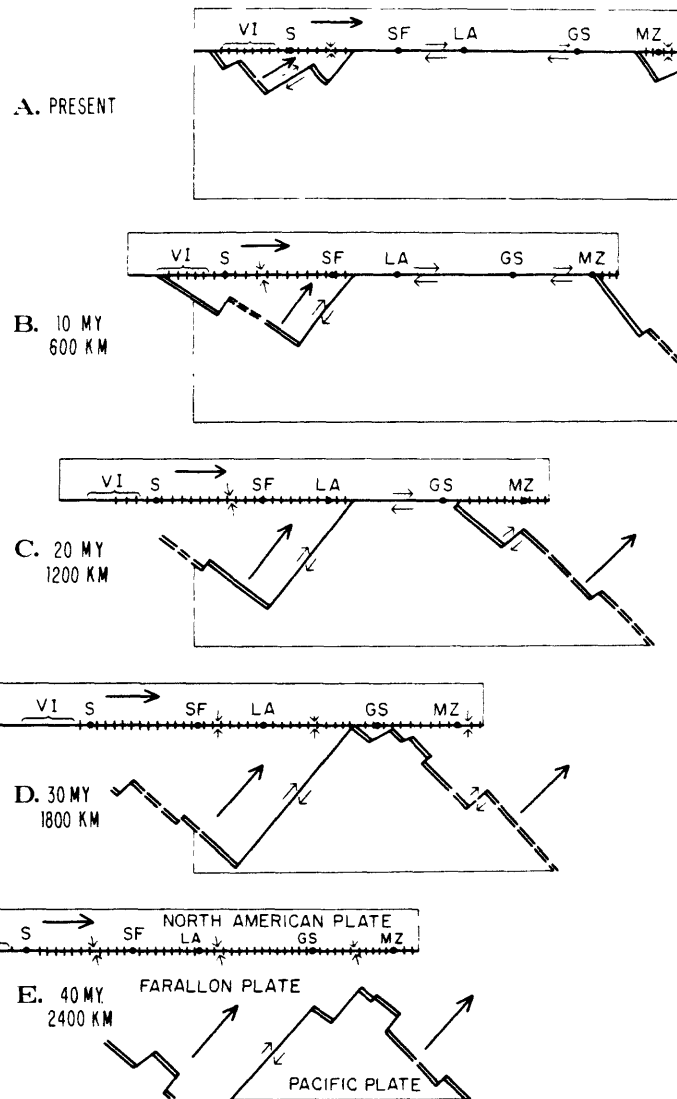
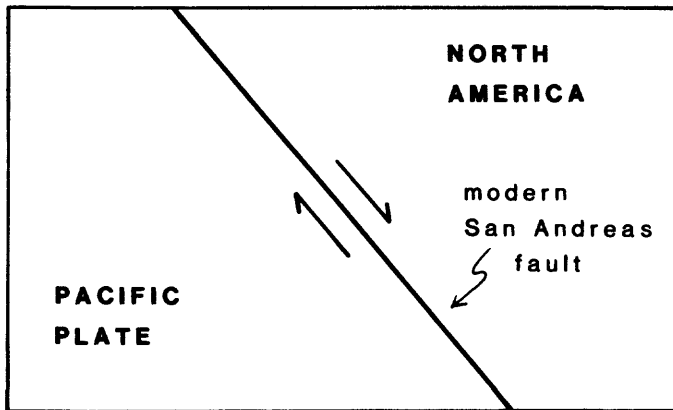
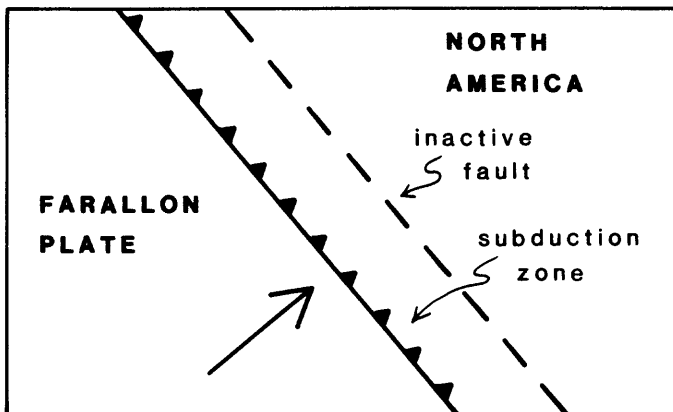


Figure 3. Schematic model of plate interactions along the west coast of North America, from Atwater (1970). The coast is approximated as parallel to the trench and to the San Andreas fault. Initials are as follows: VI = Vancouver Island, S = Seattle, SF = San Francisco, LA = Los Angeles, GS = Guaymas, MZ = Mazatlan. Single lines are transform faults, double lines are spreading centers, and hatched lines are zones of subduction (trenches). Large arrows show motions of plates with respect to Pacific plate which is arbitrarily held fixed. Small arrows show relative motions of points along plate boundaries. Captions show the time represented by each sketch in millions of years before present, and the distance that the North American plate must subsequently be displaced to reach its present position with respect to the Pacific plate.

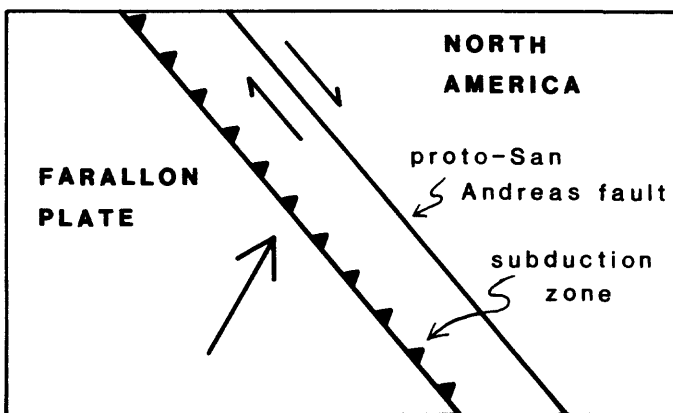
Three-stage history of plate interactions
and the San Andreas fault in central
California, modified from Carlson (1982).



30 m.y. ago
to present:
RIGHT-SLIP



42 to 30 m.y. ago:
**NORMAL
CONVERGENCE**



prior to
42 m.y. ago:
**OBLIQUE
CONVERGENCE**

Figure 4. Schematic illustration of inferred three-stage history of plate interactions and the San Andreas fault in central California, much modified from Carlson (1982). No scale. For simplicity, both the modern San Andreas and proto-San Andreas fault systems are shown as single lines.

including the La Honda basin.

(2) Between 42 and 30 m.y. ago convergence along the California coast was nearly normal (i.e., the motion of the Farallon plate was perpendicular to the offshore trench). Many of the basins formed during the earlier period of oblique subduction—including the La Honda basin—continued to subside and accumulate sediment, although at much lower rates as shown later in this report.

(3) About 30 m.y. ago, but perhaps as late as 28 m.y. ago (Engebretson, 1982), the Farallon-Pacific spreading ridge collided with the trench, resulting in regional uplift (T. H. Nilsen, unpublished report, 1982), the creation of the Mendocino and Rivera triple junctions, and the birth of the modern San Andreas transform. The length of the transform increased as the Mendocino and Rivera triple junctions migrated north and south, respectively. The Mendocino triple junction may have slid past the La Honda basin about 20 m.y. ago, and its passage may be related to a period of volcanism, rapid subsidence, and marine transgression in the basin (Dickinson and Snyder, 1979). This possibility is discussed later in this report.

In addition to the major changes in plate interactions at 42 m.y. and 30 m.y. noted above, other minor readjustments in the rates and azimuths of plate motions at about 55-50 m.y., 37 m.y., 10 m.y., and 4.5-5 m.y. have been reported in the literature. These minor readjustments may have had tectonic effects that are recorded in the rock record. For example, a major regional unconformity in the La Honda basin at the Eocene-Oligocene boundary may be related to an episode of tectonism associated with the change in plate motions at 37 m.y. noted above. Along translational margins, changes in the azimuth of plate motions can result in components of convergence or divergence that cause regional compression or extension and episodes of uplift, subsidence, or volcanism. A major period of basin expansion in central California about 10 m.y. ago may have been caused by extension due to a shift in the relative motion of the Pacific and North American plates (Blake and others, 1978). Another change in plate motions about 5 m.y. ago resulted in a component of convergence along the Pacific-North American transform boundary and may have been partly responsible for the dramatic late Cenozoic folding and uplift of the Coast Ranges (Engebretson, 1982, p. 148).

Interpretation of the rock record in terms of plate motions is further complicated by other regional events that are only indirectly related to plate motions. For example, an episode of widespread uplift and erosion that formed a regional unconformity at about the Paleocene-Eocene boundary may have been associated with a major reorganization of plate motions in the Pacific basin about 55-56 m.y. ago (Engebretson, 1982; Carlson, 1982) or, alternatively, may be related to the collision of the Salinian block with coastal California (J. G. Vedder and others, unpublished report, 1981).

It is clear that changes in plate motions can strongly affect the development of sedimentary basins along active continental margins. In practice, however, correlations of specific plate tectonic events with specific events in the rock record are subject to uncertainties. Calculations of Tertiary plate motions are based on several assumptions that are widely accepted but may be in error (Molnar and Stock, 1981; Carlson, 1982; Engebretson, 1982). In addition, due to biostratigraphic problems discussed later in this report, the timing of some major events in the rock record of the La Honda basin is only generally known. For these reasons, my correlations of plate tectonic events with events in the La Honda basin, while reasonable, are only tentative and may have to be revised as better tectonic models and more refined dating become available.

Climate and Eustasy

Although the major controls on sedimentation in the La Honda basin were probably tectonic, worldwide changes in climate and sea level may also have played a role. The Oligocene was an unusual period in earth history. Compared to the Eocene and Miocene, world climate during the Oligocene was generally cooler and more extreme, based on evidence from oxygen isotopes and the fossil record (Savin, 1977; Ingle and others, 1976; Ingle, 1979; Leckie and Webb, 1983; Snyder and others, 1984). Perhaps as a

result, many groups of organisms--plants and animals, marine and terrestrial--suffered higher than normal rates of extinction during the Oligocene (Cifelli, 1969; Addicott, 1970; Kurten, 1971; Fischer and Arthur, 1977). The extinctions and resulting low species diversity are of practical consequence, for the resolution of biostratigraphic zonations based on planktic microfossils is much lower for the Oligocene than for the Eocene or Miocene (Moore and Romine, 1981).

The middle Tertiary climatic changes were associated with major worldwide changes in sea level, although the causes and precise timing of these eustatic events are controversial (Vail and others, 1977; Donovan and Jones, 1979; Mathews and Poore, 1980; Kerr, 1980; Heller and Flessa, 1981; Miller and Olsson, 1981). A major eustatic sea level fall occurred about 29 m.y. ago during the late Oligocene, and according to Vail and Hardenbol (1979) sea level dropped "considerably more than 200 meters in a period of one to two million years." This event is recorded by unconformities and regressive sequences on continental margins over most, but perhaps not all, of the world (Pitman, 1978; Ingle, 1979; Vail and Hardenbol, 1979; Angstadt and others, 1983). In the La Honda basin and several other central California basins the record of the 29 m.y. eustatic drop is masked by a regional unconformity and major regression caused by an important episode of tectonic uplift associated with collision of the Farallon-Pacific spreading center with the continent, also about 29-30 m.y. ago. This cruel coincidence between major eustatic and tectonic events is discussed in detail in a later section of this report.

Other major sea level drops also occurred during the middle Tertiary about 40 and 22.5 m.y. ago (Vail and Hardenbol, 1979), but in the La Honda basin the records of these also are apparently masked by tectonic events. In general, the effects of eustatic sea level changes are difficult to recognize in basins along tectonically active continental margins because the rates of eustatic changes are often less than rates of sedimentation and tectonically controlled subsidence (Howell and von Huene, 1981). As a practical matter, the correlation of specific unconformities and regressive sequences with Vail and Hardenbol's eustatic drops depends in large part on precise biostratigraphic correlation, something that is very difficult to achieve in the La Honda and other Tertiary basins in central California.

METHODS

Research Strategy

The principal goal of this research is to reconstruct the middle Tertiary paleogeography and geologic history of the La Honda basin. To achieve this goal I used an approach to basin analysis similar to that used by Graham (1976) in his comprehensive study of the Salinas basin. The main components of my research strategy are discussed in some detail below.

Depositional Systems

A major focus of this research was the recognition of major depositional systems (Dickinson and Graham, 1975), their ages, and their relationships to each other in time and space. Sedimentary structures and stratigraphic cycles observed in the field were interpreted as products of depositional processes, environments, and systems by analogy with published studies of modern and ancient sedimentation. The ages and stratigraphic relations of depositional systems in the La Honda basin are based mainly on previous studies of biostratigraphy and map relations, but also partly on my own field work and interpretations of well logs.

Field work for this study was conducted intermittently from 1979 to 1982. My field investigations consisted mainly of reconnaissance traverses along several dozen streams and roads in the area. Several of these traverses covered stratigraphic sections that were previously measured and described in the literature, but I also measured several new sections. In all these traverses and sections my major emphasis was on the description and interpretation of sedimentary structures and textures, and stratigraphic cycles. I also collected several hundred rock specimens for planned future studies of sedimentology and sedimentary petrology.

Laboratory examination of rock samples for this report was limited. I briefly examined several dozen polished sections and thin-sections stained for calcite and potassium feldspar using standard procedures (Friedman, 1971; MacKinnon, 1980). X-ray diffraction was used to identify silica and carbonate minerals in some mudrocks, and carbonate cements in some sandstones.

The bedding terminology used in this report is that of Campbell (1967, p. 19). The naming of limestones, sandstones, and mudstones follows the classifications of Dunham (1962), Dott (1964), and Blatt (1982, p. 57), respectively. Deep-sea sandstones and mudrocks were classified and interpreted, where possible, using the scheme of Mutti and Ricci Lucchi (1972).

Paleocurrents

Paleocurrents are critical in identifying sediment source areas, in determining basin configuration, and in recognizing some depositional systems. Paleocurrent data from the middle Tertiary of the La Honda basin, consisting of 166 individual measurements from 52 outcrops, are summarized in Appendix 5 and were obtained as follows. The orientations of directional sedimentary structures such as flute casts, groove casts, cross-stratification, and clast imbrication were measured in the field, and then later (in the office) restored to their presumed depositional orientations with a stereonet by simple rotation about the strike of bedding (Potter and Pettijohn, 1977, p. 371-374). No additional corrections were made for other structural complications such as fold plunge or tectonic rotation, because in most cases the data necessary for these corrections are not known. Because of the small size of the data set, statistical analysis of paleocurrent data was limited to calculation of vector mean and vector strength or "consistency ratio" (Potter and Pettijohn, 1977, p. 376) for each locality and for a few arbitrary groupings of the data (see Appendix 5 and Figures 41 and 53).

The paleocurrent information in this report should be regarded as preliminary due to poor outcrop and the reconnaissance nature of my field studies. Paleocurrent data are difficult to obtain from middle Tertiary rocks of the La Honda basin because of the patchy distribution and poor, two-dimensional nature of most exposures. Much better data on cross-stratification could be obtained by excavation of large numbers of outcrops to obtain the necessary three-dimensional exposures. Additional data could probably be obtained by field measurement of paleoslope indicators such as syn-sedimentary folds (Nilsen and Simoni, 1973), by laboratory studies of grain orientation (Potter and Pettijohn, 1977, p. 70-72), and by measurements of magnetic susceptibility (Galehouse, 1968).

Subsurface Investigations

Most of the stratigraphic information used in this study came from outcrop sections, but additional data came from wells drilled in the search for oil and gas. I examined files on more than 75 wells in the La Honda basin. Most of these wells were drilled in the northern part of the basin, particularly in the La Honda quadrangle, where the lower and middle Tertiary section is largely hidden by the upper Tertiary Purisima Formation, and where some small oil fields have been established (Figures 5, 6, and 7; Table 1). Nearly all of the well files contained electric logs, which I used in conjunction with other kinds of logs—for example, mudlogs, core descriptions, and paleontologic reports—to estimate the lithology and age of the rocks encountered by each well, and to correlate with other wells and with outcrop sections. Most of the well files also contained dipmeter logs that allowed the conversion of drilled thickness to stratigraphic thickness. My subsurface data are summarized in Appendix 4.

Thickness Maps

Thickness (isopach) maps can be used to infer lateral facies changes, sediment dispersal directions, and patterns of subsidence and uplift. Thickness maps are important in interpreting paleotectonics because they can be used to recognize folds and faults that were active at the time of sedimentation of a

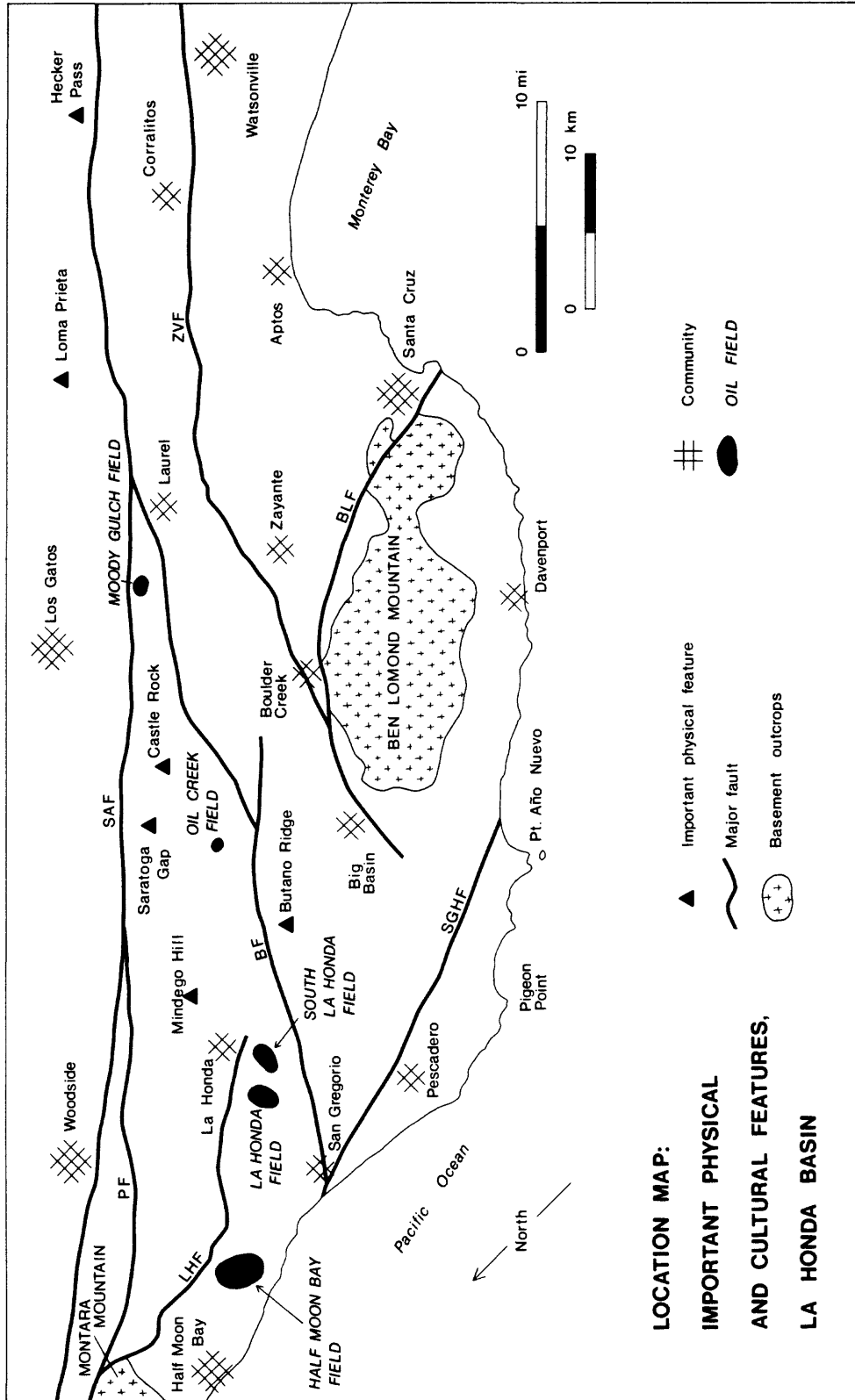
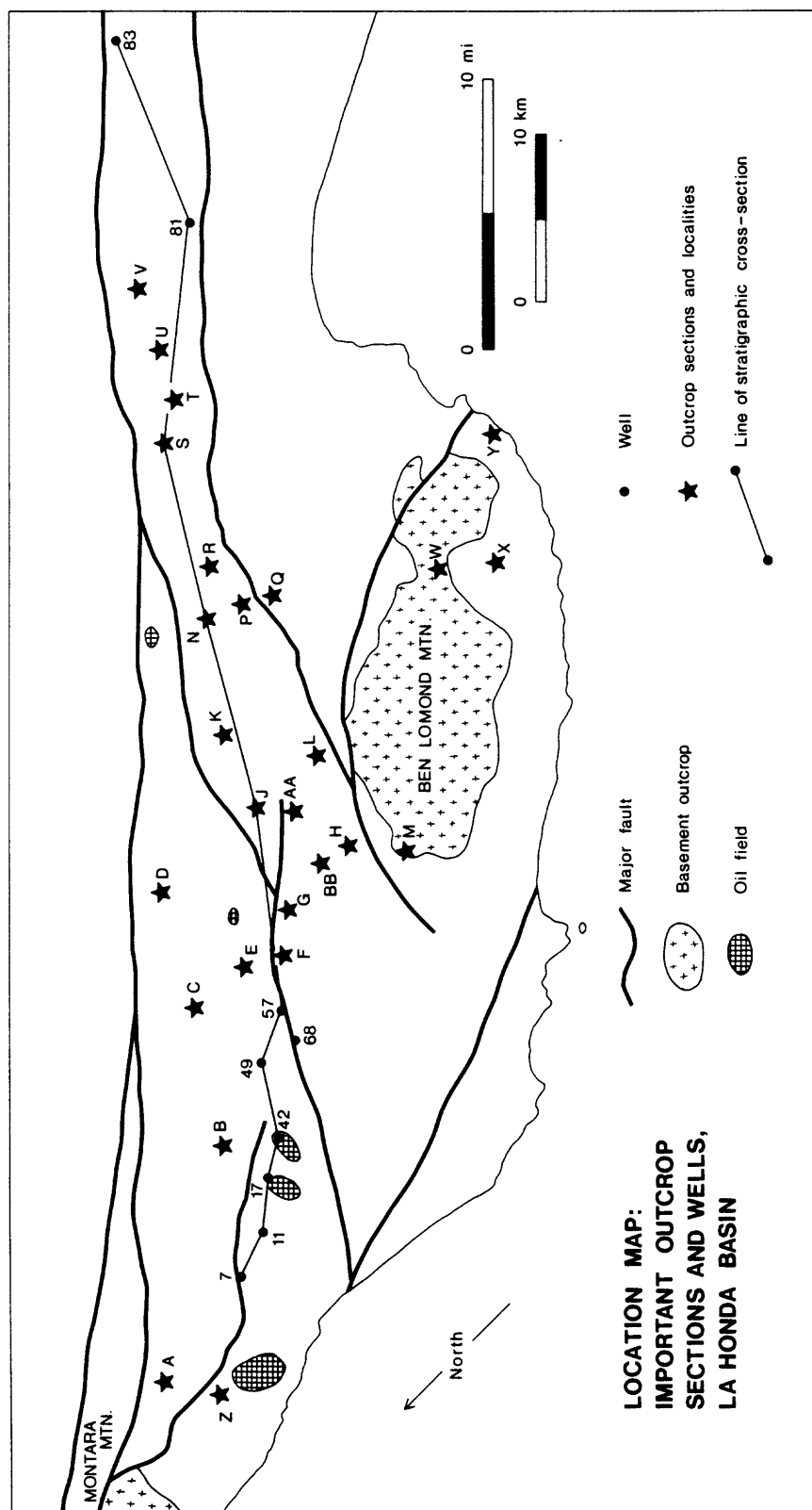


Figure 5. Location map of important physical and cultural features in the La Honda basin area. Major faults labeled as follows: BF = Butano fault, BLF = Ben Lomond fault, LHF = La Honda fault, PF = Pilarcitos fault, SAF = San Andreas fault, SGHF = San Gregorio-Hosgri fault, ZVF = Zayante-Vergeles fault.

Figure 6. Location map of important outcrop sections and wells in the La Honda basin. Major faults labeled as in Figure 5. Shown is the line of stratigraphic cross-section in Figure 15. Wells numbered as in Appendix 4. Outcrop sections and localities mentioned in text are as follows. A = Woodside-Half Moon Bay area, B = La Honda Creek (type section of the Mindego Basalt), C = Lambert and Peters creeks (type section of the Lambert Shale), D = Saratoga Gap, E = Slate Creek, F = Fall Creek, G = Little Boulder Creek (type section of the Butano Sandstone), H = Blooms Creek, J = Kings Creek (type sections of the Twobar Shale and Rices Mudstone), K = Bear Creek, L = Twobar Creek, M = Tuck's Creek (type section of the Locatelli Formation), N = Upper Zayante Creek, P = Lower Zayante Creek (type section of the Zayante Sandstone), Q = East Zayante Road (type section of the Lompico Sandstone), R = Mountain Charlie Gulch, S = Soquel Creek, T = Hinckley Creek, U = Aptos Creek, V = Corralitos Creek, W = Smith Grade-Empire Grade area, X = Majors Creek, Y = Moore Creek (type section of the Santa Cruz Mudstone), Z = Purisima Creek (type section of the Purisima Formation), AA = San Lorenzo River at Riverside Grove, BB = Upper Boulder Creek.



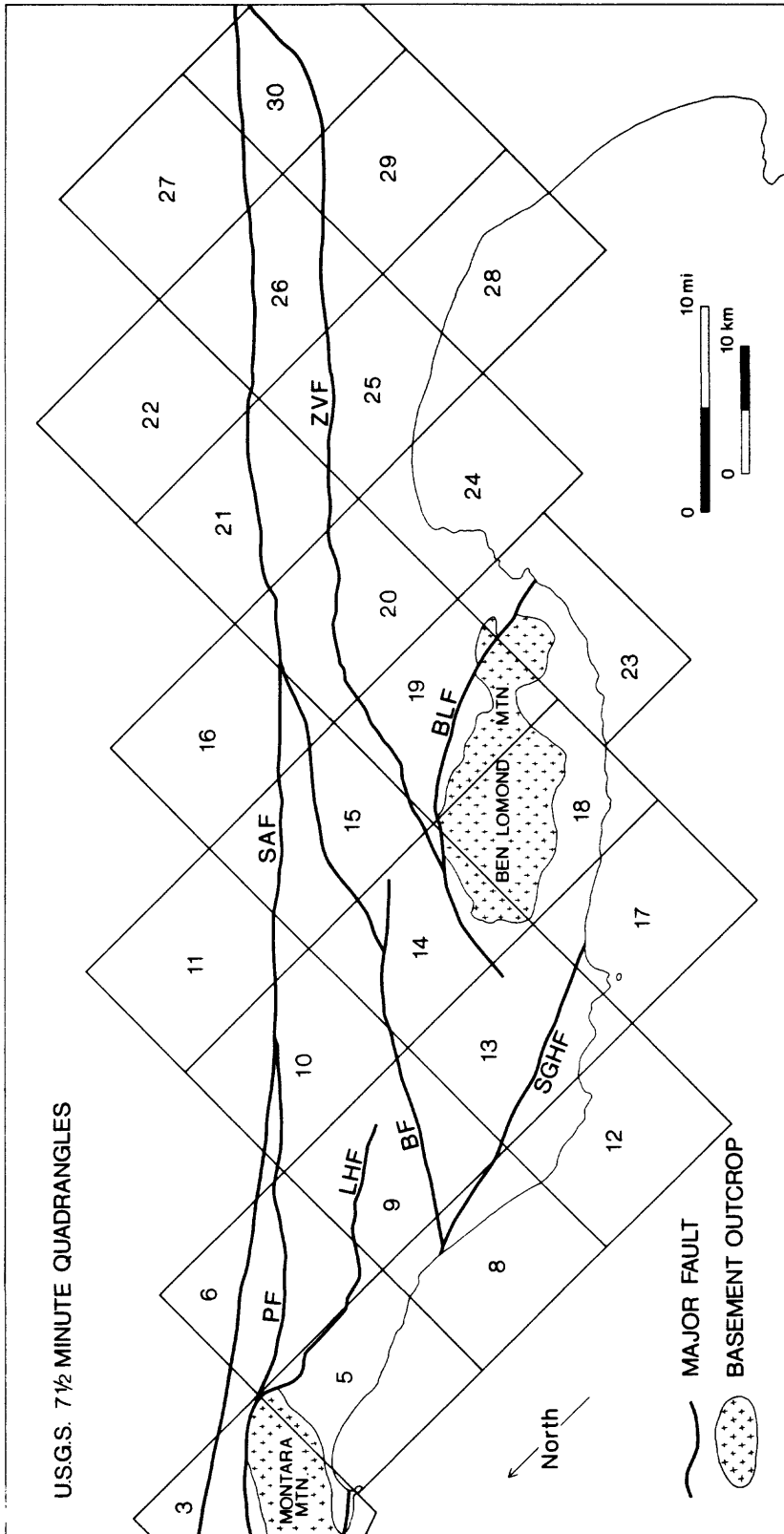


Figure 7. Index to U.S. Geological Survey 7.5 minute quadrangles in the La Honda basin area. Major faults labeled as follows: BF = Butano fault, BLF = Ben Lomond fault, LHF = La Honda fault, PF = Pilarcitos fault, SAF = San Andreas fault, SGHF = San Gregorio-Hosgri fault, ZVF = Zayante-Vergeles fault. Quadrangles numbered as follows: 3 = Montara Mountain, 5 = Half Moon Bay, 6 = Woodside, 8 = San Gregorio, 9 = La Honda, 10 = Mindego Hill, 11 = Cupertino, 12 = Pigeon Point, 13 = Franklin Point, 14 = Big Basin, 15 = Castle Rock Ridge, 16 = Los Gatos, 17 = Año Nuevo, 18 = Davenport, 19 = Felton, 20 = Laurel, 21 = Loma Prieta, 22 = Mt. Madonna, 23 = Santa Cruz, 24 = Soquel, 25 = Watsonville West, 26 = Watsonville East, 27 = Chittenden, 28 = Moss Landing, 29 = Prunedale, 30 = San Juan Bautista.

TABLE 1

LA HONDA BASIN OIL FIELDS

(Data compiled from California Division of Oil and Gas, 1973 and 1982b)

	<u>MOODY GULCH</u>	<u>HALF MOON BAY</u>	<u>OIL CREEK</u>	<u>LA HONDA</u>	<u>SOUTH LA HONDA</u>
YEAR OF DISCOVERY	1878	1882	1955	1956	1959
1981 OIL PRODUCTION	-	945 bbl.	3,100 bbl.	4,071 bbl.	9,262 bbl.
GAS	-	-	248 Mcf	4,093 Mcf	-
CUMULATIVE OIL PRODUCTION to 12/31/81	98 Mbbl.	44 Mbbl.	170 Mbbl.	783 Mbbl.	477 Mbbl.
GAS	44 MMcf	20 MMcf	76 MMcf	103 MMcf	39 MMcf
OIL GRAVITY - °API	40-45	45	41-44	Butano: 32-40 Lambert/Mindego: 24	Mindego: 16-17 Vaqueros: 17-18 Butano: 31
PRODUCING ZONES	3 sands in Twobar Shale (?) and fractured shales in the "Pacheco zone" of Purisima Formation	Various sands	"Tony" and "Costa" sands in Butano Sandstone	"Costa sand" in Butano Sandstone; minor production from Lambert Shale or Mindego Basalt	"Burns sand", a limestone in Mindego Basalt; minor production from Vaqueros and Butano sandstones

Table 1, continued

	<u>MOODY GULCH</u>	<u>HALF MOON BAY</u>	<u>OIL CREEK</u>	<u>LA HONDA</u>	<u>SOUTH LA HONDA</u>
TRAP	Local rollover or fault on steeply-dipping homocline.	Uncertain. At least one small anticline; may also be fault traps and lenticular sands.	Faulted anticline.	Buried anticline; Butano Sandstone truncated updip by unconformity at base of Purisima Formation.	Buried anticline; Burns sand truncated updip by unconformity at base of Purisima Formation.
OLDEST FORMATION PENETRATED IN FIELD	Twobar Shale (Eocene) - ?	"Eocene Sand" - ?	Butano Sandstone (Eocene)	Butano Sandstone (Eocene)	Butano Sandstone (Eocene)
ADDITIONAL REFERENCES	Krueger, 1943	Crandall, 1943; Horn, 1983	Fothergill, 1962b	Fothergill, 1962a	-

given unit, but have since been covered by younger strata or obscured by younger structures. In this study, thickness maps were constructed for selected stratigraphic intervals in the La Honda basin using data from both outcrops and wells (Appendices 3 and 4).

Paleobathymetry

General Principles

Patterns in the distribution of fossil benthic foraminifers have been used with great success in interpreting the paleobathymetry of several Tertiary basins in California, including the San Joaquin, Salinas, Ventura, Los Angeles, and Cuyama basins (Bandy and Arnal, 1969; Graham, 1976; Ingle 1980; Lagoe, 1984). The rationale for paleobathymetric analysis has been discussed in detail elsewhere (Bandy and Arnal, 1960, 1969; Ingle, 1975a, 1975b, 1980; Graham, 1976) and is summarized below.

Quantitative studies of living populations of benthic foraminifers along the eastern margin of the Pacific Ocean have shown that the most distinctive and significant changes in these populations are those that occur with increasing depth of water and distance from shore (e.g., Bandy and Arnal, 1960; Bandy, 1961; Ingle, 1967; Ingle and Keller, 1980). In addition, these studies have recognized recurring assemblages of species, or biofacies, that are strongly correlated with water depth. Many of these species (or their near relatives) are found as fossils in the Cenozoic sedimentary record and therefore have been used as paleoecologic indicators to infer the paleobathymetry of ancient marine environments.

The use of benthic foraminifers as paleobathymetric indicators has a number of problems and uncertainties. For example, the contamination of deeper-water faunas by downslope transport of shallower-water species is common in modern environments and therefore to be expected in ancient sediments, especially in turbidite and slope deposits. Consequently, assemblages of fossil foraminifers must be interpreted using the deepest-dwelling species as indicators of the minimum depth of deposition (Ingle, 1980).

Another source of uncertainty is the possibility, due to organic evolution, that ancient species and genera may not have had the same ecological preferences and requirements as their Recent descendants. Most studies of paleobathymetry, including my study of the La Honda basin, attempt to mitigate this problem by basing interpretations of paleodepth on *assemblages* of two or more species rather than on the occurrence of individual species.

How reliable are the numerical estimates of paleodepth obtained by this method? There is no pat answer to this question. The major source of uncertainty arises from our lack of knowledge about the exact physical and biological controls on the distribution of benthic foraminifers. Most modern investigators now believe that the foraminiferal biofacies are controlled not by depth itself but by other environmental factors—in particular, water mass characters such as temperature, salinity, illumination, and oxygen content—that change in concert with depth (Ingle, 1980; Ingle and Keller, 1980; Blake and Douglas, 1980). Some of these environmental factors (e.g., the maximum depth of the penetration of light) are fairly constant in the modern oceans and probably were the same in the past. But others, especially water mass characters such as temperature, salinity, and oxygen, are not so closely tied to depth and in many cases are strongly controlled by local oceanographic conditions (Ingle, 1980; Ingle and Keller, 1980). Therefore, it is possible that at least some of the water masses, along with their associated foraminiferal biofacies, may have varied in depth over geologic time as a result of changes in ocean circulation and worldwide climate.

A well-known example of local variation in the bathymetry of water masses is the occurrence of silled basins in the southern California continental borderland. In each of these basins, the water mass characters of the entire basin are uniform, rather than stratified as in the open ocean, and they are similar to the characters of water occurring at the same depth as the basin sill in the adjacent open sea. Thus, if the sill occurs at shallow depths, the deeper water organisms that would otherwise be expected to occur may be absent from the deepest part of the basin (Graham, 1976; Ingle and Keller, 1980). In general, it is

difficult to detect such silled basins in the ancient record simply by analysis of biofacies (Lagoe, 1982). However, in some of these basins the entire water column is anoxic because the sill depth occurs within the oxygen minimum zone, and such basins should be easily identifiable in the rock record because of the distinctive sediments--thin-bedded to laminated, organic-rich, and often phosphatic dark-colored shales--that form under anoxic conditions (Garrison, 1981; Pisciotto and Garrison, 1981).

A potentially greater obstacle to paleobathymetric analysis is the possibility that worldwide climatic changes may have caused major variations in the bathymetry of oceanic water masses in the geologic past. For example, Blake and Douglas (1980) have proposed that, during the latest Pleistocene glaciation, the deep, cold water mass associated with the lower bathyal biofacies may have been as shallow as 1400 m, and not at 2000 m as in the Recent oceans. This interesting interpretation is based on a study of the distribution of only one species rather than a species assemblage so that it may not be widely applicable. Nevertheless, the conclusions of Blake and Douglas pose a difficult challenge to the paleobathymetric analysis of Tertiary basins in California. It is not yet known whether such dramatic shoaling of the lower bathyal zone may have also occurred at other times, for example during the Oligocene climatic refrigeration.

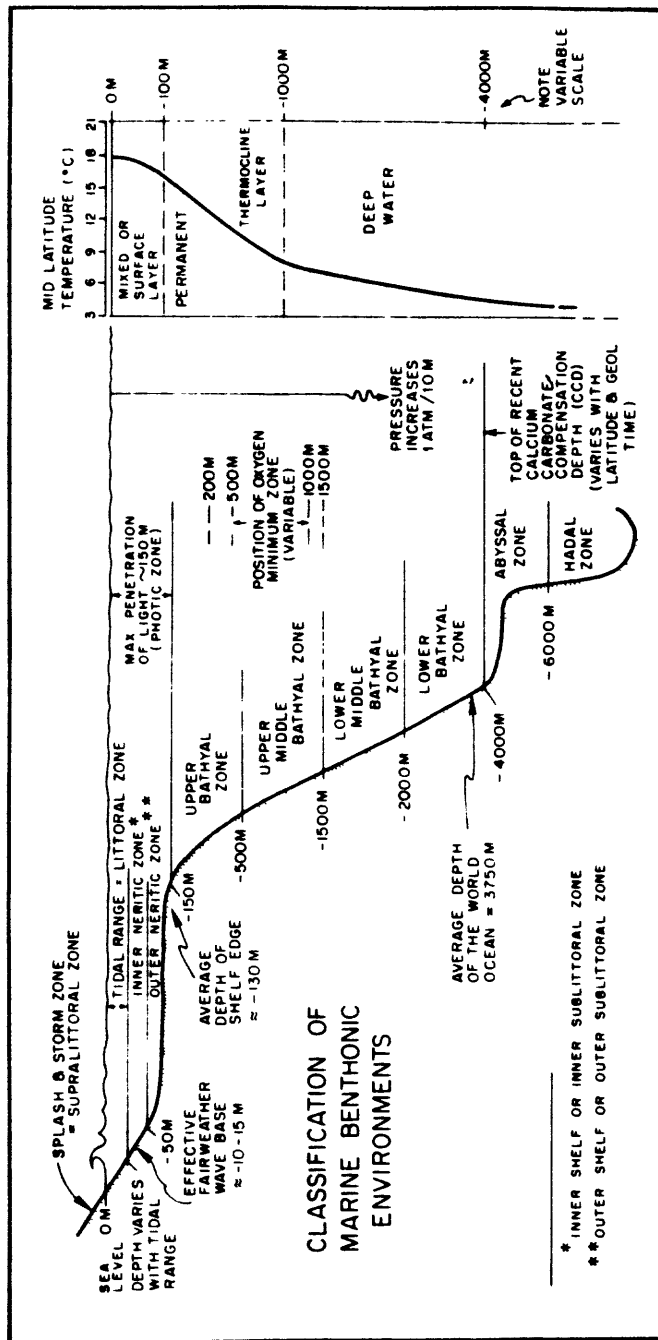
In summary, it appears that the benthic foraminiferal biofacies have remained in relatively the same depth-stratified sequence through time, but it is also clear that we must be cautious in using the bathymetry of Recent biofacies to assign numerical values of paleodepth to the fossil biofacies in ancient sedimentary basins (Ingle, 1975a; Ingle and Keller, 1980). Despite these problems, I continue to regard the analysis of paleobathymetry as an important technique of basin analysis. Other techniques, such as studies of paleocurrents and lithofacies, can provide important information on paleoenvironmental gradients such as the transition from basin to shelf, but do so only in a *qualitative* way. Paleobathymetric analysis is an important complement to such sedimentological studies because it is the only method yet developed that can give *quantitative* estimates of water depth. This information can be combined with other data, in particular measurements of stratigraphic thickness, to estimate rates and amounts of uplift, subsidence, and depth of burial, as discussed later in this report.

Application to the La Honda Basin

The faunal data used in my paleobathymetric analysis of the La Honda basin are listed in Appendix 1. These data consist of over 800 faunal lists, each of which is a list of fossil species from a single rock specimen, outcrop, or drilled interval. The lists were compiled from over 30 published and unpublished reports, and from subsurface information generously provided by Exxon USA, Gulf Oil Co., and Occidental Petroleum Co. Each list was examined and interpreted in terms of paleodepth by comparison with the bathymetric biofacies of Ingle (1980).

The age of each faunal list, also given in Appendix 1, is from the original reference unless otherwise noted. I revised an age interpretation only when I felt confident that a "better" one could be made--for example, a more specific "lower Zemorrian" rather than simply "Zemorrian." These revisions are based on the criteria of Kleinpell (1938, 1980) and also on unpublished information kindly provided by Dr. K.A. McDougall of the U.S. Geological Survey. Many of my interpretations of age and depth were personally checked by Dr. McDougall and by Dr. J.C. Ingle of Stanford University, but responsibility for errors rests solely with me.

Ten maps, each depicting the paleobathymetry of the La Honda basin for a different time horizon, were constructed in the following manner. The location of each faunal list was plotted on a 1:125,000-scale base map corresponding to a specific stratigraphic interval, usually one of the provincial benthic foraminiferal stages. Each "data point" on the maps (for example, see Figure 66) corresponds to one or more faunal lists and an inferred paleodepth. Some of the data points on the maps are based on only a single faunal list, but many data points represent several lists from the same outcrop or nearby outcrops; in these cases, the *deepest* paleodepth is assumed correct. The contour lines, or paleoisobaths, were drawn at intervals corresponding to the estimated depths of the biofacies boundaries of Ingle (1980) (Figure 8).



Classification of benthonic marine environments in terms of depth and positions of critical oceanographic boundaries or transitional zones in the modern world ocean. Note that water depths are given in meters. This classification is a modification of that presented by Hedgpeth (1957); from Ingle (1973a).

Figure 8. Classification of marine benthic environments, from Ingle (1980).

The data points on my maps include only those faunal lists that could confidently be assigned to *both* a specific bathymetric biofacies *and* a specific stratigraphic interval; thus, not all of the faunal lists in Appendix 1 are plotted on the maps.

My analysis of paleobathymetry is subject to a number of possible errors. The most important of these are inherent in the paleoecological models themselves—for examples, problems caused by redeposition, organic evolution, and changes in paleoceanography—as discussed earlier in this report. A few other problems are worth mentioning here.

The faunal lists that I used were compiled from the works of many different paleontologists, so taxonomic assignments may not be consistent. In some cases, I attempted to correct for this lack of consistency by applying commonly accepted synonymies that were kindly provided by J.C. Ingle and K.A. McDougall; otherwise, all species identifications were accepted as valid. I ignored species whose identities or occurrences were questioned in the original reference. In most cases, I also ignored species whose relative abundance in a single faunal list was reported as "rare" or "very rare."

The number of faunal lists available for the La Honda basin is large but not evenly distributed geographically or stratigraphically. Excellent data are available from the central Santa Cruz Mountains, but only sparse data are available at present from the areas north and west of La Honda and southeast of Soquel Creek. Data from the Monterey Formation are few because outcrops of this unit are generally poor and widely scattered. Data from units younger than the Monterey Formation are very few owing to the general lack of well-preserved benthic foraminifers in these rocks.

My estimates of paleodepth are based solely on analysis of the biofacies of benthic foraminifers. However, the paleobathymetric analyses of a few other Tertiary basins in California have been done not just by examining biofacies but by using more elaborate paleoecologic techniques, such as the quantitative analysis of arenaceous-planktic-calcareous species ratios, numbers of foraminifera, numbers of radiolarians, etc. (Bandy and Arnal, 1960, 1969; Bandy, 1967; Ingle, 1975a, 1975b, 1980). Such quantitative analysis was not possible in my study of the La Honda basin because no quantitative data are available; most of my sources of data listed the abundances of species only in relative terms, if at all.

A few additional notes on the organization and presentation of paleontologic data in Appendix 1 are appropriate here. A large number of the faunal lists examined in this study could not be interpreted in terms of Ingle's bathymetric biofacies because the benthic foraminiferal assemblages were too small or consisted of nondiagnostic species. These assemblages are identified in Appendix 1 by the notation "NED," meaning "not enough data." In some cases, however, these assemblages contained common to abundant planktic foraminifers or radiolaria, suggesting that they represent outer shelf or greater depths (Ingle, 1975a, and personal communication, 1982). These assemblages are identified in Appendix 1 by the notation "DW," or "deep water," without any more specific interpretation of paleodepth.

A few benthic foraminiferal assemblages consist entirely or almost entirely of arenaceous species, and these are identified in Appendix 1 by the designation "ARF." The paleoecological interpretation of these arenaceous assemblages is clear in most but not all cases. Most of these assemblages appear to represent shelf or bathyal faunas from which the calcareous species have been leached by weathering or other post-depositional processes; this interpretation is supported by the occurrence of foraminiferal molds in some outcrops. However, it is possible that at least a few of the arenaceous assemblages represent deposition at truly abyssal depths, near or below the lysocline (LCD) and the calcium carbonate compensation depth (CCD). In the modern oceans, the dissolution of calcareous foraminiferal tests below the LCD and the CCD increases the relative abundance of arenaceous foraminifers (Ingle, 1980). Some of the Tertiary arenaceous assemblages from the La Honda basin—particularly those from the Butano Sandstone and Twobar Shale—may represent sub-lysocline faunas because (1) these units also contain calcareous assemblages indicative of lower bathyal deposition, and (2) the arenaceous assemblages include representatives of several genera identified by Ingle (1980) as being common at abyssal depths, including *Bathysiphon*, *Cyclammina*, *eggerella*, *Haplophragmoides*, and *Rhabdammina*. The interpretation of these faunas as abyssal is still uncertain, however, because they could also represent lower bathyal faunas from

which the calcareous elements have been leached. No direct sedimentologic evidence of sub-LCD or sub-CCD deposition, such as the occurrence of radiolarian cherts or other abyssal pelagic sediments, has been reported from the La Honda basin, but such evidence may have been masked by the relatively rapid deposition of clastic sediments that occurred throughout the Tertiary history of the basin.

Some of the foraminiferal assemblages from the Twobar Shale and Lambert Shale consist of only a few species--usually representatives of the upper bathyal and upper middle bathyal biofacies--and are dominated by common to abundant individuals of only one or two species. In the Twobar Shale, the dominant species is usually *Bulimina microcostata* Cushman and Parker, while in the Lambert Shale the dominant species is usually *Globobulimina pacifica* Cushman, or rarely *Chilostomella ovoidae* Reuss. All three of these species are thought to be indicative of anaerobic bottom conditions produced by water of low oxygen content (Ingle, 1980; Milam and Ingle, 1982). Therefore, the low-diversity foraminiferal assemblages that are dominated by low-oxygen species are here interpreted as faunas that lived in the oxygen minimum zone, and are identified in Appendix 1 by the designation "OMZ." Some of these assemblages may be redeposited, but it is probably significant that they occur most commonly in the Twobar Shale and Lambert Shale, formations that consist largely of thin-bedded to laminated organic-rich shales that on sedimentological grounds are thought to have been deposited in anaerobic environments, as discussed later in this report.

The OMZ assemblages are bathymetrically anomalous, however, for while they consist mainly of species from the upper bathyal and upper middle bathyal biofacies, their stratigraphic occurrence is often closely bracketed, above and below, by assemblages indicative of lower bathyal or lower middle bathyal depths. This situation can be interpreted in at least three ways. (1) The upper bathyal and upper middle bathyal assemblages were transported from shallower water into deeper water. This interpretation is supported by the common occurrence, in both the Twobar and Lambert Shales, of sandstone turbidites, indicating extensive redeposition of sediment. (2) Alternatively, the entire basin may have actually shoaled during deposition of the Twobar Shale and then again during deposition of the Lambert Shale to upper bathyal or upper middle bathyal depths. This requires rapid basin-wide tectonic "hiccups" that are not supported by independent evidence such as unconformities. (3) My preferred interpretation is that both the Twobar Shale and the Lambert Shale represent basin-wide anoxic events that were caused by the development of sills, at upper bathyal to upper middle bathyal depths, that partially blocked the deep circulation between the La Honda basin and the Pacific Ocean. Thus, the paleoceanographic conditions in the La Honda basin during the late Eocene and again during the early Miocene may have been analogous to conditions in some of the present-day silled basins of the southern California continental borderland, where the development of a sill within the oxygen minimum zone has resulted in anoxic bottom conditions throughout the entire water column, even to depths of 2000 m or more. This notion of at least two basin-wide anoxic events is further supported by the observation that both the Twobar and the Lambert shales are laterally extensive throughout the preserved part of the La Honda basin. The possible locations of these sills are discussed in a later section of this report.

To the best of my knowledge, the paleobathymetric maps in this report are the first ever prepared for the La Honda basin. However, several previous workers have made estimates of paleobathymetry, based on benthic foraminifers, for individual sections or small areas. In most cases, my inferred paleodepths agree with or are more specific than previous interpretations; for example, the Butano Sandstone, Rices Mudstone, and Vaqueros Sandstone are all interpreted simply as "bathyal" by Fairchild and others (1969) but as lower bathyal by me. In a few other cases, my interpretations differ substantially from previous ones. For example, the Rices Mudstone in Soquel Creek is interpreted as bathyal to outer neritic by Smith (1971), but as lower bathyal by me. Other examples of new or revised interpretations are discussed elsewhere in this report.

Biostratigraphy and Time Scale

Traditionally, in the Santa Cruz Mountains and the rest of the Coast Ranges, the ages of rock units are given in terms of the provincial benthic foraminiferal stages (Schenck and Kleinpell, 1936; Kleinpell,

1938; Mallory, 1959) or the provincial molluscan stages (Addicott, 1972). In general, the benthic foraminiferal stages are best developed and most useful in fine-grained clastic rocks deposited in the outer shelf and bathyal zones, while the molluscan stages are most useful in coarse-grained shelf deposits (Addicott, 1978).

The correlation of the provincial foraminiferal and molluscan stages with the European standard section and the absolute time scale is one of the long-standing problems of California geology (see Brabb and others, 1977, for a concise history). Recent advances in planktic biostratigraphy have allowed the direct correlation of a few sections in the Santa Cruz Mountains and elsewhere in the Coast Ranges with sections in Europe and with boreholes of the Deep Sea Drilling Project (see, for example, Bukry and others, 1977; Poore and Brabb, 1977; Warren and Newell, 1980). However, these advances have fanned a new controversy: several investigators have suggested that many, if not all, of the benthic foraminiferal stages are not good time-stratigraphic units, but are time-transgressive with respect to zonations based on planktic foraminifers and calcareous nannofossils (e.g., Ingle, 1973, 1980; Crouch and Bukry, 1979; Arnal, 1980; Poore, 1980). The planktic microfossils are assumed to be superior for long-distance correlation of different sedimentary basins because of the uniformity of surface waters over large areas of the world ocean (Addicott, 1980). On the other hand, the species assemblages that are the basis for the benthic foraminiferal stages are believed to be more strongly influenced by *local* environmental changes, especially climate. These benthic assemblages appear to have migrated north and south along the eastern margin of the North Pacific Ocean in response to major climatic events of the Cenozoic (Ingle, 1973).

The controversy over the validity of the benthic foraminiferal stages as time-stratigraphic units has not yet been resolved. Like it or not, benthic foraminifers remain the major correlation tool in the Santa Cruz Mountains and elsewhere in California for both practical and historical reasons. Benthic foraminifers occur throughout the Cenozoic section in abundance, whereas the occurrence of other microfossil groups is sporadic (Poore, 1980, p. C7). In addition, nearly 50 years of experience have shown that the benthic foraminiferal stages are of proven utility for short-range correlations. In the view of many West Coast micropaleontologists, benthic foraminiferal stages *within a single basin*--for example, the restored La Honda-San Joaquin basin--are probably good time-stratigraphic units, but correlations *between different basins* based on the benthic foraminiferal stages may be time-transgressive and therefore seriously in error, especially if the basins are separated by wide spans of latitude (J.C. Ingle, Stanford University, personal communication, 1979).

The time scale used in this thesis (Figure 9) is an attempt to take these issues into account. The correlation of the European standard section with the absolute time scale is from the most recently published version of the Exxon sea level curves (Vail and Hardenbol, 1979) and was used so that transgressive and regressive events in the La Honda basin could be compared with worldwide changes in sea level. The correlation of the California provincial benthic foraminiferal stages with the European standard section is modified from Ingle (1980) and incorporates some new information from the Santa Cruz Mountains and elsewhere in California (Poore, 1980; Warren and Newell, 1980; Poore and others, 1981). It appears that some of the benthic foraminiferal stage boundaries are more time-transgressive or more precisely dated than others, and this is implied by the variable slant of the stage boundaries in Figure 9.

The interpretations given in Figure 9 are based in large part on studies in the Santa Cruz Mountains. Planktic foraminifers and calcareous nannofossils are locally abundant in Ynezian and Narizian strata and indicate that the Ynezian is upper Paleocene and the Narizian is middle to upper Eocene (Berggren and Aubert, 1977; Haq, 1977; Poore and Brabb, 1977). In contrast, over 40 samples from Refugian and Zemorrian rocks have been processed for planktic microfossils but most have been barren or yielded only long-ranging species that span several zones (Bukry and others, 1977; Poore, unpublished data, 1981; Poore and Brabb, 1977; Warren and Newell, 1980). No planktic microfossils have been reported from Saucesian or Luisian strata in the Santa Cruz Mountains, and only one assemblage of questionable lower or middle Miocene nannofossils has been recovered from Relizian rocks (Bukry and others, 1977).

Figure 9. Time scale used in this thesis. Correlation of the European standard section with the radiometric scale is from Vail and Hardenbol (1979). Correlation of the California benthic foraminiferal stages with the European standard section is slightly modified from Ingle (1980) using data presented by Poore (1980), Warren and Newell (1980), and Poore and others (1981). The slant of the stage boundaries reflects their probable time-transgressive nature as well as uncertainties in age assignment. Some of the stage boundaries are more time-transgressive, or are less well dated, than others, as implied by the variable slant of the stage boundaries. Correlation of the California molluscan stages with the benthic foraminiferal stages is from Addicott (1972, 1978).

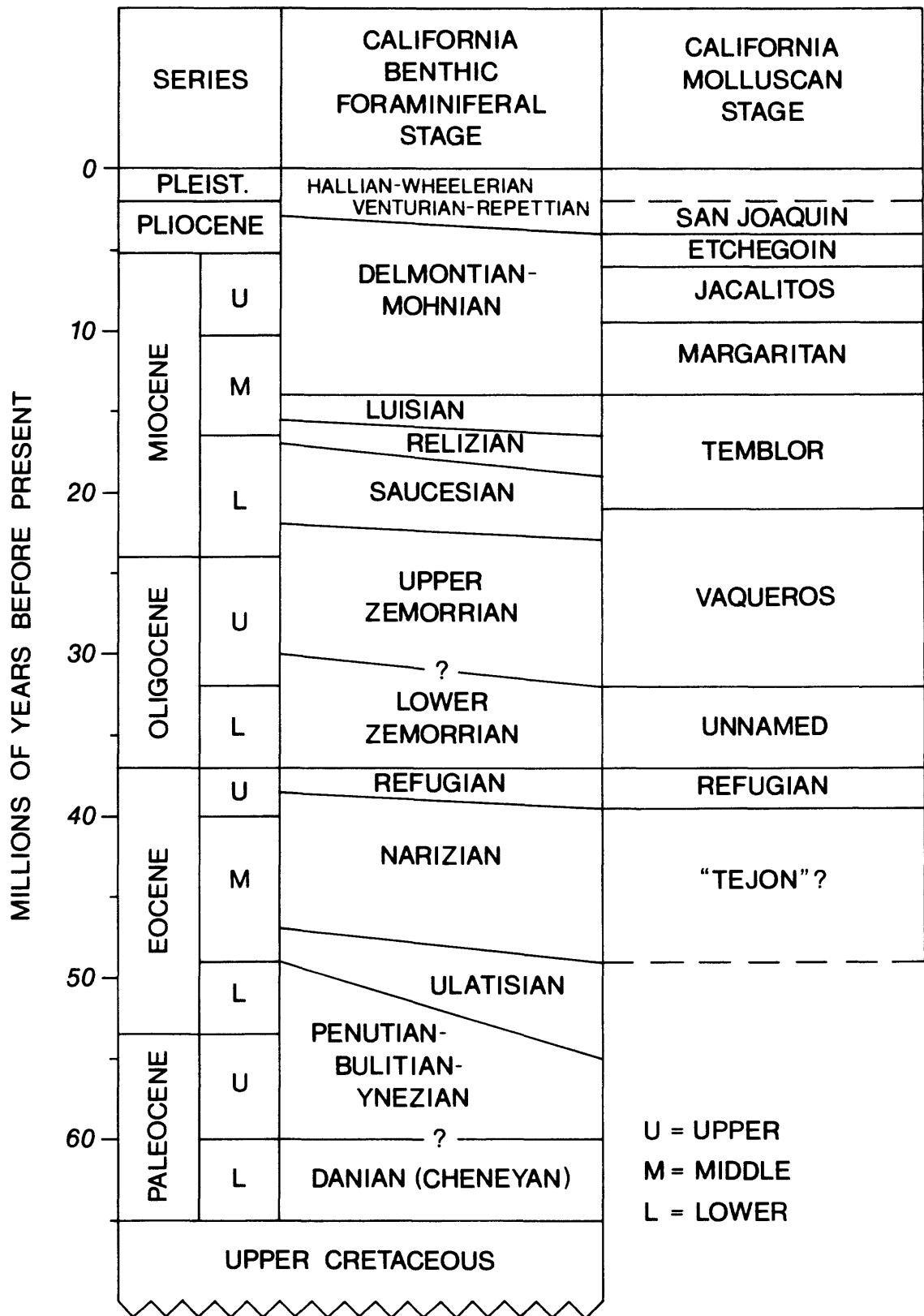
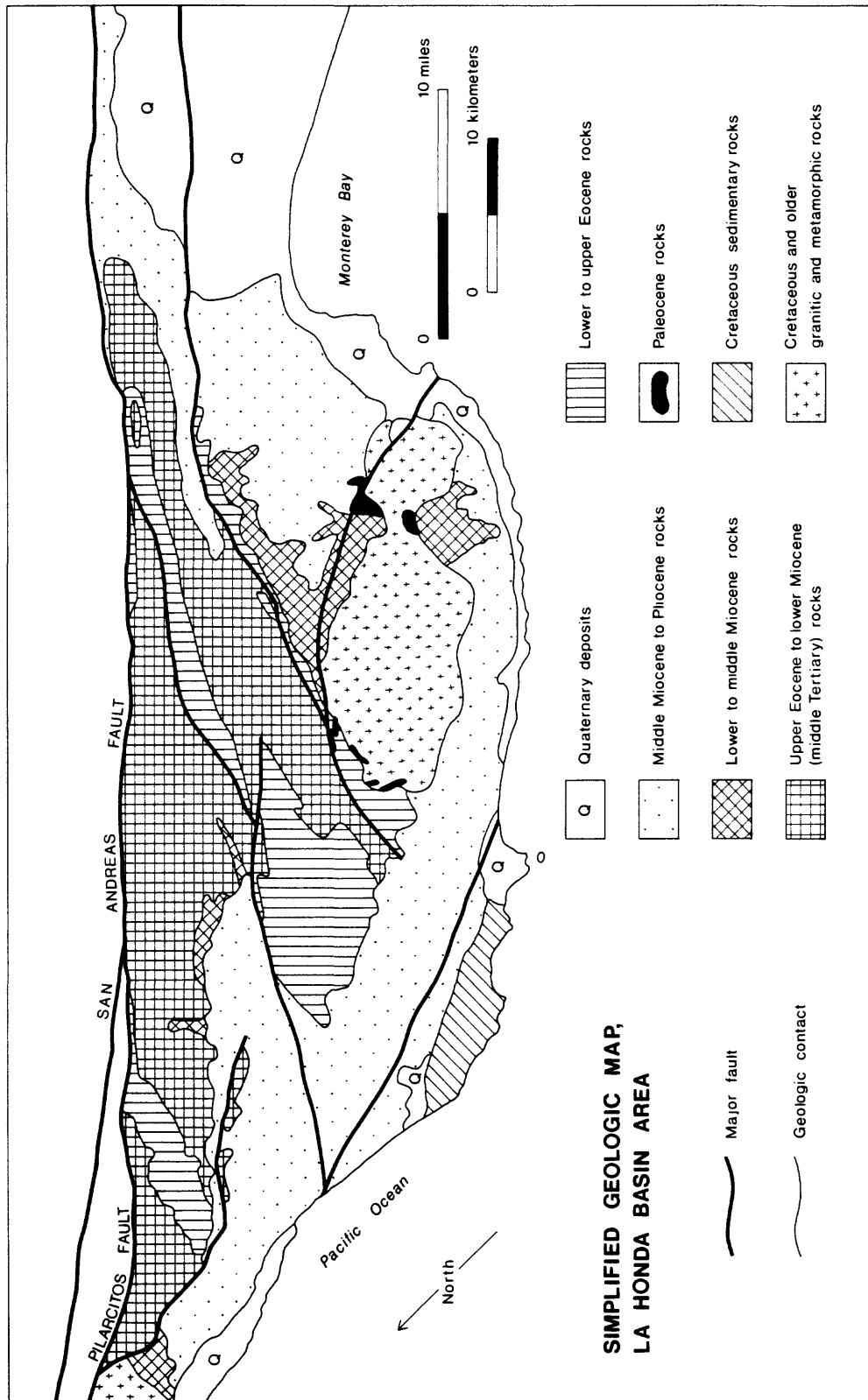


Figure 10. Simplified geologic map of the La Honda basin area, southwest of the San Andreas and Pilarcitos faults. Major faults shown as in Figure 5. Formations included in map units are as follows. Cretaceous sedimentary rocks: Pigeon Point Formation. Paleocene rocks: Locatelli Formation. Lower to upper Eocene rocks: Butano Sandstone, Twobar Shale. Upper Eocene to lower Miocene (middle Tertiary) rocks: Rices Mudstone, Vaqueros Sandstone, Zayante Sandstone, Mindego Basalt, Lambert Shale. Lower to middle Miocene rocks: Lompico Sandstone, Monterey Formation. Middle Miocene to Pliocene rocks: Santa Margarita Sandstone, Santa Cruz Mudstone, Purisima Formation. Map compiled from many sources, but mainly Brabb (1970), Dibblee and Brabb (1978a, 1978b, 1978c, 1980), and Dibblee and others (1978).



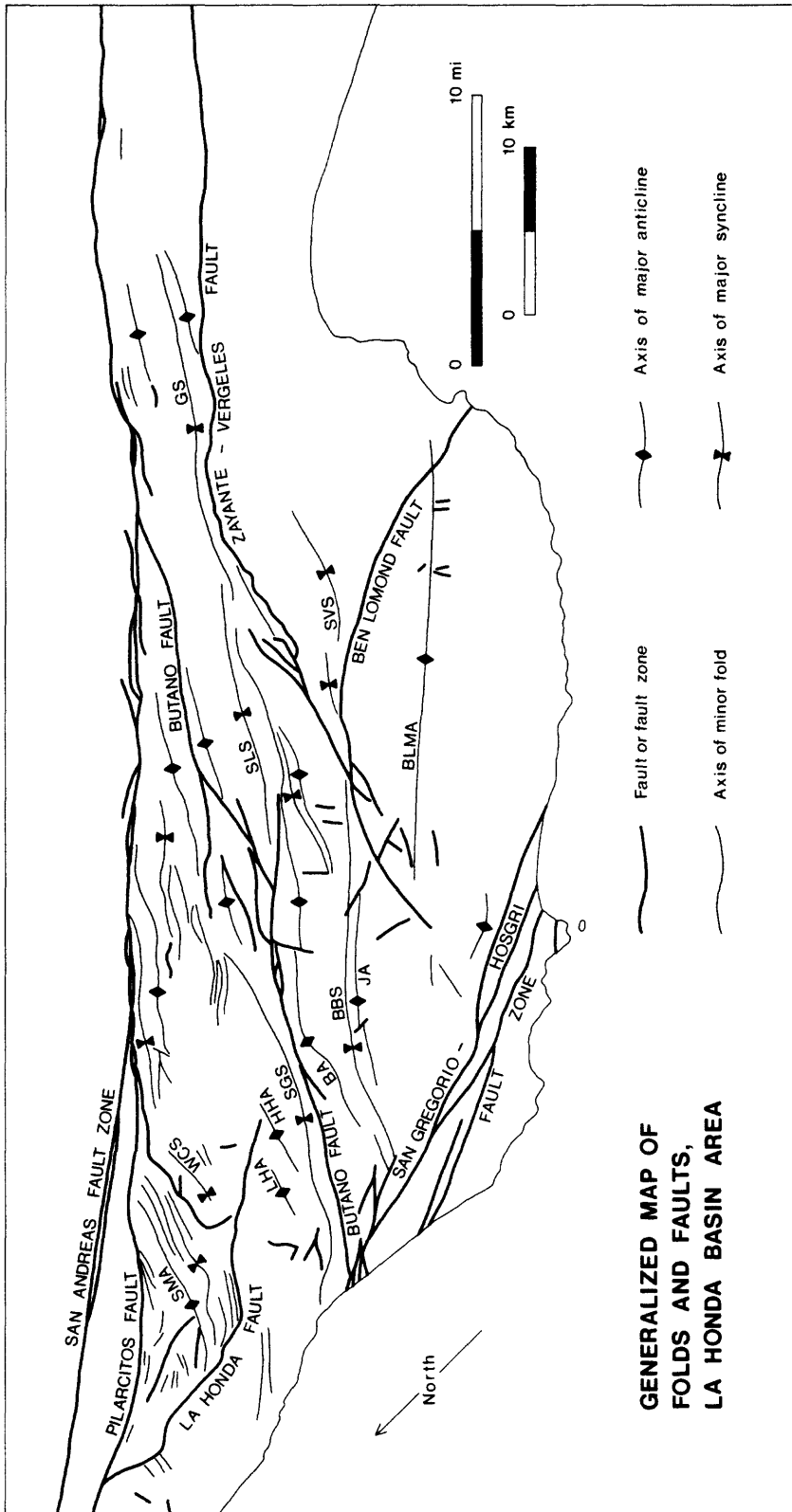


Figure 11. Generalized map of folds and faults in the La Honda basin area, southwest of the San Andreas and Pilarcitos faults. Major folds labeled as follows: BA = Butano anticline, BBS = Big Basin syncline, BLMA = Ben Lomond Mountain anticline, GS = Glenwood syncline, HHA = Haskin Hill anticline, JA = Johansen anticline, LHA = La Honda anticline, SGS = San Gregorio syncline, SLS = San Lorenzo syncline, SMA = Sierra Morena anticline, SVS = Scotts Valley syncline, WCS = Weeks Creek syncline. Map compiled from same references as Figure 10 with the addition of Weber and Lajoie (1980).

Additional stratigraphic control is provided by a few radiometric dates on volcanic rocks associated with age-diagnostic fossil assemblages. In Zayante Creek, a pillow basalt that occurs just a few meters below the biostratigraphic Zemorrian-Saucesian boundary gave a K-Ar date of 23.1 ± 0.7 m.y. (Turner, 1970; Clark and others, 1979). In Peters Creek, another basalt that is underlain and overlain by mudstones with upper Zemorrian faunas gave a K-Ar age of 19.7 ± 1.2 m.y., but this is regarded as a minimum age due to "incipient alteration of the dated plagioclase" (Turner, 1970).

The correlation of the lower Zemorrian-upper Zemorrian boundary with planktic zonations and the radiometric scale is uncertain. The tentative interpretation shown in Figure 9 is that of Warren and Newell (1980) who cautiously suggest--with numerous question marks--that this important boundary occurs within Zone P20 of the worldwide planktic foraminiferal zonation, dated at about 30 to 32 m.y.

In summary, the benthic foraminiferal stages in the La Honda basin can be correlated to the worldwide time scale with varying degrees of confidence. In general, the Narizian stage is middle to upper Eocene, the Refugian is entirely upper Eocene, the Zemorrian is Oligocene and lowermost Miocene, the Saucesian and Relizian are lower Miocene, and the Luisian is middle Miocene. These correlations are based on a few radiometric dates and scattered data on planktic microfossils from the Santa Cruz Mountains and elsewhere in California. Attempts to correlate geologic events in the La Honda basin with regional tectonics or worldwide changes in sea level must take these uncertainties into account.

GENERAL GEOLOGY OF THE LA HONDA BASIN

Limits of Study

This report discusses in some detail upper Eocene (Refugian) to lower Miocene (Saucesian) strata of the La Honda basin. Rocks older than Refugian and younger than Saucesian are also discussed, but in considerably less detail, so that later in this report the middle Tertiary history can be placed in the context of the overall evolution of the La Honda basin. Geographically, this report focuses on the central part of the La Honda basin, or roughly the area between the towns of La Honda and Corralitos (Figure 5). Much less attention is paid to the northwestern and southeastern extremes of the basin--the Woodside-Half Moon Bay and northern Gabilan areas, respectively--because outcrops in these areas are generally poor, biostratigraphic control is limited, and stratigraphic correlations with the central part of the basin are uncertain.

The entire La Honda basin has been mapped geologically by previous investigators, and I relied heavily on these maps in interpreting stratigraphy and structure. A compilation by Brabb (1970) served as my geologic base map in the northern and central parts of the basin (i.e., the area northwest of Highway 17). Maps by Dibblee and Brabb (1978b, 1980) and Dibblee and others (1978) guided my work in the southern area. Additional information was obtained from maps by Brabb (1980), Brabb and Dibblee (1979), Brabb and Pampeyan (1972), Clark (1966, 1970, 1981), Clark and Rietman (1973), Cummings and others (1962), Dibblee (1966), Dibblee and Brabb (1978a, 1978c), Stanley and McCaffrey (1983), and Weber and Lajoie (1980). Information from all the above maps was used to construct the simplified geologic and structure maps in Figures 10 and 11, as well as the formation distribution maps in Figures 16, 22, 32, 55, and 61.

Geologic investigations in the Santa Cruz Mountains have been hampered by complex structure and stratigraphy, poor outcrop, and difficult access. The warm and humid climate, with an annual rainfall of over 50 inches (125 cm) in places, has encouraged growth of an unusually thick cover of vegetation that hides outcrops and creates impenetrable brushy thickets. Deep weathering of the bedrock has created soil profiles that commonly are several meters thick. The heavy winter rains, combined with thick soils and steep topography, have caused landslides that have obscured or removed many outcrops. Good exposures are found in fresh headwall scarps of landslides and in fresh roadcuts, but where these outcrops occur on hillsides they are commonly out of place due to downhill creep of large coherent blocks. Failure to recognize such blocks can lead to incorrect interpretations of structure and stratigraphy. The best outcrops in the area are found along streams in the deep canyons, where running water has carved and

polished beautiful exposures in which sedimentary structures and other details are superbly displayed. Unfortunately, these stream outcrops come and go, as each winter new floods and landslides cover up old outcrops and create new ones. These processes ensure that there will be plenty of new field data gathered in the Santa Cruz Mountains for years to come. Finally, increasing urbanization of the area and the proliferation of fences and large dogs have made access to some sections difficult.

Structural Geology

Structural Blocks and Basement

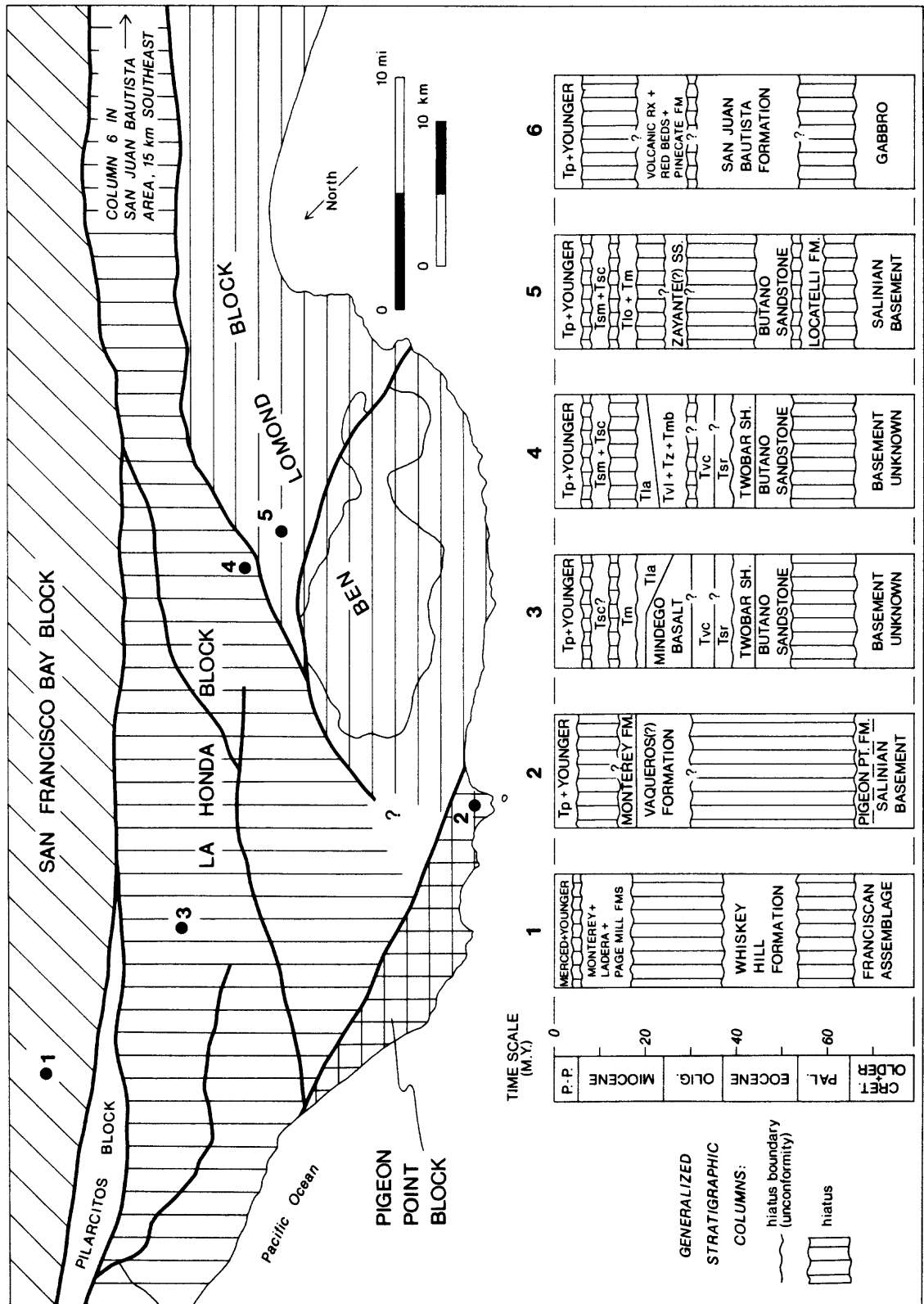
The Santa Cruz Mountains area is divided by major faults into a series of structural blocks that may be viewed as crustal slivers within the braided San Andreas fault system (Clark and Brabb, 1978; Nilsen and Brabb, 1979). Each fault-bounded block contains a stratigraphic section that differs from the sections on adjacent blocks (Figure 12). The present configuration of the blocks is due in large part to Neogene strike-slip faulting. For example, during the past 10 to 15 m.y., the San Francisco Bay block presumably has moved about 300 km relatively southeastward along the San Andreas fault before reaching its present location alongside the La Honda block. Similarly, the Pigeon Point block is believed to have arrived at its present position after 105 to 160 km of relatively northwestward movement along the right-lateral San Gregorio-Hosgri fault (Graham and Dickinson, 1978a, 1978b; Nagel and Mullins, 1983; Clark and others, 1984).

In contrast to these large-scale movements, the Ben Lomond and La Honda blocks are believed to have remained in about the same relative geographic position since at least the middle Eocene, although the history of movement along the Zayante-Vergeles fault which separates the two blocks is controversial (see discussion below). Together, the Ben Lomond and La Honda blocks form the structural underpinnings of the La Honda basin. It is important to note that Cenozoic strata on the Pigeon Point, San Francisco Bay, and probably the Pilarcitos, blocks are *not* part of the Tertiary La Honda basin; these blocks are newcomers to the area, having been brought there by relatively recent movements on the San Andreas and San Gregorio-Hosgri faults.

In most of central California, the San Andreas fault is the boundary between Franciscan basement on the east and Salinian granitic and metamorphic basement on the west. However, the distribution of basement rocks in the Santa Cruz Mountains is somewhat more complicated (Figure 12). The Franciscan Complex underlies both the San Francisco Bay and Pilarcitos blocks (Nilsen and Brabb, 1979); the latter occurrence suggests that the Pilarcitos fault may be an older, inactive trace of the San Andreas fault. The Pigeon Point block is believed to be underlain by Salinian granitic basement, on the basis of geophysical evidence (McCulloch and others, 1977; Howell and Joyce, 1981). The entire Ben Lomond block, including much of Monterey Bay, is underlain by Salinian granitic and metamorphic basement as shown by extensive outcrops on Ben Lomond Mountain, scattered outcrops elsewhere in the Santa Cruz area, and numerous well logs and geophysical data (Clark and Rietman, 1973; Ross and Brabb, 1973; Greene, 1977; Greene and Clark, 1979).

Beneath the La Honda block, however, the nature and distribution of the basement rocks are complex and largely unknown. At the northern tip of the block, Salinian granitic and metamorphic rocks crop out on Montara Mountain (Brabb and Pampeyan, 1972; Pampeyan, 1981). At the southern end of the La Honda block, near Logan and San Juan Bautista, the basement is a 156-m.y.-old gabbro (Ross, 1970, 1978). Between Logan and Montara Mountain, a linear distance of about 90 km, there are no basement outcrops and no wells have drilled deep enough to penetrate the basement. Various geophysical studies have suggested that this covered interval may be underlain by Salinian granitic and metamorphic basement (Clark and Rietman, 1973); gabbro similar to that exposed at Logan (Hanna and others, 1972; Ross, 1978); or rocks of the Franciscan Complex (Ross and Brabb, 1973; Olson and others, 1980). Knowledge of the nature of the basement is critical to understanding the evolution of the La Honda basin and the history of the Zayante-Vergeles fault. For example, differences in the basement and crustal structure beneath the La Honda and Ben Lomond blocks may help explain why the La Honda block subsided to receive 2 to 3 km of sediment during the middle Tertiary, while the adjacent granitic Ben

Figure 12. Fault-bounded blocks and representative stratigraphic columns in the La Honda basin area. The names and boundaries of the blocks are modified from Clark and Brabb (1978). Major faults are shown as in Figure 5. The Zayante-Vergeles fault probably continues westward and abuts against the San Gregorio-Hosgri fault, but this relationship has not yet been definitely established. Formation abbreviations are as in Table 2. Map and stratigraphic columns were compiled and slightly modified from the same references as Figure 10 with the addition of Beaulieu (1970), Brabb and others (1977), and Clark and Brabb (1978).



Lomond block remained structurally high and served as a sedimentary source area. Furthermore, if the La Honda block is underlain by Franciscan material as has been suggested, then the Zayante-Vergeles fault which separates the La Honda and Ben Lomond blocks must be a major strike-slip fault.

Patterns of Folding and Faulting

There are some significant differences in structural style between the Ben Lomond and La Honda blocks. The structure of the Ben Lomond block is characterized by broad, open folds and block faulting (see cross-sections of Greene, 1977; Clark and Rietman, 1973; and Clark, 1981). In contrast, the structure of the La Honda block is much more complex and characterized by a much greater degree of folding. The folds become tighter and of shorter wavelength near the San Andreas fault, and locally are overturned and nearly isoclinal (see cross-sections of Cummings and others, 1962; and Dibblee, 1966). The differences in structural style between the Ben Lomond and La Honda blocks probably reflect (1) the presence of shallow, rigid granitic basement beneath the Ben Lomond block, versus the more deeply buried--and possibly more ductile and non-granitic--basement of the La Honda block, and (2) the closer proximity of the La Honda block to the San Andreas fault.

Folds and faults in the Santa Cruz Mountains strike generally NW to WNW (Figure 11), a structural pattern that is typical of the central California Coast Ranges and is probably the result of Neogene wrench tectonism along the San Andreas and San Gregorio-Hosgri faults. The intensities of folding and faulting increase near these two major strike-slip faults (Cummings and others, 1962), further underscoring their dominant role in the Neogene structural evolution of the area. Wrench-related folding and faulting have probably occurred continuously throughout the Neogene in the Santa Cruz Mountains as in the San Joaquin Valley and elsewhere along the San Andreas system (Harding, 1976). Some of the major folds in the Santa Cruz Mountains--for example, the Scotts Valley, and Glenwood, and San Lorenzo synclines--are believed to record two or more periods of Neogene deformation because older strata are more strongly folded than younger strata in these structures (Clark, 1981).

Several pre-Neogene anticlinal structures occur in the subsurface in the La Honda-San Gregorio area but do not appear on the map in Figure 11 because they are covered by younger rocks--in particular, the upper Miocene to Pliocene Purisima Formation--and have little or no surface expression. Two of these buried anticlines produce oil from lower and middle Tertiary reservoirs in the La Honda and South La Honda fields (Figure 5; Table 1). Two other buried structures--the "San Gregorio high" and the "Tarwater Creek high"--are inferred from thickness data presented later in this report and probably were important Paleogene and early Neogene features.

Faults

The two biggest faults in the area--the San Andreas and San Gregorio-Hosgri--are strike-slip faults with very large lateral displacements, and their slip histories have been intensely studied. In contrast, surprisingly little is known about the slip histories of other faults in the Santa Cruz Mountains. The Pilarcitos fault is widely believed to be a right-lateral strike-slip fault, and perhaps an abandoned trace of the San Andreas or proto-San Andreas, but the amount of strike separation along it is unknown (Cummings and others, 1962; Graham and Dickinson, 1978b, p. 17; Dickinson and others, 1979, p. 1463). The Ben Lomond fault is a minor normal-slip(?) fault that was active during deposition of the Santa Margarita Sandstone in late Miocene time (Stanley and McCaffrey, 1983). The Butano fault consists of a collection of vertical to steeply-dipping, northwest-trending fractures that locally show very strong topographic expression. Dip separation on the Butano fault may be as much as 1800 m (Cummings and others, 1962), but the amount of strike separation is unknown, and little is known about the slip history of this fault. Similarly, little is known about the history of the La Honda fault; it may have been active during an interval of basaltic volcanism in the late Oligocene or early Miocene, as shown by variations in thickness and facies discussed later in this report.

Zayante-Vergeles Fault

The Zayante-Vergeles fault, which separates the Ben Lomond and La Honda blocks, is a complicated zone of northwest-trending and vertical to steeply-dipping fractures. The fault is a major structural boundary in the Santa Cruz Mountains and appears to have had a long and complicated history of movement. Unfortunately, the early and middle Tertiary history of the fault is poorly known because the record has been obscured by Neogene deformation.

Along the Zayante-Vergeles fault, dip separation of the base of the Tertiary section is believed to be about 2000 to 3000 m and down to the northeast, but this estimate may be in error because it is based in large part on gravity evidence and the presumption that the relatively downthrown La Honda block is underlain by granitic basement (Clark and Rietman, 1973). The amount of strike separation is unknown, and as a result the slip history of the fault is poorly understood and controversial. The fault was interpreted as mainly a dip-slip fault by Clark (1966, 1981) and Clark and Rietman (1973), who suggested that most of the 2000 to 3000 m of vertical displacement was accomplished in Oligocene and early Miocene time. However, the Zayante-Vergeles fault is subparallel to the San Andreas fault, suggesting that it may be a right-lateral strike-slip fault. In addition, the Zayante-Vergeles is vertical or nearly-vertical for most of its length, is laterally persistent for at least 90 km, and is generally linear but locally consists of a braided system of vertical fractures; these geometric features are typical of strike-slip faults in the California Coast Ranges, but atypical of normal-slip and reverse-slip faults. If the basement beneath the La Honda block is gabbro or Franciscan as has been suggested, then at some early time the Zayante-Vergeles fault must have been a major strike-slip fault with a minimum displacement equal to the length of the fault, or about 90 km. This early strike-slip motion, if it really occurred, probably ended prior to deposition of the lower to middle Eocene Butano Sandstone, because this unit occurs on both sides of the fault (Brabb, 1970; Nilsen, 1979).

During the Oligocene and early Miocene, the Zayante-Vergeles fault was active and strongly controlled patterns of sedimentation and volcanism in the La Honda basin, as noted by Clark and Rietman (1973) and discussed in detail in a later section of this report. Major movement on the fault must have occurred before deposition of the middle to upper Miocene Santa Margarita Sandstone, because the outcrop belt of this sandstone in the western Big Basin area strikes across the fault without noticeable offset (see geologic map of Brabb, 1970). Minor movements along the fault during the late Cenozoic have resulted in small offsets of units as young as Quaternary. The local presence of fault-related geomorphic features and the occurrence of small earthquakes along the fault suggest that it is an active fracture in the modern San Andreas system (Coppersmith, 1979).

Summary of Structural Geology

In summary, the structure of the Santa Cruz Mountains is dominated by folds and faults that trend generally to the northwest and are probably related to Neogene wrench tectonism along the San Andreas and San Gregorio-Hosgri faults. Tectonic deformation has occurred through much of the Tertiary, as shown by (1) numerous unconformities, both local and regional, (2) patterns of sedimentation along faults such as the Zayante-Vergeles and Ben Lomond that were active during deposition, (3) folds in which older strata are more strongly deformed than younger strata, and (4) buried anticlinal structures with little or no surface expression. The most recent period of major deformation began during the late Pliocene and has resulted in folding, faulting, and uplift of the modern Santa Cruz Mountains (Cummings and others, 1962). The timing and amounts of strike-slip displacement on several important faults in the area—including the La Honda, Butano, and Zayante-Vergeles—are largely unknown, and this lack of knowledge hampers the preparation of palinspastic paleogeographic maps, as well as paleotectonic interpretations.

NATURE OF THE STRATIGRAPHIC FILL

Introduction

The stratigraphy of the Santa Cruz Mountains was established early in this century by Haehl and Arnold (1904) and by Branner and others (1909). These early investigators made many astute observations and laid the necessary foundation for future studies, but they also were responsible for applying formation names borrowed from the Salinas Valley stratigraphic nomenclature, an unfortunate circumstance that has caused much confusion among succeeding generations of geologists. Subsequent work has shown that while formations such as the Vaqueros, the Monterey, and the Santa Margarita in the Santa Cruz Mountains are superficially similar in lithology to their identically-named counterparts in the Salinas Valley, there are also important differences in sedimentary facies, age, and stratigraphic relationships. As discussed later in this report, it appears that the La Honda and Salinas basins shared similar histories but were rarely if ever physically connected. Through most of the early and middle Tertiary the two basins evidently were separated by a major granitic island or peninsula--located in the present position of Monterey Bay--that served as a sedimentary source for both basins (Graham, 1976, 1978). Given the similarities in basin history and provenance, the use of Salinas Valley formation names in the Santa Cruz Mountains by the earliest investigators was very reasonable, although in hindsight it was confusing.

Following the pioneering work of Haehl and Arnold (1904) and Branner and others (1909), the stratigraphy of the Santa Cruz Mountains was substantially revised (and the Salinas Valley names retained) by a series of Ph.D. theses completed during the 1950s and 1960s at Stanford University. These studies were highly successful in using benthic foraminiferal biostratigraphy to make detailed correlations in this area of rapid lateral facies changes, complex structure, and patchy, discontinuous outcrops. The results of the Stanford studies are summarized in reports and maps by Cummings and others (1962), Brabb (1970), Brabb and others (1977), Clark and Brabb (1978), and Clark (1981), which are now the standard references on the stratigraphy of the area.

Stratigraphic Packaging and Nomenclature

The Tertiary rocks of the La Honda basin are here divided into five unconformity-bounded sequences (Figure 13) following a scheme modified from that of Brabb (1970) and Clark and Brabb (1978). Each sequence is bounded above and below by major unconformities of regional extent and is roughly equivalent to the concept of "depositional sequence" defined by Mitchum and others (1977). The sequences recognized here are the Paleocene, Eocene to lower Miocene, lower to middle Miocene, middle to upper Miocene, and upper Miocene to Pliocene. This packaging scheme provides a logical framework for discussion; however, it is somewhat arbitrary and may need future revision because some of the sequences also contain internal unconformities that may be regionally extensive.

The formation and unit names used in this report are from Brabb (1970) with minor changes and additions. Several new and informal stratigraphic units are named and described in later sections of this report. These include the "Blooms Creek sandstone" unit of the Rices Mudstone, and three subdivisions of the Vaqueros Sandstone of Brabb (1970). The "Laurel" and "Castle Rock" units of the Vaqueros Sandstone represent shelf and submarine fan depositional systems, respectively, and together with the Zayante Sandstone form a northward-thinning wedge of coarse sediment in the central part of the La Honda basin (Figure 14). The "Vaqueros Sandstone of the Woodside area" occurs only in the extreme northwestern corner of the basin and forms a southward-thinning wedge of coarse sediment that apparently is not physically connected to the wedge that comprises the Castle Rock and Laurel units (Figure 14).

Also recognized for the first time in this report is an inferred mid-Oligocene unconformity along the southwestern margin of the basin. This unconformity is discussed in the section on the Laurel unit of the Vaqueros Sandstone.

DEPOSITIONAL SEQUENCES AND FORMATIONS
OF THE LA HONDA BASIN

BRABB, 1970, AND CLARK AND BRABB, 1978		THIS REPORT	
UPPER MIOCENE TO PLIOCENE SEQUENCE	PURISIMA FORMATION SANTA CRUZ MUDSTONE SANTA MARGARITA SANDSTONE	PURISIMA FORMATION	UPPER MIOCENE TO PLIOCENE SEQUENCE
MIDDLE MIOCENE SEQUENCE	MONTEREY SHALE (OR MONTEREY FORMATION) LOMPICO SANDSTONE	SANTA CRUZ MUDSTONE SANTA MARGARITA SANDSTONE	MIDDLE TO UPPER MIOCENE SEQUENCE
EOCENE TO LOWER MIOCENE SEQUENCE	LAMBERT SHALE MINDEGO BASALT VAQUEROS SANDSTONE ZAYANTE SANDSTONE SAN LORENZO FORMATION: --RICES MUDSTONE MEMBER --TWOBAR SHALE MEMBER BUTANO SANDSTONE	LAMBERT SHALE MINDEGO BASALT ZAYANTE SANDSTONE VAQUEROS SANDSTONE OF THE WOODSIDE AREA VAQUEROS SANDSTONE: --LAUREL UNIT --CASTLE ROCK UNIT SAN LORENZO FORMATION: --RICES MUDSTONE MEMBER ----BLOOMS CREEK SANDSTONE --TWOBAR SHALE MEMBER BUTANO SANDSTONE	EOCENE TO LOWER MIOCENE SEQUENCE
PALEOCENE SEQUENCE	LOCATELLI FORMATION	LOCATELLI FORMATION	PALEOCENE SEQUENCE
SALINIAN BASEMENT.		SALINIAN BASEMENT ON BEN LOMOND BLOCK; BASEMENT UNKNOWN ON LA HONDA BLOCK.	

Figure 13. Depositional sequences and formations of the La Honda basin. The present report differs slightly from older reports in stratigraphic nomenclature and packaging. Wavy lines indicate nonconformities and angular unconformities of regional extent.

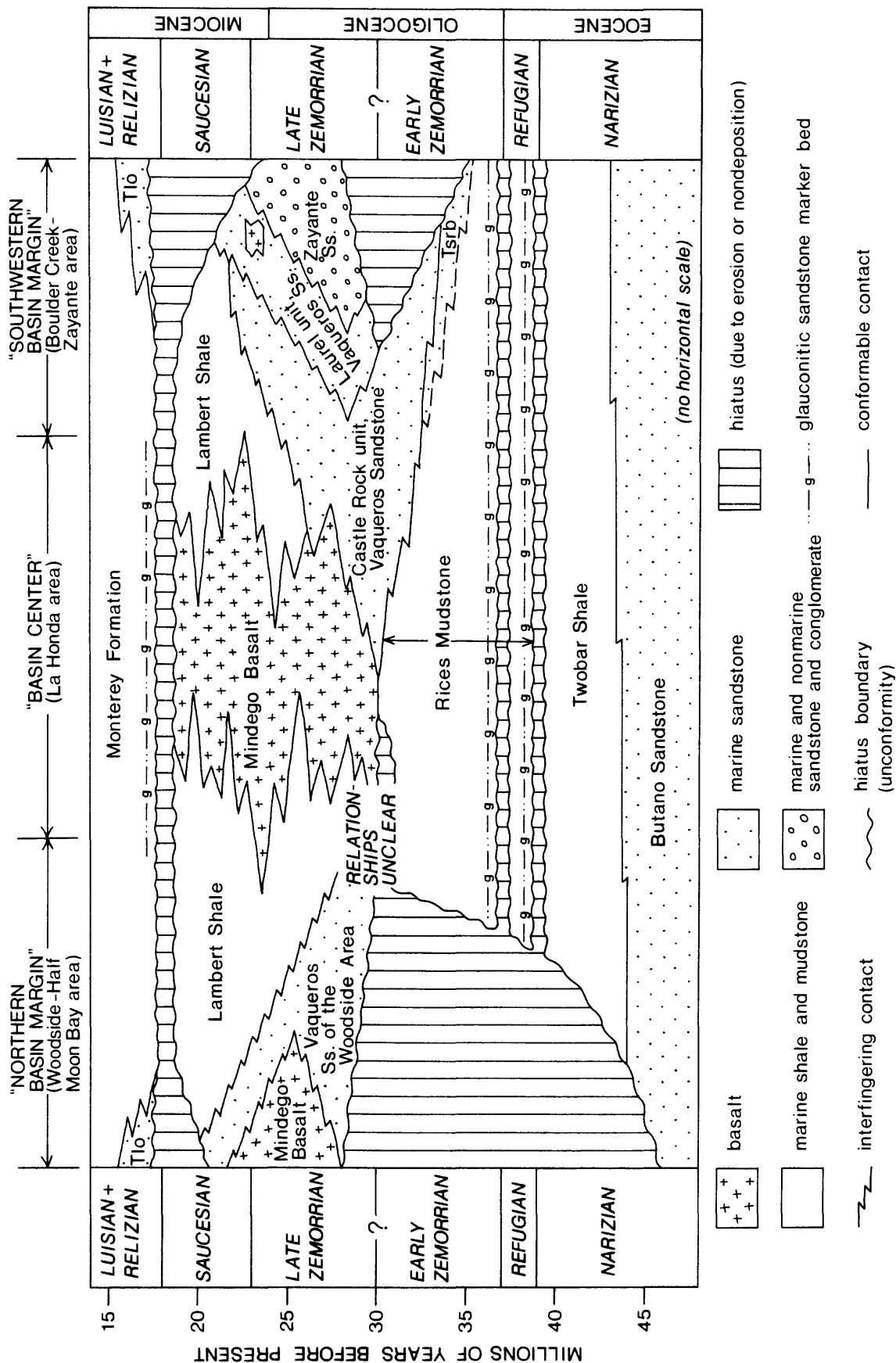
TABLE 2

FORMATION SYMBOLS USED IN THIS REPORT

Tp	Purissima Formation
Tsc	Santa Cruz Mudstone
Tsm	Santa Margarita Sandstone
Tm	Monterey Formation
Tlo	Lompico Sandstone
Tla	Lambert Shale
Tmb	Mindego Basalt
Tz	Zayante Sandstone
Tvw	Vaqueros Sandstone of the Woodside area
Tvl	Vaqueros Sandstone, Laurel unit
Tvc	Vaqueros Sandstone, Castle Rock unit
Tv	Vaqueros Sandstone, undivided
Tos	Lambert Shale and San Lorenzo Formation, undivided
Tsrb	Rices Mudstone, Blooms Creek sandstone
Tsr	Rices Mudstone, undivided
Tst	Twobar Shale
Tsl	San Lorenzo Formation, undivided (may include Rices Mudstone and/or Twobar Shale)
Tb	Butano Sandstone
Tsj	San Juan Bautista Formation
Tl	Locatelli Formation
R-S	Composite stratigraphic interval from base of Refugian Stage to top of Saucesian stage

Figure 14. Tentative middle Tertiary chronostratigraphic correlation chart along a north-south transect of the La Honda basin, inspired by similar charts presented by Vail and others (1977). Vertical axis is time (not thickness). Horizontal axis is map distance, but is not drawn at any particular scale. This diagram is an attempt to summarize the known and inferred stratigraphic relations in the area. Correlations of rock units to the absolute time scale are based primarily on fossil evidence, radiometric dates, and field relations, and secondarily on postulated relationships to eustatic and tectonic events as discussed in the text. Some of the indicated relations are highly speculative, e.g., the local unconformity at the base of the Mindego Basalt (Touring, 1959). Abbreviations are as follows: Tlo = Lompico Sandstone; Tsrbb = Blooms Creek sandstone of the Rices Mudstone.

LA HONDA BASIN: MIDDLE TERTIARY CHRONOSTRATIGRAPHIC CHART



Stratigraphy and Sedimentation

Each formation in the La Honda Basin is discussed below and interpreted in terms of its age, depositional systems, and significance to paleogeography. The main focus is on units of Refugian to Saucian age; other units are treated only briefly.

PALEOCENE SEQUENCE

Locatelli Formation

The Locatelli Formation consists of feldspathic (arkosic) sandstone, mudstone, and conglomerate that are exposed in small, discontinuous patches on Ben Lomond Mountain and in Henry Cowell Redwoods State Park (Figure 10). The Locatelli Formation was named by Brabb (1960, p. 13) for exposures on Vince Locatelli's ranch at the northern end of Ben Lomond Mountain. Brabb designated a type section along Tuck's Creek, a small tributary to Scott Creek.

The Locatelli Formation rests nonconformably on granitic basement rocks and is overlain unconformably by the Butano Sandstone (Brabb, 1960). The Locatelli is at least 305 m thick; its original thickness is unknown because the top of the formation is everywhere eroded.

The Locatelli Formation is of late Paleocene age, as shown by molluscs of the so-called "Martinez Stage" (Clark, 1966, 1981), benthic foraminifers of the Ynezian Stage (Brabb, 1960; Clark, 1966, 1981), planktic foraminifers of the upper Paleocene P4 to P5 Zones (Berggren and Aubert, 1977) and upper Paleocene discoasters of the NP 5 Zone (Haq, 1977). Based on these data and the time scale of Vail and Hardenbol (1979), the Locatelli Formation was deposited sometime between 59 and 54 m.y. ago.

The sedimentology of the Locatelli Formation has not been studied in detail, so the discussion here is based on the available literature and on my own limited field observations. There are substantial vertical and lateral variations in lithology in the Locatelli Formation. Near the intersection of Smith Grade and Empire Grade, and locally in Cowell Park, the lower part of the Locatelli consists mainly of bioturbated sandstone that contains abundant shallow-water molluscs, echinoids, and calcareous benthic foraminifers (Clark, 1966, 1968, 1981; Clark and others, 1979). This sandstone was probably deposited on a marine shelf (Clark, 1981). Gradationally overlying this shelf sandstone are siltstone and silty mudstone that contain abundant arenaceous foraminifers and may have been deposited at bathyal to abyssal depths (Clark, 1981). Thus, in the Smith Grade-Empire Grade and Cowell Park areas, the Locatelli Formation is a transgressive sequence that records rapid deepening.

In contrast, this just described basal fossiliferous shelf sandstone has not been reported from the Locatelli Formation at the northern end of Ben Lomond Mountain. Instead, in this northern area, the Locatelli Formation consists of the following lithologies. (1) Dark colored silty mudstones, although poorly exposed, contain benthic foraminiferal assemblages indicative of deposition at lower bathyal depths (Appendix 1). (2) Interbedded with these mudstones are thin to thick bedded, fine to medium grained sandstones that are commonly normally graded and exhibit partial to complete Bouma sequences, rip-up clasts, and sharp lower contacts; these are interpreted as turbidity current deposits. (3) Thick to very thick bedded, fine to coarse grained sandstones and pebbly sandstones are present locally; these exhibit both normal and reverse grading, plane to low-angle cross-laminations, sharp lower contacts, and amalgamated beds, and were probably deposited by large turbidity currents or other sediment gravity flow processes. (4) Pebble, cobble, and boulder conglomerates, composed of well-rounded granitic, metamorphic, and volcanic framework clasts in a sandy matrix, appear to fill large channels cut into the underlying finer-grained strata. (5) Pebbly mudstones, with rounded clasts of granitic and metamorphic rocks, are common in the type section and interpreted by me as debris-flow deposits. Based on these preliminary observations and interpretations, I infer that the Locatelli Formation on the northern end of Ben Lomond Mountain was deposited on the upper part of a submarine fan or slope. The thick to very thick bedded sandstones and conglomerates may represent channel-fill deposits, while the mudstones and thinner sandstone beds probably accumulated in the interchannel areas.

Shelf sandstones are present in the Smith Grade-Empire Grade and Cowell Park areas, but are absent from the northern end of Ben Lomond Mountain, suggesting that the Locatelli Formation was deposited in a basin that deepened to the north. This interpretation is supported by a single paleocurrent measurement, a flute cast at the base of a sandstone bed in Tuck's Creek with an azimuth of N38E and indicating flow to the northeast. The feldspathic mineralogy of the sandstones in the Locatelli Formation suggests derivation from a granitic source area, probably the Salinian block.

The Locatelli Formation has not been found in outcrop on the La Honda block, nor has it been positively identified anywhere in the subsurface. As a result, little is known about the stratigraphic relationships between the Locatelli Formation and other nearby Paleocene units, including the Carmelo Formation at Point Lobos, and the unnamed turbidite sequence at Point San Pedro. Paleogeographically, these three Paleocene units may represent three small, separate sedimentary basins in the early Tertiary continental borderland of central California (Nilsen and Yount, 1981). A fourth occurrence of Paleocene strata at Point Reyes may represent yet another borderland basin, or alternatively may be part of the Locatelli Formation that has been offset at least 100 km laterally by strike-slip movement on the San Gregorio-Hosgri fault (Graham and Dickinson, 1978b, p. 18).

EOCENE TO LOWER MIOCENE SEQUENCE

The stratigraphy of the Eocene to lower Miocene sequence is extremely complex owing to numerous unconformities and lateral facies changes. The schematic chronostratigraphic chart in Figure 14 summarizes my tentative interpretation of this complexity. Figure 14 is based on a synthesis of lithostratigraphic and biostratigraphic information compiled from the literature, and also on the correlations of available well logs with outcrop sections shown in Figure 15.

Within the Eocene to lower Miocene sequence, the original thickness of the middle Tertiary (Refugian + Zemorrian + Saucian) interval is impossible to determine because the top of the section is everywhere eroded and because there are several internal unconformities from which unknown thicknesses of strata are missing.

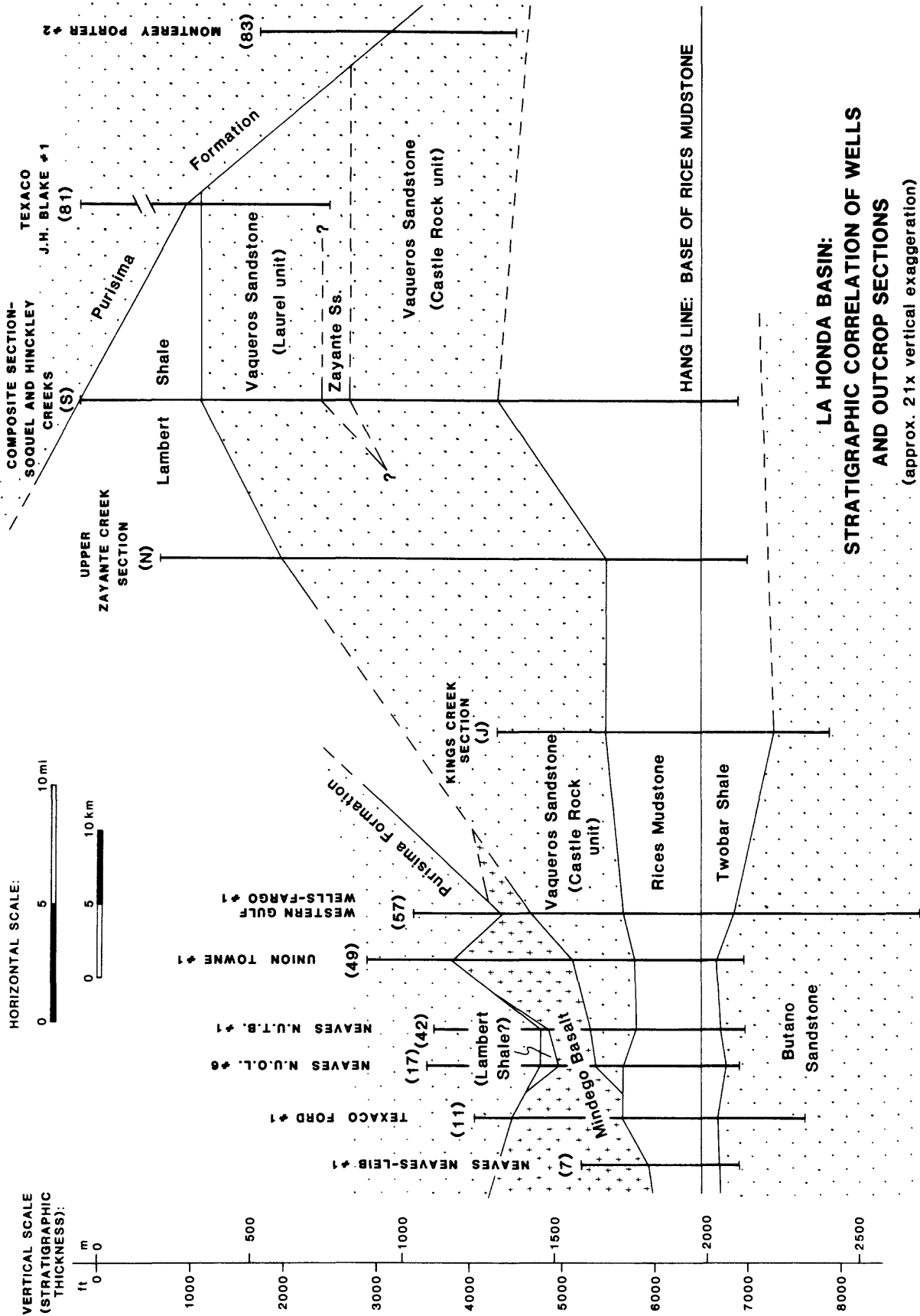
The situation is further complicated by lateral facies changes. The total of the maximum thicknesses of all five middle Tertiary formations is 5900 m, but owing to lateral facies changes there is no place in the basin where the middle Tertiary is that thick. My best estimates of the thickness of the middle Tertiary interval range from 2000 m in the Soquel Creek area to nearly 3000 m in the La Honda area (Appendices 3 and 4).

Butano Sandstone

The Butano Sandstone consists of interbedded feldspathic sandstone, mudstone, and conglomerate and represents part of an Eocene submarine fan (Nilsen, 1979). The Butano was named by Branner and others (1909) for exposures on Butano Ridge north of Big Basin, and a type section was designated by Cummings and others (1962) along Little Boulder Creek. Geographically, the Butano Sandstone is widely distributed in outcrop and in the subsurface in the Santa Cruz Mountains and is present on both the La Honda and Ben Lomond blocks. Modest amounts of petroleum have been produced from the Butano Sandstone in the La Honda and Oil Creek fields (Table 1; Figure 5; Fothergill, 1962a, 1962b).

On the Ben Lomond block, the Butano Sandstone rests nonconformably on granitic basement (Clark, 1968, p. 170) and unconformably on the Locatelli Formation (Cummings and others, 1962). On the La Honda block, however, the base of the Butano has never been observed, even in the deepest wells. The Butano is overlain conformably by the Twobar Shale (Cummings and others, 1962). No complete section of the Butano is exposed, so its total thickness is unknown. Its minimum thickness is at least 1500 m (Nelson and Nilsen, 1974), and it may be 3000 m thick or more (Appendix 3).

Figure 15. Stratigraphic correlation of wells and outcrop sections from northwest (left) to southeast (right) in the La Honda basin along the line shown in Figure 6. Wells numbered as in Appendix 4. Outcrop sections labeled as in Figure 6.



**LA HONDA BASIN:
STRATIGRAPHIC CORRELATION OF WELLS
AND OUTCROP SECTIONS**
(approx. 21x vertical exaggeration)

The Butano Sandstone is apparently of early to middle Eocene age. Benthic foraminifers are locally abundant and indicate that the Butano ranges in age from Bulitian(?) to Narizian, although most of the Butano seems to have accumulated during Narizian time (Appendix 1; Cummings and others, 1962; Nilsen and Simoni, 1973; Nilsen, 1979; Clark, 1966, 1981). The Butano has also yielded planktic foraminifers of the lower Eocene P8 and middle Eocene P13 to P14 Zones (Berggren and Aubert, 1977; Poore and Brabb, 1977), and calcareous nannofossils of the lower to middle Eocene NP 12 to NP 17 Zones (Haq, 1977; Warren and Newell, 1980). These data and the time scale of Vail and Hardenbol (1979) indicate that most of the Butano Sandstone accumulated between 52 and 44 m.y. ago.

Sedimentological studies by Tor Nilsen and his colleagues show that the Butano Sandstone was deposited by northward-flowing turbidity currents and other kinds of sediment gravity flows on a submarine fan (Nilsen and Simoni, 1973; Nelson and Nilsen, 1974; Nilsen, 1979). During deposition of the Butano, the La Honda basin was one of several deep and rapidly-subsiding basins in the early Tertiary continental borderland of central California (Nilsen and Clarke, 1975). The Butano Sandstone accumulated mainly at lower bathyal and possibly abyssal depths, according to benthic foraminiferal paleobathymetry (Appendix 1). Sediment deposited on the Butano fan was derived from an area of uplifted Salinian granitic rocks to the southwest of the La Honda basin; this source area was probably an island or peninsula located in the same position as the modern Monterey Bay. Sediments from this granitic source were transported directly across a narrow shelf and into deep water via at least two conglomerate-filled submarine channels (Nilsen and Simoni, 1973).

The northeastern part of the submarine fan has been truncated by 305 to 310 km of Neogene right-lateral movement on the San Andreas fault. The missing fan fragment is represented on the other side of the fault by the Point of Rocks Sandstone of the Temblor Range, west of Bakersfield (Clarke and Nilsen, 1973). The reconstructed Butano-Point of Rocks fan probably measured about 120 to 160 km long and 80 km wide (Nelson and Nilsen, 1974).

Twobar Shale

The Twobar Shale consists mainly of laminated clay-shale and mud-shale with minor amounts of bioturbated mudstone, turbidite sandstone, and calcareous concretions. The formation was named by Brabb (1964, p. 671) for exposures near Twobar Creek, but its type section is along Kings Creek (Figure 6).

On the La Honda block the Twobar Shale is widely distributed both in outcrop and in the subsurface (Figure 16). However, the formation is not present on the northern end of the La Honda block in the Woodside-Half Moon Bay area, nor does it occur on the Ben Lomond block. Presumably, the Twobar Shale was deposited in both these areas but removed by later erosion.

The Twobar Shale rests conformably on the Butano Sandstone. The Butano-Twobar contact is generally poorly exposed and has been variously described as abrupt (Brabb, 1964), gradational (Cummings and others, 1962; Clark, 1981, p. 13), and possibly interfingering (Beaulieu, 1970, p. 133 and p. 136). The Twobar Shale is overlain abruptly and disconformably by the Rices Mudstone (Brabb, 1960, 1964). This contact is marked by a glauconitic sandstone marker bed that occurs at the base of the Rices Mudstone and is traceable in outcrop and in the subsurface over much of the La Honda basin.

The original depositional thickness of the Twobar Shale is impossible to determine because the upper contact of the formation is everywhere a disconformity. An unknown but perhaps minor thickness of the formation was removed by erosion during the late Eocene prior to deposition of the overlying Rices Mudstone. Limited thickness data presented in Appendices 3 and 4 suggest that, at the beginning of deposition of the Rices Mudstone, the Twobar Shale was a sheetlike body between 50 m and 250 m thick that thickened gradually northeastward toward the San Andreas fault (Figure 17).

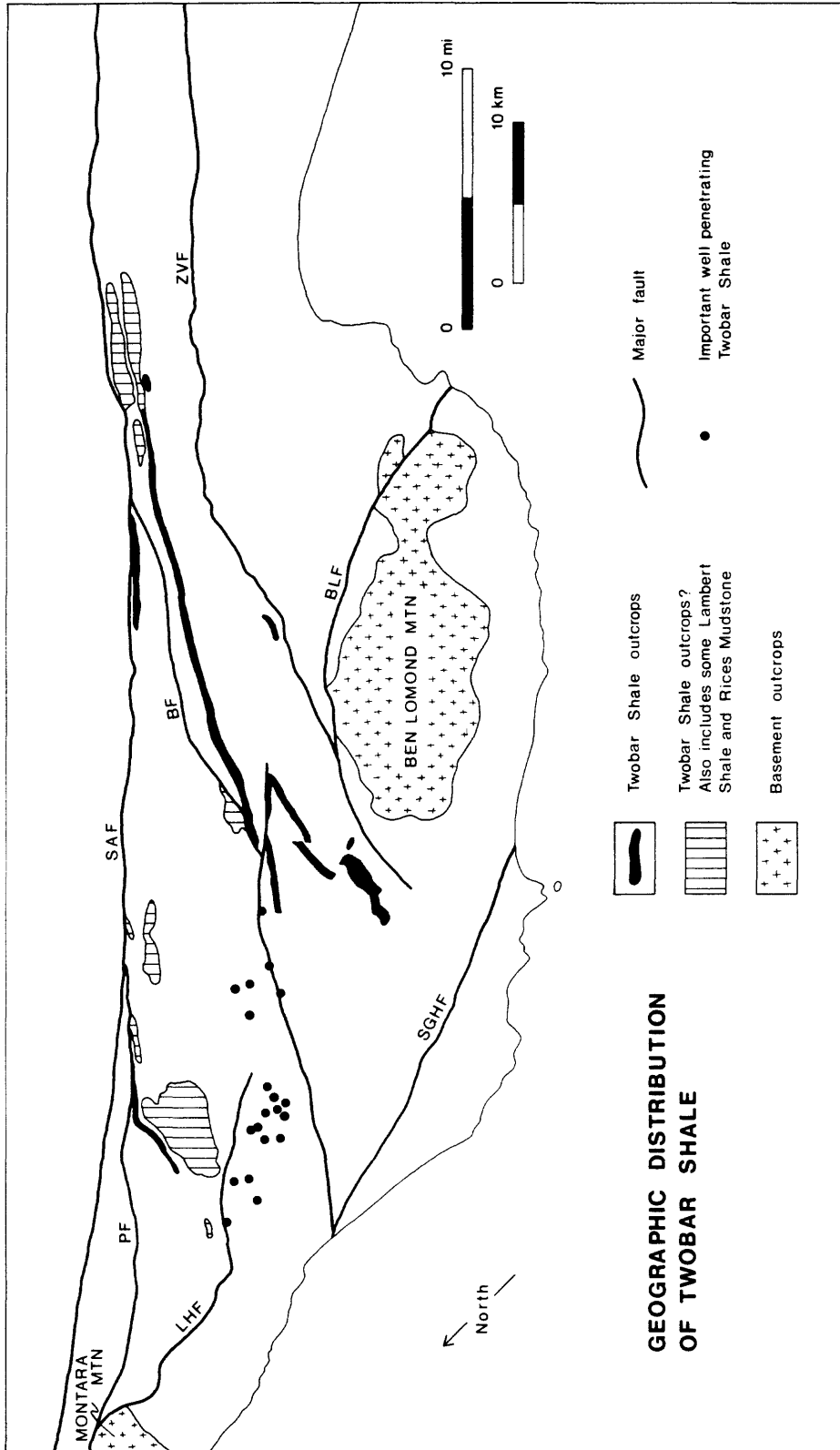


Figure 16. Map of the geographic distribution of the Two-Bar Shale in the La Honda basin. Major faults labeled as follows: BF = Butano fault, BLF = Ben Lomond fault, LHF = La Honda fault, PF = Pilarcitos fault, SAF = San Andreas fault, SGHF = San Gregorio-Hosgri fault, ZVF = Zayante-Vergeles fault.

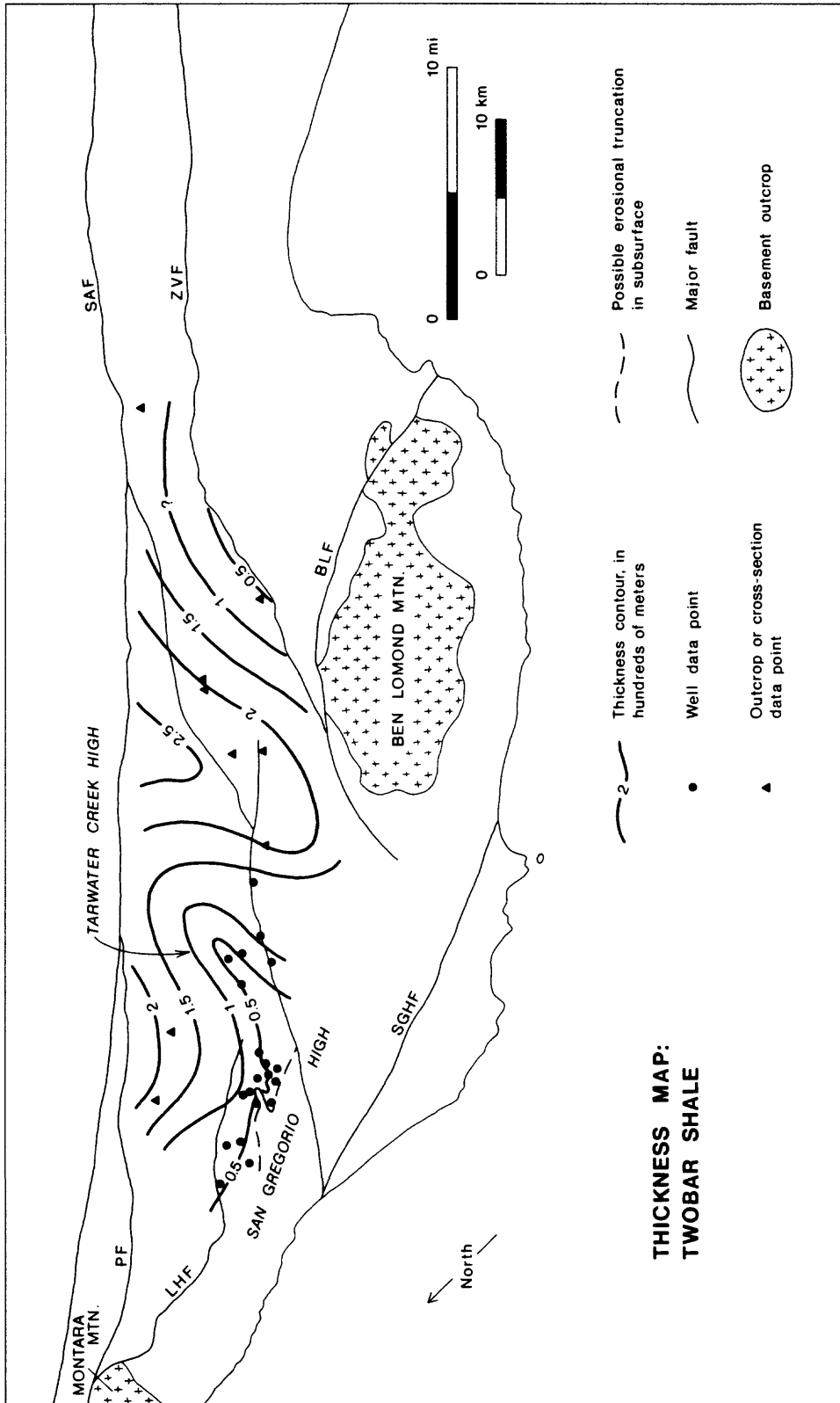


Figure 17. Map of the thickness of the Two-Bar Shale, based on data in Appendices 3 and 4. Major faults labeled as in Figure 16. The "Tarwater Creek high" and the "San Gregorio high" are areas of anomalous thinning that may have been structurally positive--i.e., areas that were uplifted, or that subsided less rapidly than the surrounding region--during middle to late Eocene deposition of the Two-Bar Shale.

Two other areas of anomalous thinning, both on the La Honda block, are interpreted by me as Eocene structural highs. The "Tarwater Creek high" (Figure 17) is an east-west trending feature that occurs in the subsurface southeast of La Honda. This structure persisted as a positive area through much of middle Tertiary time as shown by thickness maps of the Rices Mudstone and Vaqueros Sandstone (Figures 24 and 33). A second area of thinning of the Twobar Shale occurs in the subsurface west of La Honda and is inferred to represent depositional thinning and onlap of the Twobar Shale onto the eastern flank of a large feature herein named the "San Gregorio high." My subsurface data are insufficient to define the shape or lateral extent of the San Gregorio high, but I speculate that it is a north to northwest-trending structural salient that is probably bounded on the west by the San Gregorio-Hosgri fault. The San Gregorio high was a long-lived structure, for it is recognizable in thickness maps of the Rices Mudstone, Vaqueros Sandstone, and Mindego Basalt (Figures 24, 33, and 56). The San Gregorio high also was an important late Cenozoic feature, because less than 2 km west of the La Honda and South La Honda oil fields--on the presumed "top" of the high--the Twobar Shale is missing and the Butano Sandstone is overlain in angular unconformity by the upper Miocene to Pliocene Purisima Formation.

The Twobar Shale is of middle to late Eocene age as shown by locally abundant foraminifers of the Narizian Stage. The formation is mainly of late Narizian age (Cummings and others, 1962; Brabb, 1964; Smith, 1971) but in the San Lorenzo River section (Figure 19) the boundary between the upper and lower substages of the Narizian may fall in the lower part of the Twobar Shale (K. A. McDougall, unpublished report, 1979). The formation has also yielded planktic foraminifers of the middle to upper Eocene P14 to P16 Zones (Poore, 1977; Poore and Brabb, 1977; R. Z. Poore, unpublished data, 1978) and calcareous nannofossils of the middle to upper Eocene NP15 to NP20 Zones (Bukry and others, 1977; Haq, 1977; Warren and Newell, 1980). Using these data and the time scale of Vail and Hardenbol (1979), I infer that most of the Twobar Shale accumulated between 44 m.y. and 39 m.y. ago, during the late Narizian. The middle Eocene-upper Eocene boundary of international usage, dated at 40 m.y. by Vail and Hardenbol (1979), falls within the Twobar Shale but does not seem to be associated with any physical surface that can be observed in the field.

The sedimentology of the Twobar Shale has not been studied in detail, so the following discussion is based on the available literature and my own limited field observations. More than 90% of the formation is composed of dark brown to black, thin to very thin bedded, organic-rich clay-shale and mud-shale that splits readily parallel to planes of stratification (Figure 20). In most outcrops the shale is finely laminated on a millimeter scale, and the laminae are defined by aligned particles such as mica flakes, fish scales, foraminifers, and silt-size grains of quartz and feldspar. Cream-colored phosphatic nodules and laminae are common. Microfossils are abundant and include benthic and planktic foraminifers, diatoms, radiolarians, and calcareous nannofossils, although the relative proportions of these different kinds have not been determined (Brabb, 1960, 1964; Bukry and others, 1977). Megafossils are exceedingly rare, but a few bivalves and plant fragments have been reported (Brabb, 1964; Clark, 1981).

These shales were probably deposited in low-oxygen environments, as suggested by the ubiquitous laminations, high organic content, near-absence of megafossils, and abundance of phosphatic nodules and laminae. These features are common in low-oxygen muds in modern environments, and also in other inferred anoxic shales from the ancient record (Garrison, 1981; Pisciotto and Garrison, 1981; Soutar and others, 1981). In addition, many benthic foraminiferal assemblages from the Twobar Shale are dominated by common to abundant individuals of *Bulimina microcostata* Cushman and Parker, an extinct Paleogene species thought by Milam and Ingle (1982) to have had a special affinity for low-oxygen environments. The processes by which the low-oxygen muds were deposited are unknown, but by analogy with modern environments most of the fine sediment probably reached the sea floor as fecal pellets or by downslope movement of resuspended sediments (Garrison, 1981, p. 23).

The deepest-dwelling foraminiferal assemblages indicate that the shales were deposited at lower middle bathyal to lower bathyal and possibly abyssal depths (Appendix 1). The presence of abundant planktic foraminifers indicates that the surface waters in the basin were of normal marine salinity and connected directly to the open ocean (Sullivan, 1962; Brabb, 1964; Smith, 1971).

LITHOLOGIC SYMBOLS FOR STRATIGRAPHIC COLUMNS

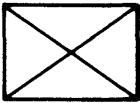
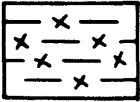
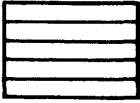

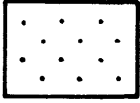
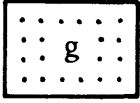
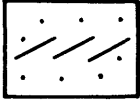
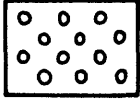
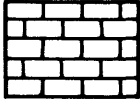
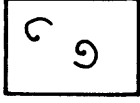
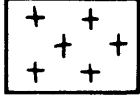
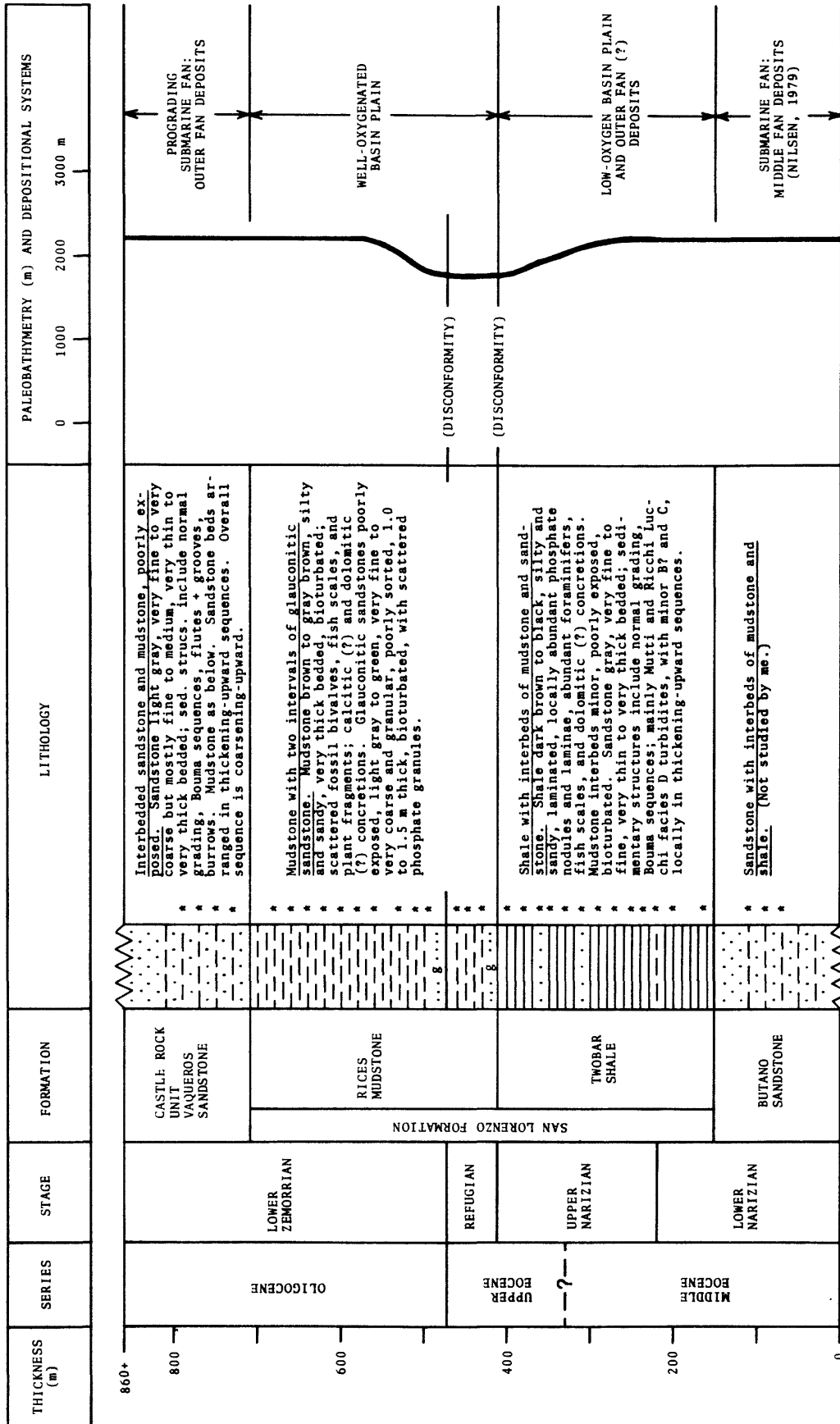
	COVER
	CHERT
	SHALE
	MUDSTONE AND SILTSTONE
	SANDSTONE
	GLAUCONITIC SANDSTONE
	CROSS-STRATIFIED SANDSTONE
	CONGLOMERATE
	LIMESTONE
	FOSSILS
	IGNEOUS ROCK

Figure 18. Lithologic symbols for stratigraphic columns in this report.

Figure 19. Inferred stratigraphy, paleobathymetry, and depositional systems for the San Lorenzo River section at Riverside Grove. See Figure 6 for location. Stratigraphic nomenclature and thicknesses modified from Brabb (1960) and Brabb and others (1977). Lithology shown schematically. The boundary between the middle Eocene and upper Eocene is based on planktic nannofossil data reported by Warren and Newell (1980). The boundary between the lower Narizian and upper Narizian is based on benthic foraminiferal data reported by K. A. McDougall (unpublished data, 1979). Paleontological sample locations are shown schematically; many more samples have been collected and processed but could not be shown at the scale of this figure.

SAN LORENZO RIVER SECTION AT RIVERSIDE GROVE



**=Paleontological sample location.

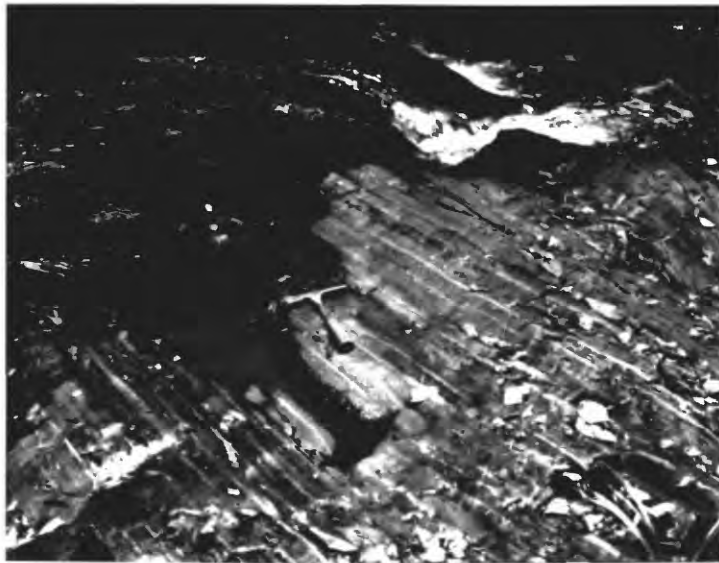


Figure 20. Outcrops of the Two-bar Shale along the San Lorenzo River north of San Lorenzo Park. Hammer handle in both photos is about 28 cm long. **Top:** Dark laminated shale with lighter-colored phosphate nodules and laminae dipping steeply to the left; light orange dolomitic concretion near stratigraphic top of outcrop. **Bottom:** Dark laminated shale with very thin to thin interbeds of lighter-colored sandstone interpreted as Mutti and Ricci Lucchi facies D turbidites. Beds dip steeply to right; stratigraphic top to right.

Thin to medium interbeds of massive, bioturbated mudstone occur sporadically and constitute less than 1% of the Twobar Shale. Individual burrows in these beds are poorly defined by color and textural mottling and generally are oriented parallel to or at a slight angle to stratification. No detailed study of the burrows has been made, however. The bioturbated beds probably represent brief episodes in which low-oxygen conditions abated and burrowing organisms could survive, by analogy with bioturbated intervals in cores from modern low-oxygen environments (Soutar and others, 1981).

Sandstone interbeds are scattered throughout the Twobar Shale and locally make up as much as 10% of the section (Brabb, 1964). The sandstones are feldspathic arenites and wackes that are similar in mineralogy to the underlying Butano Sandstone (Cummings and others, 1962). Most of the sandstones in the Twobar Shale are very fine to medium grained, moderately to well sorted, and normally graded. The beds are most commonly very thin to medium in thickness and laterally persistent. The lower contacts of the beds are generally sharp and planar, but sometimes irregular and marked by load casts, groove casts, and small scours. The upper contacts of most beds are abrupt, but in many cases are gradational into the overlying shale. Common sedimentary structures in these beds include plane lamination, ripple cross-lamination, convolute lamination, and small rip-up clasts of shale. The sandstone beds strongly resemble the facies D sandstones of Mutti and Ricci-Lucchi (1972) and were probably deposited by dilute, low-density turbidity currents. In most outcrops the sandstones in the Twobar Shale are not obviously arranged into thinning- or thickening-up sequences and therefore were probably deposited on a flat to very gently sloping basin plain, by analogy with the depositional models of Mutti and Ricci-Lucchi (1972), Rupke (1978), and Howell and Normark (1982).

Thick to very thick bedded, normally graded, medium to coarse sandstones also occur in the Twobar Shale but are volumetrically unimportant. Good exposures are in Soquel Creek, where these beds exhibit sharp, erosional lower contacts and gradational upper contacts. Most of these beds are massive, but faint parallel laminations, dish structures, rip-up clasts, and mud diapirs were noted in some. These beds resemble the facies B and facies C sandstones of Mutti and Ricci-Lucchi (1972) and may have been deposited by large turbidity currents or grain flows that spilled out onto the basin plain.

Cummings and others (1962) noted that sandstone interbeds in the Twobar Shale are thicker and more abundant to the west and south, suggesting that they were derived from the same southwestern source area as the turbidites in the underlying Butano Sandstone. However, this hypothesis should be tested by detailed paleocurrent studies.

The wide geographic distribution of the Twobar Shale (Figure 16) suggests that low-oxygen conditions prevailed throughout the La Honda basin, and not just along the basin margins, during late Narizian time. The causes of this basin-wide anoxic event are unknown, and may have involved complicated interactions of both tectonics and climate. The simplest explanation for a basin-wide anoxic event, based on analogy with modern and Neogene margin basins in central and southern California (e.g., Ingle, 1980), is that a sill formed across the connection between the La Honda basin and Pacific Ocean. This hypothetical sill, if it formed at the same depth as the oxygen minimum zone in the Pacific, would have caused low-oxygen conditions at depths greater than the "effective depth" of the sill in the La Honda basin. However, at depths shallower than this effective depth, free circulation of surface waters between the Pacific Ocean and the La Honda basin would have continued, and the normal marine character of plankton in the La Honda basin would have been preserved. In addition to sill formation, a general cooling of world climate during the middle and late Eocene may have led to increased upwelling and productivity along the California continental margin, resulting in thickening and intensification of the oxygen minimum zone (Milam and Ingle, 1982).

The conformable contact between the Butano Sandstone and the overlying Twobar Shale records a change from rapid deposition of coarse sediment to relatively slow hemipelagic deposition of fine-grained material. The reasons for this change are unknown, but may have involved any or all of the following. (1) A relative rise in sea level—due to tectonic subsidence, eustatic changes, or both—could have cut off the supply of coarse sediment to the basin by drowning the sediment source areas or by trapping the sediment in bays, estuaries, and deltas on the basin margins. (2) A change in climate—for example, a dramatic

reduction in rainfall--could have caused reduced rates of weathering, erosion, and sediment production in the source areas adjacent to the basin. (3) The transportation of coarse sediment to the basin may have been interrupted by a physical barrier, such as an uplifted area that blocked current flow, or a downdropped trough that trapped sand and gravel but not mud. (4) The sedimentary source area may have been reduced by erosion to a low-relief plain that no longer contributed sediment to the basin.

In summary, stratigraphic, sedimentologic, and paleontologic evidence suggest that the Twobar Shale was deposited at water depths of 1500 m or more in low-oxygen environments on a flat or very gently sloping basin plain. The Twobar Shale was deposited between 44 m.y. and 39 m.y. ago and records two major events in the history of the La Honda basin: (1) a basin-wide anoxic event, and (2) the cessation of coarse-sediment deposition on the Butano-Point of Rocks submarine fan. The coincidence in time of these two events suggests that they shared a common cause. I speculate that these two events were related to tectonic readjustments that accompanied the change from oblique subduction to normal subduction along the California margin about 42 m.y. ago (Carlson, 1982). The change in plate motions may have had local tectonic effects, perhaps including folding or block faulting to form a sill across the connection between the La Honda basin and Pacific Ocean and subsequent widespread anoxic conditions in the La Honda basin. The location of the sill is unknown; it may have been the San Gregorio high or another as-yet unidentified structural salient in the subsurface farther to the west.

With the end of oblique subduction along the California margin about 42 m.y. ago, wrench tectonism on the proto-San Andreas fault system probably ceased. The La Honda basin, which formed during the earlier interval of wrench tectonism, persisted as a deep-water basin following the change to normal subduction about 42 m.y. ago, but the wrench-related uplift of the granitic highlands adjacent to the basin probably came to a halt. These highlands, which formerly supplied abundant coarse sediment to the Butano-Point of Rocks submarine fan, were quickly eroded to a low-relief plain, and as a result, sedimentation in the La Honda basin changed from predominantly sand to predominantly mud. Thus, I infer that the Butano Sandstone-Twobar Shale contact may be roughly correlated with changes in local tectonic style that accompanied the shift from oblique subduction to normal subduction along the California continental margin during the late middle Eocene.

Palinspastic restoration of 305 to 310 km of right-lateral displacement along the San Andreas fault suggests that the Twobar Shale is the offset correlative of the Kreyenhagen Formation in the southern San Joaquin basin (Clarke and Nilsen, 1973). Like the Twobar Shale, the Kreyenhagen is of middle to late Eocene age and was deposited in low-oxygen environments at bathyal depths (Milam and Ingle, 1982).

Rices Mudstone

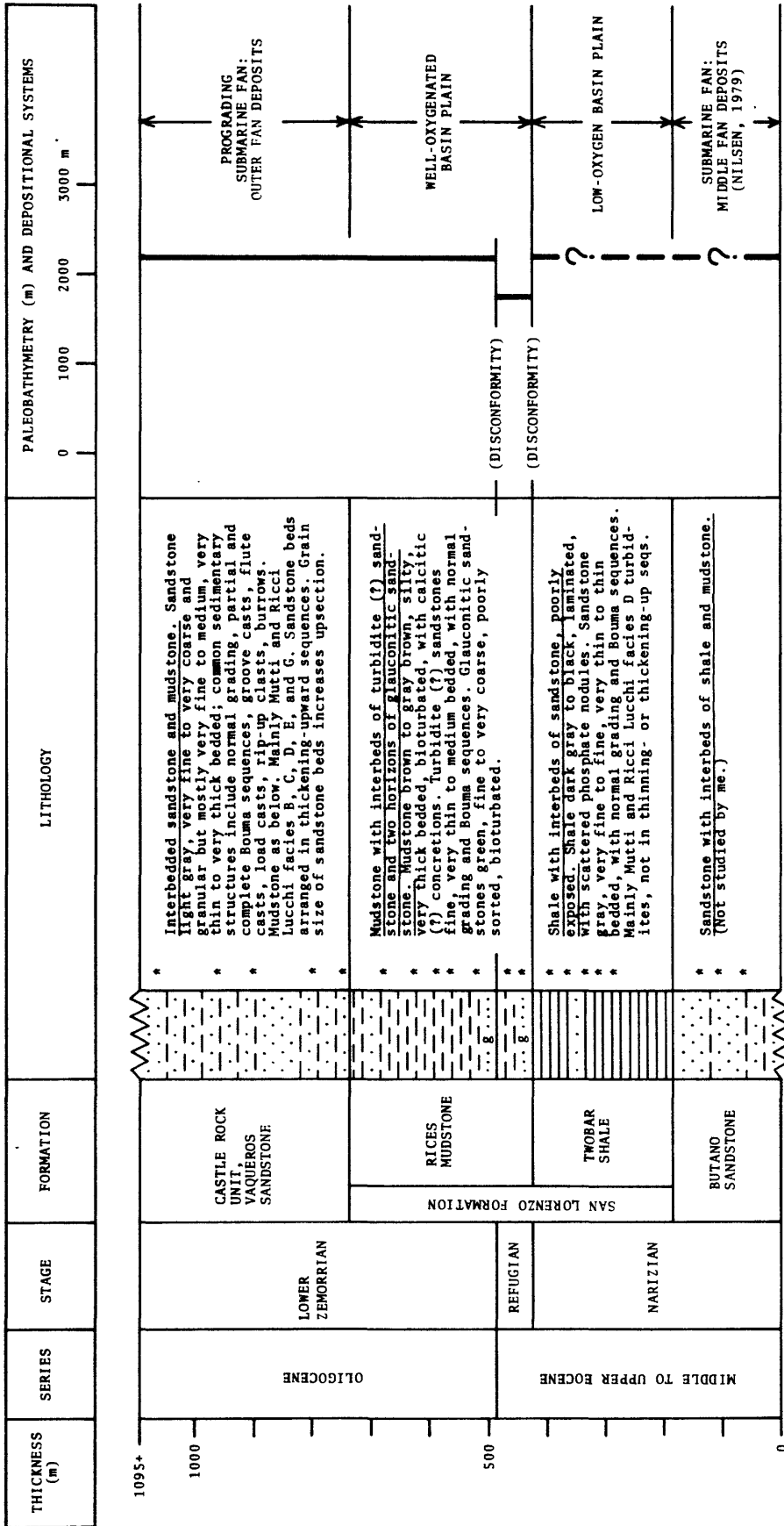
Introduction

The Rices Mudstone consists mainly of bioturbated mudstone, siltstone, and fine sandstone, with lesser amounts of turbidite sandstone and bioturbated glauconitic sandstone. The unit was named by Brabb (1960, 1964), who designated a type section along Kings Creek about 4 km north of "Rices Junction" (Figures 6, 21).

The Rices Mudstone is widely distributed both in outcrop and in the subsurface on the La Honda block (Figure 22). However, it is missing from the Woodside-Half Moon Bay area on the northern part of the La Honda block, and also from the entire Ben Lomond block. The formation was probably removed from these areas by middle Tertiary erosion, according to stratigraphic relations and paleoenvironmental interpretations discussed below.

During the 1979 to 1982 field seasons, the best exposed sections of the Rices Mudstone occurred along Soquel Creek (Figure 23) and along the San Lorenzo River at Riverside Grove (Figure 19). Good exposures of the "Blooms Creek sandstone" an informal unit introduced in this report for the convenience of discussion, were located in the Big Basin area along Blooms Creek and Kelly Creek (Figure 22) and in

KINGS CREEK SECTION



*-Paleontological sample location.

Figure 21. Inferred stratigraphy, paleobathymetry, and depositional systems for the Kings Creek section. See Figure 6 for location. Stratigraphic nomenclature and thicknesses modified from Brabb (1960) and Brabb and others (1977). Lithology shown schematically.

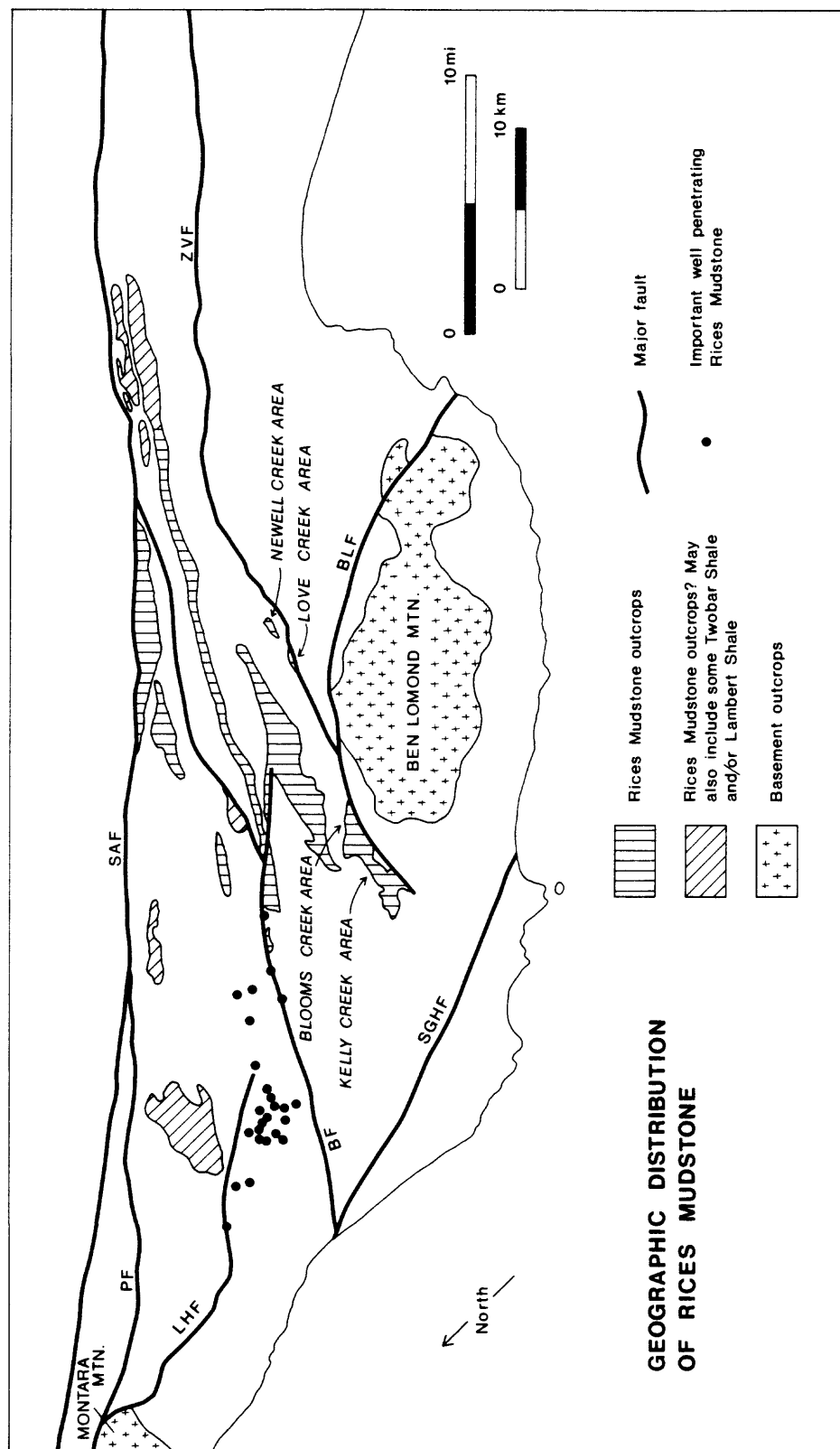
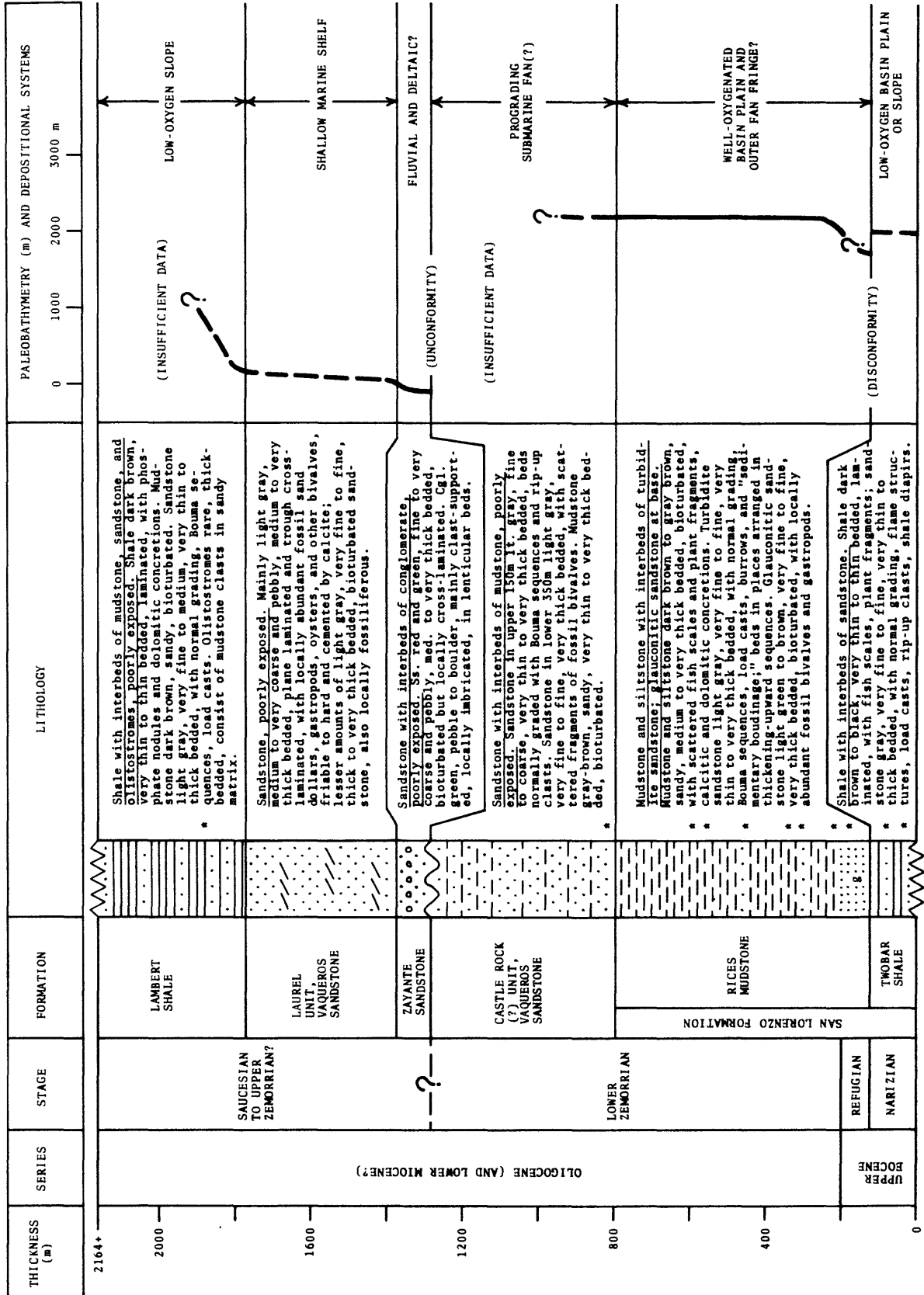


Figure 22. Map of the geographic distribution of the Rices Mudstone in the La Honda Basin. The "Blooms Creek sandstone," informally named in this report, is well exposed in the Blooms Creek and Kelly Creek areas, and similar rocks are reportedly present in the Love Creek and Newell Creek areas. Major faults are labeled as follows: BF = Butano fault, BLF = Ben Lomond fault, LHF = La Honda fault, PF = Pilarcitos fault, SAF = San Andreas fault, SGHF = San Gregorio-Hosgri fault, ZVF = Zayante-Vergeles fault.

Figure 23. Inferred stratigraphy, paleobathymetry, and depositional systems for the Soquel Creek-Hinckley Creek area. See Figure 6 for location. Stratigraphic nomenclature and thicknesses modified from Smith (1971) and Dibblee and others (1978). Lithology shown schematically. Lithologic descriptions of Twobar Shale, Rices Mudstone, and Zayante Sandstone based on field observations made along both Soquel and Hinckley creeks. Lithologic descriptions of Vaqueros Sandstone and Lambert Shale based mainly on field observations made along Hinckley Creek. Most of the paleontologic data are from Soquel Creek.

COMPOSITE SECTION: SOQUEL CREEK-HINKLEY CREEK AREA



*Paleontological sample location.

roadcuts along Highway 236 (Sec. 9-9S-3W) and Little Basin Road (Sec. 9-9S-3W).

Age and Stratigraphic Relations

The Rices Mudstone is of late Eocene to Oligocene age, as indicated by abundant Refugian and lower Zemorrian benthic foraminiferal assemblages (Brabb, 1960, 1964; Smith, 1971; K. A. McDougall, unpublished data, 1979) and sparse planktic microfossils. Refugian strata from the San Lorenzo River section at Riverside Grove (Figure 19) have yielded calcareous nannofossils tentatively assigned to the NP19-NP20 zones by Warren and Newell (1980). Lower Zemorrian strata from the San Lorenzo River section and from Mountain Charlie Gulch have yielded planktic foraminifers of the Oligocene P19-P20 zones and low-diversity assemblages of calcareous nannofossils of the Oligocene NP23-NP25 zones (Bukry and others, 1977; Poore, 1977 and 1980; Poore and Brabb, 1977; Warren and Newell, 1980). Based on these sparse data and the correlations in Figure 9, I infer that most of the Rices Mudstone was deposited about 39-30(?) m.y. ago.

The contact between the Rices Mudstone and the underlying Twobar Shale is a disconformity that coincides with the Narizian-Refugian stage boundary and is marked by a laterally extensive bed of glauconitic sandstone (Brabb, 1960, 1964). Higher up in the Rices Mudstone, a similar glauconitic sandstone marks the Refugian-Zemorrian stage boundary, which also appears to be a disconformity (Brabb, 1960, 1964); this important stratigraphic horizon apparently coincides with the Eocene-Oligocene boundary of international usage (Warren and Newell, 1980) which occurred about 37 m.y. ago (Vail and Hardenbol, 1979).

Over most of the La Honda basin, the Rices Mudstone is conformably overlain by the Castle Rock unit of the Vaqueros Sandstone. This contact has been previously described as gradational (Brabb, 1960, 1964; Cummings, 1960; Cummings and others, 1962). The contact was exposed in 1982 along Twobar Creek, Kings Creek, and along the San Lorenzo River near Paradise Park; in these areas, the contact is a transition over a few meters stratigraphically from a lower sequence of mudstone with few or no sandstone interbeds to an upper sequence of sandstone with numerous mudstone interbeds. On a regional scale, the upper part of the Rices Mudstone is laterally equivalent to the lower part of the Castle Rock unit of the Vaqueros Sandstone (Brabb, 1960, 1964). This lateral equivalence is particularly well displayed in the La Honda area, where electric log correlations by Touring (1959, his Plate 17) show that sandstone beds of the Vaqueros thin from south to north and eventually pinch out into the Rices Mudstone.

About 5 km north of La Honda, the Vaqueros Sandstone is missing and the Rices Mudstone is directly overlain by the Mindego Basalt (Figures 14, 15). In this area the Rices-Mindego contact is poorly exposed and controversial. In much of the La Honda quadrangle this contact is possibly a disconformity or slightly angular unconformity (Touring, 1959, p. 67) but in some places it may be conformable (Cummings and others, 1962, p. 193).

Locally, near the Zayante-Vergeles fault, the Rices Mudstone is reportedly overlain by the Zayante Sandstone. This contact was inferred to be conformable by Clark (1966, 1981) but it may be an unconformity, as discussed in the section of this report on the Zayante Sandstone.

Thickness

Patterns of thickening and thinning of the Rices Mudstone (Figure 24) are very similar to those of the underlying Twobar Shale (Figure 17). The Rices Mudstone thickens gradually to the northeast, away from the Ben Lomond block and toward the San Andreas fault. Stratigraphic relationships discussed earlier in this report suggest that at least part of this northeastward thickening is due to lateral facies changes; the upper part of the Rices Mudstone to the northeast was probably deposited at the same time as the lower part of the Castle Rock unit of the Vaqueros Sandstone to the southwest.

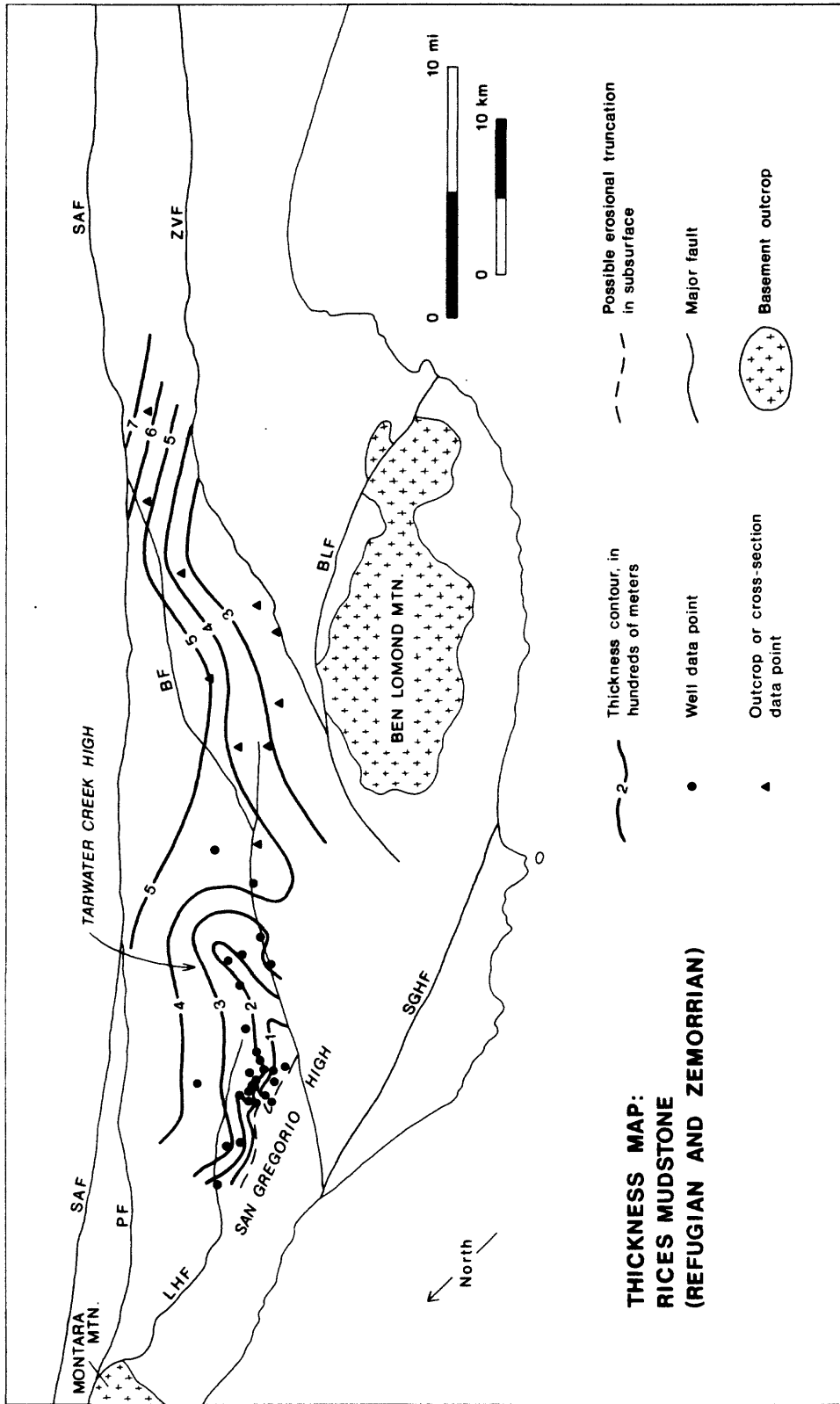


Figure 24. Map of the thickness of the Rices Mudstone, based on data in Appendices 3 and 4. The thickness shown is that of the entire formation, including both the Refugian and Zemorrian stages and the Blooms Creek sandstone. Major faults labeled as in Figure 22. The "Tarwater Creek high" and the "San Gregorio high" are areas of anomalous thinning that may have been structurally positive during the late Eocene and early Oligocene deposition of the Rices Mudstone.

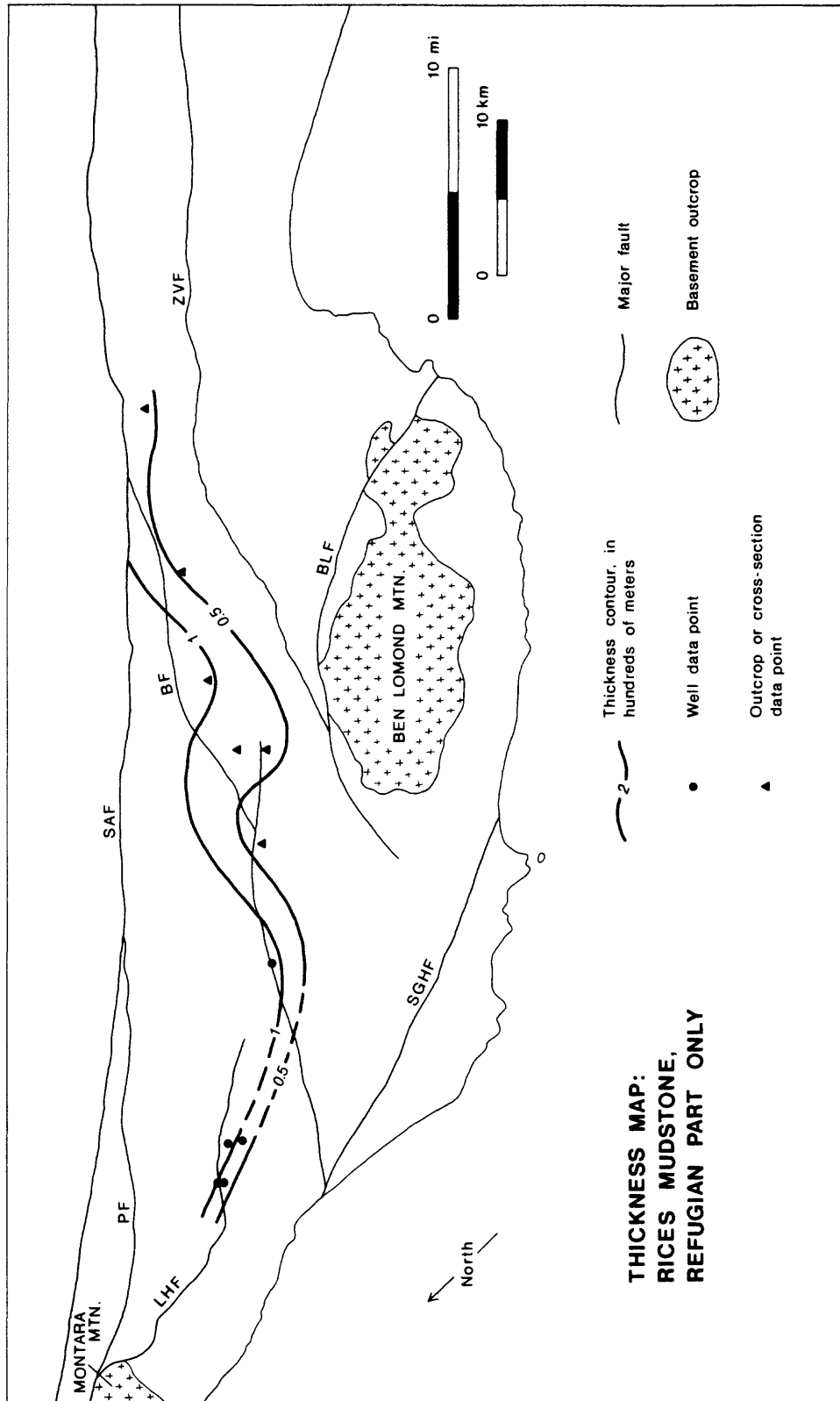


Figure 25. Map of the thickness of the Refugian part of the Rices Mudstone, based on data in Appendices 3 and 4. Major faults labeled as in Figure 22.

Near La Honda, the Rices Mudstone thins over the inferred Tarwater Creek high. The formation also thins westward onto the flank of the inferred San Gregorio high.

The Rices Mudstone is missing from the northern part of the La Honda block in the Woodside-Half Moon Bay area. Figure 24 shows an implied east-west truncation of north-trending thickness contours in this area. This truncation suggests that the Rices Mudstone was deposited in the Woodside-Half Moon Bay area and then removed by erosion, probably prior to deposition of the Vaqueros Sandstone in that area (Figure 14).

The Rices Mudstone is also missing from the area southwest of the Zayante-Vergeles fault, and from the crest of the inferred San Gregorio high. The pattern of thickness contours in Figure 24 suggests that the Rices Mudstone, if it ever was deposited in these areas, was thinner than over most of the rest of the La Honda basin.

Data on the thickness of the Refugian part of the Rices Mudstone are limited but show that the Refugian Stage in the La Honda basin thickens gradually to the northeast toward the San Andreas fault (Figure 25). In addition, these data suggest that Refugian strata are present in the subsurface in the area northwest of Big Basin. This interpretation differs from that of Brabb (1960, p. 50), who inferred on the basis of other data that Refugian strata were removed from this area by early Zemorrian erosion. However, paleontologic reports provided by Gulf Oil Co., Exxon USA, and Texaco USA show that Refugian faunas are present in several wells in the area, including the Western Gulf Wells Fargo #1 (Figure 26), the Humble Santa Cruz Lumber Co. #1 (Figure 27), and the Texaco Ford #1.

Lithology

The major categories of rocks in the Rices Mudstone, recognized mainly on the basis of field characteristics, are as follows: (1) bioturbated mudrocks, which comprise most of the formation; (2) bioturbated sandstones, which occur as interbeds throughout the formation but make up 90% or more of the unit in the Blooms Creek and Kelly Creek areas; (3) turbidite sandstones; and (4) glauconitic sandstones. The latter two categories make up less than 5% of the formation.

Bioturbated mudrocks. --

Mudrocks in the Rices Mudstone range from claystone to siltstone, but mudstone is the most common. In outcrop these different mudrocks grade almost imperceptibly from one to another and into the bioturbated sandstones described below.

Most mudrocks are gray brown to brown on fresh surfaces. Thin-sections show that the mudrocks consist chiefly of angular grains of silt and fine sand in a light brown argillaceous matrix. Most of the silt and sand grains are quartz and feldspar, but biotite, muscovite, chlorite, hematite, and glauconite are also common as detrital grains. Microfossils are abundant and include foraminifers, fish fragments, echinoid spines, and sponge spicules; radiolarians, diatoms, and calcareous nannofossils are also present but are much less numerous (Brabb, 1960). Megafossils are common in some outcrops and include many species of bivalves and gastropods as well as plant fragments (Arnold, 1908; Brabb, 1960). Tellinid bivalves are particularly common and occur as articulated shells and disarticulated valves scattered at random orientations in the mudrocks.

In most outcrops the mudrocks are apparently unstratified or only crudely stratified, with bedding poorly defined by elongate concretions or by subtle variations in resistance to weathering. Sedimentary structures are difficult to observe due to the chippy and spheroidal weathering of most outcrops, and perhaps as a result the mudrocks have been described in the past as "massive" (e.g., Brabb, 1960, 1964). However, detailed observation of dozens of water-polished outcrops and sawn slabs show that virtually all of the seemingly "massive" mudrocks are bioturbated (Figure 28), an important feature that has not been

WESTERN GULF WELLS FARGO NO. 1 WELL

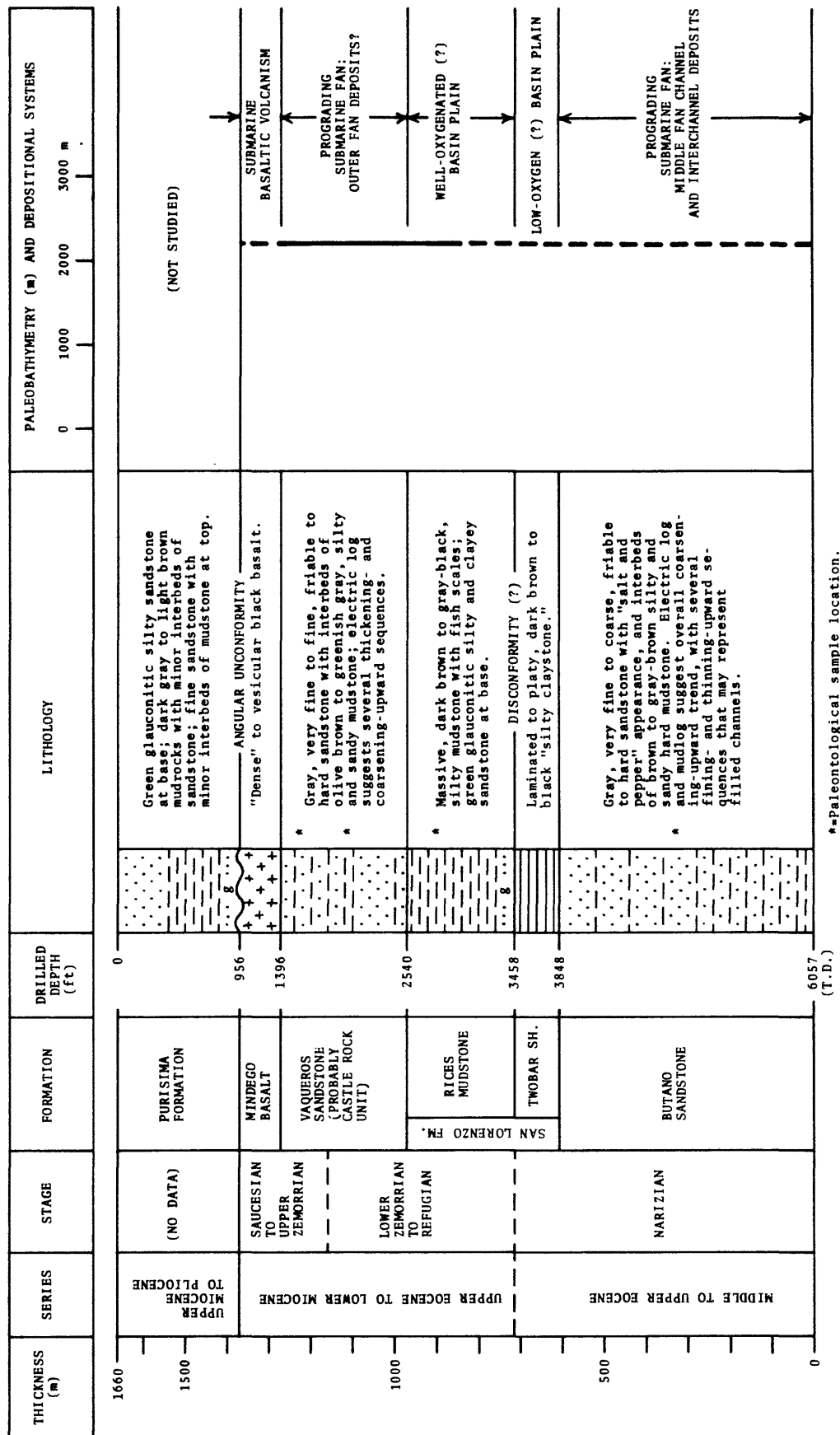


Figure 26. Inferred stratigraphy, paleobathymetry, and depositional systems for the Western Gulf Wells Fargo #1 well. See Figure 6 for location. Interpretations are based on electric logs, mudlog, core descriptions, paleontologic reports, and dipmeter data kindly provided by Gulf Oil Co. Thickness shown is "true" stratigraphic thickness, calculated using available dipmeter results and drilled intervals from electric logs.

HUMBLE SANTA CRUZ LUMBER NO. 1 WELL

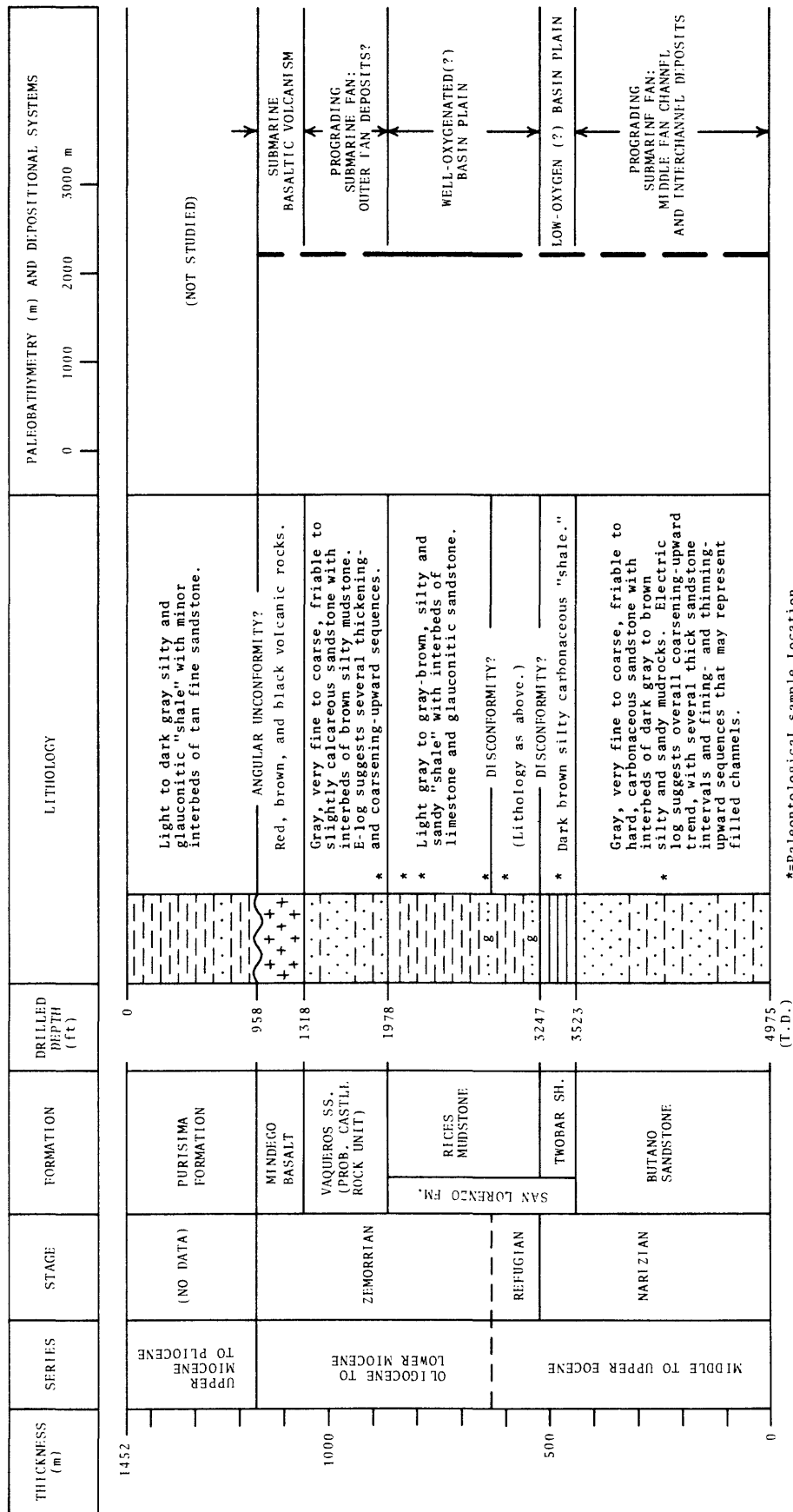


Figure 27. Inferred stratigraphy, paleobathymetry, and depositional systems for the Humble Santa Cruz Lumber Co. #1 well. See Figure 6 for location. Interpretations are based on electric logs, core descriptions, and paleontologic reports kindly provided by Exxon Co., USA. Thickness shown is "true" stratigraphic thickness, calculated using available dipmeter results and drilled intervals from electric logs.

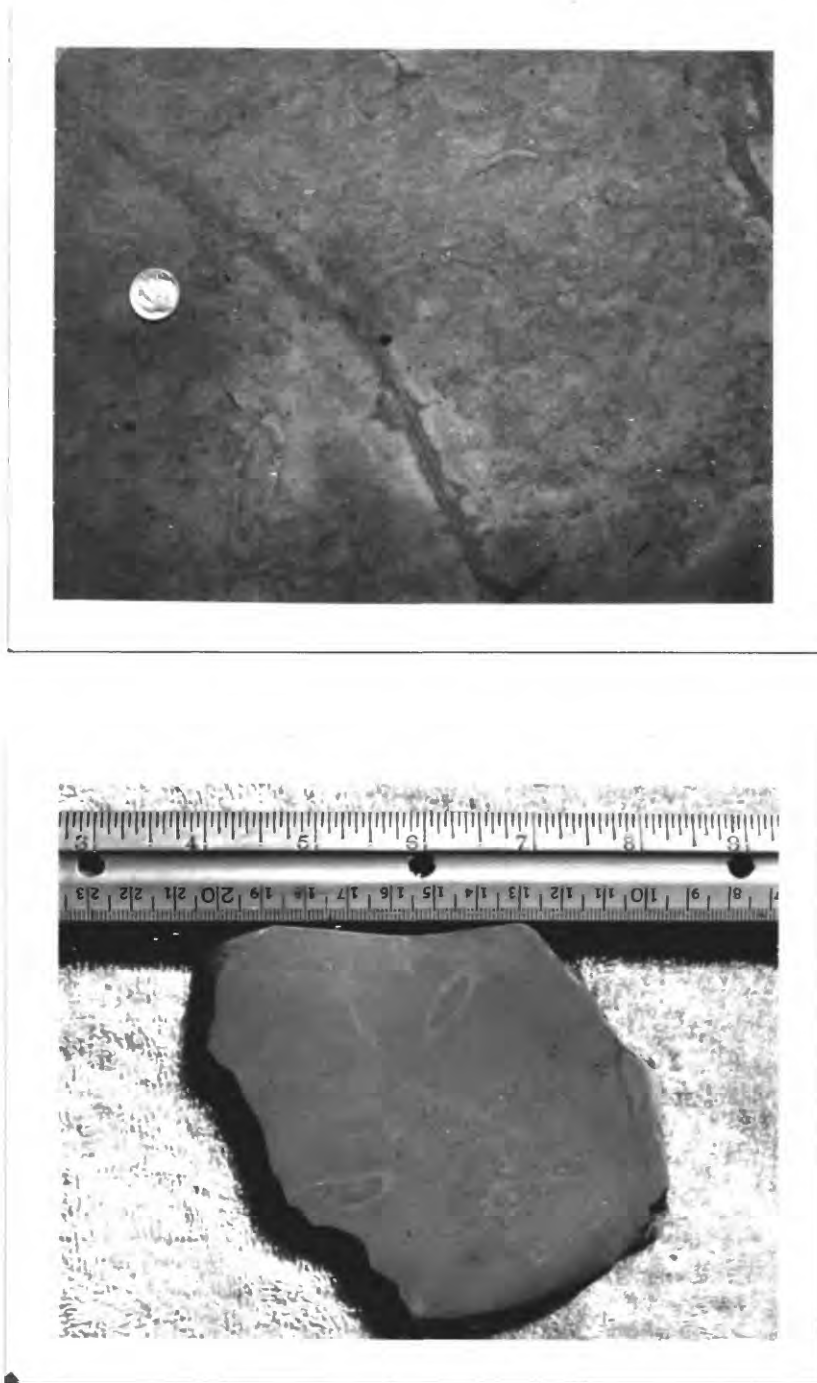


Figure 28. Bioturbated mudrocks of the Rices Mudstone. Top: Outcrop of bioturbated siltstone cemented by calcite, near the base of the Corralitos Creek section (Figure 38). Bottom: Sawn slab of bioturbated mudstone, from along the San Lorenzo River near Riverside Grove. Scale in inches and centimeters.

noted previously in the literature. Individual burrows, where distinct, are defined by textural and color mottling; they are generally oriented parallel or subparallel to stratification, but some burrows are at high angles to stratification. I made no detailed study of the trace fossils, but by comparing sawn slabs with illustrations in Chamberlain (1978) I was able to tentatively identify *Helminthoida*, *Planolites*, *Teichichnus*, "rind burrows," "halo burrows," and possible *Chondrites* and *Terebellina*.

Calcareous concretions are common and generally weather out in relief from the softer mudrocks that surround them. The concretions range in shape from spherical and ellipsoidal to lenticular, and may be 2 m or more in stratigraphic thickness. X-ray diffraction and chemical staining of thin-sections show that some concretions are cemented by dolomite and others by calcite, but I made no attempt to estimate the relative abundance of these different kinds. Aside from the carbonate cements, the sedimentary textures and structures in the concretions—including the bioturbation—are identical to the soft mudrocks in which the concretions are found.

Benthic foraminiferal assemblages from the mudrocks indicate deposition in the lower middle bathyal to lower bathyal zones, at water depths greater than 1500 to 2000 m (Appendix 1; Figures 19, 21, 23, 26, and 27). The fine texture of the sediment also suggests deposition in quiet, deep water. The bioturbation of the mudrocks indicates that the bottom waters were well-oxygenated and supported an active sediment-churning infauna. Bioturbation has destroyed any physical sedimentary structures that might indicate the processes by which the muddy sediment was transported and deposited. However, by analogy with modern California margin basins, most of the fine sediment was probably deposited by fecal pellets falling from the overlying water column and by downslope movement of resuspended sediments (Garrison, 1981).

Bioturbated fine sandstone. --

Bioturbated very fine to fine sandstone occurs in two different stratigraphic settings in the Rices Mudstone.

(1) Over most of the La Honda basin, horizons of bioturbated fine sandstone occur here and there as interbeds in the bioturbated mudrocks described above. The contacts between adjacent horizons of sandstone and mudrock are often gradational and difficult to locate precisely, even in areas of good outcrop.

(2) Along the southwestern margin of the preserved part of the La Honda basin near the Zayante-Vergeles fault, bioturbated mudrocks in the stratigraphically lower part of the Rices Mudstone grade vertically upsection and laterally to the southwest into bioturbated fine sandstone. This coarser-grained part of the Rices Mudstone is termed the "sandy siltstone facies" by Brabb (1960), but in the present report it is treated as an informal stratigraphic unit, the "Blooms Creek sandstone" (Figure 14). The unit is named for excellent exposures along Blooms Creek in the Big Basin area. About 10 to 12 km east of Blooms Creek, lithologically similar rocks may occur in the Newell Creek and Love Creek areas according to Clark (1981), and I tentatively correlate them with the Blooms Creek sandstone (Figure 22).

Bioturbated sandstone in the Blooms Creek sandstone and elsewhere in the Rices Mudstone is light gray to light brown on fresh surfaces but white on dry weathered outcrops. The sandstone is very fine to fine grained, and ranges from well-sorted "clean" arenite with calcite cement and little or no matrix to poorly sorted "dirty" wacke with argillaceous matrix and mud-filled burrows. Mineralogically, the sandstone is feldspathic arenite and wacke composed mainly of quartz and feldspar with lesser amounts of biotite. Other detrital minerals are minor and include muscovite, glauconite, and rock fragments. Well-rounded granules of quartz and granitic rock are present but uncommon in some outcrops. Megafossils are common locally and include several species of bivalves and gastropods as well as barnacle fragments and plant remains (McCollom, 1959; Brabb, 1960). These fossils occur scattered at random orientations in the sandstone, probably as a result of bioturbation. Benthic foraminifera are present but scattered, and are visible only in thin-section.

The sandstone is everywhere bioturbated and as a result bedding is not easy to see in outcrop. In some exposures, stratification can be inferred from subtle changes in resistance to bedding, from the orientation of elongate concretions, and from subtle changes in texture and truncation of burrows along amalgamation surfaces. Individual burrows are defined by color mottling and subtle textural mottling; some burrows stand out in knobby relief on weathered outcrop surfaces. Most of the burrows are cylindrical in shape, less than 2 cm in diameter, and oriented more or less parallel to stratification, but many are also at high angles to stratification (Figure 29). No detailed study of the trace fossils has been made.

Calcareous concretions are common, generally spheroidal to ellipsoidal in shape, and often 2 m or more in diameter (Figure 29). X-ray diffraction and chemical staining of thin-sections from several outcrops showed the presence of calcite cement but no dolomite.

The processes and environments of deposition of these bioturbated sandstones are difficult to interpret because bioturbation has destroyed any physical structures that could indicate the processes by which the sand was transported and deposited. Therefore, the bioturbated sandstones are probably best interpreted by examining their stratigraphic association with other, better-understood rocks. In much of the Rices Mudstone, bioturbated sandstones occur interbedded with mudrocks that contain benthic foraminiferal faunas indicative of deposition at water depths of 1500 to 2000 m or greater. Based on this close stratigraphic association, I infer that these bioturbated sandstones were also deposited at lower middle bathyal to lower bathyal depths. I speculate that the sand may have been carried into deeper water by turbidity currents derived from the same source as the turbidite sandstones described below, but that the Bouma sequences and other physical sedimentary structures were subsequently destroyed by biological reworking of the sediment.

The stratigraphic relationships of the Blooms Creek sandstone suggest that it also was deposited at bathyal depths. In the Big Basin area, the Blooms Creek sandstone conformably and gradationally overlies mudrocks in the lower part of the Rices Mudstone that were deposited at depths of 2000 m or more based on benthic foraminifers. The contact between these mudrocks and the overlying Blooms Creek sandstone is truly gradational and is fairly well exposed along Sempervirens Creek (Sec. 8-9S-3W), where the transition from mudrock to sandstone occurs over a stratigraphic interval about 80 m thick. The Blooms Creek sandstone is conformably overlain by the Castle Rock unit of the Vaqueros Sandstone, which consists of turbidite sandstones and mudrocks that were deposited at water depths greater than 2000 m based on benthic foraminifers. Finally, the Blooms Creek sandstone, which occurs at the stratigraphic top of the Rices Mudstone in the Blooms Creek and Kelly Creek areas, is laterally equivalent to bathyal mudrocks that occur at the top of the Rices Mudstone in more basinward settings, most notably in the Kings Creek and Twobar Creek sections about 5 km east of the Blooms Creek area (Figure 21 and 34), and the Western Gulf Wells Fargo #1 and Humble Santa Cruz Lumber Co. #1 wells about 12 km to the north (Figures 26 and 27). Thus, the Blooms Creek sandstone is bracketed stratigraphically and conformably above and below, and is laterally equivalent to rocks that were deposited at lower middle bathyal to lower bathyal depths (Figure 14). Based on this stratigraphic setting, I infer that the Blooms Creek sandstone also was deposited at lower middle bathyal to lower bathyal depths.

The processes by which the sand in the Blooms Creek sandstone was transported and deposited are unknown. I speculate that the Blooms Creek sandstone was formed by intense biological reworking of a sequence of interbedded turbidite sandstone and mudstone with a high sand-to-mud ratio.

The Blooms Creek sandstone has previously been interpreted as "neritic" (Brabb, 1960, 1964) and "shallow marine" (Nilsen and Brabb, 1979, p. 77), apparently on the basis of its sandy texture, bioturbation, and presumed shallow-water fossil fauna. This interpretation is rejected here for the following reasons. The sandy texture and bioturbation could have resulted from the biological reworking of deep-water redeposited sands as noted above. The fossil fauna reportedly contains some shallow-water genera such as *Solen* sp. and *Panope* sp. (both bivalves) but also some deeper-dwelling species such as the tellinid bivalve *Acila dalli* (Nilsen and Brabb, 1979, p. 77). The presence of both shallow-water and deep-water organisms in the same deposit suggests that the shallow-water fossils were transported into deeper

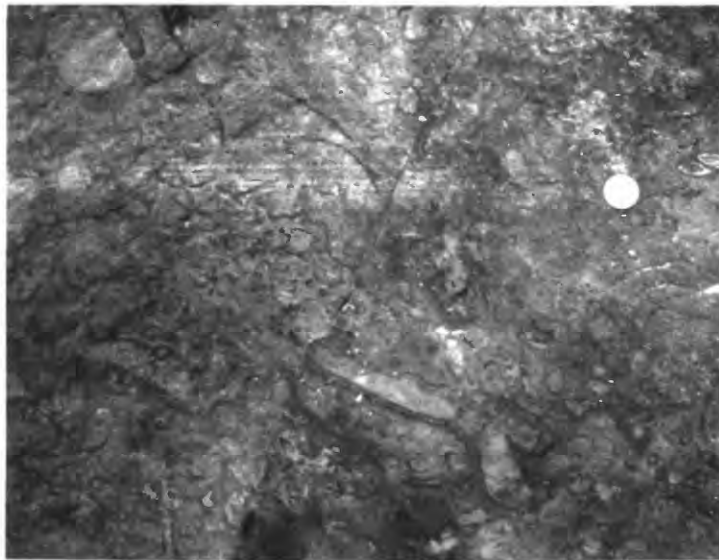


Figure 29. Outcrops of the Blooms Creek sandstone of the Rices Mudstone. **Top:** Very thick bedded, very fine "massive" (bioturbated) sandstone with large calcite concretions, in roadcut along Highway 236 near Blooms Creek. Stratification is not discernible in this photograph, but probably dips about 60° to the right. **Bottom:** Very thick bedded, bioturbated, very fine sandstone, from landslide scarp near the headwaters of Kelly Creek. Bedding has an apparent dip of about 25° to the right in this photo. Penny for scale. White elliptical objects near penny are unidentified burrows.

water and redeposited. In addition, no independent sedimentological evidence for shallow-water deposition has been found in the Blooms Creek sandstone. Such evidence could include, for example, medium to thick sets of tabular or trough cross-stratified sandstones, upper flow regime plane laminated coarse sandstones, oyster reefs, or fossil calcareous algae. These features are present in other Tertiary shallow marine sandstones in the La Honda basin, including the Santa Margarita Sandstone, the Lompico Sandstone, and the Laurel unit of the Vaqueros Sandstone. Finally, a shallow-marine origin for the Blooms Creek sandstone is difficult to reconcile with the stratigraphic relationships noted previously. If the Blooms Creek sandstone was deposited at water depths of 150 m or less, I would expect the contact between the sandstone and the underlying lower bathyal mudrocks to be an unconformity, rather than conformable and gradational as is exposed along Sempervirens Creek.

Turbidite sandstone. --

Turbidite sandstone occurs in a few outcrops of the Rices Mudstone as interbeds in the bioturbated mudrocks. The best exposures of turbidite sandstone are in Soquel Creek and near the top of the formation in Bear Creek (Figure 30).

In most outcrops the turbidite sandstones are light gray to light brown on fresh surfaces, very fine to fine grained, and moderately to well sorted. Mineralogically, the sandstones are feldspathic arenites and wackes composed mainly of quartz and feldspar with minor biotite, muscovite, glauconite, chlorite, and fragments of chert, mudstone, and granitic rocks. X-ray diffraction and chemical staining of thin-sections show that the major cements in the sandstones are calcite and argillaceous material.

Individual beds range from very thin to very thick, but most are very thin to thin. The majority of beds are laterally persistent across the outcrop (generally less than 30 m) but some are lenticular. The lower contacts of most beds are sharp and clearly erosional because they truncate burrows and other sedimentary structures in the underlying strata (Figure 30). The upper parts of the sandstone beds are often bioturbated and gradational into the overlying bioturbated mudrocks.

Common sedimentary structures include normal grading, plane lamination, convolute lamination, and ripple cross-lamination. However, these current-formed structures are commonly modified by bioturbation as shown in Figure 30. Bouma T_{bce} and T_{ce} sequences are common. Load casts, groove casts, and flute casts are rarely observed, perhaps because of the generally poor exposures. Only two paleocurrent measurements were obtained from turbidite sandstones in the Rices Mudstone: a weak parting lineation trending NW-SE, and a flute cast indicating flow from southwest to northeast (Appendix 5).

These sandstones are interpreted as turbidites because: (1) they exhibit normal grading, Bouma sequences, and other sedimentary structures that are common in turbidity current deposits, and (2) the sandstones occur interbedded with mudrocks that were deposited at water depths greater than 1500 m to 2000 m, based on benthic foraminiferal paleobathymetry.

Most of these sandstone beds resemble the facies C, D, and E turbidites of Mutti and Ricci Lucchi (1972), but facies B is also present in a few outcrops. In most exposures the turbidite sandstones occur as single beds or in groups of a few beds that are not obviously arranged in thickening-upward or thinning-upward sequences. This lack of organization suggests deposition on a basin plain according to the models of deep-sea siliciclastic sedimentation proposed by Mutti and Ricci Lucchi (1972), Rupke (1978), and Howell and Normark (1982). However, thickening-upward sequences occur in some outcrops along Soquel Creek, and also near the stratigraphic top of the Rices Mudstone in Bear Creek, Twobar Creek, and along the San Lorenzo River south of San Lorenzo Park. These thickening-upward sequences suggest deposition at the outer fringe of a prograding submarine fan or slope, according to the models of Mutti and Ricci Lucchi (1972) and others cited above.



Figure 30. Turbidite sandstone in the Rices Mudstone. Top: Outcrop of very thin to medium beds of resistant sandstone and less resistant mudstone, interpreted as Mutti and Ricci Lucchi facies D, E, and G, along Soquel Creek near localities B-7117, B-7118, and B-7119 of Smith (1971). Beds dip steeply to left and face left. Hammer handle about 28 cm long. Bottom: Sawn slab of thin beds of laminated and bioturbated sandstone, interpreted as Mutti and Ricci Lucchi facies D turbidites, from near the top of the Rices Mudstone along Bear Creek near its confluence with Deer Creek. See Figure 6 for location. Stratigraphic top to right. Scale in inches and centimeters.

Glauconitic sandstone. --

Two horizons of glauconitic sandstone in the Rices Mudstone occur along important biostratigraphic boundaries and inferred disconformities. The contact between the Rices Mudstone and the underlying Twobar Shale, which corresponds to the Narizian-Refugian stage boundary, is marked by a glauconitic sandstone that is traceable in outcrop and in the subsurface from the Soquel Creek-Hinckley Creek area to the southern edge of the Woodside quadrangle, a distance of more than 50 km (Figure 15). A second horizon of glauconitic sandstone occurs within the Rices Mudstone at the Refugian-Zemorrian stage boundary and is traceable for a distance of about 40 km from the Zayante Creek area to the Woodside quadrangle. During the 1980, 1981, and 1982 field seasons, good exposures of these glauconitic sandstones occurred along Soquel Creek, Hinckley Creek, Upper Boulder Creek, and Kings Creek (Figures 21, 23, and 31).

The thickness of the basal Refugian glauconitic sandstone ranges from about 15 cm in the upper Pescadero Creek area (Brabb and others, 1977, p. 15) to about 60 m in the Soquel Creek-Hinckley Creek area (Figure 23). The basal Zemorrian glauconitic sandstone is generally thinner, ranging from less than 20 cm thick along the San Lorenzo River near Camp Campbell to about 2 m thick along the same river near Waterman Gap.

Both the basal Refugian and basal Zemorrian glauconitic sandstones have knife-sharp lower contacts that are clearly erosional, as shown by: (1) the common occurrence of cylindrical borings, generally 1 or 2 cm in diameter, that extend as far as 17 cm downward into the underlying mudrock and are filled with glauconitic sandstone from above; and (2) the occurrence in some outcrops of thin, laterally discontinuous lenses of phosphate granules and pebbles, interpreted as lag deposits, along the contacts. Where exposed, the upper parts of the glauconitic sandstones grade upward into the overlying bioturbated mudrocks.

The lithologies of the basal Refugian and basal Zemorrian glauconitic sandstones are apparently identical. They are generally green, gray green, or brown on fresh surfaces, but weather to shades of orange brown. They are generally very fine to fine grained and poorly sorted, with scattered granules and pebbles up to 5 cm in diameter. The amount of glauconite in the sandstones ranges from less than 10% of the detrital grains in the basal Zemorrian near Riverside Grove to 90% in the basal Refugian along Little Boulder Creek (Brabb and others, 1977, p. 15), but is generally between 10% and 30%. Quartz and feldspar make up most of the rest of the detrital grains, but biotite, muscovite, rock fragments, fish fragments, skeletal carbonate grains, phosphate ooids, and phosphate granules and pebbles also occur.

The individual grains of glauconite range from green to nearly black in reflected light. Most grains are in the fine to medium sand range. The grains vary in shape from ovoid and well-rounded to highly irregular and angular. The irregular shape of many grains is apparently the result of deformation during compaction, because many of the glauconite grains have been squeezed between detrital grains of quartz and feldspar. Most of the glauconite grains are composed of homogeneous microcrystalline glauconite with no apparent internal structure. In a few thin-sections I found biotite grains that are partly replaced by glauconite. Glauconite also fills some hairline fractures in detrital grains of quartz and feldspar.

Well-rounded granules and pebbles of phosphate are common in some outcrops. They are generally white to cream colored on freshly broken surfaces but many are coated with a black material that may be manganese oxide. The phosphate granules and pebbles occur scattered in the glauconitic sand but in some places are concentrated in burrows or in lag deposits along the basal contacts of the glauconitic horizons.

Fossils are present locally in the glauconitic sandstones. Bivalves and gastropods are abundant in the basal Refugian glauconitic sandstone along Soquel Creek (Smith, 1971) and along Hinckley Creek.

The glauconitic sandstones are everywhere bioturbated. Individual burrows in water-polished outcrops and sawn slabs are defined by color and textural mottling (Figure 31). Glauconite grains and phosphate nodules are commonly concentrated in individual burrows. Other than bioturbation, the only



Figure 31. Outcrops of glauconitic sandstone of the Rices Mudstone. Top: Sharp contact between the Two-bar Shale and the overlying basal Refugian glauconitic sandstone of the Rices Mudstone, along Upper Boulder Creek just downstream from the China Grade culvert. See Figure 6 for location. Hammer is on the contact, which dips gently to the left in the photo. Hammer handle is about 28 cm long. Bottom: Bioturbated glauconitic sandstone, in float block near the contact between the Two-bar Shale and the Rices Mudstone along Hinckley Creek. See Figure 6 for location. Pencil is about 13 cm long.

other sedimentary structures observed were the granule and pebble lags noted above and a faint stratification in some outcrops defined by the parallel alignment of the shells of fossil bivalves.

The glauconitic sandstones range from friable to very hard and cemented by calcite. Euhedral crystals of pyrite are abundant in some outcrops.

The two horizons of glauconitic sandstone described above appear to mark significant regional disconformities. Evidence for the disconformities is as follows:

(1) By analogy with well-studied glauconitic sediments in both modern environments and ancient rocks, the two horizons of glauconitic sandstone in the Rices Mudstone probably record long intervals of very slow deposition or nondeposition and prolonged exposure on the sea floor (McRae, 1972; Kennedy and Garrison, 1975a, 1975b; Garrison and others, 1979; Odin and Matter, 1981).

(2) The two glauconitic horizons apparently coincide with two important biostratigraphic breaks, the Narizian-Refugian and Refugian-Zemorrian stage boundaries (Brabb, 1964).

(3) The lower contacts of both glauconitic horizons are knife-sharp and clearly erosional, and marked by borings made by unidentified bioeroding organisms into the underlying rocks.

Thus, each of the two disconformities consists of two components: (a) a sharp lower contact that represents erosion of the underlying rocks, and (b) an overlying glauconitic sandstone that probably represents an interval of very slow deposition or nondeposition. However, the thickness of section that is missing due to erosion and the amount of geologic time represented by the erosional surface and glauconitic sandstone are unknown. No local formations or biostratigraphic units appear to be missing along these disconformities (Brabb, 1964) with one possible exception. In the San Lorenzo River section at Riverside Grove (Figure 19), a subzone of the lower Refugian Stage *may* be missing from the base of the Rices Mudstone, with the missing interval represented by the basal Refugian disconformity (K. A. McDougall, unpublished report, 1979).

The origins of the glauconite and phosphate grains in these sandstones are unknown. Petrographic evidence noted above suggests that some of the glauconite formed by replacement of detrital biotite, perhaps in the manner proposed by Galliher (1935). Most of the glauconite grains, however, are not obviously replacements of biotite and may have formed in other ways, perhaps by replacement of fecal pellets, fossil fragments, and other materials (Odin and Matter, 1981). The phosphate granules and pebbles may have been derived by erosion and winnowing of the underlying Twobar Shale, which contains abundant phosphate nodules as noted previously. Alternatively, the phosphate pebbles may have formed by complex burial-exhumation cycles analogous to those inferred by Kennedy and Garrison (1975b) for the Cretaceous of England. No detailed petrographic studies have attempted to test these hypotheses.

The two disconformities in the Rices Mudstone probably formed at bathyal depths, based on the following evidence. First, both the basal Refugian and basal Zemorrian disconformities are underlain and overlain by marine mudrocks that were deposited at water depths greater than 1500 m to 2000 m, according to benthic foraminiferal paleobathymetry in the San Lorenzo River section (Figure 19), the Soquel Creek-Hinckley Creek section (Figure 23), the Humble Santa Cruz Lumber Co. #1 well (Figure 27), and the Kings Creek section (Figure 21). Second, there is no physical or paleontological evidence of erosion or deposition in shallow marine or nonmarine environments. A possible exception is the occurrence of presumably shallow-water molluscs in the basal Refugian glauconitic sandstone in the Soquel Creek area (Smith, 1971), but these fossils may have been transported into deeper water and redeposited. Both the basal Refugian and basal Zemorrian disconformities must have been created by events that were regional in scope, because they are correlatable over almost the entire length of the preserved part of the La Honda basin. The detailed nature of these events is unknown. Presented below are three working hypotheses that may account for the origins of the disconformities.

(1) One or both of the disconformities may have formed as a result of eustatic changes in sea level. Vail and others (1981) have identified glauconitic "marine condensed sections" that represent substantial intervals of geologic time and form during rapid eustatic rises of sea level. During a rapid rise, terrigenous sediments are trapped on the shelves, leading to cessation of terrigenous sedimentation in deeper water and creation of a "starved basin" in which glauconitic sediments form. The glauconitic sediments are commonly underlain by erosional surfaces formed during the preceding lowstand of sea level. The processes that create these erosional surfaces are not known but may include erosive turbidity currents or "major deep ocean boundary currents" (Vail and others, 1980). The basal Zemorrian disconformity in the La Honda basin may have formed in the same manner as these "marine condensed sections," and may be correlated with a eustatic fall in sea level and subsequent rapid rise that occurred at the Eocene-Oligocene boundary about 37 m.y. ago (Vail and Hardenbol, 1979). The basal Refugian disconformity in the La Honda basin, however, does not appear to correlate with Vail and Hardenbol's sea level curves. A major eustatic drop in sea level occurred at the middle Eocene-upper Eocene boundary about 40 m.y. ago (Vail and Hardenbol, 1979); but, as mentioned earlier, available biostratigraphic evidence shows that this boundary occurs within the Twobar Shale and is not marked by any obvious physical surface.

(2) One or both of the disconformities may have formed as a result of local or regional tectonic events. Rapid tectonic subsidence and bathymetric deepening of the entire basin, accompanied by the drowning of sediment source areas and the trapping of terrigenous sediments on the shelves, could have created starved-basin conditions favoring erosion by bottom currents and the formation of glauconite. Such an explanation has been invoked to explain the origin of glauconitic sandstones in the Tertiary record of the Salinas basin (Graham, 1976; Garrison and others, 1979). The basal Zemorrian glauconitic sandstone in the La Honda basin may have formed in an analogous manner. This interpretation is supported by evidence from foraminiferal paleobathymetry, which indicates that an abrupt deepening of several hundred meters occurred at the Refugian-Zemorrian boundary in the Kings Creek area (Figure 21) and possibly also in the Soquel Creek area (Figure 23). Speculatively, this rapid deepening may reflect rapid tectonic subsidence, and may be related to a change in the rate of spreading on the Farallon-Pacific ridge about 37 m.y. ago (Engebretson, 1982). This hypothesis of rapid deepening and tectonic subsidence, however, does not explain the origin of the basal Refugian glauconitic sandstone in the La Honda basin, which is associated with rapid *shallowing* according to benthic foraminiferal paleobathymetry in the Kings Creek and possibly the Soquel Creek areas (Figures 21 and 23).

(3) One or both of the disconformities may have formed by erosion, winnowing, and removal of fine sediment by high energy bottom currents. Some possible causes of episodic powerful bottom currents include: (a) local or regional tectonic events that cause changes in basin morphology and therefore affect current patterns; (b) climate changes that lead to intensified current activity in the world oceans, and (c) meteorite impacts (Fischer and Arthur, 1977; Angstadt and others, 1983). The basal Refugian disconformity records a significant environmental change from anoxic deposition of the laminated Twobar Shale to well-oxygenated deposition of the bioturbated Rice Mudstone. I speculate that this change was caused by tectonic events that destroyed the sill that had previously maintained low-oxygen conditions in the La Honda basin during deposition of the Twobar Shale. Sudden removal of the sill would result in rapid reorganization of water masses in the La Honda basin; the homogeneous low-oxygen water mass of the silled basin would be quickly replaced by the stratified system of water masses that prevailed in the adjacent open ocean. The rapid exchange of waters between the La Honda basin and the Pacific Ocean may have been accompanied by vigorous bottom currents that eroded and winnowed an unknown thickness of sediment from the upper part of the Twobar Shale. The glauconitic sand, in this scenario, represents mainly a lag deposit left behind by winnowing and removal of the silt and clay fractions of the Twobar Shale.

To speculate further, an equally catastrophic event may explain the basal Zemorrian disconformity in the La Honda basin. Data from oxygen isotopes suggest that a major episode of rapid cooling of the world ocean occurred about 37 m.y. ago at the Eocene-Oligocene boundary (Shackleton and Kennett, 1975; Savin, 1977). This cooling was associated with increased rates of convection in the oceans and vigorous bottom currents that resulted in erosion and the development of widespread submarine unconformities (Rona, 1973; Fischer and Arthur, 1977; Kennett, 1977; Olsson and others, 1980). The

basal Zemorrian disconformity in the La Honda basin, which formed about 37 m.y. ago according to available biostratigraphic evidence, may have formed during this episode of worldwide deep-sea commotion and erosion.

Depositional Systems and Provenance

The Rices Mudstone was deposited during the late Eocene and early Oligocene in a marine basin at water depths greater than 1500-2000 m. The bottom waters of the basin were well-oxygenated and supported an active and abundant burrowing infauna, as well as many species of molluscs, benthic foraminifers, and other marine invertebrates. Most of the formation consists of bioturbated mudstone, siltstone, and fine sandstone that accumulated on a basin plain that was flat or sloped gently to the north and northeast. However, turbidite sandstones arranged in thickening-upward sequences occur locally and suggest that parts of the formation were deposited on the outer fringes of a prograding submarine fan.

In the lower part of the formation, the lower and upper boundaries of the Refugian Stage are regional disconformities marked by horizons of glauconitic sandstone. The disconformities represent basin-wide episodes of at least minor erosion and sediment starvation, but the causes of these episodes—whether eustatic, tectonic, or more exotic—are unknown. The two disconformities could have formed by the same or by different mechanisms.

The upper part of the Rices Mudstone becomes coarser-grained to the southwest, suggesting that the main source of terrigenous sediment lay in that direction (Brabb, 1960, 1964). A sediment source to the southwest is also suggested by (1) a single paleocurrent measurement on a flute cast indicating flow toward the northeast, and (2) the mineralogy of the sandstones, which consist mainly of quartz, feldspar, and biotite that were most likely derived from the nearby Salinian granitic terrane to the southwest.

Vaqueros Sandstone

Introduction

The name "Vaqueros" was originally applied to arkosic sandstones in the Los Vaqueros Valley area of the Salinas basin by Hamlin (1904). The term was subsequently applied by Haehl and Arnold (1904) and Branner and others (1909) to sandstones in the La Honda basin that are generally similar in lithology and fossil content to those in the Los Vaqueros Valley. The use of the name "Vaqueros" in the La Honda basin has persisted up to the present time even though the type section of the Formation is in the Salinas basin (Thorup, 1943), and despite recent investigations which show that the Salinas and La Honda basins are distinct and separate accumulations of strata that were deposited in two different marine embayments during the middle Tertiary (Graham, 1976, 1978).

In the La Honda basin, strata mapped as Vaqueros Sandstone by Cummings and others (1962) and by Brabb (1970) consist of Oligocene and lower Miocene sandstone, mudstone, and minor conglomerate that have a wide geographic distribution (Figure 32). The internal stratigraphy of the Vaqueros, and its stratigraphic relationships with surrounding formations, are complex (Figure 14). Data on thickness and stratigraphic relationships described below show that the Vaqueros consists of two large basinward-thinning wedges of coarse sediment, one on the north and the other on the south (Figures 14 and 33).

At the northwestern tip of the basin, the Vaqueros Sandstone of the Woodside area forms a southward-thinning wedge that was derived from a granitic source area to the northwest (Mack, 1959). This wedge of sandstone apparently pinches out and is not physically connected to the rest of the Vaqueros Sandstone to the southeast (Figures 14 and 33), but the details of this relationship are unclear due to poor outcrops and sparse well control.

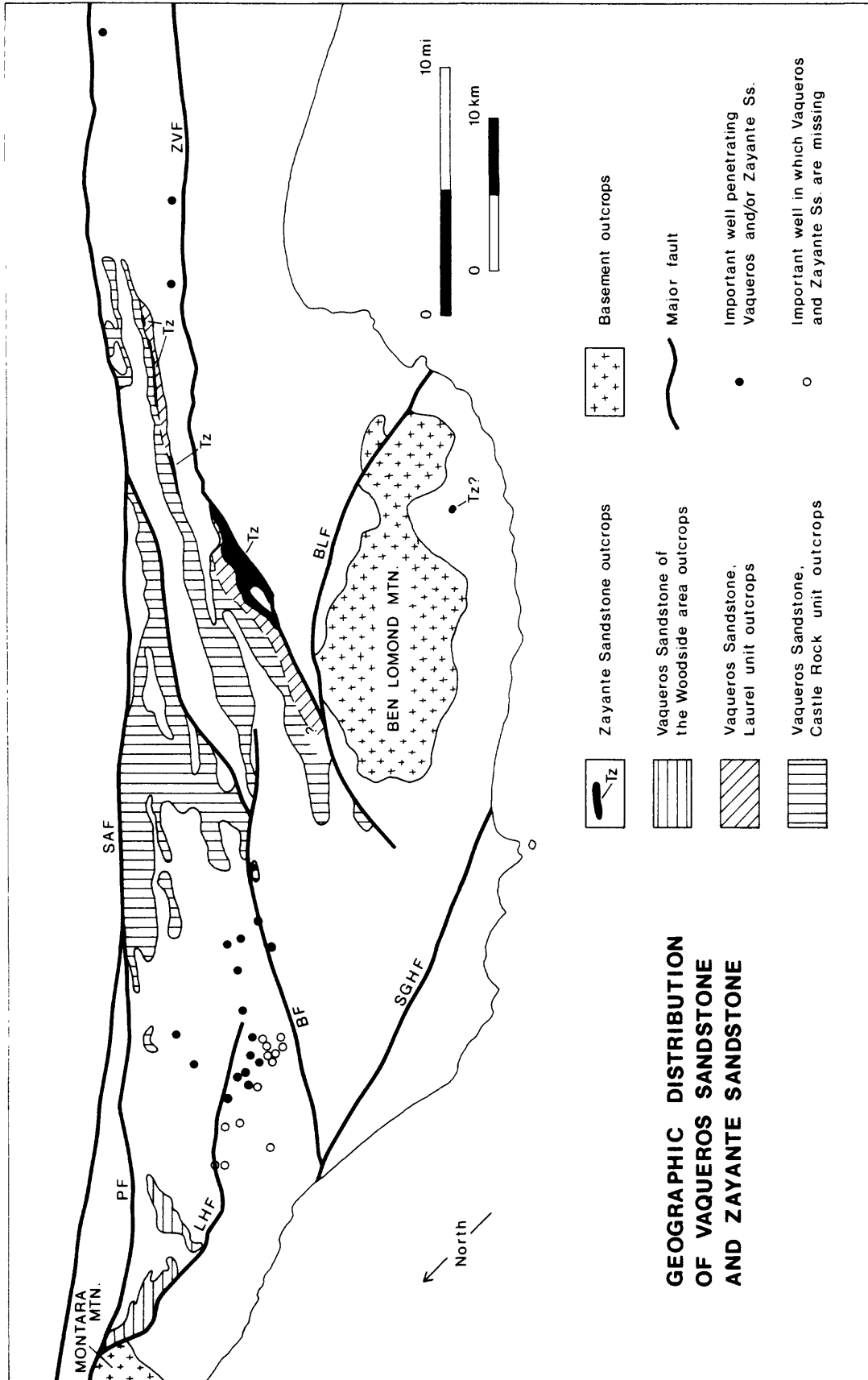


Figure 32. Map of the geographic distribution of the Vaqueros Sandstone and Zayante Sandstone in the La Honda basin. Major faults are labeled as follows: BF = Butano fault, BLF = Ben Lomond fault, LHF = La Honda fault, PF = Pilarcitos fault, SAF = San Andreas fault, SGHF = San Gregorio-Hosgri fault, ZVF = Zayante-Vergeles fault.

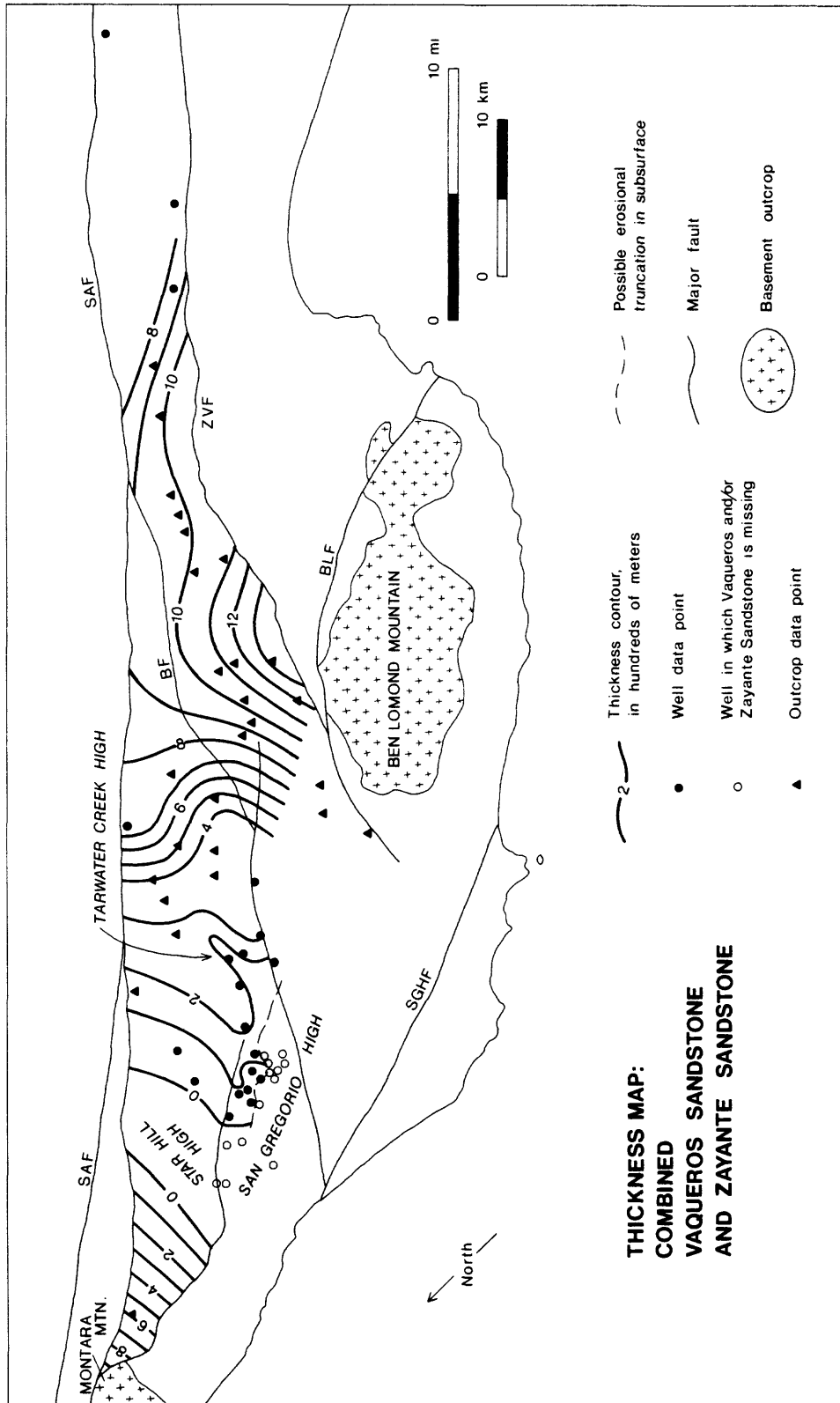


Figure 33. Map of the thickness of the combined Zayante Sandstone and Vaqueros Sandstone intervals, based on data in Appendices 3 and 4. Major faults labeled as in Figure 32. The "Star Hill high," "Tarwater Creek high," and "San Gregorio high" are areas of anomalous thinning inferred to have been structurally positive during Oligocene and early Miocene(?) deposition of the Vaqueros and Zayante sandstones.

A second and much larger wedge of coarse sediment reaches a thickness of more than 1200 m in the Bear Creek-Zayante Creek area near the Zayante-Vergeles fault (Figure 33). This wedge is composed of three stratigraphic units: the "Castle Rock" and "Laurel" units of the Vaqueros Sandstone which represent submarine fan and shelf depositional systems, respectively, and the Zayante Sandstone which probably represents coarse-grained fluvial and deltaic systems (Figure 14). The similarities and differences between these units are summarized in Table 3.

From the depocenter in the Bear Creek-Zayante Creek area, the great wedge of coarse sediment formed by the Vaqueros and Zayante sandstones thins radially to the southeast, east, and north (Figure 33). The northward thinning and eventual pinchout of the Vaqueros Sandstone in the La Honda area is due mainly to lateral interfingering with the Rices Mudstone, Mindego Basalt, and Lambert Shale (Figure 14; Touring, 1959; Cummings, 1960; Cummings and others, 1962). Also in the La Honda area, sparse well control suggests the presence of three areas of anomalous thinning that are interpreted as structural positives. Two of these--the Tarwater Creek and San Gregorio highs--also appear on thickness maps of the Twobar Shale and Rices Mudstone, and therefore persisted from at least the late Eocene to the Oligocene (Figures 17 and 24). A third structure--the Star Hill high--is inferred to have separated the Vaqueros Sandstone of the Woodside area from the northward-thinning wedge of Vaqueros in the central La Honda basin.

Castle Rock unit of the Vaqueros Sandstone

Introduction

The Castle Rock unit consists mainly of feldspathic sandstone interbedded with mudstone and shale, along with minor olistostromes and bioturbated glauconitic sandstone. Lenses of basaltic volcanic rocks occur locally and are described in the section of this report on the Mindego Basalt.

The Castle Rock unit is named informally in this report for the Castle Rock Ridge quadrangle, where it is well-exposed in the Kings Creek, Twobar Creek, and upper Zayante Creek sections (Figures 21, 34, and 35) as well as along Bear Creek and in roadcuts along Skyline Boulevard.

Age

The Castle Rock unit ranges in age from early Oligocene to early Miocene as shown by locally abundant microfossils and a few megafossils. Benthic foraminifers from outcrops and wells indicate that the Castle Rock unit ranges from early Zemorrian to Saucian, but most of the unit seems to have accumulated during the Zemorrian (Appendix 1; Klempell, 1938; Cummings and others, 1962; Fairchild and others, 1969; Smith, 1971; K. A. McDougall, unpublished report, 1979). Fossil molluscs, though not abundant and often fragmentary, have been collected from the unit at several localities and include *Pecten sanctaecruzensis* Arnold, which is characteristic of the unnamed lower Oligocene stage of Addicott (1972), and *Macrochlamis magnolia* (Conrad) and *Turritella inezana*, Conrad, which are characteristic of Addicott's Vaqueros Stage (Burchfiel, 1958; Brabb, 1960; Cummings, 1960; Cummings and others, 1962). Calcareous nannofossils collected from the Castle Rock unit in the Bear Creek, Zayante Creek, and Mountain Charlie Gulch areas are representative of the Oligocene NP23 to NP25 zones, but could not be assigned to specific zones because the assemblages consist mainly of long-ranging species (Bukry and others, 1977; R. Z. Poore, unpublished data, 1981). These data indicate that the Castle Rock unit was deposited between 37 m.y. and 18 m.y. ago, an unusually long interval of time.

TABLE 3
COMPARISON OF ZEMORRIAN SANDSTONES IN THE LA HONDA BASIN

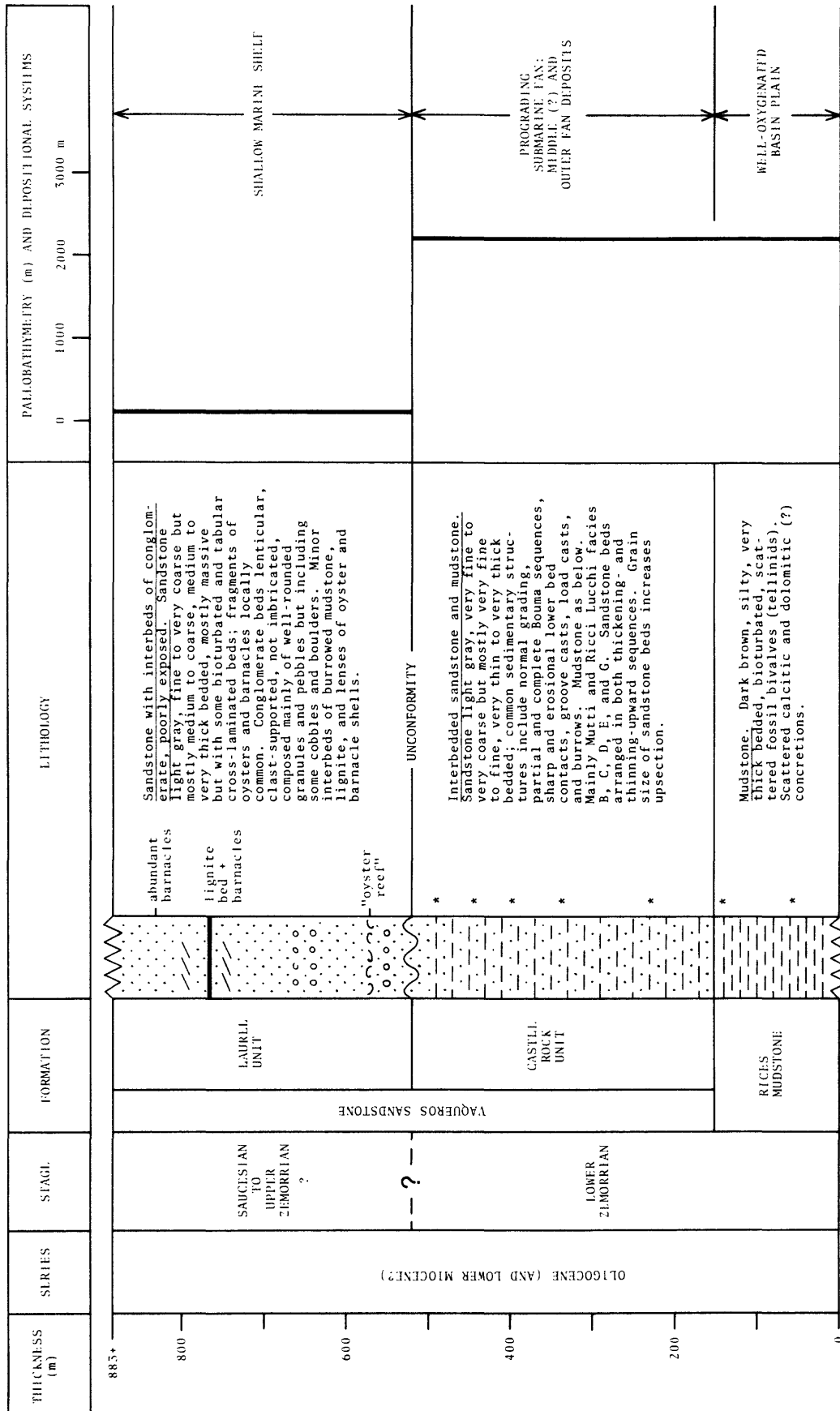
	Vaqueros Sandstone		
	Castle Rock unit	Laurel unit	Zayante sandstone
Rocks	Mainly interbedded feldspathic sandstone and mudrocks: facies A, B, C, D, E, G, and minor F of Mutti and Ricci Lucci (1972).	Mainly bioturbated and massive to cross-laminated feldspathic sandstone; minor mudrocks and conglomerates.	Mainly conglomerate and and feldspathic sandstone with minor mudrocks; facies Gm, Gt, St, Sp, Sr, Sh and Fl of Miall (1977, 1978).
Sandstone Colors	Light gray.	Light gray.	Green, red, gray.
Glauconite	Scattered grains in sandstones; two laterally persistent horizons with >20% glauconite.	Scattered grains in sandstones.	None.
Fossils	Abundant benthic forams in mudrocks; scattered molluscs in sandstones.	Locally abundant molluscs, barnacles, and echinoids; benthic forams in mudrocks.	Rare fragments of molluscs; one serpulid reef with molluscs, barnacles, and echinoids.

Table 3, continued

	Vaqueros Sandstone		Zayante Sandstone
	Castle Rock unit	Laurel unit	
Paleocurrents	Generally to the north and northeast	Insufficient data.	Generally to the north and northeast.
Geographic Distribution	Covers most of the La Honda block.	Only along the southwestern margin of the La Honda block.	Only along the southwestern margin of the La Honda block.
Age	Lower Zemorrian to Saucian.	Upper(?) Zemorrian to Saucian.	Upper(?) Zemorrian.
Paleo-bathymetry	Mainly middle and lower bathyal (>1500 m).	Mainly shelf (0-150 m).	Mainly nonmarine; some inner shelf (0-50 m).
Depositional System	Submarine fan.	Shallow marine shelf.	Fan-delta.
Provenance	Granitic.	Granitic.	Granitic.

Figure 34. Inferred stratigraphy, paleobathymetry, and depositional systems for the Twobar Creek section. See Figure 6 for location. Stratigraphic nomenclature and thicknesses modified from Brabb (1960) and Brabb and others (1977). The Castle Rock and Laurel units are roughly equivalent to cosets M and N, respectively, of Brabb (1960) and Brabb and others (1977). Lithology shown schematically. Assignment of the Laurel unit of the Vaqueros Sandstone to the Saucesian and Upper Zemorrian stages is based on correlation with well-dated rocks of similar lithology and stratigraphic position in the lower Zayante Creek section, located along strike about 10 km east of the Twobar Creek section.

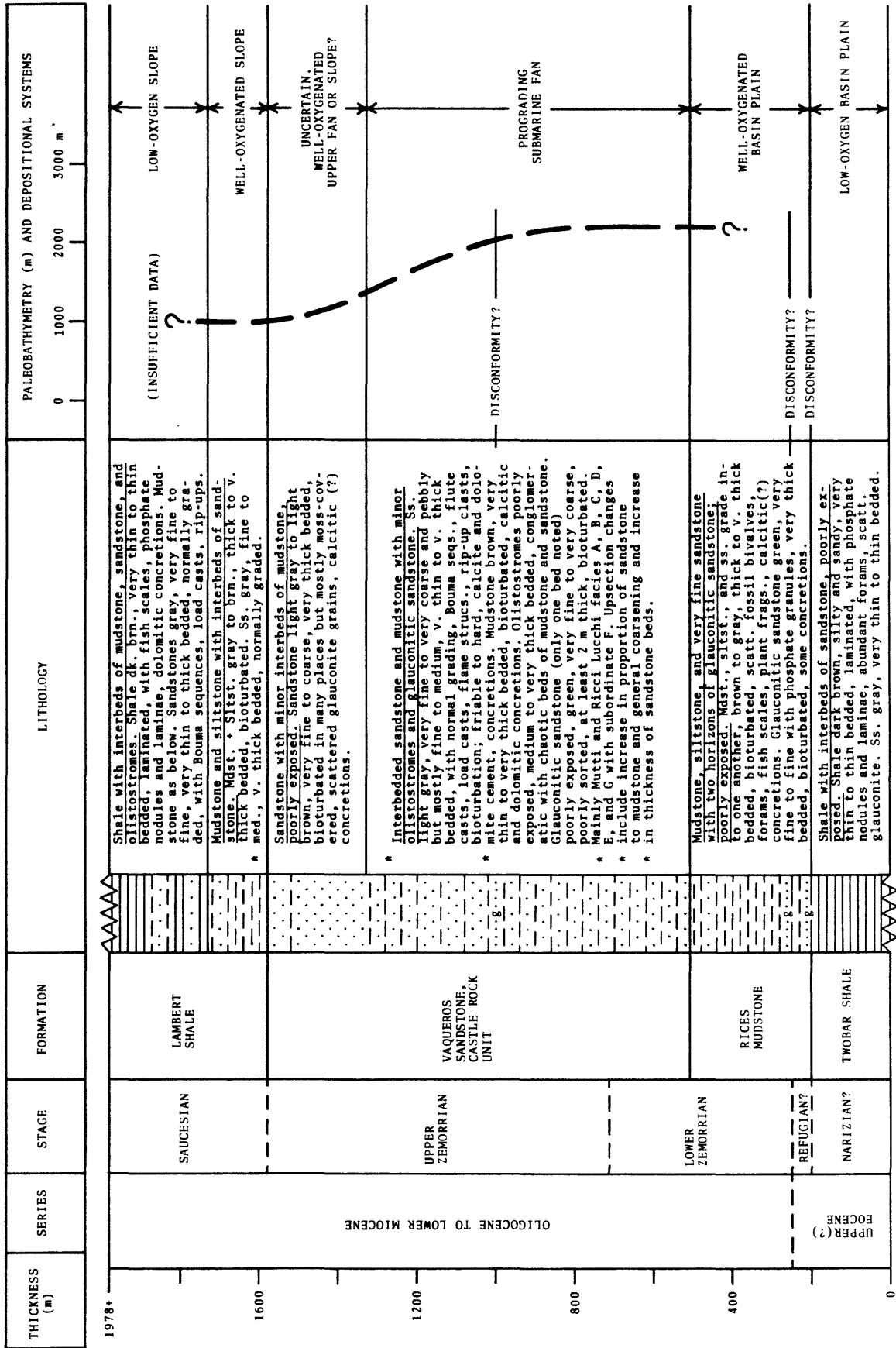
TWOBAR CREEK SECTION



*=Paleontological sample location.

Figure 35. Inferred stratigraphy, paleobathymetry, and depositional systems for the upper Zayante Creek section, on the north limb of the San Lorenzo syncline. See Figure 6 for location. Stratigraphic nomenclature and thicknesses in part from Brabb and others (1977). Lithology shown schematically. The entire Vaqueros Sandstone in this section is tentatively assigned to the Castle Rock unit, but the upper 250 m of the Vaqueros is very poorly exposed and may include strata of the Laurel unit.

UPPER ZAYANTE CREEK SECTION, NORTH LIMB OF SAN LORENZO SYNCLINE



*=Paleontological sample location.

Stratigraphic Relations

The Castle Rock unit conformably overlies the Rices Mudstone over nearly the entire La Honda block from southeast of Corralitos to the pinchout northeast of La Honda (Figures 14, 15, and 33). As mentioned earlier, the pinchout occurs in the subsurface and is due mainly to lateral interfingering with the Rices Mudstone, Mindego Basalt, and Lambert Shale. However, *some* of the thinning may be due to Oligocene or early Miocene erosion. Based on subsurface data, Touring (1959, his Plate 17) suggested that in some places the Castle Rock unit is overlain unconformably by the Mindego Basalt. Thus, some of the thinning of the Castle Rock unit may be the result of erosion that occurred prior to accumulation of the Mindego Basalt.

Farther south, the Castle Rock unit is overlain by and partly laterally equivalent to the Laurel unit of the Vaqueros Sandstone, and also the Zayante Sandstone (Figures 14, 15). Stratigraphic relationships in this area are discussed in detail in the section of this report on the Laurel unit.

The Castle Rock unit is missing from the Ben Lomond block. If it ever was deposited there, it was removed by Oligocene or early Miocene erosion prior to deposition of the lower Miocene (Relizian) Lompico Sandstone, which rests nonconformably on the granitic basement.

Lithology

The major categories of rocks in the Castle Rock unit are as follows: (1) feldspathic sandstones, which make up most of the unit; (2) mudrocks, which are interbedded with the sandstones and locally make up 30% to 50% of the section; (3) olistostromes; and (4) bioturbated glauconitic sandstones. The latter two categories together make up less than 1% of the Castle Rock unit.

Feldspathic sandstones. --

Feldspathic arenite and wacke are the most abundant and typical rocks in the Castle Rock unit. In most outcrops they are light gray to light brown on fresh surfaces and weather various shades of brown.

Visual estimates of composition from thin-sections and sieve samples by Cummings (1960) and Brabb (1960) show that the sandstones generally consist of 40-80% quartz, 20-50% feldspar, and 0-10% lithic fragments, with up to 5% biotite and lesser amounts of other minerals. Potassium feldspar is generally more abundant than plagioclase. The most common lithic fragments are chert, silicic volcanic rocks, and granitic rocks; less common are fine sandstone and siltstone, quartzite, mica schist, and unidentified foliated metamorphic rocks. Fresh fragments of basalt occur in some beds and probably were derived from local volcanic centers that were active during the late Oligocene and early Miocene and are discussed in the section of this report on the Mindego Basalt.

The sandstones range from highly weathered and friable to hard and well-cemented. The most common cements are calcite and dolomite, but laumontite occurs locally in the Saratoga Gap area (Madsen and Murata, 1970). Argillaceous material is a common cement in many outcrops, but it is not clear whether the clay minerals are detrital, formed during deep burial diagenesis, or are merely products of surface weathering. Calcitic and dolomitic concretions are common.

The sandstones of the Castle Rock unit can be divided very generally into three groups on the basis of recurrent associations of bed thickness, grain size, and sedimentary structures: (1) thick to very thick bedded, coarse grained, massive sandstones that are commonly amalgamated to form intervals from one to many m thick; (2) thin bedded, fine grained sandstones that commonly exhibit normal grading and Bouma sequences and are interbedded with roughly equal amounts of mudrock; and (3) thick to very thick bedded, fine grained, thoroughly bioturbated sandstones. The thick bedded coarse sandstones probably represent deposition in channels on a submarine fan while the thin bedded sandstones and bioturbated sandstones probably were deposited in interchannel areas. These three categories of sandstones are

discussed in further detail below.

(1) Thick bedded coarse sandstone.

Intervals of seemingly "massive" sandstone ranging in thickness from less than one m to more than 60 m form numerous cliffs along Castle Rock Ridge (Figure 36), as well as monoliths such as Castle Rock and Goat Rock, and numerous cliffs and waterfalls in the stream valleys of the Santa Cruz Mountains. The sandstones range in texture from fine to very coarse and pebbly but most are medium to coarse grained. The sorting ranges from poor to moderate, and the shapes of the sand grains range from angular to rounded. The granules and pebbles are generally well-rounded and consist mainly of silicic volcanic and granitic rocks. Megafossils are uncommon, but gastropods, pectinids, oysters, and other bivalves have been discovered in several areas including the Corralitos Creek, Kelly Creek, Twobar Creek, and Kings Creek sections (Burchfiel, 1958, 1964; McCollom, 1959). Most of these megafossils are broken, suggesting that they were transported for some distance prior to deposition (Cummings and others, 1962).

Close inspection of good outcrops reveals that nearly all of these very thick intervals of sandstone are composite and made up of two or more amalgamated beds ranging from 30 cm to more than 100 cm thick. The amalgamation surfaces are defined by abrupt changes in texture, by truncations of sedimentary structures such as convolute laminations and burrows, and by thin, laterally discontinuous horizons of mudrocks. Both the amalgamation surfaces and the bases of the amalgamated intervals are sharp and erosional, generally scoured and irregular, and sometimes marked by flute casts, groove casts, load casts, and flame structures (Figure 37). The amalgamated intervals are commonly laterally persistent and of constant thickness across single outcrops (usually less than 10 m) but probably are lenticular on a large scale because individual amalgamated intervals cannot be correlated between adjacent creeks, which in general are separated by distances of one km or more.

Relatively few sedimentary structures are found in these sandstones. Most beds are massive, but some exhibit planar to low-angle lamination. In some cases, plant fragments are concentrated along these laminae. Rip-up clasts of mudrocks and fine sandstone are fairly common. Normal grading is present in some beds but is commonly restricted to the upper parts of the beds. The tops of some beds exhibit convolute laminations, while the tops of others are bioturbated. No dish structures were observed.

These sandstones resemble the facies A and B turbidites of Mutti and Ricci Lucchi (1972). The processes by which such sandstones are deposited are poorly understood, but probably include high-velocity turbidity currents, grain flows, sandy debris flows, and other types of sediment gravity flows (Mutti and Ricci Lucchi, 1972; Middleton and Hampton, 1976; Howell and Normark, 1982). I infer that the thick bedded coarse sandstones in the Castle Rock unit represent channel deposits on a submarine fan, based on their large-scale lenticularity, erosional lower contacts, stratigraphic association with the turbidite sandstones and bathyal mudrocks described below, and analogy with similar deposits in the submarine fan models of Mutti and Ricci Lucchi (1972) and Walker (1978, 1979).

(2) Thin bedded fine sandstones.

The thick bedded coarse sandstones described above alternate with intervals of thin bedded fine sandstone and interbedded mudrocks that range from less than one m to more than 100 m thick. In general, the ratio of sandstone to mudrocks within these intervals is about 1:10 to 2:1; however, ratios of 20:1 and higher occur in places, for example along the Big Basin Road (Highway 236) near Blooms Creek, and also along the same road about 1.1 km south of Waterman Gap (Figure 6).

The sandstones range in texture from fine to coarse, but most are very fine to fine. The sands range from poorly sorted to well sorted, and the grains are angular to subrounded.

The sandstones range from very thin to medium bedded, but most are very thin to thin. Most beds are laterally persistent across the outcrop (generally less than 10 m), but lenticular beds that appear to fill small-scale channels are common locally and are particularly well exposed in the Corralitos Creek section



Figure 36. Outcrops of the Castle Rock unit of the Vaqueros Sandstone. **Top:** View of part of Castle Rock State Park looking northeast from airplane. Bedding dips away from the camera at about 30° and is right side up. Light colored sandstone cliffs are interpreted as middle-fan channel deposits of an ancient submarine fan; thin covered intervals are mainly interbedded mudrocks and thin bedded sandstone interpreted as interchannel deposits. **Bottom:** Thinning- and fining-upward sequence of light brown sandstone beds and dark mudstone interbeds, interpreted as a channel-fill deposit. Roadcut is along Eureka Canyon Road and is stratigraphically equivalent to part of the nearby Corralitos Creek section. Beds are nearly vertical and face left. Hammer handle is about 28 cm long.

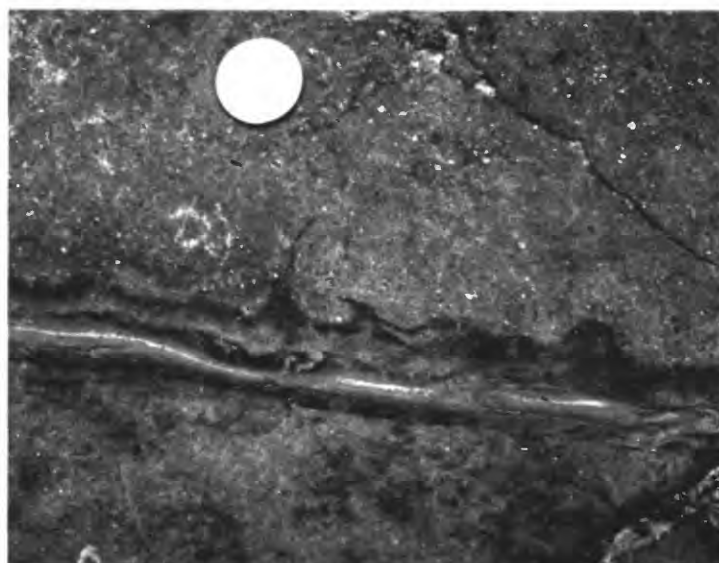


Figure 37. Sedimentary structures in sandstones of the Castle Rock unit of the Vaqueros Sandstone. **Top:** Giant flute casts at the base of coarse sandstone interpreted as Mutti and Ricci Lucchi facies A, in the Corralitos Creek section. View is perpendicular to the strike of bedding; bed is vertical and facing away from the camera. Giant flute casts, in particular the ones above the 1.5 m Jacob's staff, indicate paleoflow from right to left. **Bottom:** Load casts and flame structures at the base of a bed of very coarse sandstone. Outcrop is in the headwall scarp of a landslide at the headwaters of Kelly Creek (Big Basin quadrangle, Sec. 7-9S-3W). Quarter for scale.

(Figure 38). The lower contacts of both the laterally persistent and the lenticular beds are sharp and often clearly erosional, as shown by the common occurrence of scours and the truncation of burrows and laminations in the underlying beds. The tops of the sandstone beds are abrupt in places but usually gradational into the overlying mudrocks (Figure 39).

Sedimentary structures are abundant in these thin bedded sandstones and are best observed in water-polished outcrops and in sawn slabs. The most common structures include normal grading, plane lamination, ripple and climbing ripple cross-lamination, convolute lamination, and bioturbation. Less common are flute casts, groove casts, load casts, flame structures, rip-up clasts, escape structures, and parting lineation. Bouma Tbce, Tbe, and Tce sequences are abundant, and Tabce sequences occur in some outcrops. Plant fragments and mica are in many cases concentrated along laminations. In many beds, laminations and other current-formed structures have been disrupted or completely obliterated by bioturbation (Figure 40).

These thin bedded sandstones are interpreted as turbidity current deposits because: (1) they exhibit normal grading, Bouma sequences, and other sedimentary structures that are common in both modern and ancient turbidites (Middleton and Hampton, 1976; Walker, 1979); and (2) the sandstones are interbedded with mudrocks, described below, that were deposited at water depths greater than 1500 m to 2000 m based on benthic foraminiferal paleobathymetry. The thin bedded sandstones in the Castle Rock unit strongly resemble the facies C, D, and E turbidites of Mutti and Ricci Lucchi (1972) and the "classical turbidites" of Walker (1978, 1979).

Vertical sequences and stratigraphic associations suggest that the thin bedded sandstones of the Castle Rock unit were deposited in several different settings on a submarine fan. In the lower part of the unit the sandstone beds in places are arranged in poorly-defined thickening- and coarsening-upward sequences. These sequences are interpreted as prograding outer-fan lobes, by analogy with the submarine fan models of Mutti and Ricci Lucchi (1972) and Walker (1978). The thickening- and coarsening-upward sequences generally range in thickness from about 1 m to 3 m thick, but some are more than 10 m thick; they are best exposed in the Twobar Creek and Kings Creek sections (Figures 21 and 34), along Bear Creek on the north limb of the San Lorenzo syncline, and along the San Lorenzo River near San Lorenzo Park.

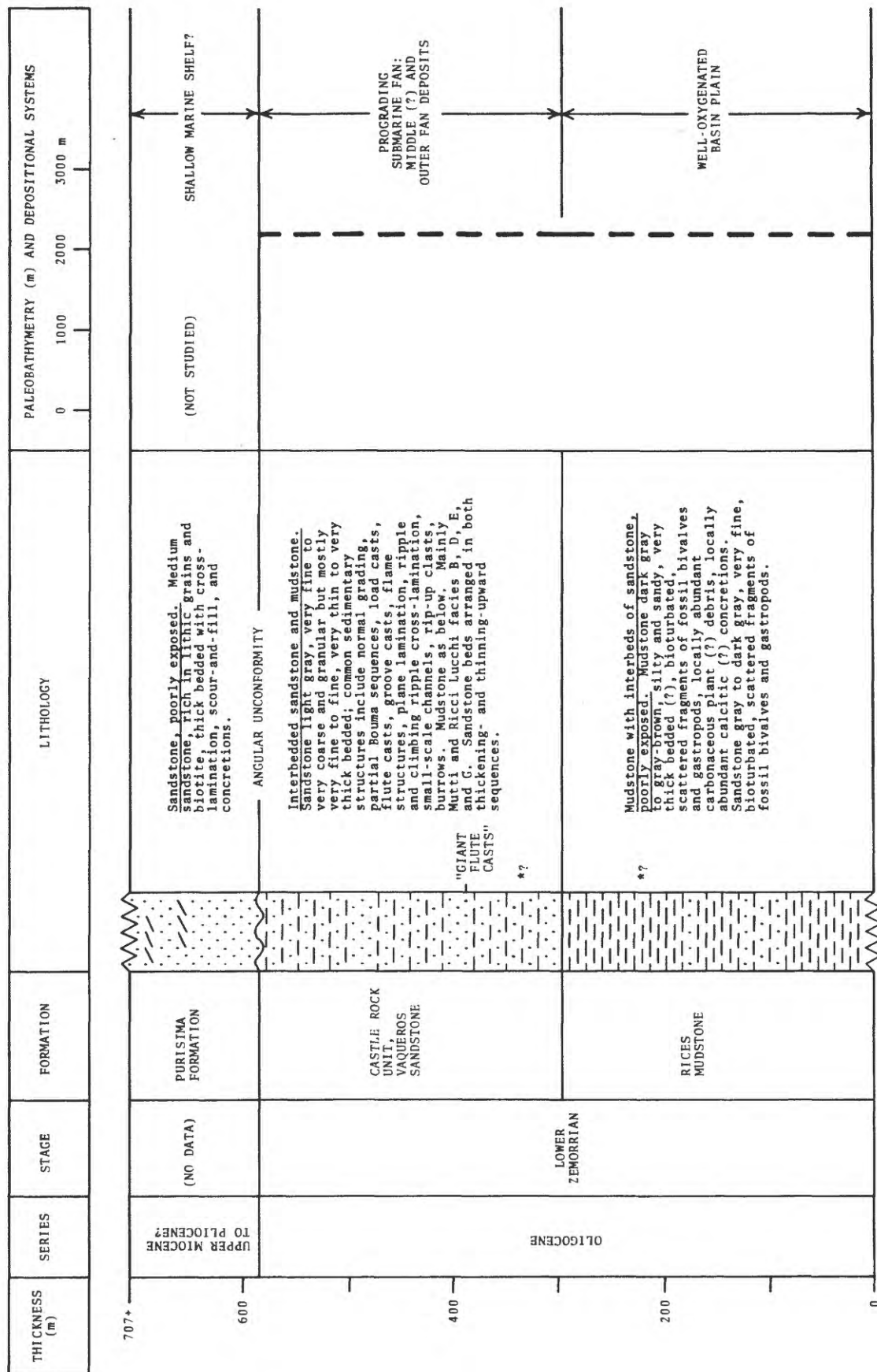
Higher up in the Castle Rock unit, intervals of thin bedded sandstone and mudrock alternate with packets of amalgamated sandstone. These are interpreted as middle-fan interchannel and channel deposits, respectively, by analogy with the submarine fan models of Mutti and Ricci Lucchi (1972) and Walker (1978). The thin bedded sandstones probably represent mainly overbank deposits that were deposited by turbidity currents that spilled out of the main channels on the Castle Rock fan and flowed across broad interchannel areas where they eventually slowed and deposited their sediment load. In some outcrops the sandstone beds are arranged in thinning- and fining-upward sequences that probably represent middle-fan channel-fill deposits (Figure 36; Nilsen and Brabb, 1979, p. 76).

The stacking of middle-fan channel and interchannel deposits is strikingly revealed along Castle Rock Ridge, where the channel sandstones form bare cliffs and prominent knobs, while the interchannel deposits are generally recessive-weathering and covered by brush (Figure 36).

(3) Bioturbated fine sandstones.

Intervals of thick to very thick bedded, bioturbated, very fine to fine sandstone occur locally in the Castle Rock unit. These rocks are lithologically similar to the bioturbated sandstones that occur in the Rices Mudstone and are described in an earlier part of this report. The bioturbated sandstones in the Castle Rock unit are generally poorly exposed but appear to range from less than one m to several tens of m thick. In the upper Zayante Creek and Soquel-Hinckley sections (Figures 23 and 35) these bioturbated sandstones are clearly interbedded with the turbidite sandstones and mudrocks that are most typical of the Castle Rock unit. Based on stratigraphic association, I infer that the bioturbated sandstones were deposited at bathyal depths on the interchannel areas of the Castle Rock submarine fan. The bioturbated

CORRALITOS CREEK SECTION



*Paleontological sample location, shown approximately.

Figure 38. Inferred stratigraphy, paleobathymetry, and depositional systems for the Corralitos Creek section. See Figure 6 for location. This section was measured with tape and Brunton compass in September 1981 by H. Gibbons and R. Stanley. Lithology shown schematically.



Figure 39. Outcrops of the Castle Rock unit of the Vaqueros Sandstone. Top: Thick to very thick and amalgamated beds of sandstone resembling facies A and B of Mutti and Ricci Lucchi (1972) and interpreted as middle fan channel deposits, alternating with intervals of thin bedded sandstone and mudrocks resembling facies D, E(?), and G of Mutti and Ricci Lucchi and interpreted as interchannel deposits. Roadcut along Big Basin Road (Highway 236) near Blooms Creek (see Figure 6 for location). Bottom: Interbedded sandstone (light) and mudstone (dark) resembling Mutti and Ricci Lucchi facies D and G and interpreted as interchannel deposits. Note the sharp bases and gradational tops of the sandstone beds. Beds are vertical and face to the right. Hammer handle is about 28 cm long. Water-polished outcrop is in the upper Zayante Creek section (Figures 6 and 35).

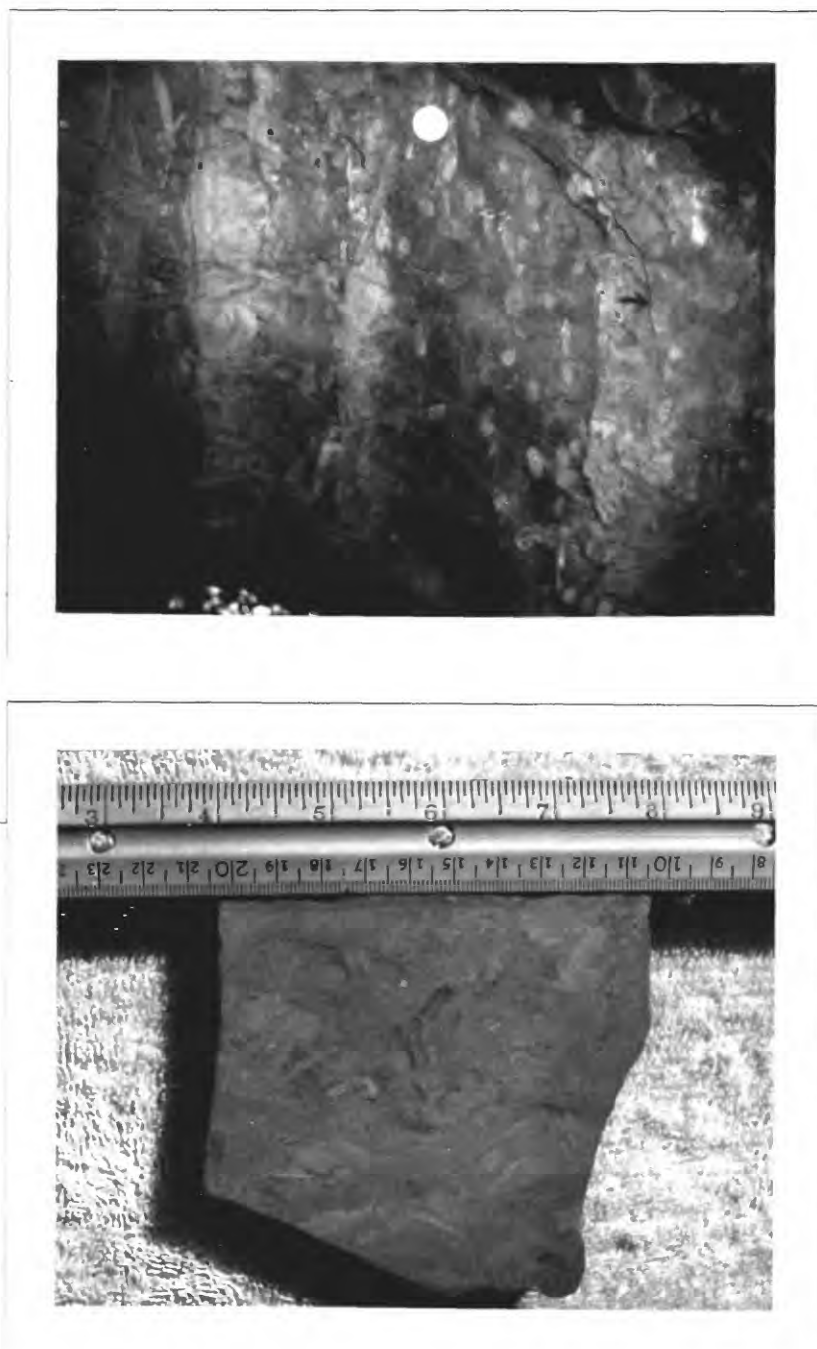


Figure 40. Bioturbated rocks in the Castle Rock unit of the Vaqueros Sandstone. **Top:** Outcrop of bioturbated dark gray mudstone and light brown sandstone in the upper Zayante Creek section. Beds are nearly vertical and face to the right. Note that bedding has been nearly obliterated by intense bioturbation. Penny for scale. **Bottom:** Sawn slab of bioturbated siltstone from the Corralitos Creek section. Scale in inches and centimeters.

sandstones formed at certain times when, for reasons that are unclear, rates of sedimentation were low compared to rates of biological reworking of the sediment.

Mudrocks. --

Mudrocks occur as interbeds throughout the Castle Rock unit of the Vaqueros Sandstone. The mudrocks are generally very thin to thin bedded, but in places form horizons that are several tens of m thick. The mudrocks are generally poorly exposed and chippy-weathering in roadcuts and on hillsides, but are well-exposed in water-polished outcrops along the bottoms of stream valleys.

Mudrocks in the Castle Rock unit include bioturbated claystone, mudstone, and siltstone, as well as laminated shale. Bioturbated mudstone and siltstone (Figure 40) make up more than 90% of the mudrocks in the unit and were most likely deposited in well-oxygenated bottom waters. These bioturbated mudrocks are nearly identical in lithology to those in the underlying Rices Mudstone and described in an earlier part of this report.

Laminated dark-colored shales occur in places near the top of the Castle Rock unit and suggest a change from well-oxygenated to anaerobic bottom conditions. The shales are fairly well exposed along Fall Creek and in roadcuts along Highway 9 near Saratoga Gap (Figure 6). These laminated shales are similar in lithology to those in the overlying Lambert Shale described in a later part of this report.

Assemblages of benthic foraminifers from both the bioturbated mudrocks and the laminated shales indicate deposition in lower middle bathyal to lower bathyal environments, and water depths greater than 1500 m to 2000 m (Appendix 1). The processes by which the muds were deposited are unclear. The interbedding of the mudrocks with turbidite sandstones suggests that the mud was deposited by the fine-grained "tails" of sandy turbidity currents, or by muddy, low-density turbidity currents. However, much of the mud may have been deposited as fecal pellets falling from the overlying water column, by analogy with modern California margin basins (Garrison, 1981).

Olistostromes. --

Olistostromes, or probable debris-flow and slump deposits, are uncommon in the Castle Rock unit and generally poorly exposed. Several olistostromal beds occur in the upper Zayante Creek section stratigraphically above the prominent glauconitic sandstone (Figure 35), and a single olistostrome is fairly well exposed in a roadcut along Big Basin Road (Highway 236) about 1.1 km south of Waterman Gap (Figure 6).

The thickness of the olistostromal beds ranges from about 25 cm to more than 2 m. In general, the deposits consist of cobble to boulder sized clasts of mudstone, sandstone, quartzite, and other rock types in a matrix of fine to coarse sandstone. Most of the mudstone and sandstone clasts are angular and irregular in shape, and similar in lithology to the interchannel deposits of the Castle Rock unit described earlier in this report. Also present in some beds are large blocks, up to 2 m long, of chaotically deformed intervals of interbedded sandstone and mudstone; these are interpreted as large chunks of interchannel deposits that were eroded from channel walls or slump scars.

The depositional processes and significance of the olistostromes in the Castle Rock unit are difficult to pin down because the exposures are few and poor. The ones in the upper Zayante Creek section occur stratigraphically in an interval interpreted as middle fan channel and interchannel deposits, and therefore may represent sediments that slumped or were eroded from the sides of channels and were subsequently redeposited by channelized debris flows. These and the other olistostromes in the Castle Rock unit correspond to facies F in the scheme of Mutti and Ricci Lucchi (1972).

Bioturbated glauconitic sandstones. --

At least two horizons of bioturbated glauconitic sandstone occur within the Castle Rock unit. Both horizons are laterally persistent and have been correlated and mapped from one stream valley to another by Burchfiel (1958, 1964), McCollom (1959), and Brabb and Dibblee (1979). One of these glauconitic horizons was traced from the Twobar Creek area to near Inspiration Point on Highway 17, a distance of about 12 km, by McCollom (1959).

The glauconitic sandstones are poorly exposed. During the 1980-1982 field seasons I examined an outcrop in a landslide in the upper Zayante Creek section (Figure 35) and two outcrops along Bear Creek south of the Bear Creek Road bridge (Figure 6). In none of these outcrops are the upper or lower contacts exposed, but the glauconitic horizons appear to be about 2-4 m thick.

The glauconitic sandstones are green on fresh surfaces and weather to shades of reddish and orangish brown. They are generally medium to coarse grained and pebbly, and poorly sorted. They are thoroughly bioturbated; the burrowing is defined by textural and color mottling, and by knobby weathering surfaces.

Mineralogically, the sandstones consist of about 20-80% green glauconite, 15-60% quartz, 5-30% feldspar, and 0-5% lithic fragments. The glauconite grains are generally fine to medium sand size and ovoid to irregular in shape. The irregular grains appear to have originated as ovoid grains that were squashed between harder grains of quartz and feldspar during compaction. Some of the glauconite grains appear to be aggregates of several smaller grains cemented together by glauconite cement; apart from this, no internal microstructure was observed in the glauconite grains. The feldspars include both potassium feldspar and plagioclase. The lithic fragments are mainly chert, silicic volcanic rocks, and granitic rocks; granitic pebbles and cobbles occur scattered in the sandstone in the two outcrops along Bear Creek. Other mineral grains in the glauconitic sandstones include biotite, garnet, zircon, and other heavy minerals, but together these make up less than 1-2% of the rock. I found vertebrate bones up to 20 cm long in the upper Zayante Creek exposure; bones also occur in the Bear Creek and Twobar Creek areas, according to Burchfiel (1958).

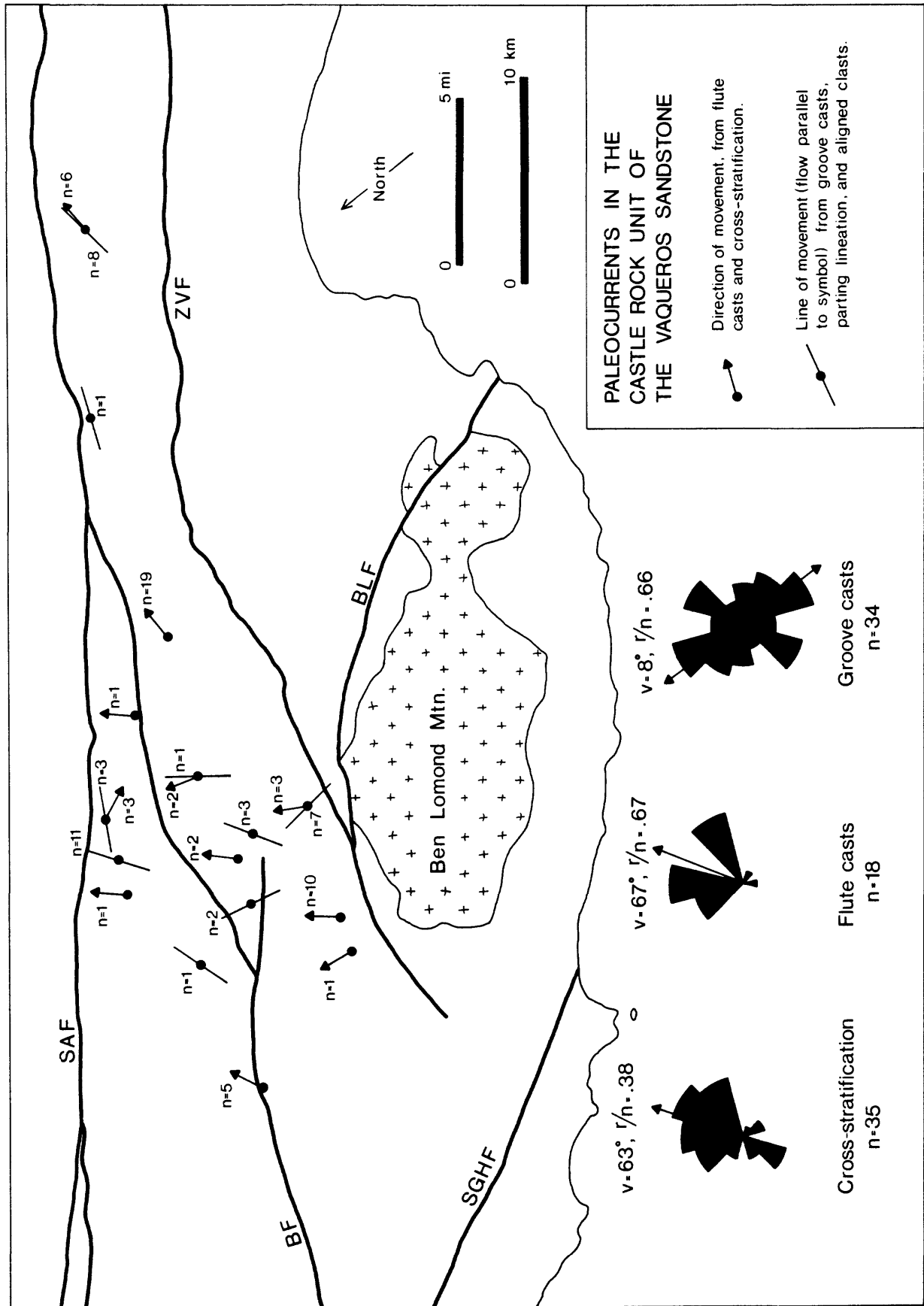
The glauconitic sandstones range from friable to hard. The most common cement is a nearly isotropic, very fine grained material apparently composed of clays and limonite(?), but small amounts of glauconite and calcite cement also occur.

The origin and stratigraphic significance of the glauconitic sandstones are unknown, in large part because the exposures are so poor. They *may* represent sands that were transported from shallow water and redeposited in deeper water on the Castle Rock fan; however, the sandstones are thoroughly bioturbated and no evidence of deposition from turbidity currents or other sediment gravity flows has been observed. Alternatively, the Castle Rock glauconitic sandstones may be analogous to the basal Refugian and basal Zemorrian glauconites of the Rices Mudstone, and may represent periods during which sedimentation on the Castle Rock submarine fan slowed considerably and perhaps stopped altogether. However, the glauconitic horizons of the Castle Rock unit do not correspond to any important biostratigraphic breaks, at least as far as is known. Speculatively, the Castle Rock glauconitic horizons may mark disconformities and represent periods of abrupt subsidence or abrupt eustatic rises in sea level that resulted in drowning of sediment sources, trapping of sediments in shallow-marine and nonmarine settings, and temporary cessation of sedimentation on the Castle Rock submarine fan.

Paleocurrents

About 90 paleocurrent measurements, mainly from flute casts, groove casts, and ripple cross-lamination, were obtained from the Castle Rock unit (Figure 41, Appendix 5). The measurements were made in the field without regard to stratigraphic position, but most of them appear to be from the lower Zemorrian part of the unit.

Figure 41. Paleocurrents in the Castle Rock unit of the Vaqueros Sandstone. Map shows vector mean (v) and number of measurements (n) at each locality. Major faults labeled as follows: BF = Butano fault, BLF = Ben Lomond fault, SAF = San Andreas fault, SGHF = San Gregorio-Hosgri fault, ZVF = Zayante-Vergeles fault. Rose diagrams summarize measurements from all localities on cross-stratification, flute casts, and groove casts; r/n = vector strength.



These limited data suggest that the dominant direction of sediment transport was to the north and northeast. The paleocurrents define a generally radial pattern emanating from a weakly-defined vertex in the Boulder Creek area (Figure 41). This radial pattern is consistent with interpretation of the Castle Rock unit as an ancient submarine fan. The scatter in the paleocurrent data, viewed in terms of the model of sediment dispersal on submarine fans proposed by Nilsen and Simoni (1973), probably is the result of downfan transport of sediment along channels that were meandering and braided (rather than straight), as well as overbank transport of sediment out and away from the channels.

Large-scale Variations in Lithology

Maps of sandstone grain size and sandstone-to-mudstone ratio prepared by McCollom (1959) show that the Castle Rock unit of the Vaqueros Sandstone becomes generally finer grained to the north and northeast of the Boulder Creek area (Figure 42). McCollom's maps, combined with the paleocurrent data in Figure 41, suggest that the main source of sediment for at least the lower part of the Castle Rock submarine fan was located southwest of the Zayante-Vergeles fault in the general area of Boulder Creek.

Measured stratigraphic sections by me and by Burchfiel (1958, 1964), McCollom (1959), Brabb (1960), and Brabb and others (1977) show the following vertical trends in the Castle Rock unit: (1) an upward increase in the average grain size of sandstone beds; (2) an upward increase in the average thickness of sandstone beds; and (3) an upward increase in the ratio of sandstone to mudstone. This general upward coarsening, combined with evidence discussed earlier in this report that the lower part of the Castle Rock unit was deposited on outer-fan lobes while higher parts were deposited in middle-fan environments, suggests that the Castle Rock unit represents a prograding submarine fan that records a major Oligocene regression.

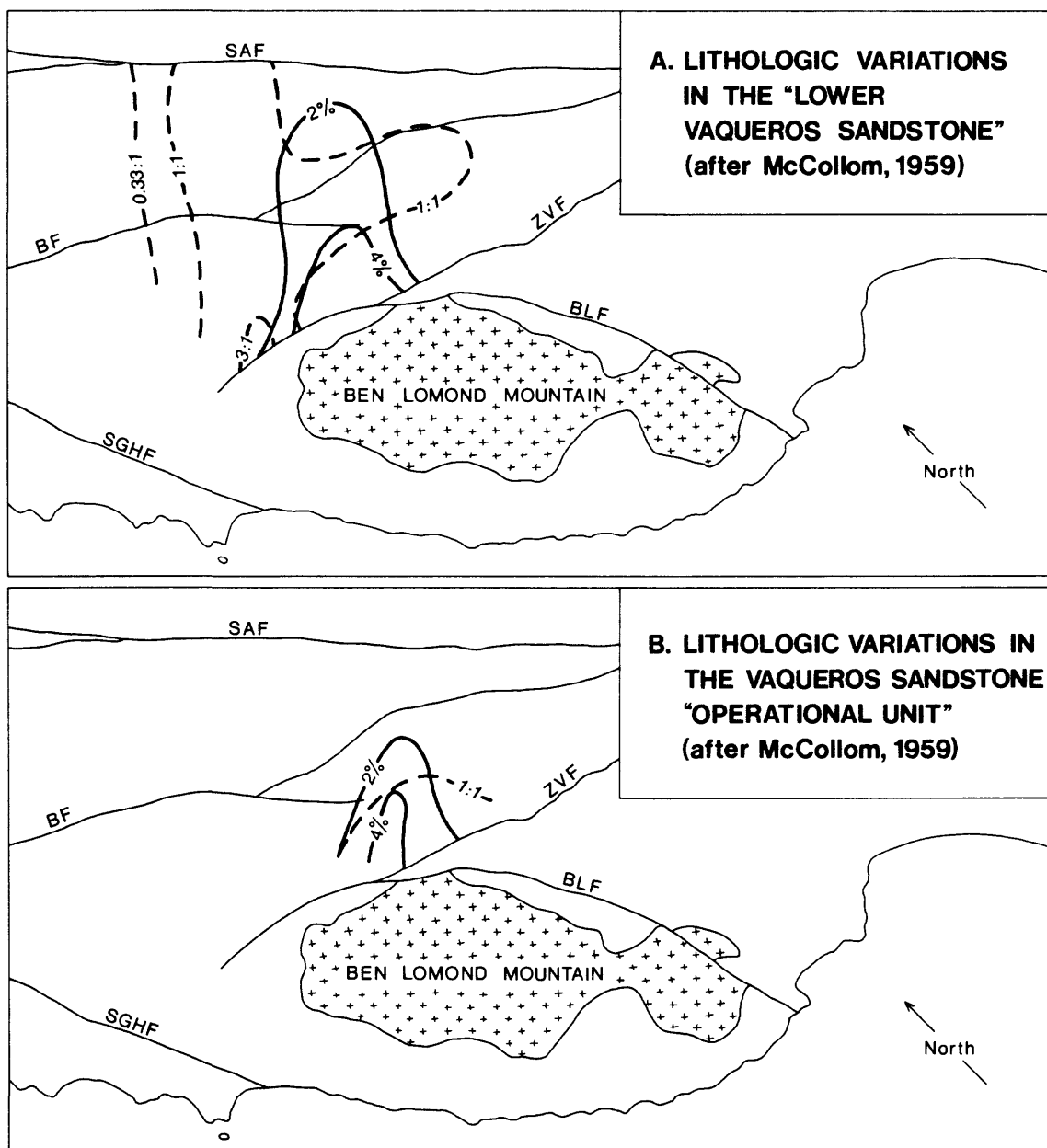
Depositional Systems and Provenance

The Castle Rock unit of the Vaqueros Sandstone most likely was deposited by north- and northwest-flowing turbidity currents and other kinds of sediment gravity flows on a prograding submarine fan. A submarine fan origin is supported by: (1) evidence from foraminiferal paleobathymetry of deposition in water deeper than 1500 m to 2000 m; (2) abundant evidence from sedimentary textures and structures of deposition by turbidity currents and related processes; (3) the occurrence of identifiable outer-fan lobe and middle-fan channel and interchannel deposits; (4) the generally radial paleocurrent pattern; and (5) the generally radial patterns of changes in sandstone grain size and sandstone-to-mudstone ratio.

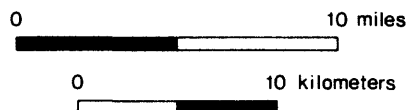
The main source of sediment for the Castle Rock submarine fan was probably an area of uplifted granitic basement located southwest of the Zayante-Vergeles fault. Evidence for a granitic provenance includes the quartzofeldspathic mineralogy of the sandstone, the presence of up to 5% fresh grains of detrital biotite, the common occurrence of granitic granules and pebbles, and the compositions of the heavy mineral assemblages studied by Beveridge (1958, 1960).

QFL plots (Figure 43) show that the composition of the Castle Rock unit is similar to that of the Eocene Butano Sandstone, suggesting that both the Castle Rock and Butano sands were derived from the same source area southwest of the Zayante-Vergeles fault. The composition of the Castle Rock unit is also generally similar to, but somewhat less lithic than coeval sandstones in the Salinas basin (Figure 43). This similarity in composition is consistent with the conclusion of Graham (1976, 1978) that a mountainous granitic peninsula, located roughly in the area of the modern Monterey Bay, served as a sediment source for both the La Honda and Salinas basins. Sediment shed northward from this granitic highland was probably transported by rivers to deltaic and shelf environments represented by the Zayante Sandstone and the Laurel unit of the Vaqueros Sandstone; much of this sediment was eventually carried into deeper water and deposited on the Castle Rock submarine fan. Sediment shed southward from the granitic peninsula into the Salinas basin was deposited mainly in nonmarine and shallow-marine shelf

Figure 42. Maps of lithologic variation in the Vaqueros Sandstone, redrawn from McCollom (1959). A: Variations in the "lower Vaqueros Sandstone," defined by McCollom as the stratigraphically lowest 900 feet (275 m) of the formation above the contact with the underlying Rices Mudstone. B: Variations in the "operational unit" of the Vaqueros Sandstone, defined by McCollom as the stratigraphic interval from the contact with the Rices Mudstone upward to a distinctive bed of glauconitic sandstone that McCollom found in several places in the Boulder Creek area. Both the "operational unit" and the "lower Vaqueros Sandstone" of McCollom are included within the Castle Rock unit of the Vaqueros Sandstone. Major faults are labeled as in Figure 41.



**SCALE AND KEY
FOR MAPS "A" AND "B":**







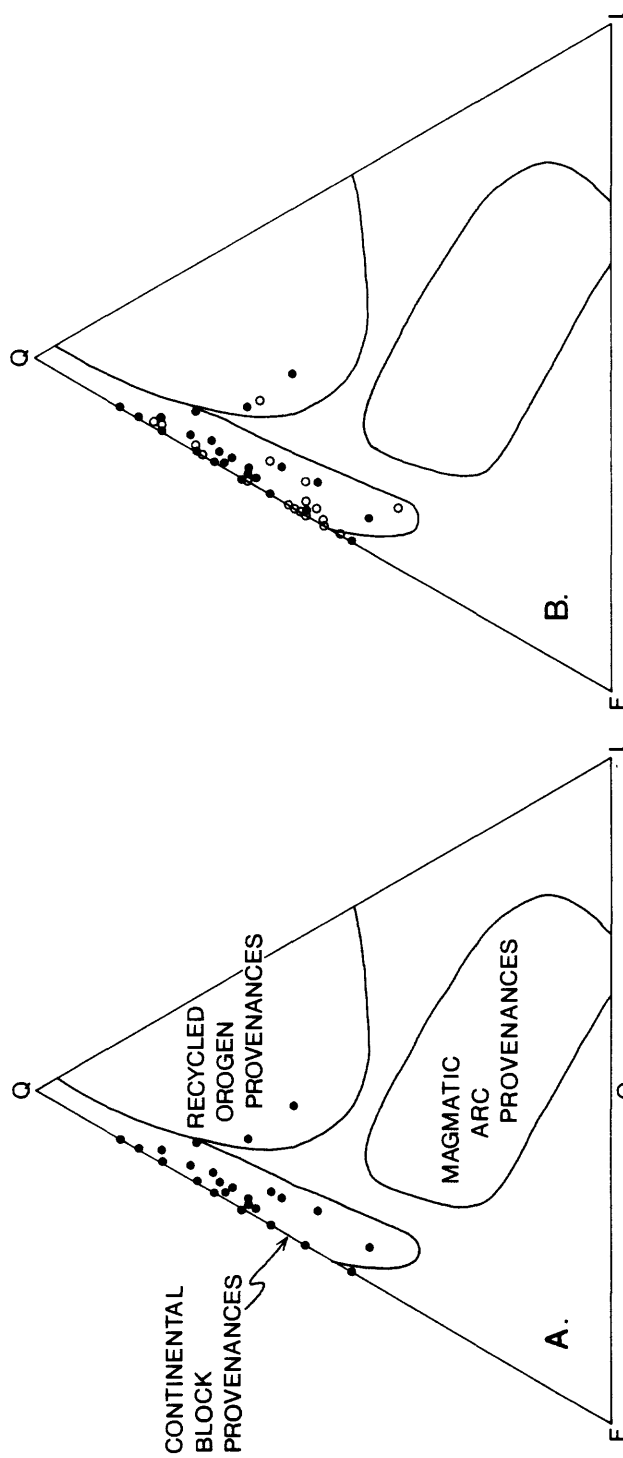
- | | |
|---|--|
|  | Ratio of sandstone to mudstone |
|  | Percentage of grains coarser than medium sand (0.5 mm) |
|  | Major fault |
|  | Basement outcrop |

Figure 43. QFL (quartz, feldspar, lithic) plots of the detrital mineralogy of some middle Tertiary sandstones in the La Honda and Salinas basins. Data for the Castle Rock unit of the Vaqueros Sandstone and the Butano Sandstone were compiled from petrographic and sieve data of Cummings (1960, p. 198-199) and Brabb (1960, p. 25 and p. 60), and recalculated using the categories of Dickinson (1970). A: Comparison of the composition of the Castle Rock unit with the provenance fields of Dickinson and Suczek (1979). B: Comparison of the composition of the Castle Rock unit (Oligocene and lower Miocene) with that of the Butano Sandstone (Eocene). C: Comparison of the Castle Rock unit with Oligocene and lower Miocene sandstones of the Salinas basin reported by Graham (1976).



SANDSTONE COMPOSITIONS

- Castle Rock unit of the Vaqueros Sandstone, La Honda basin
- Butano Sandstone, La Honda basin
- + Oligocene and lower Miocene sandstones of the Salinas basin (Graham, 1976)

environments represented by the Berry Formation and the Vaqueros Sandstone (Graham, 1976).

Detrital grains of glaucophane are present but extremely rare in the Vaqueros Sandstone of the La Honda basin (Beveridge, 1958, 1960). Nevertheless, the occurrence of glaucophane was cited by Cummings and others (1962) as evidence that some of the sand in the Vaqueros was derived from an area of uplifted Franciscan rocks located east of the San Andreas fault. This interpretation is rejected here because of the small amount of glaucophane actually found, and because paleocurrents and other data (Figures 41 and 42) show that most if not all of the sediment was derived from the southwest, with no evidence for an eastern source. In addition, no detrital grains of serpentine, radiolarian chert, or other "typical" Franciscan lithologies have been reported from the Vaqueros Sandstone of the La Honda basin.

Laurel unit of the Vaqueros Sandstone

Introduction

The Laurel unit consists mainly of bioturbated and massive to cross-laminated sandstone with minor interbeds of conglomerate and mudrocks. In some places, for example in the lower Zayante Creek section (Figure 44), basalt and fossiliferous limestone occur near the base of the unit; these rocks are described later in this report in the section on the Mindego Basalt.

The Laurel unit is named informally in this report for intermittent exposures along Hinckley Creek in the Laurel Quadrangle (Figure 23). Other outcrops of the Laurel unit occur along Twobar Creek (Figure 34) and along lower Zayante Creek (Figure 44) but in none of these areas are the exposures good enough to allow detailed studies of sedimentology.

Geographically, the Laurel unit is restricted in outcrop and in the subsurface to a narrow belt parallel and adjacent to the Zayante-Vergeles fault (Figure 32).

Age

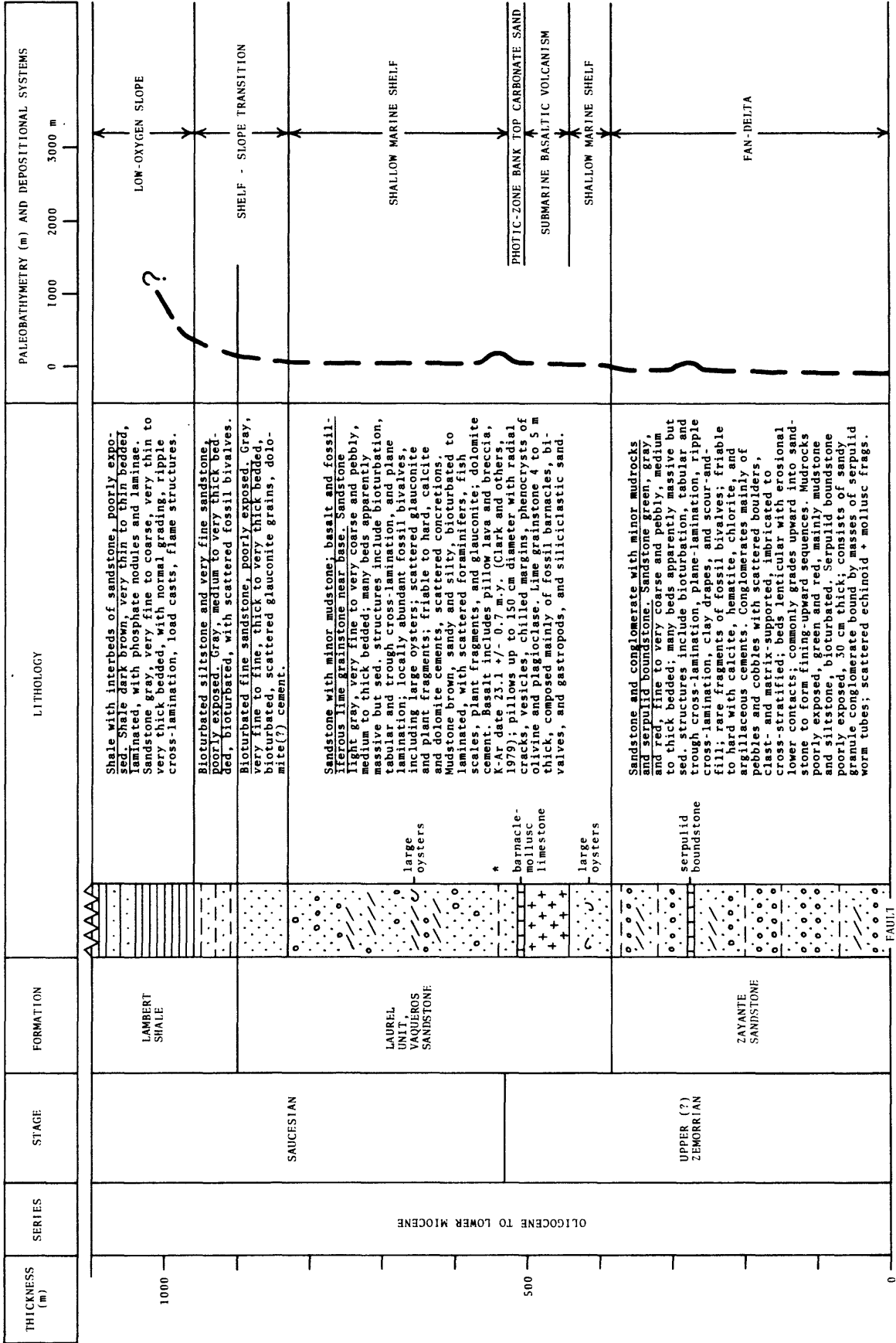
The age of the Laurel unit has been determined with confidence only in the lower Zayante Creek section (Figure 44). In this area, a horizon of basaltic pillow lava that occurs about 80 m stratigraphically above the base of the unit has been dated at 23.1 ± 0.7 m.y. by the potassium-argon method (Turner, 1970). The basalt is immediately overlain by a fossiliferous limestone that contains an abundant and diverse assemblage of molluscs assigned by Clark (1966, 1981) to the uppermost Vaqueros Stage of Addicott (1972) and the uppermost Zemorrian Stage of Kleinpell (1938). About 30 to 45 m stratigraphically above the basalt, Clark (1966, 1981) collected benthic foraminifers of the Saucesian Stage from a mudstone interbed. Thus, in the lower Zayante Creek section, the Laurel unit is of late Zemorrian and Saucesian age.

In the Corralitos area, about 24 km southeast of the lower Zayante Creek section, the Texaco J.H. Blake #1 well encountered the Saucesian Lambert Shale at drilled depths of 5097 to 5373 feet (Figure 15; Appendix 4). Beneath the Lambert and down to the total drilled depth of 7522 feet, the well penetrated a sequence of coarse sandstone, conglomerate, and mudrock that reportedly contains "very weak" Saucesian to Zemorrian fossils. I correlate this sequence with the Laurel unit in the lower Zayante Creek section on the basis of similar lithology and stratigraphic position.

In summary, available data from outcrops and a single well indicate that the Laurel unit is of late Zemorrian and Saucesian age and was deposited sometime between 30 m.y. and 18 m.y. ago, using the correlations with the radiometric time scale in Figure 9. In the lower Zayante Creek section, most of the unit was deposited after the eruption of a basaltic pillow lava about 23 m.y. ago.

Figure 44. Inferred stratigraphy, paleobathymetry, and depositional systems for the lower Zayante Creek section, on the south limb of the San Lorenzo syncline. See Figure 6 for location. Stratigraphic nomenclature and thicknesses in part from Brabb and others (1977). Thickness of Zayante Sandstone measured with tape and Brunton compass in October 1980 by H. Gibbons and R. Stanley. Lithology shown schematically.

LOWER ZAYANTE CREEK SECTION, SOUTH LIMB OF SAN LORENZO SYNCLINE



*=Paleontological sample location.

Stratigraphic Relations

The stratigraphic relations of the Laurel unit are complex (Figure 14). In general, the Laurel unit consists of shallow marine shelf sandstones that are laterally equivalent to the nonmarine Zayante Sandstone to the southwest, and deeper-water sandstones and mudrocks of late Zemorrian to Saucesian age—including the Castle Rock unit and the Lambert shale—to the northeast. Along the southwestern margin of the La Honda block, the Laurel unit rests unconformably on the older, lower Zemorrian part of the Castle Rock unit (Figure 14). Evidence for these interpretations is discussed below.

The lateral equivalence of the Laurel unit and the Zayante Sandstone is suggested by the conformable and interfingering contact between the two units. This contact is well-exposed along an unnamed dirt road in Mountain Charlie Gulch about 2 km east of the lower Zayante Creek section (Figure 45). The interfingering of the Laurel unit and the Zayante Sandstone occurs over an interval that stratigraphically is at least 175 m thick.

The inferred lateral equivalence of the Laurel unit to parts of the Castle Rock unit and Lambert Shale is based mainly on biostratigraphic evidence. In the lower Zayante Creek section (Figure 44) the Laurel unit is of late Zemorrian and Saucesian age, as previously discussed. Less than 2 km to the north in the upper Zayante Creek section (Figure 35), the shelf sandstones of the Laurel unit are missing, and in their place are upper Zemorrian to Saucesian deeper-water sandstones and mudrocks of the Castle Rock unit and the Lambert shale.

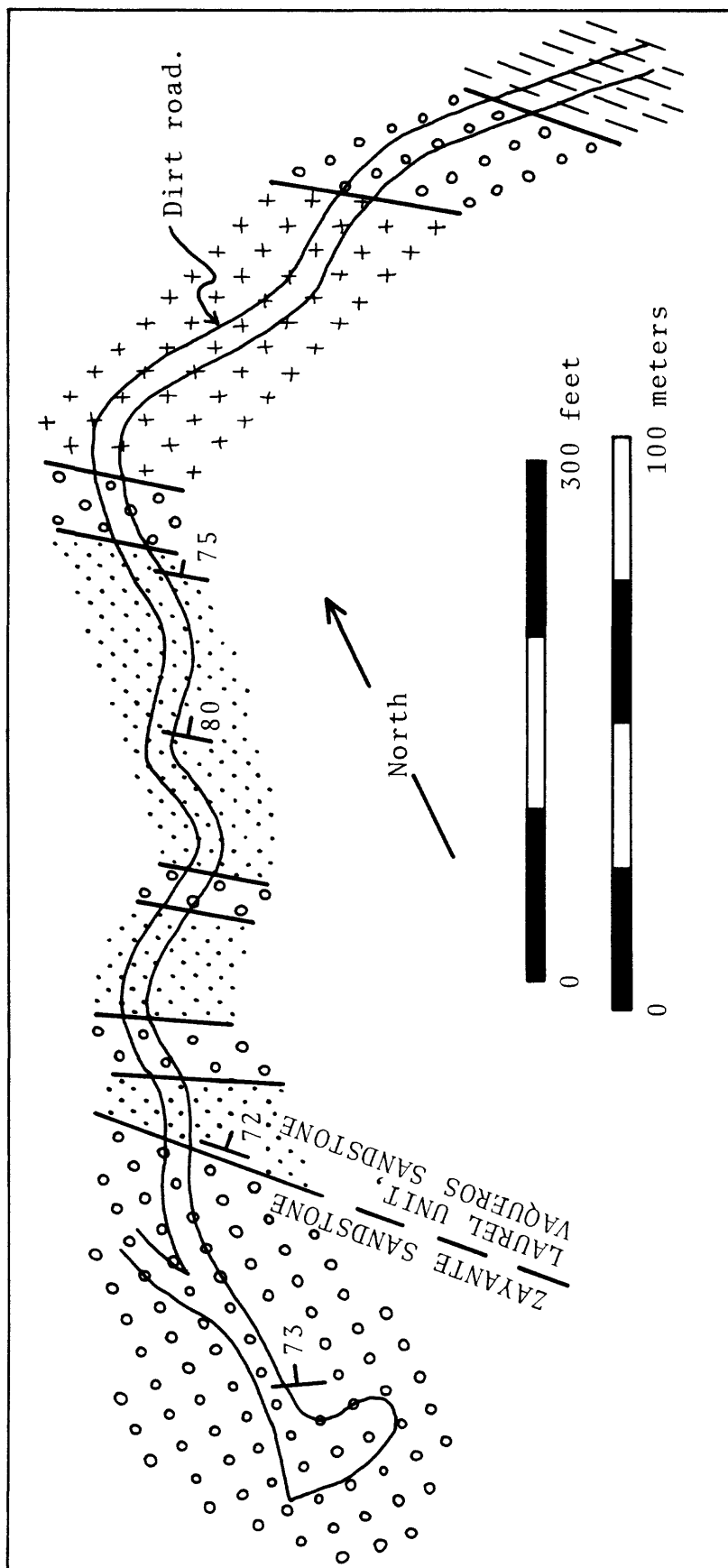
Middle Oligocene Unconformity

A major unconformity of probable middle Oligocene age occurs along the southwestern margin of the La Honda block near the Zayante-Vergeles fault. The unconformity is nowhere clearly exposed but is inferred from evidence discussed below. Along this inferred unconformity, deeper water strata of early Zemorrian age—including the Castle Rock unit of the Vaqueros Sandstone and possibly also the Rices Mudstone—are abruptly overlain by shallow marine and nonmarine strata of late Zemorrian to Saucesian age, including the Laurel unit of the Vaqueros Sandstone and the Zayante Sandstone (Figure 14).

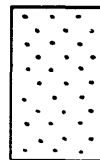
In the Twobar Creek section (Figure 34), the Castle Rock unit is overlain by the Laurel unit. The contact between the two units is covered by vegetation but is probably abrupt, because the covered stratigraphic interval is less than 5 m thick. Bedding attitudes in the two units appear to be concordant. The Castle Rock and Laurel units contrast strongly with each other in lithology and inferred depositional setting. The Castle Rock unit consists mainly of turbidite sandstone and mudrocks that were deposited on the outer to middle(?) parts of a submarine fan at water depths greater than 2000 m. The Laurel unit, as discussed below, consists of bioturbated and massive to cross-laminated sandstone that was deposited on a shallow marine shelf at water depths less than 150 m. Thus, the contact between the Castle Rock and Laurel units represents a sudden change in depositional setting from middle fan to shelf. Missing from the contact are upper fan, feeder channel, and slope facies that would be expected in a conformable regressive sequence from middle fan to shelf, using Walther's law and the submarine fan models of Walker (1978) and Mutti and Ricci Lucchi (1972). In addition, the contact represents a very quick shoaling of about 2000 m from lower bathyal to shelf depths. Because of the missing facies and abrupt shoaling, I conclude that the contact between the Castle Rock and Laurel units is best interpreted as an unconformity.

In the Soquel Creek-Hinckley Creek section (Figure 23) about 20 km southeast of the Twobar Creek section, the Castle rock unit is overlain by the Zayante Sandstone. The contact is not exposed and is apparently concordant, but is inferred to be an unconformity because lower bathyal turbidites of the Castle Rock unit are abruptly overlain by nonmarine red and green sandstones of the Zayante Sandstone (Figure 23). I tentatively correlate this unconformity with the one between the Castle Rock and Laurel units in the Twobar Creek section, based on the presumption that the Laurel unit and the Zayante Sandstone are for the most part laterally equivalent to each other (Figure 14).

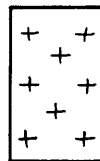
Figure 45. Geologic sketch map of the inferred interfingering contact between the Zayante Sandstone and the overlying and laterally equivalent Laurel unit of the Vaqueros Sandstone. The unnamed dirt road is on the east side of Mountain Charlie Gulch, at the eastern edge of the Felton quadrangle (Sec. 32-9S-1W). Surveyed with tape and Brunton compass in October 1980 by H. Gibbons and R. Stanley.



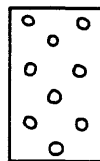
Santa Cruz Mudstone(?)



Rocks "typical" of the Laurel unit, Vaqueros Sandstone: white-weathering, well-sorted, fine to coarse sandstone, cross-laminated to bioturbated; interbeds of pebble conglomerate and white to brown mudstone.



Basalt, poorly exposed.



Rocks "typical" of the Zayante Sandstone: orange-weathering pebble and cobble conglomerate, with interbeds of orange-weathering, fine to very coarse, poorly sorted sandstone and minor interbeds of green mudstone.

The unconformity in the Twobar Creek and Soquel-Hinckley sections is probably of middle Oligocene age, based on the following evidence. In both areas the unconformity occurs at the top of lower Zemorrian strata of the Castle Rock unit, and therefore can be no older than the base of the lower Zemorrian, or about 37 m.y. (Figure 9). The unconformity is overlain by the Laurel unit and by the Zayante Sandstone, which have yielded no age-diagnostic fossils in either the Twobar Creek or Soquel-Hinckley areas. However, as discussed earlier, the base of the Laurel unit in the lower Zayante Creek section must be older than about 23 m.y., based on radiometric dating of a basaltic pillow lava within the unit. Thus, the unconformity between the Castle Rock and the overlying Laurel and Zayante Sandstone must be older than 23 m.y.; in fact, it may be several million years older, because more than 380 m of the Laurel unit and Zayante Sandstone occur *below* the dated basalt in the lower Zayante Creek section (Figure 44). To summarize, available radiometric and biostratigraphic data indicate that the unconformity is no older than 37 m.y. and no younger than 23 m.y.

I speculate that this unconformity is correlative with major eustatic and/or tectonic events that occurred about 29 to 30 m.y. ago. According to Vail and Hardenbol (1979), eustatic sea level fell more than 200 m about 29 m.y. ago. The amount of this drop—about 200 m—is an order of magnitude less than the 2000 m of shoaling indicated by foraminiferal paleobathymetry in the Twobar Creek and Soquel-Hinckley sections (Figures 23 and 34). Thus, much or all of the shoaling must have been caused by tectonic uplift. The uplift may have been associated with movement during the Oligocene along the Zayante-Vergeles fault (Clark, 1966; Clark and Rietman, 1973). Uplift in the Twobar Creek and Soquel-Hinckley areas, as well as movement along the Zayante-Vergeles fault, may have been among the tectonic effects of the collision of the Farallon-Pacific spreading center with the Farallon-North America trench about 29 to 30 m.y. ago (Atwater, 1970; Atwater and Molnar, 1973; Nilsen, 1982).

Lithology

The major categories of rocks in the Laurel unit of the Vaqueros Sandstone are: (1) massive to bioturbated and cross-laminated feldspathic sandstones; (2) conglomerate; and (3) mudrocks. More than 90% of the Laurel unit is sandstone, while conglomerate and mudrocks each make up less than 5%.

Sandstones. --

Feldspathic arenite and wacke are the most abundant rocks in the Laurel unit, and typically form fern- and moss-covered cliffs and waterfalls along stream valleys. The sandstones are generally light gray to bluish gray on fresh surfaces, and weather brown to white where not covered by vegetation. They range from very fine to very coarse and pebbly; some beds contain scattered cobbles and boulders of granitic rocks. Sorting ranges from moderate to good in the fine and medium sandstones, but is generally poor in the coarser ones. Rounding also appears to be correlated with grain size, with the coarser sand grains and larger clasts generally better rounded than the medium and smaller sand grains.

Mineralogically, the sandstones consist of about 40-70% quartz, 15-30% potassium feldspar, 5-20% plagioclase, 5-25% lithic fragments, and 0-15% biotite, based on visual estimates of 16 thin-sections. The feldspars and biotite are generally fresh-appearing and relatively unaltered. The lithic fragments include granitic rocks, chert, silicic and basaltic volcanic rocks, fine sandstone and siltstone, mica schist, quartzite, and other unidentified lithologies. Also present are detrital sand-sized grains of glauconite, muscovite, hornblende, zircon, and other heavy minerals, but together these make up less than 1-2% of most specimens. Shell fragments—mainly rounded pieces of molluscs and echinoids—are locally abundant and make up more than 20% of some rocks. The sandstones range from friable to hard and well-cemented; calcite and dolomite are the most common cements, and calcitic and dolomitic concretions are fairly common.

Stratification and sedimentary structures in the sandstones are difficult to study in detail because most outcrops are covered by moss. In general, the sandstone occurs as intervals from one m to several tens of m thick. Most of these intervals appear to be composed of amalgamated medium to very thick

beds. Most of the beds are apparently massive, but bioturbation, tabular and trough cross-lamination, and plane lamination are visible in some outcrops (Figures 46 and 47). The bioturbation is marked mainly by textural and color mottling (Figure 47) but in some outcrops individual burrows weather out in knobby relief. The amalgamation horizons are marked by abrupt changes in grain size and by erosional truncations of burrows and cross-lamination. In outcrops where amalgamation horizons are not visible, stratification is often crudely defined by differential resistance to weathering and by the alignment of lenticular concretions parallel to bedding.

Megafossils and fossil fragments are common and include oysters and other bivalves, gastropods, barnacles, and sand dollars (Figure 46). Many of the megafossils appear to be well-preserved but could not be extracted from the well-cemented sandstones without destroying them, and therefore they were not collected or further identified.

The megafossils and fossil fragments generally occur scattered in bioturbated or cross-laminated sandstones (Figure 46) but in some outcrops they are concentrated in lenses. One such lens in the Twobar Creek section (Figure 34) is about one m thick at its thickest point, and consists of fragments and whole fossils of oysters that form a clast-supported network with a matrix of medium sandstone. This oyster-shell accumulation may represent an ancient oyster reef similar to modern reefs found along the Gulf and Atlantic coasts of the United States (Price, 1968; Milliman, 1974). Alternatively, it may represent a shelly lag deposit left behind by storms, such as is found on the modern Oregon shelf in water depths of 20 to 30 m (Dupre and others, 1980, p. 107). Other lenses of fossil shells, some consisting of unidentified bivalves other than oysters, are exposed along the lower Zayante Creek section (Figure 44) as well as along Hinckley and Aptos Creeks (Figure 6).

Plant fragments are scattered in many of the sandstones but generally make up less than 1-2% of the rock. However, a bed near the top of the Twobar Creek section (Figure 34) consists of large angular clasts of lignite, well-preserved barnacles, and well-rounded pebbles scattered in a sandstone matrix. The bed is about 30 cm thick and consists of about 20-30% lignite. Another lignite interbed along Love Creek was mined for local use around the turn of the century according to Clark (1981); I was unable to visit this outcrop, but map relationships suggest that it probably occurs stratigraphically within the Laurel unit.

Conglomerates. --

Beds of clast-supported granule and pebble conglomerate are scattered through most of the Laurel unit but are volumetrically unimportant. The beds are generally 10 to 50 cm thick; most are lenticular and pinch out along the outcrop, but a few are laterally persistent for 15 m or more. Some of the beds exhibit clast imbrication. Most beds consist of well-rounded granules and pebbles of granitic rocks, black chert, white quartz, porphyritic and banded silicic volcanic rocks, and mica schist. In addition, angular cobbles and boulders of granitic rocks and mica schist occur locally, and seem to be most common in the Twobar Creek section. Most of the conglomerate beds have a sandstone matrix and are cemented by calcite or dolomite.

Mudrocks. --

Mudrocks in the Laurel unit are volumetrically unimportant and poorly exposed. Most are various shades of brown on both fresh and weathered surfaces. The beds range from a few cm to more than 2 m thick. Most are bioturbated sandy mudstones and siltstones with scattered fossil foraminifers, fish scales, plant fragments, glauconite, and rare fossil bivalves. However, laminated shales occur in some outcrops, and the laminae are defined by the parallel alignment of mica flakes and fish scales.

A small assemblage of benthic foraminifers collected by Clark (1981) from mudrocks about 30 to 45 m stratigraphically above the basalt in the lower Zayante Creek section suggests deposition at water depths of about 150 m or greater (Figure 44, Appendix 1).



Figure 46. Outcrops of cross-laminated coarse sandstone in the Laurel Unit of the Vaqueros Sandstone. Top: Medium to thick bedded sandstone along the San Lorenzo River near the top of the Twobar Creek section (Figure 34). Bedding is emphasized by differential cementation and weathering of sandstone, dips gently to left, and is right side up. Note the tabular(?) cross-laminated beds at the waterline and at the hammer handle, which is about 28 cm long. Bottom: Cross-laminated sandstone with abundant fragments of sand dollars along Hinckley Creek. See Figure 6 for location. Bedding is nearly vertical and facing to the left. Hammer head is about 17 cm across.



Figure 47. Bioturbated fine sandstone in an outcrop near the top of the Laurel unit of the Vaqueros Sandstone in the upper Zayante Creek section (Figure 35). See Figure 6 for location. Both photographs are from the same outcrop; the pen is about 15 cm long. Top: Very thick bedded, bioturbated sandstone dipping away from camera at about 30° . Bed is right side up, but stratification is not visible in this photograph. Bottom: Detail of the same bed, showing bioturbation defined mainly by color mottling.

Paleocurrents

Only seven paleocurrent measurements, mainly on tabular(?) cross-stratification in the Twobar Creek section, were obtained from sandstones of the Laurel unit (Figure 48). The small data set reflects the poor outcrop and the lack of reliable bedding attitudes in areas of steep dips and complicated structure. The available paleocurrent data provide weak evidence for currents flowing predominantly to the southeast, or nearly perpendicular to the northeastward paleoslope indicated by paleocurrents and other data in the Castle Rock unit of the Vaqueros Sandstone (Figure 41) and in the Zayante Sandstone (Figure 53). The southeastward-flowing paleocurrents in the Laurel unit are roughly parallel to the inferred shoreline in paleogeographic reconstructions presented later in this report, and therefore may reflect sediment transport by longshore drift.

Depositional Systems and Provenance

The Laurel unit of the Vaqueros Sandstone was deposited mainly in high energy, well-oxygenated, shallow marine shelf environments. Evidence for this interpretation includes: (1) the common occurrence of fossil oysters, barnacles, and sand dollars which are typical inhabitants of modern shallow-marine environments (Heckel, 1972); (2) the occurrence of lenses of oyster and other bivalve shells, which probably represent oyster reefs and/or storm-caused lag deposits; (3) the presence of glauconite, which forms only in marine environments (Odin and Matter, 1981); (4) the coarse texture, abundant cross-lamination, good rounding and sorting, and absence of mud matrix in many of the sandstones, indicating high-energy conditions and deposition mainly by traction processes; (5) the intense bioturbation of many of the sandstones, indicating well-oxygenated bottom waters and an active burrowing infauna; and (6) the occurrence in the lower Zayante Creek section (Figure 44) of a limestone, described later in this report in the section on the Mindego Basalt, that contains abundant fossil invertebrates and calcareous algae indicative of deposition in the photic zone.

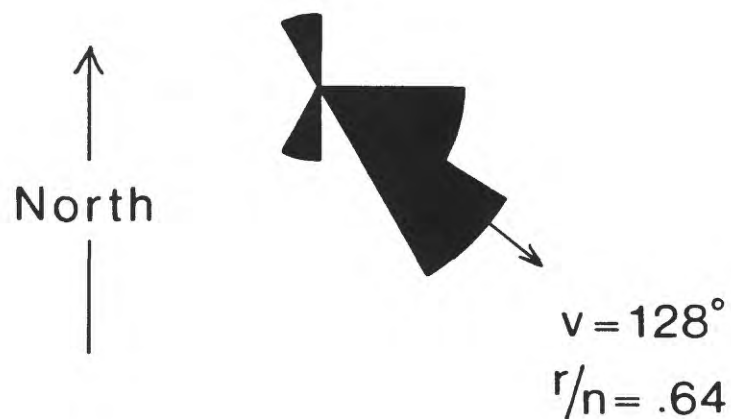
By analogy with modern shelf environments summarized by Johnson (1978), the tabular and trough cross-laminated sandstones were probably deposited by subaqueous sand waves and dunes in lower flow regime conditions, while the plane-laminated sandstones were deposited by more powerful currents of the upper flow regime. However, the specific processes that generated the depositing currents—for example, waves, storms, or tides—are unclear, mainly because the poor outcrops of the Laurel unit do not allow detailed studies of paleocurrents or recognition of critical sedimentary structures and vertical sequences (see Johnson, 1978, for criteria useful in distinguishing tidally-dominated shelves from storm- and wave-dominated shelves). The bioturbated sandstones and mudrocks probably represent periods of relatively quiet water when rates of biological reworking of the sediment exceeded rates of deposition and reworking by currents and waves.

A granitic provenance for the Laurel unit is suggested by the quartzofeldspathic mineralogy of the sand, the common occurrence of fresh detrital biotite, and the occurrence of large granitic clasts. The ultimate source of this sediment was probably the same mountainous granitic terrane that supplied sand to the Castle Rock submarine fan. Sediment eroded from the granitic source was probably transported generally north and northeastward by braided streams to a coarse-grained delta represented by the Zayante Sandstone. Sediments on the seaward fringes of this delta were reworked by marine processes to form a narrow shelf represented by the Laurel unit. Much sediment was carried seaward from this shelf and delta complex and redeposited in deeper water on the Castle Rock submarine fan.

Vaqueros Sandstone of the Woodside area

The Vaqueros Sandstone of the Woodside area consists mainly of feldspathic sandstone with interbeds of mudrocks, and minor amounts of pebble conglomerate and glauconitic sandstone. These rocks are very poorly exposed in a roughly triangular area bounded by the La Honda fault on the west, the Pilarcitos fault on the northeast, and the Sierra Morena anticline on the south (Figure 32).

PALEOCURRENTS IN THE
LAUREL UNIT,
VAQUEROS SANDSTONE



Tabular (?) cross-stratification
 $n=7$

Figure 48. Paleocurrents in the Laurel unit of the Vaqueros Sandstone. Rose diagram summarizes seven measurements on tabular (?) cross-stratification. Shown are vector mean (v), number of measurements (n), and vector strength (r/n).

The stratigraphic relations of the Vaqueros in this area are poorly understood, in large part because of the poor outcrop. The Vaqueros rests unconformably on the Narizian Butano Sandstone; this contact is evidently a disconformity in some places (Esser, 1958) and an angular unconformity in others (Classen, 1959). The Vaqueros is conformably overlain by the Lambert Shale (Mack, 1959). The thickness of the Vaqueros in the Woodside area is more than 670 m (Appendix 3), and thins southward by lateral interfingering with the overlying Lambert Shale (Figures 14 and 33). The interfingering of the Vaqueros and Lambert formations is clearly shown on geologic maps prepared by Esser (1958), Mack (1959), and Brabb (1970). Basaltic intrusions and interstratified basaltic lavas and breccias occur locally in the Vaqueros in the Woodside area and are assigned by Brabb (1970) and by me to the Mindego Basalt.

The Vaqueros Sandstone is not well dated in the Woodside area but appears to be of late Oligocene and early Miocene age. Assemblages of benthic foraminifers reported by Classen (1959) and Mack (1959) appear to be mainly of late Zemorrian age (Appendix 1). No planktic microfossils and no age-diagnostic megafossils have been reported. I infer that the Vaqueros Sandstone of the Woodside area is of late Zemorrian and Saucian age based on the microfossil assemblages noted above and on the interfingering of the Vaqueros with the overlying Lambert Shale, which is mainly of Saucian age in this area (Appendix 1; Mack, 1959).

The age of the unconformity at the base of the Vaqueros in the Woodside area is unknown, but must be younger than the Narizian Butano Sandstone and older than the upper Zemorrian Vaqueros Sandstone. The unconformity must be of Zemorrian age if, as seems likely, the Rices Mudstone was deposited in the Woodside area during the Refugian and early Zemorrian and was then removed by erosion prior to deposition of the Vaqueros during the late Zemorrian. Based on these limited data and assumptions, I speculate that the basal Vaqueros unconformity in the Woodside area is correlative with the middle Oligocene unconformity along the southwestern margin of the La Honda block (Figure 14).

The sedimentology of the Vaqueros Sandstone in the Woodside area has not been studied in detail. The following discussion is based mainly on the literature and on less than one day of field reconnaissance by me. The unit consists mainly of sandstone with interbedded mudrocks. The sandstones are very thin to very thick bedded, fine to very coarse and pebbly, generally poorly sorted, and consist mainly of feldspathic arenite and wacke. Mineralogically, they consist of 40-50% quartz, 35-50% feldspar, 5% lithics, and up to 5% biotite, suggesting a granitic provenance (Mack, 1959). Most beds are apparently massive but normal grading, plane lamination, ripple cross-lamination, and "flysch figures" (probably load casts and flame structures) also occur (Mack, 1959). The mudrocks range from mudstone to shale and contain assemblages of benthic foraminifers that indicate deposition at water depths of 500 m and greater (Appendix 1). Green glauconitic sandstones occur locally and may mark minor disconformities within the Vaqueros (Esser, 1958; Beaulieu, 1970).

These limited stratigraphic, paleontologic, and sedimentologic data suggest that the Vaqueros Sandstone of the Woodside area was deposited mainly at bathyal depths on a southward-sloping surface. Deposition may have been by turbidity currents on a submarine fan, but detailed sedimentological information to support this interpretation is not available. The main source of sediment was a granitic terrane to the north, perhaps Montara Mountain or a more northerly part of the Salinian block (Mack, 1959).

Zayante Sandstone

Introduction

The Zayante Sandstone consists mainly of conglomerate, green and red coarse sandstone, and green mudrocks. The formation was named by Clark (1966, 1981) who designated a type section along Zayante Creek on the south limb of the San Lorenzo syncline (Figures 6 and 44). The Zayante Sandstone was interpreted by Clark (1966, 1981) as representing an ancient alluvial fan, but new evidence discussed below suggests that the formation was deposited on a fan-delta by braided streams that flowed directly

into the marine La Honda sea.

Geographically, the Zayante Sandstone is limited to the southwestern part of the La Honda block (Figure 32). The formation is generally poorly exposed. During the 1980-1982 field seasons, intermittent exposures were present in the type section along Zayante Creek, and also along Lompico Creek, Soquel Creek, Hinckley Creek, and Mountain Charlie Gulch (Figure 6).

Thickness, Stratigraphic Relations, and Age

In its type section the Zayante Sandstone is at least 384 m thick (Figure 44, Appendix 3), but the lower part of the formation is not exposed due to faulting. In the Lompico Creek area, about 2.5 km west of the type section, the formation is about 550 m thick (Clark, 1981). From this depocenter in the Zayante-Lompico area, the Zayante Sandstone thins and pinches out to the west, north, and east, apparently by lateral interfingering with the Vaqueros Sandstone (Figure 14). In the Soquel Creek area about 11 km southeast of the type section, the Zayante Sandstone is only about 90 m thick (Appendix 3).

Map relations and sedimentological evidence suggest that the base of the Zayante Sandstone is a low-angle angular unconformity. In the Laurel and Loma Prieta quadrangles the Zayante Sandstone overlies the Castle Rock unit of the Vaqueros Sandstone (Dibblee and others, 1978; Dibblee and Brabb, 1980), but in the Newell Creek area of the Felton quadrangle the Zayante Sandstone overlies the Rices Mudstone (Clark, 1966, 1981).

During the 1980-1982 field seasons, the base of the Zayante Sandstone was nowhere clearly exposed. For example, along Hinckley Creek in the Laurel quadrangle, the thickness of the covered stratigraphic interval between the base of the exposed Zayante Sandstone and the top of the exposed Castle Rock unit of the Vaqueros Sandstone is about 40 to 50 m. Bedding attitudes in the two formations appear to be concordant, but the contact between the two is inferred to be an unconformity because of the strong contrast in depositional settings represented by the two units; the nonmarine Zayante Sandstone overlies the submarine fan turbidites of the Castle Rock unit without the intervening shelf and slope deposits that would be expected in a conformable regressive sequence.

In the Love Creek and Newell Creek areas, the contact between the Zayante Sandstone and the underlying Rices Mudstone is interpreted by Clark (1966, 1981) to be conformable and interfingering. Clark's interpretation is difficult to reconcile with the observations and conclusions presented in the two preceding paragraphs. During the 1980-1982 field seasons I was unable to examine Clark's key outcrops and confirm or refute his interpretations. The outcrops that Clark studied in the 1960s in Newell Creek are now covered by the Loch Lomond reservoir, and his outcrops along Love Creek are now evidently covered by soil and vegetation.

No age-diagnostic fossils have been found in the Zayante Sandstone, but the formation must be Zemorrian because it is stratigraphically sandwiched between two formations of Zemorrian age, the Rices Mudstone and the Vaqueros Sandstone (Figure 14; Clark, 1966, 1981). As discussed earlier in this report, the Zayante Sandstone and Laurel unit of the Vaqueros Sandstone may have been deposited following an episode of erosion due to regional uplift and a eustatic fall in sea level about 29-30 m.y. ago.

Lithology

The major categories of rocks in the Zayante Sandstone are (1) conglomerates, (2) sandstones, (3) mudrocks, and (4) serpulid boundstone. More than 90% of the exposed part of the formation is composed of conglomerate and sandstone; these two rock types commonly occur together in crude fining-upward sequences. About 10% of the formation is made up of mudrocks, but these are very poorly exposed and therefore their apparent abundance in outcrop may be less than their "true" relative abundance as might be measured in a core. Serpulid boundstone was found in only one outcrop and probably makes up less

than 1% of the formation.

Conglomerates. --

Conglomerates in the Zayante Sandstone are composed mainly of clasts of granitic rocks, mica schist, and silicic volcanic rocks, with lesser amounts of white quartz, quartzite, chert, older conglomerate, laminated shale, and calcite-cemented feldspathic sandstone. Most of the clasts are well-rounded and range from granule to cobble size, but angular boulders of granitic rock as much as 120 cm in diameter occur in some beds (Clark, 1981).

The conglomerates range from clast-supported to matrix-supported. The matrix in both types is poorly sorted coarse sandstone; no conglomerates with mud matrix have been noted. In places, both clast-supported and matrix-supported conglomerates are cemented by calcite. Calcitic concretions occur in some outcrops.

Most of the conglomerate beds are lenticular and enclosed by sandstone. The lenticularity of the conglomerates is fairly well exposed on the face of a cliff more than 30 m high that occurs at a right-angle bend in Mountain Charlie Gulch at the eastern edge of the Felton quadrangle (Sec. 32-9S-1W). The conglomerate lenses generally are 30-100 cm thick but some are more than 200 cm thick. Many of these lenses have sharp, erosional bases and clearly fill channels cut into the underlying strata.

Many of the conglomerates exhibit clast imbrication, and most are massive or crudely stratified (Figure 49). These conglomerates strongly resemble facies Gm in the classification of braided stream deposits proposed by Miall (1977, 1978), and therefore are interpreted as representing deposition during periods of high water flow on longitudinal and mid-channel bars in a braided stream.

Some of the channel-filling conglomerates in the Zayante Sandstone are trough cross-stratified and resemble facies Gt in the scheme of Miall (1977, 1978). The origin of such deposits is unclear. The trough cross-stratified conglomerates may represent: (1) deposition on the downstream faces of migrating gravelly dunes or other bedforms; (2) filling of scours or minor channels; or (3) lateral accretion on point bar surfaces or the low-angle margins of diagonal bars (Miall, 1977, 1978; Harms and others, 1982).

Some conglomerates in the Zayante Sandstone are partly or completely bioturbated, and generally occur as lenses that are entirely enclosed by bioturbated sandstone (Figure 50). These conglomerates have no counterpart in the braided stream lithofacies of Miall (1977, 1978), and their origin is uncertain. Perhaps the coarse sediment was deposited as gravel bars during floods and then reworked by sediment-churning organisms during periods of quiet water.

The facies Gm and Gt conglomerates in the Zayante Sandstone in many cases grade upward into coarse sandstone to form crude fining-upward sequences (Figure 51). Uncommonly, the sandstones in these sequences grade upward into mudrocks. These gravel-rich, mud-poor fining-upward sequences are generally similar to those in the "Donjek-type" model of braided stream deposition (Miall, 1977, 1978). The interpretation of such sequences is debatable; they may represent channel fill and abandonment, or alternatively they may represent lateral accretion by the growth of point bars (Miall, 1977).

Sandstones. --

Sandstones in the Zayante Sandstone are feldspathic arenites and wackes that exhibit a wide range of colors, textures and sedimentary structures. About 5-10% of the sandstones are red; most of the rest are green or gray on fresh surfaces and brown to orangish brown on weathered ones (Figures 50 and 52). Thin-section observations suggest that the colors reflect the mineralogy of both the cement and the detrital grains. The red sandstones are cemented by a very fine-grained material that is dark red and nearly isotropic in thin-section and appears to be a mixture of hematite and clay minerals. The green sandstones are generally rich in detrital biotite, which in most cases is partially or completely altered to green chlorite. Some of the green sandstones are cemented by calcite, but many are cemented by a very

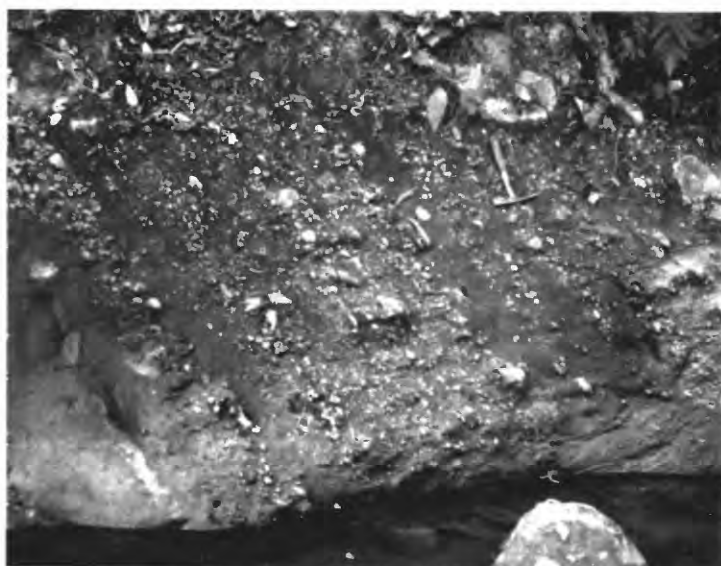


Figure 49. Outcrops of the Zayante Sandstone along the lower Zayante Creek section. See Figure 6 for location. Hammer handle in both photographs is about 28 cm long. Top: Green bioturbated muddy sandstone overlain by tabular cross-laminated coarse sandstone with several reactivation surfaces defined by laminae of green mudstone. Outcrop is about 250-300 m upstream (generally north) of the East Zayante Road bridge, Felton quadrangle, Sec. 30-9S-1W. Bottom: Plane- to cross-stratified coarse sandstone and conglomerate. Note imbrication of some clasts suggesting paleoflow generally to the right. Outcrop is about 150 m downstream (generally southwest) of the East Zayante Road bridge, Felton quadrangle, Sec. 31-9S-1W.

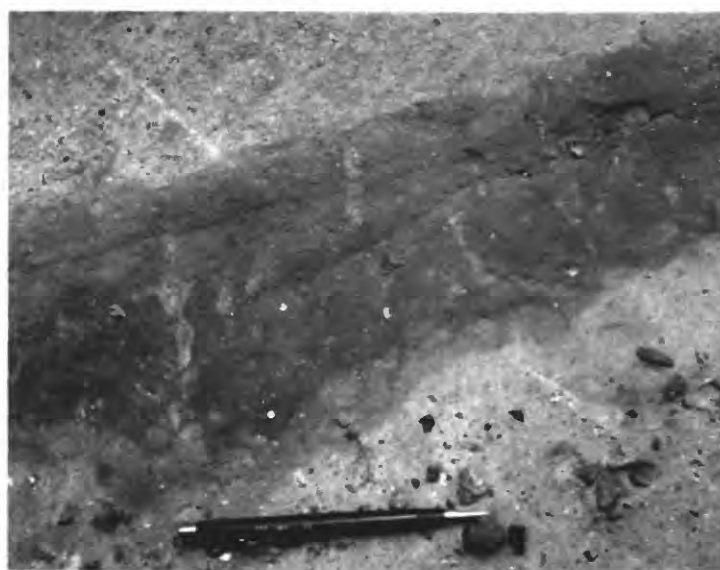
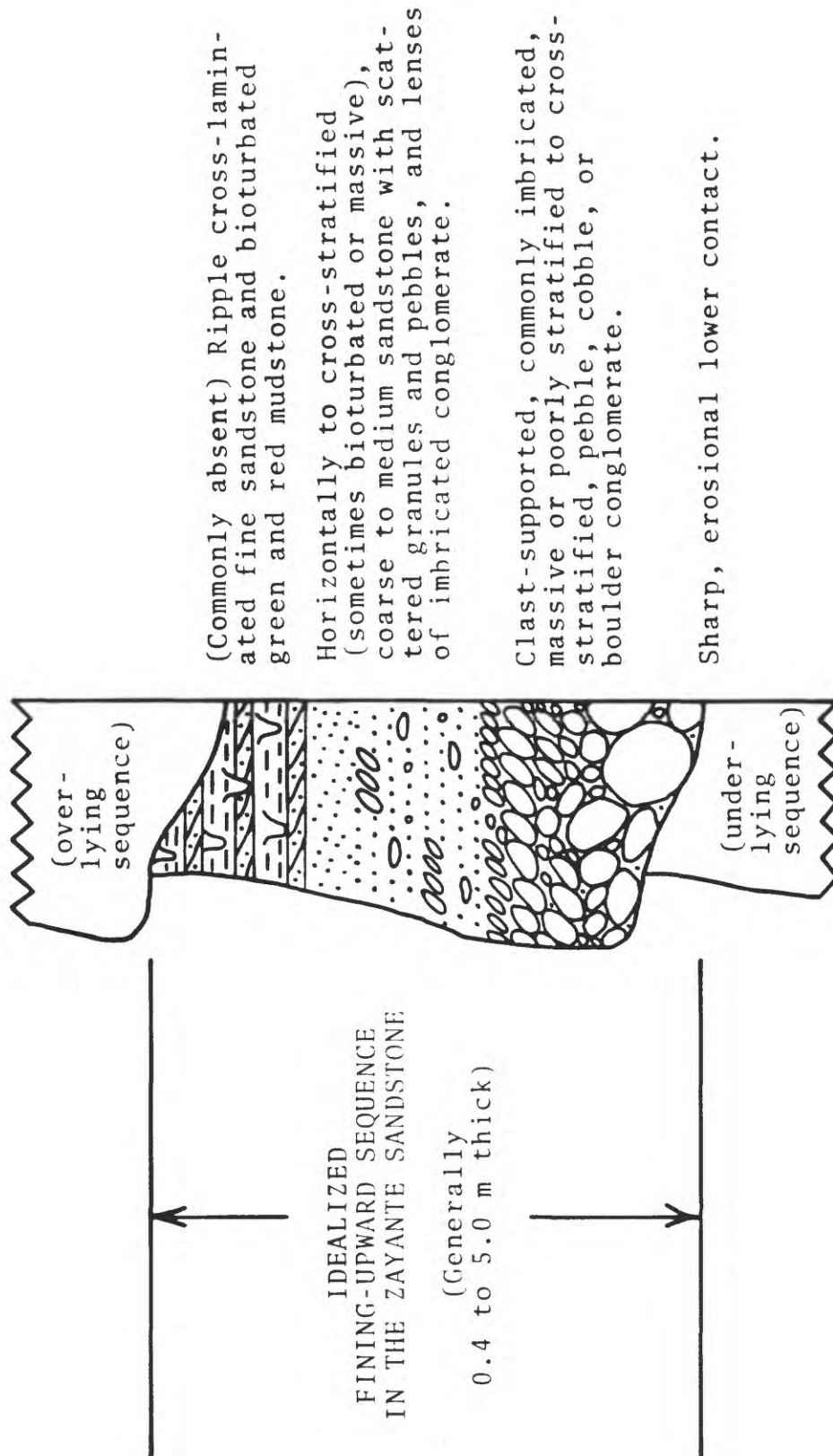


Figure 50. Sandstone and conglomerate in an outcrop of the Zayante Sandstone in an unnamed southward-flowing tributary to Mountain Charlie Gulch, center of Sec. 31-9S-1W in the Felton quadrangle. Top: Lenses of partly bioturbated pebble conglomerate enclosed by bioturbated red, green, and gray sandstone. Hammer handle is about 28 cm long. Bottom: Detail of bioturbated sandstone. Pencil is about 14 cm long.



(Commonly absent) Ripple cross-laminated fine sandstone and bioturbated green and red mudstone.

Horizontally to cross-stratified (sometimes bioturbated or massive), coarse to medium sandstone with scattered granules and pebbles, and lenses of imbricated conglomerate.

Clast-supported, commonly imbricated, massive or poorly stratified to cross-stratified, pebble, cobble, or boulder conglomerate.

Sharp, erosional lower contact.

Figure 51. Idealized fining-upward sequence in the Zayante Sandstone, based on observations of many outcrops along Lompico Creek, Mountain Charlie Gulch, and the lower Zayante Creek section. The origin of these fining-upward sequences is uncertain; they may represent fluvial channel-fill and abandonment, or lateral accretion by the growth of point bars.



Figure 52. Sandstones in the Zayante Sandstone. **Top:** Sawn slab of bioturbated (?) red and green mottled coarse sandstone from outcrop along Soquel Creek in the Laurel quadrangle. Scale in inches and centimeters. **Bottom:** Outcrop of bioturbated coarse sandstone with bivalve shell fragment, in the lower Zayante Creek section. Blue cap of pen is about 6 cm long. Outcrop is on the northeast side of the creek, about 200–250 m downstream (generally southwest) of the East Zayante Road bridge, Felton quadrangle, Sec. 31-9S-1W.

finely crystalline material with a platy habit and yellowish-green color that may consist of clays, chlorite, or a mixture of the two. The gray sandstones generally are cemented by calcite.

Sandstones in the Zayante Sandstone range from very fine to very coarse and pebbly. Most are poorly sorted with abundant angular grains, and some look like granitic grus. Well-sorted sandstones with mostly rounded grains also occur, however, and appear to be more abundant near the stratigraphic top of the formation.

Mineralogically, the sandstones consist of about 30-60% quartz, 10-35% potassium feldspar, 5-25% plagioclase, 0-20% lithic fragments, and 0-20% biotite, based on visual estimates of 29 thin-sections. Many of the feldspar grains are angular and relatively fresh. The most common lithic grains are chert, silicic volcanic rocks, granitic rocks, and fine sandstone and siltstone; also present but less common are basaltic(?) volcanic rocks, quartzite, mica schist, and unidentified foliated metamorphic rocks. Other detrital mineral grains in the sandstones include muscovite, chlorite, hematite, amphibole, zircon, and other heavy minerals, but these generally make up less than 1-2% of the rock.

The sandstones are generally lenticular and range from very thin to very thick bedded, but most are medium to thick bedded.

Common sedimentary structures in the medium to very coarse sandstones include tabular and trough cross-lamination, plane-lamination, scour-and-fill, and bioturbation (Figures 49, 50, and 52). Some beds are apparently massive. Reactivation surfaces, marked by clay drapes and very thin intervals of ripple cross-laminated sandstone, were observed in a tabular cross-laminated unit near the top of the formation in the lower Zayante Creek section (Figure 49). Scattered in some beds are angular clasts, generally 2-10 cm in diameter, of green mudstone and fine sandstone; these are interpreted as fragments of levee(?) and overbank deposits that were eroded from the sides and floors of fluvial channels and incorporated into the sandstone.

Common sedimentary structures in the very fine to fine sandstones include ripple cross-lamination, plane lamination, bioturbation, and small flakes of green mudstone that may represent dried mud chips eroded from mudcracks. (However, no mudcracks were observed in outcrop.) Clay drapes on ripple cross-laminated sandstone were noted in a few outcrops.

Bioturbation in the sandstones of the Zayante Sandstone is defined mainly by textural and color mottling, and ranges from discrete burrows scattered in thin cross-laminated beds to thoroughly burrowed and homogenized intervals several m thick. The organisms that caused the bioturbation are unknown. Some of the individual burrows are tubelike and backfilled, and most likely were created by burrowing invertebrates. Some of the bioturbation may be the result of terrestrial plant growth or trampling by terrestrial vertebrates but no definite root traces or isolated vertebrate tracks were noted.

Fossils are very rare and poorly preserved in the sandstones. A single bivalve fragment was found in a bioturbated sandstone along the lower Zayante Creek section (Figure 52). A second bivalve fragment was found in a concretion in cross-laminated coarse sandstone along Mountain Charlie Gulch, about 150 m north of a prominent right-angle bend in the gulch on the eastern edge of the Felton quadrangle (Sec. 32-9S-1W). Neither of these bivalve fragments was further identified.

Sandstones in the Zayante Sandstone exhibit a wide range of sedimentary textures and structures and probably represent a number of different depositional processes and environments within a braided-stream system. The cross-laminated and plane-laminated sandstones are similar to facies St, Sp, Sr, and Sh of Miall (1977, 1978) and probably represent deposition by migrating subaqueous dunes, sand waves, ripples, and other bedforms generated by fluvial currents. The bioturbated sandstones probably represent biological reworking of facies St, Sp, Sr, and Sh during periods of relatively quiet water. The origin of the massive sandstones in the Zayante Sandstone is unknown; they may only *appear* to be massive due to poor outcrop or lack of a sufficient range of different grain sizes and minerals to define bioturbation, laminations, or other structures. Alternatively and very speculatively, they may be truly structureless

and represent deposition by sandy debris flows or some other kind of sediment gravity flow.

Mudrocks. --

Mudrocks in the Zayante sandstone are very poorly exposed. Most are green, but many are red or mottled green and red. Sandy mudstone and siltstone are most common, but claystone occurs in places. Most of the mudrocks are bioturbated, but a few are laminated and the laminae defined by aligned flakes of mica.

Most of the mudrocks in the Zayante Sandstone occur at the tops of fining-upward sequences (Figure 51) where they generally are very thin to thin bedded and interstratified with ripple cross-laminated fine to very fine sandstone. These fine-grained sediments are similar to facies F1 and Fm in the classification of braided-stream lithofacies proposed by Miall (1977, 1978). Most of these fine-grained rocks probably represent levee and overbank deposits; some of the thicker horizons of mudrock may represent abandoned channel fills.

Serpulid boundstone. --

In the lower Zayante Creek section (Figure 44), a bed of serpulid boundstone about 30 cm thick forms a resistant low mound in the center of the creek about 100 m upstream (generally north) of the East Zayante road bridge (Felton quadrangle, Sec. 30-9S-1W). The rock is a sandy granule conglomerate that appears to have been bound at the time of deposition by masses of serpulid worm tubes. The tubes were identified as those of serpulid worms by their external morphology and by the similarity of their wall microstructure, as seen in thin-section, to illustrations in Majewske (1969). Other fossils and fossil fragments found in outcrop and in thin-sections include bivalves, gastropods, barnacles, and echinoid spines and plates. Also found was a single poorly preserved fossil keyhole limpet, tentatively identified by David Lindberg (personal communication, 1982) as a unit of the family Fissurellidae, and probably either *Fissurella* or *Diodora*.

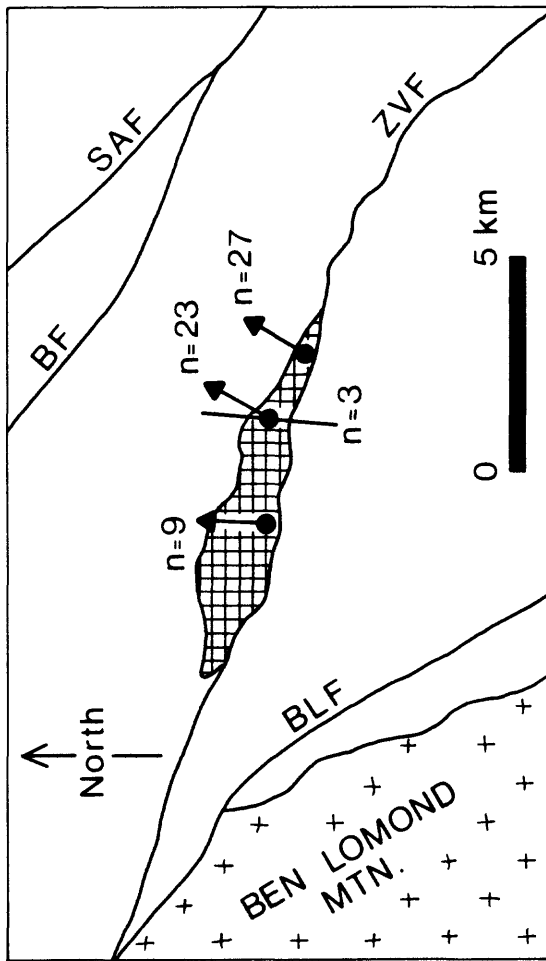
The serpulid boundstone was most likely deposited in water of normal marine salinity because it contains the fossil remains of stenohaline organisms such as limpets and echinoids. The coarse texture of the sediment and the occurrence together of barnacles and limpets suggests that deposition occurred in very shallow water. The serpulid boundstone may represent a reef deposit broadly analogous to the modern serpulid reefs that occur in coastal lagoons along the southeastern Gulf Coast of Texas and are briefly described by Milliman (1974). According to Milliman, the serpulid reefs in Texas are subtidal and occur at average water depths of one meter or less.

The serpulid boundstone is anomalous and important because it is a marine deposit that occurs in a thick section of apparently nonmarine rocks that were deposited by fluvial processes. The simplest explanation for this interstratification of marine and nonmarine rocks, as discussed below, is that the Zayante Sandstone was deposited by braided streams on a coarse-grained delta that built out into the La Honda sea. The exact depositional setting of the serpulid reef on this delta is unknown. Perhaps the reef grew on a gravel bar or on the gravelly floor of an abandoned delta distributary channel.

Paleocurrents

About 60 paleocurrent measurements were obtained from the Zayante Sandstone, most of them from clast imbrication in conglomerates and cross-stratification in sandstones (Figure 53, Appendix 5). These limited data suggest that the dominant direction of sediment transport was to the north and northeast.

Paleocurrent directions from clast imbrication in the conglomerates are unimodal and arguably radial, and are interpreted as representing flow in radiating fluvial distributary channels on a coarse-grained delta.



PALEOCURRENTS IN THE ZAYANTE SANDSTONE

Direction of movement, from pebble/cobble imbrication and cross-stratification.



Line of movement (flow parallel to symbol) from grain alignment and parting lineation.

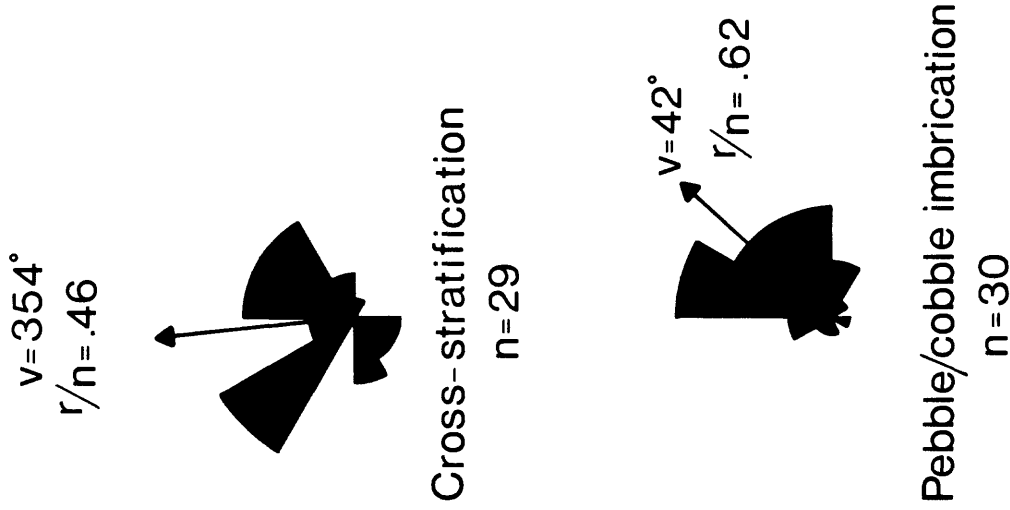


Figure 53. Paleocurrents in the Zayante Sandstone. The generalized outcrop area of the Zayante Sandstone is shown by crosshatching. Map shows vector mean (v) and number of measurements (n) at each group of outcrops. BF = Butano fault, BLF = Ben Lomond fault, SAF = San Andreas fault, ZVF = Zayante-Vergeles fault. Rose diagrams summarize measurements from all outcrops on cross-stratification and pebble/cobble imbrication; r/n = vector strength.

Paleocurrent directions from cross-stratification in the sandstones show a roughly trimodal distribution. The number of modes and their orientations may not be significant in view of the small number of measurements, so the following interpretations are tentative. The northeastward-flowing mode probably represents the movement of sand down the fluvial delta-distributary channels hypothesized above. The northwestward-flowing and southwestward-flowing modes, as well as the other scattered paleocurrent directions, may represent any of the following: (1) flow along meandering or braided fluvial channels; (2) overflow transport away from the channels due to crevasse-splays and other overbank processes; (3) reworking of sediments on the delta by marine processes such as tidal currents, longshore currents, or waves; and (4) "noise" due to post-depositional tectonic rotation, about a vertical axis, of the cross-stratified beds in which the paleocurrent measurements were made.

Depositional Systems and Provenance

The Zayante Sandstone includes deposits of both nonmarine and marine origin. Most of the Zayante Sandstone consists of interstratified conglomerate, sandstone, and minor mudrocks that most likely were deposited by braided streams. These fluvial deposits, however, enclose a serpulid reef that contains a marine fossil fauna and probably was deposited in very shallow water of normal marine salinity. On a more regional scale, the braided stream deposits of the Zayante Sandstone interfinger with and apparently are laterally equivalent to the shallow-marine sandstones of the Laurel unit of the Vaqueros Sandstone, as discussed earlier in this report. The simplest explanation for this interbedding and interfingering of fluvial and shallow-marine deposits is that the Zayante Sandstone represents a coarse-grained delta in which braided streams emptied directly into the La Honda sea. The Zayante delta may have been a fan-delta similar to those reported from modern environments and from the ancient record by Wescott and Ethridge (1980, 1983).

Much of the Zayante Sandstone may have been deposited by braided streams in a nonmarine setting analogous to the "lower fan-delta plain" in the model of Wescott and Ethridge (1983). Evidence for a braided-stream origin for much of the Zayante Sandstone includes: (1) the common occurrence of several of the braided stream lithofacies of Miall (1977, 1978), including facies Gm, Gt, St, Sp, Sr, Sh, and Fl; (2) the common occurrence of these lithofacies in fining-upward sequences that resemble those reported from other braided-stream deposits, particularly those of the "Donjek-type" (Miall, 1977, 1978); (3) the unimodal paleocurrent directions exhibited by clast imbrication in the conglomerates; (4) the general lack of marine fossils in these rocks, and in particular the lack of benthic foraminifers in the finer-grained sediments (Clark, 1966); and (5) the occurrence of red and green coloring, which is a characteristic feature of nonmarine sequences (Turner, 1980).

The main source of sediment for the Zayante Sandstone was probably an uplifted terrain of Salinian granitic rocks located southwest of the Zayante-Vergeles fault. Evidence for this interpretation includes: (1) the quartzofeldspathic mineralogy of the sandstones; (2) the abundance of detrital biotite in the sandstones; (3) the presence of numerous clasts of granitic rock, ranging from sand size to more than 120 cm in diameter, in both the sandstones and conglomerates; and (4) the north- and northeast-directed paleocurrents, which suggest sediment transport from the south and southwest.

The source area of the Zayante Sandstone was underlain mainly by granitic rocks, but metamorphic and sedimentary rocks were also present. The scattered clasts of mica schist and other metamorphic rocks in the Zayante Sandstone may have been derived from one or more of the metamorphic roof pendants that are common throughout the Salinian terrane, for example the nearby Santa Lucia and Gabilan ranges and Ben Lomond Mountain (Ross, 1977). The fragments of unmetamorphosed sandstone and mudrocks in the Zayante Sandstone may have been eroded from a carapace of older sedimentary rocks—perhaps including the Paleocene Locatelli Formation or the Eocene Butano Sandstone—that overlay the Salinian granitic and metamorphic basement rocks. The source of the well-rounded silicic volcanic clasts in the Zayante Sandstone is unknown. No roof pendants or other large exposures of such rocks occur on the Salinian block. However, clasts of well-rounded silicic volcanic rocks are common in Mesozoic and lower Cenozoic conglomerates in the Monterey Bay area, including the Cretaceous Pigeon

Point Formation, the Paleocene Locatelli Formation, and the Eocene Butano Sandstone. Perhaps the silicic volcanic clasts were eroded from these older conglomerates and redeposited in the Zayante Sandstone.

Rates of erosion in the source area and rates of sediment transport to the Zayante fan-delta were probably very high, as suggested by: (1) the angularity and large size of some of the granitic clasts; (2) the relatively fresh appearance of many of the detrital grains of feldspar; and (3) the grus-like appearance of some of the sandstones in the Zayante Sandstone.

High rates of erosion in the sediment source area, combined with evidence for a major unconformity at the bases of the Zayante Sandstone and the Laurel unit of the Vaqueros Sandstone, suggest that a major episode of tectonic uplift occurred along the southwestern margin of the La Honda basin during Oligocene time. The uplift may have been accompanied by movement along the Zayante-Vergeles fault, as hypothesized by Clark (1966, 1981) and Clark and Rietman (1973).

Zayante(?) Sandstone of the Majors Creek Area

Stratigraphic Relationships

Along Majors Creek on the southwestern flank of Ben Lomond Mountain is a sequence of green mudstone and sandstone with minor conglomerate and chert (Figure 54). These rocks were tentatively assigned by Clark (1966, 1981) to the Zayante Sandstone on the basis of their lithologic similarity to the Zayante Sandstone in its type area. However, neither the age nor the stratigraphic relations of the beds in Majors Creek are clear. No fossils diagnostic of age have been recovered and the upper and lower contacts are not exposed. My reconnaissance mapping along Majors Creek suggests that the stratigraphically lowest part of the Zayante(?) Sandstone is in fault contact with the Cretaceous Ben Lomond Quartz Diorite, and that this contact may represent a faulted nonconformity. The contact between the Zayante(?) Sandstone and the overlying Relizian Lompico Sandstone is also covered, but must be either a fault or an angular unconformity because bedding attitudes in the two formations are discordant. Based on these relationships, the Zayante(?) Sandstone along Majors Creek can be of any age, but most likely between Cretaceous and lower Miocene. My reconnaissance mapping suggests that the formation is at least 50 m thick.

Lithology

The Zayante(?) Sandstone along Majors Creek consists mainly of mudstone and sandstone with minor interbeds of conglomerate and chert. Exposures occur only along the bottom of the canyon and are generally poor.

Mudstone. --

Mudstone in the Zayante(?) Sandstone is gray green to brown, sandy and silty, very thin to thick bedded, and massive to bioturbated. The sand and silt grains include quartz, feldspar, biotite, and rock fragments including red chert. Exposures are exceptionally poor.

Sandstones. --

Sandstones in the Zayante(?) Sandstone include feldspathic arenite and minor feldspathic wacke. Colors on presumed fresh surfaces range from gray to gray green to orange brown. The grain size ranges from fine to very coarse and pebbly, and most beds are poorly sorted. The mineralogy of the sandstones, based on field observations and visual estimates of two thin-sections, is about 50% quartz, 20% plagioclase, 15-20% potassium feldspar, 5-10% biotite, and 5% "other" grains including lithic fragments,

MAJORS CREEK SECTION

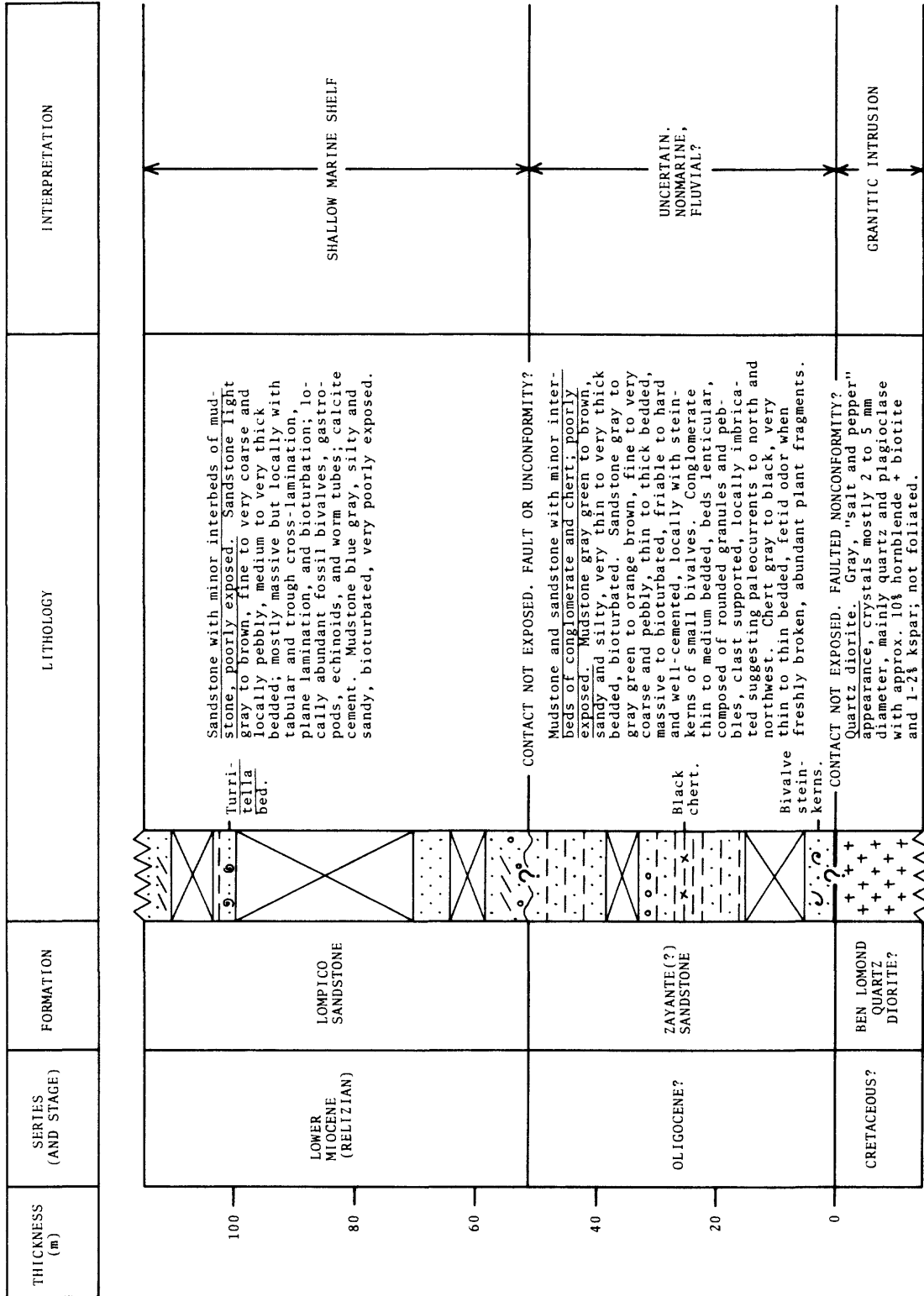


Figure 54. Inferred stratigraphy and depositional systems for the Majors Creek section on the southwest flank of Ben Lomond Mountain (see Figure 6 for location). Measured with tape and Brunton compass in July 1982 by H. Gibbons and R. G. Stanley. Lithology shown schematically.

hornblende, muscovite, and opaque minerals. The feldspar and quartz grains are mostly angular, while the lithic fragments--mainly chert and silicic volcanic rocks, with minor sandstone, mudstone, and basalt--are generally well-rounded. The sandstones range from friable to hard and well cemented; the cements include chlorite(?), clay minerals, and opal. Bed thicknesses range from thin to thick. Most beds are apparently massive, but some are bioturbated, with the individual burrows defined by color and textural mottling and a knobby appearance on weathered surfaces. A bed of bioturbated gray green sandstone near the base of the formation contains steinkerns of unidentified fossil bivalves.

Conglomerates. --

Interbeds of conglomerate make up less than 5% of the exposed section along Majors Creek. The conglomerates are lenticular, thin to medium bedded, and composed mainly of well-rounded granules and pebbles of porphyritic and banded silicic volcanic rocks. Most of the conglomerate beds are clast supported and some are weakly imbricated, with the imbrication suggesting paleocurrents directed to the north and northwest.

Chert. --

Thin beds of chert occur as interbeds in bioturbated mudstone about 25 m stratigraphically above the base of the formation (Figure 54). The chert is dark gray to black, aphanitic, and hard and brittle; it is cut by numerous fractures and quartz-filled veinlets, and in places has a brecciated appearance. Thin-sections show that the chert is composed mainly of silicified plant fragments. Most of the fragments are needlelike in shape and 1 to 3 mm in diameter; they appear to be the leaves, stems, and roots of unidentified vascular plants that have been replaced by microcrystalline quartz. Fine details of the plant microstructure, including the tracheids and other cells, are remarkably well preserved. These chertified fragments occur in a matrix of opaline silica that is translucent brown in thin-section and has a vaguely pelleted structure. (The presence of both quartz and opal-CT was confirmed by X-ray diffraction.) Orange brown organic material occurs in both the chertified plant fragments and the opaline matrix, and constitutes 5-10% of the rock. This organic material is probably responsible for the dark color of the chert, and also the fetid odor that issues from freshly broken pieces of the chert. Detrital grains of quartz sand constitute less than 1% of the rock. In places the chert is crudely stratified with the stratification defined by the parallel alignment of stems and roots.

Depositional Systems and Provenance

Exposures of the Zayante(?) Sandstone along Majors Creek are too poor to allow more than a tentative interpretation of depositional systems and provenance. Little can be said about the processes that deposited the sandstones and mudstones because they are all bioturbated or apparently massive. A nonmarine and perhaps fluvial depositional setting is suggested by the general similarity of the rocks in Majors Creek with the Zayante Sandstone in its type area, including the green color of the mudrocks and sandstones, the lack of marine fossils, and the lenticularity of the conglomerates. The rocks in the two creeks are also generally similar in sandstone mineralogy and conglomerate clast composition, suggesting a common provenance.

The origin of the black plant-rich cherts in the Zayante(?) Sandstone along Majors Creek is unknown. Perhaps the cherts represent accumulations of plant material in quiet ponds or marshes. The diagenetic history of these cherts--including the source of the silica, the geochemical conditions under which replacement of the plant fragments occurred, and the reasons for the coexistence of both opal and quartz--is unknown and worthy of detailed investigation.

Mindego Basalt

Introduction

Mafic volcanic rocks of late Zemorrian and Saucesian age are widespread in the La Honda basin (Figure 55) and are mapped as the Mindego Basalt by Brabb (1970). These volcanics include both extrusive and intrusive rocks, which in some outcrops are difficult to tell apart. The extrusives consist mainly of tuffs and breccias, but minor amounts of pillow lava and "massive" lava also occur. The intrusive rocks consist of dikes and sills that probably represent the subsurface conduits through which lava flowed to the surface to form the extrusive rocks. In places, the extrusive rocks are overlain by laterally discontinuous bodies of fossiliferous limestone that are included with Mindego Basalt for the convenience of discussion.

The name "Mindego" has been used inconsistently as a stratigraphic term. The name is derived from Mindego Hill (Figure 5), where the volcanic pile is thickest. The "Mindego Formation" was proposed as a stratigraphic unit by Touring (1959), who designated a type section along La Honda Creek (Figure 6). However, Touring's Mindego Formation included not just volcanic rocks, but also substantial volumes of feldspathic sandstone and mudrock; these sedimentary rocks were subsequently assigned to the Vaqueros Sandstone and Sandholdt Formation (=Lambert Shale of this report) by Cummings (1960), who proposed a new unit, the "Mindego Volcanics," consisting of rocks of volcanic origin only. Confusingly, a report by Cummings and others (1962) used essentially the same terminology as Touring (1959). Still another stratigraphic unit, the "Mindego basalt," was proposed by Dibblee (1966) but restricted by him to only those basaltic rocks that were "mappable continuous" with the type section along La Honda Creek. The term "Mindego Basalt" was subsequently extended by Brabb (1970) and Clark and Brabb (1978) to include all volcanic rocks of Zemorrian and Saucesian age in the central and northern Santa Cruz Mountains, regardless of their physical continuity with the volcanics exposed along La Honda Creek. The present report follows this last usage.

Stratigraphic Relations

The stratigraphic relations of the Mindego Basalt are complex and in some respects unresolved (Figure 14). In the La Honda and Mindego Hill quadrangles, the Mindego Basalt overlies the San Lorenzo Formation; conformably overlies and is laterally equivalent to parts of the Vaqueros Sandstone; is conformably overlain and laterally equivalent to parts of the Lambert Shale; and is unconformably overlain by the Monterey Formation and the Purisima Formation (Cummings, 1960; Dibblee, 1966; Brabb, 1970). The contact between the Mindego Basalt and the underlying San Lorenzo Formation is thought to be conformable over most of the area, but may be a disconformity or slightly angular unconformity in the subsurface in the La Honda quadrangle (Touring, 1959; Cummings, 1960).

The Mindego Basalt also includes small, isolated bodies of volcanic rocks--generally basaltic tuffs, breccias, and pillow lavas--that are interstratified with and entirely enclosed by the Vaqueros Sandstone and Lambert Shale; these are scattered here and there in the Half Moon Bay, Woodside, Big Basin, Castle Rock Ridge, Felton, and Laurel quadrangles (Mack, 1959; Classen, 1959; Clark, 1966, 1981; Dibblee, 1966; Brabb, 1970; Hector, 1976; Dibblee and others, 1978; Brabb and Dibblee, 1978).

Age

Radiometric dates on volcanic rocks and assemblages of fossils recovered from intercalated sedimentary rocks show that the Mindego Basalt is of late Oligocene and early Miocene age. A potassium-argon date of 23.1 ± 0.7 m.y. was obtained by Turner (1970) for a pillow lava in the lower Zayante Creek section (Figure 44). A second potassium-argon date of 19.7 ± 1.2 m.y. was obtained by Turner (1970) on a basalt in Peters Creek, about 8 km southwest of the type section in La Honda Creek (Figure 6). However, the 19.7 m.y. date is regarded by Turner (1970) as a minimum age due to incipient

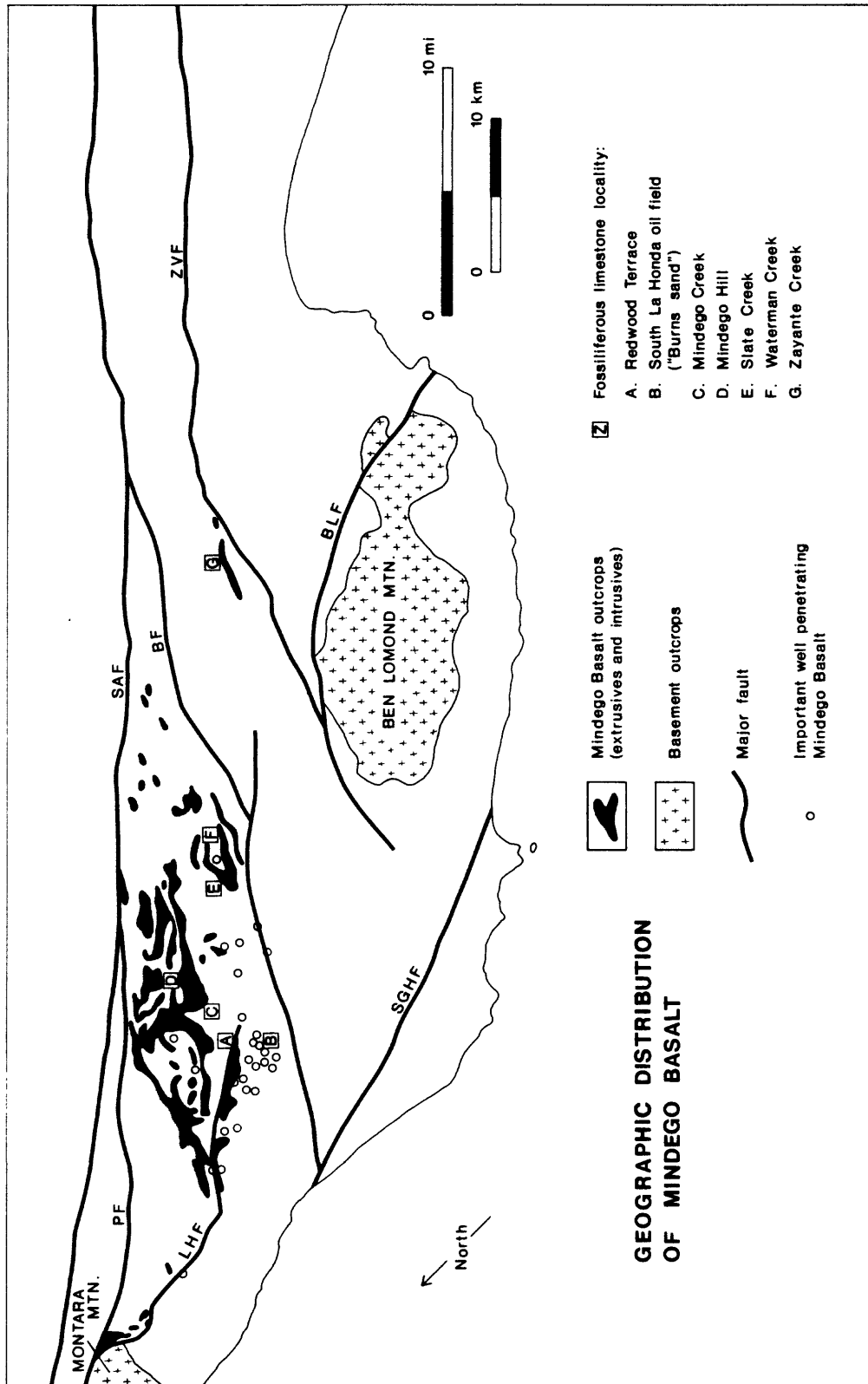


Figure 55. Map of geographic distribution of the Mindego Basalt in the La Honda basin. Shown also are the locations of fossiliferous limestones discussed in the text. BF = Butano fault, BLP = Ben Lomond fault, LHF = La Honda fault, PF = Pilarcitos fault, SAF = San Andreas fault, SGHF = San Gregorio-Hosgri fault, ZVF = Zayante-Vergeles fault.

alteration of the dated plagioclase.

Extrusive rocks of the Mindego Basalt are interbedded in many places with mudrocks that contain upper Zemorrian to Saucesian benthic foraminifers (Mack, 1959; Touring, 1959; Cummings, 1960; Turner, 1970; Clark, 1966, 1981). In a few places, the extrusive rocks are interstratified or closely associated with limestones and sandstones that contain megafossils of the Vaqueros Stage of Addicott (1972); these occur along Zayante Creek and Peters Creek, and possibly also along Mindego Creek and Oil Creek (Touring, 1959; Cummings, 1960; Clark, 1966, 1981). Basaltic intrusive rocks that are presumably coeval with the extrusive rocks cut strata ranging in age from Narizian to Saucesian (Touring, 1959; Cummings, 1960).

The paleontologic data and stratigraphic relationships noted above indicate that the igneous activity recorded by the Mindego Basalt occurred during late Zemorrian and Saucesian time. The limited radiometric dates suggest that most of the volcanism occurred during a somewhat narrower time interval, roughly about 20 to 25 m.y. ago.

Thickness

The stratigraphic thickness of the Mindego Basalt is difficult to determine for several reasons: (1) outcrops are generally very poor, and the structure complicated; (2) even in good outcrops, stratification in the volcanic rocks is often ambiguous or absent, and sills are often indistinguishable from extrusive lavas; and (3) over much of the La Honda Basin, the top of the formation has been eroded. Nevertheless, data compiled from wells, published cross-sections, and stratigraphic columns (Appendix 3) show that the volcanic pile reaches its greatest preserved thickness of over 1500 m in the vicinity of Mindego and Langley Hills and thins in all directions away from this central area (Figure 56). Smaller and thinner accumulations of volcanic rock occur in the Zayante area, and also in the Woodside-Half Moon Bay area southeast of Montara Mountain (Figure 56). These variations in thickness suggest that the main eruptive center was in the Mindego Hill area (Touring, 1959; Cummings, 1960), and that smaller peripheral vents occurred in the Zayante and Woodside-Half Moon Bay areas.

In the vicinity of Mindego Hill, outcrops and thickness contours of the Mindego Basalt define a generally rhomb-shaped area in map view (Figures 55 and 56). This rhomboidal geometry is strikingly similar to the model of a pull-apart basin proposed in 1974 by J. C. Crowell (compare Figures 55 and 56 with Figure 57). Thus, in the Mindego Hill area, the Mindego Basalt may have erupted and accumulated in a pull-apart between two *en echelon* strike-slip faults or "master faults" in the terminology of Rodgers (1980) and Mann and others (1983). Unfortunately, it is not clear which, if any, of the faults that are presently exposed in the area were involved in the development of the hypothesized pull-apart. Comparison of Figures 55, 56, and 57 suggests that either the San Andreas or Pilarcitos faults, or both, may have served as the master fault along the northeastern boundary of the pull-apart. Similarly, either the La Honda or Butano faults, or both, may have served as the master fault along the southwestern margin of the pull-apart. The Woodhaven fault, with its meandering trace (Figure 56) may have originated as an irregular normal-slip fault on the ragged northwestern margin of the pull-apart.

The small pod of basaltic volcanic rocks in the Zayante area (Figure 56) apparently is not physically connected to the main mass of Mindego volcanics in the Mindego Hill area (Clark, 1966). The outcrop belt of the volcanics in the Zayante area is parallel to and only a short distance from the Zayante-Vergeles fault, suggesting that a buried fracture related to this fault served as a conduit for magma rising from below. Similarly, the basaltic volcanic rocks in the Woodside-Half Moon Bay area may have erupted from vents along the La Honda fault.

Lithology

The major categories of rocks in the Mindego Basalt are: (1) extrusive rocks, mainly tuffs and breccias but also including pillow lavas and "massive" lavas; (2) intrusive rocks, consisting of dikes and

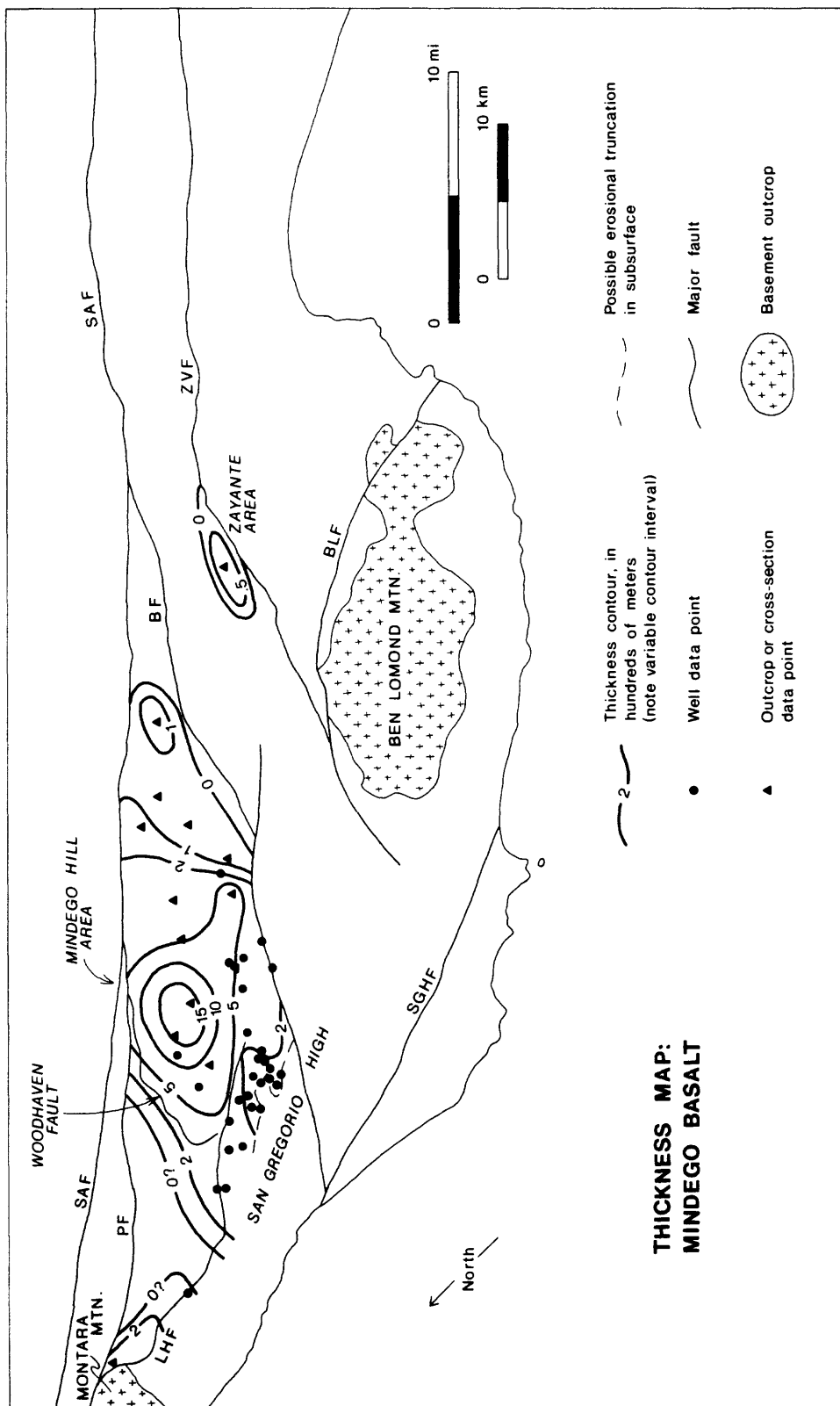


Figure 56. Map of thickness of the Mindego Basalt, based on data in Appendices 3 and 4. Major faults labeled as in Figure 55.

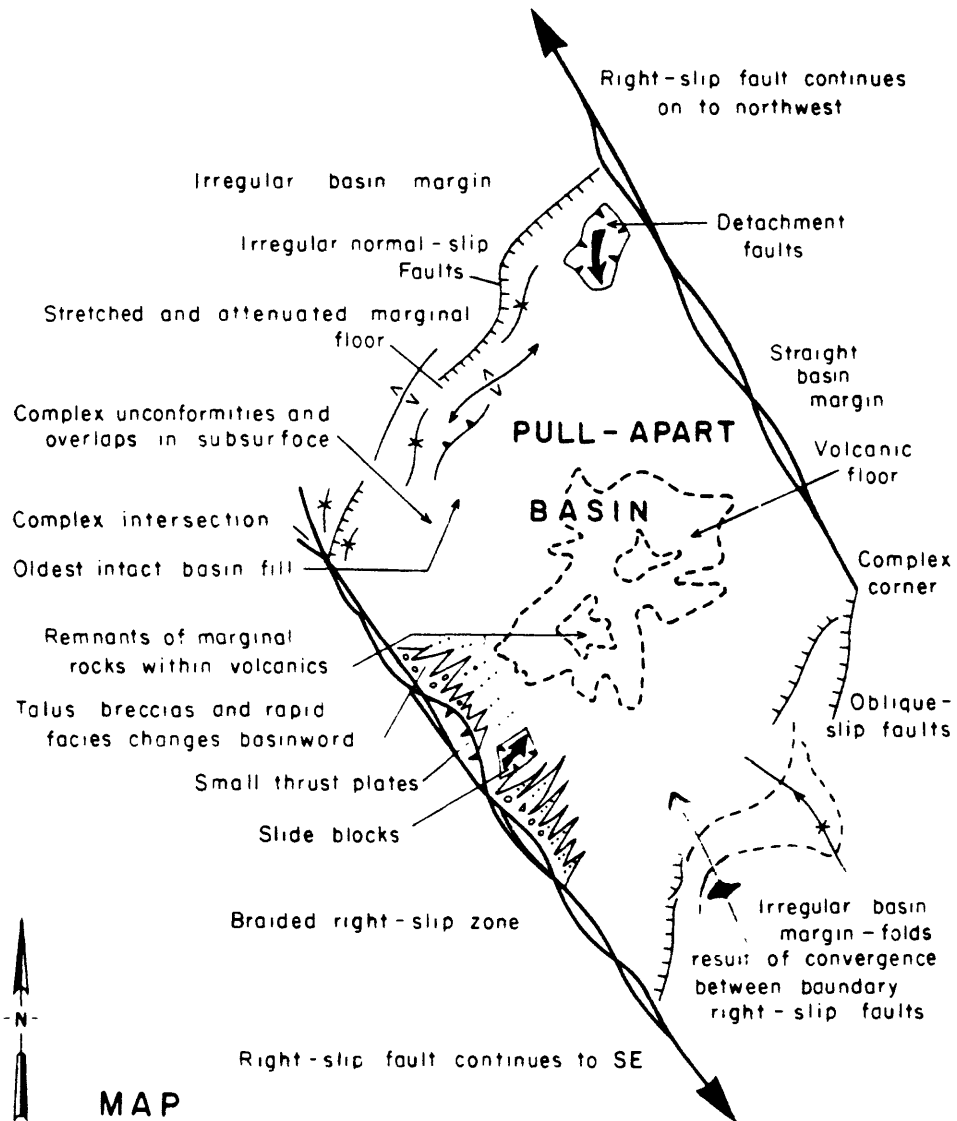


Figure 57. Sketch map of an idealized pull-apart basin (Crowell, 1974), for comparison with maps of geographic distribution and thickness of Mindego Basalt (Figures 55 and 56).

sills; and (3) fossiliferous limestones.

Most of the formation is made up of tuffs and breccias (Cummings, 1960). This is well-illustrated in the Langley Hill Quarry in the Mindego Hill quadrangle (Sec. 7-75-3W), where the formation is about 90% tuff and breccia, 5% lava, and 5% bioturbated mudrocks similar to those in the Lambert Shale and described later in this report.

I did not study the lithology of the Mindego Basalt in detail. The short descriptions and discussions presented below are based mainly on the available literature and on my own limited field observations and petrographic work. More thorough descriptions of the field relations and petrology of these volcanic rocks can be found in reports by Haehl and Arnold (1904), Mack (1959), Touring (1959), Cummings (1960), Cummings and others (1962), James (1964), Clark (1966, 1981), and Hector (1976).

Petrographically and chemically, the Mindego volcanic rocks are basalts. Many but not all of them are porphyritic. Thin-sections show that they commonly consist of phenocrysts of plagioclase and olivine (and rarely of pyroxene) in a groundmass of plagioclase microlites, finely crystalline pyroxene, glass, and magnetite (Touring, 1959; Cummings, 1960; James, 1964). The silica content of these rocks, based on two chemical analyses reported by Haehl and Arnold (1904) and studies of the index of refraction of unaltered volcanic glass by James (1964), ranges from 49% to 52%; this is within the range generally regarded as mafic (Hyndman, 1972) or basaltic (Francis, 1976, p. 131). In addition, detailed petrographic studies by James (1964) show that the mineralogic and textural features of most samples from the Mindego Basalt are characteristic of alkali-olivine basalts, although some show features more typical of tholeiitic basalts. Detailed analysis of the composition of the basalts using x-ray fluorescence is underway by students of the University of California, Santa Cruz, but the results were not available when this report was written.

Many but not all of the volcanic rocks are vesicular and amygdaloidal. The amygdules commonly are composed of calcite, chalcedony, opal, natrolite, and analcite (Touring, 1959; Cummings, 1960; James, 1964; Clark, 1966, 1981).

Extrusive rocks.--

Extrusive rocks in the Mindego Basalt consist mainly of tuffs and breccias. These volcanoclastic rocks vary widely in clast composition and texture, but typically consist of angular to rounded fragments of basalt cemented by white, coarsely crystalline calcite (Figure 58). The fragments of basalt range from sand size to more than 100 cm in diameter in some outcrops, but most are less than 20 cm in diameter. Basaltic tuffs and breccias are abundant in the Mindego Hill area, and also occur interstratified with sandstones and mudrocks of both the Castle Rock and Laurel units of the Vaqueros Sandstone in the Saratoga Gap, Castle Rock Ridge and Zayante areas (Hector, 1976; Clark, 1966, 1981). During the 1980-1982 field seasons, good exposures of tuff and breccia were present along Slate Creek, in the type section along La Honda Creek, and in the Langley Hill Quarry.

The sedimentology of the tuffs and breccias has not been studied in detail, but limited field observations suggest that they can be divided into several different categories that probably represent a variety of depositional processes. For example, some breccias are monolithologic--that is, composed of only one kind of clast (Parsons, 1969; Lajoie, 1979)--and consist of angular pieces of basalt that seem to fit together like the pieces of a jigsaw puzzle. These "jigsaw breccias" are interpreted as autoclastic deposits (Lajoie, 1979) that formed by the rapid cooling and shattering of hot lava as it came into contact with cold seawater or wet, unconsolidated sediment. Such breccias are volumetrically unimportant in the Mindego Basalt, however, and probably make up less than 5% of the formation.

More common are monolithologic tuffs and breccias that are composed of angular fragments that *do* not fit together like a jigsaw puzzle. These deposits typically are many m thick and massive to poorly stratified. The processes by which such tuffs and breccias are formed in submarine settings are poorly known (Lajoie, 1979). The angular clasts of basalt may have been produced by autoclastic fragmentation, or alternatively they may have formed by pyroclastic ejection from volcanic vents during explosive



Figure 58. Outcrops of middle Tertiary basaltic volcanic rocks in the La Honda basin. **Top:** Intensely weathered vesicular pillow lava in roadcut along Highway 9 just north of Saratoga Gap. This lava occurs as a lens within turbidite sandstone and mudstone of the Castle Rock unit of the Vaqueros Sandstone. Stratigraphic up is to upper right. Hammer handle is about 28 cm long. **Bottom:** Basaltic breccia with white calcite cement; float block along Slate Creek. Broom is about 23 cm long.

subaqueous(?) eruptions. Once created, the clasts may have simply accumulated in a pile around the vent, or they may have been transported under the influence of gravity and redeposited far from the vent by hot pyroclastic flows or cold debris flows and turbidity currents. The monolithologic character of the tuffs and breccias suggests that each deposit is the product of a single eruption from a single vent or group of closely spaced vents.

Many other tuffs and breccias in the Mindego Basalt are heterolithologic, or composed of more than one kind of clast. The clasts are nearly all basaltic, but commonly they differ from each other in features such as color; size and number of vesicles; size, number and mineralogy of phenocrysts; and degree of rounding of the clasts, which range from angular to very well-rounded. Some of these heterolithologic tuffs and breccias also contain large fragments of pillow lava, and a few contain clasts of mudrock and dolomitic limestone (Hector, 1976). The beds generally range from one m to many m thick and are massive to crudely stratified, with the stratification defined by the weak preferred orientation of elongate clasts. These heterolithologic breccias were probably not the products of single eruptive events. Instead, the variety of clast types suggests that they consist of material derived from several different eruptions and possibly from several different vents. This material was probably mixed together, reworked and rounded, and then transported and redeposited by sedimentary processes. I speculate that the heterolithologic tuffs and breccias formed when autoclastic, pyroclastic, and epiclastic material produced by several different eruptions was mixed together and transported down the slopes of submarine volcanos by debris flows or large turbidity currents. These catastrophic events may have been triggered by nearby eruptions or by earthquakes associated with eruptions.

In the Langley Hill Quarry I found several beds of tuff, ranging from one to several m in thickness, that are normally graded and grade upward into bioturbated mudstone. These tuffs are tentatively interpreted as turbidity current deposits, although no Bouma sequences were observed.

Minor amounts of pillow lava also occur in the Mindego Basalt. Pillow lavas up to 10 m thick, with pillows up to 200 cm in diameter, are interstratified with and enclosed by turbidite sandstones and mudrocks of the Castle Rock unit of the Vaqueros Sandstone in the Saratoga Gap and Castle Rock Ridge areas (Figure 58; Hector, 1976). A highly fractured pillow lava with pillows up to 150 cm in diameter occurs within the Laurel unit of the Vaqueros Sandstone in the lower Zayante Creek section (Figure 44; Clark, 1966, 1981). Several occurrences of pillow lava in the Mindego Hill area are mentioned by Cummings (1960). Pillow lavas form when fluid lava chills in contact with water (Moore, 1975), and their presence in the Mindego Basalt lends support to the notion that most if not all of the formation is of submarine origin.

Lavas described as "massive" and "crystalline" are reported from the La Honda and Mindego Hill quadrangles by Touring (1959), Cummings (1960), Cummings and others (1962), and James (1964). These lavas are described as black and commonly vesicular and amygdaloidal; in places, they exhibit columnar jointing. The massive lavas are inferred to be of subaerial origin by Cummings and others (1962), but the evidence for this interpretation is not clear.

Intrusive rocks. --

Dikes and sills of mafic intrusive rocks are common in the Mindego Hill and La Honda quadrangles, both in surface outcrops and in the subsurface where they are recognizable in electric logs from some wells (Touring, 1959; Cummings, 1960). The dikes and sills are composed of light- and dark-colored rocks variously described as diabase, diorite, and gabbro; the darker-colored varieties are apparently the most common (Haehl and Arnold, 1904). The intrusions cut across rocks as old as the Narizian Butano Sandstone and as young as the Saucian Lambert Shale, but seem to be concentrated in the Twobar Shale and Rices Mudstone (Touring, 1959; Mack, 1959; Cummings, 1960). Some of the sills are as thick as 120 m (Dibblee, 1966). The chemistry and mineralogy of these intrusive rocks is generally similar to that of the extrusive rocks of the Mindego Basalt, and for that reason the intrusives are believed to have served as feeders for the extrusives (Haehl and Arnold, 1904; Beaulieu, 1970).

Fossiliferous limestones.--

Fossiliferous limestones associated with extrusive rocks of the Mindego Basalt have been reported from a number of localities in the La Honda basin (Figure 55). I've examined outcrops in Zayante Creek and Slate Creek, and these are discussed below.

(1) Zayante Creek occurrence.

In the lower Zayante Creek section (Figure 44), an interval of basaltic breccia and pillow lava is overlain by a fossiliferous limestone about 4 or 5 m thick. This limestone was discovered by Clark (1966), and aspects of its sedimentology and paleoecology were discussed by Stanley (1973).

The limestone is a gray to orange brown skeletal lime grainstone (Figure 59). It consists mainly of whole fossils and fragments of marine invertebrates, and siliciclastic sand. The skeletal grains range from sand size to 15 cm diameter; most are angular, but rounded fragments also occur. Detrital grains of very fine to fine siliciclastic sand--mainly feldspar and quartz, but also including biotite, hornblende, and other minerals--make up 5-30% of most samples, but constitute up to 50% of some rocks. Rounded to angular, sand to boulder-sized fragments of basalt are scattered throughout the limestone but make up only 1-2% of the rock. The calcite cement ranges from microcrystalline to coarsely crystalline and is stained orange brown, presumably by iron oxides. Porosity is about 10% and is due mainly to selective leaching of skeletal grains.

Sedimentary structures are difficult to see in outcrop because of the pitted and cavernous weathering of the limestone. Polished slabs show that most of the limestone is apparently massive, possibly due to bioturbation. In some places, however, elongate bivalve and barnacle fragments exhibit a preferred orientation that defines a crude stratification in the limestone.

The fossil assemblage includes at least 23 species of invertebrates. The fauna is dominated by barnacles and bivalves, but gastropods, echinoids, bryozoans, worm tubes, scleractinian corals, ostracodes, benthic foraminifers, and calcareous red algae are also present. Some of the skeletal grains exhibit dark microcrystalline rims that resemble the micrite envelopes formed by endolithic algae on bioclasts in modern tropical carbonate sediments (Bathurst, 1975).

I interpret the lime grainstone of the Zayante Creek area as a carbonate sand that accumulated in shallow water on a sea floor knoll formed by the underlying basalt. Deposition in shallow water is indicated by: (1) the molluscan fossil fauna, which consists of mainly shallow-water species (Clark, 1966; Stanley, 1973); (2) the presence of fragments of calcareous red algae and algally-micritized grains, which must have formed in the photic zone at depths of 150 m or less; and (3) the stratigraphic occurrence of the limestone in the lower part of the Laurel unit of the Vaqueros Sandstone, which consists of siliciclastic sandstone and conglomerate that most likely were deposited on a shallow marine shelf.

Field relationships suggest the following simple history. Basaltic lava was extruded into shallow water on a marine shelf on which quartzofeldspathic sand of the Laurel unit of the Vaqueros Sandstone was accumulating. The lava cooled, and the newly-formed, bare-rock surfaces of basalt were colonized by barnacles and other epifaunal organisms. Subsequent accumulation of shell hash and lesser amounts of siliciclastic sand on top of the basalt bank provided a loose sediment substrate that was occupied by burrowing bivalves and other organisms. The elevated position of the basalt bank above the surrounding sandy sea floor may have kept the carbonate sediments from being overly diluted by siliciclastic sediment. In addition, the basaltic knoll may have created special environmental conditions such as increased illumination, better water circulation, and lessened turbidity that encouraged organic productivity and the subsequent accumulation of carbonate skeletal material.



Figure 59. Sawn slabs of fossiliferous limestones associated with middle Tertiary basaltic volcanic rocks in the La Honda basin. Scales in centimeters and inches. **Top:** Skeletal lime grainstone with large fragments of fossil bivalves and barnacles; sample collected from limestone that overlies a pillow lava in the lower Zayante Creek section (Figure 44). Note the high porosity due to selective leaching of skeletal grains. **Bottom:** Skeletal lime grainstone composed mainly of benthic foraminifers and sand-sized fragments of fossil molluscs and other organisms; sample from stratigraphic top of Mindego Basalt, Slate Creek section (Figure 60).

(2) Slate Creek occurrence.

A fossiliferous limestone about 2.5 m thick occurs at the stratigraphic top of the Mindego Basalt in Slate Creek (Figures 59 and 60). This limestone is thinner, generally finer-grained, and has a fossil fauna somewhat different from that of the limestone in Zayante Creek.

The limestone in Slate Creek is a light brown skeletal lime grainstone. It consists mainly of angular to rounded fine to medium sand sized skeletal grains, but bivalve fragments up to 2 cm long also occur. Sand to granule sized basalt fragments make up about 5% of the rock, while detrital grains of feldspar and quartz sand constitute only about 1%. The cement is very finely crystalline calcite. Porosity ranges from 5-15% and is apparently due to selective leaching of both volcanic and carbonate detrital grains. Most of the limestone is massive but in places a crude stratification is defined by the parallel alignment of elongate shell fragments and by alternating layers of coarser and finer grained material.

Many of the skeletal grains are too small to identify with certainty, but of the recognizable fragments the most common are benthic foraminifers (probably several species), echinoid spines and plates, and several species of bivalves. Other organisms present in lesser amounts include bryozoans, barnacles, gastropods, and probable calcareous green algae. A few skeletal grains have thin dark rims that I interpret as micrite envelopes of algal origin.

Several lines of evidence suggest that the lime grainstone of Slate Creek was deposited in shallow, well-agitated water on the crest or flank of a submarine volcanic knoll. The algally-micritized skeletal grains and the fragments of calcareous green algae must have formed in the photic zone. The lack of mud matrix and the high degree of fragmentation and rounding of the skeletal grains indicate winnowing by currents of at least moderate strength. The paucity of detrital quartz and feldspar sand suggests that the carbonate sediment was deposited well out of the reach of turbidity currents carrying land-derived sediments, as would be the case on a submarine knoll. The presence of a submarine topographic high in the Slate Creek area during late Zemorrian and Saucian time is also suggested by evidence from benthic foraminiferal paleobathymetry discussed later in this report and shown in Figure 66.

An alternative interpretation is that the limestone of Slate Creek is a shallow water carbonate sand that was transported into deeper water and redeposited. However, I have observed no evidence for redeposition. Such evidence could include, for example, the occurrence of sedimentary structures in the limestone indicative of deposition from turbidity currents or grain flows; and the occurrence within the limestone of interbeds of shale containing deeper-water fossil assemblages.

(3) Other limestone occurrences.

Several other lenses of limestone associated with the Mindego Basalt have been reported (Figure 55). These have not been studied in detail but may represent banktop accumulations of carbonate sediment similar to the limestones in Zayante or Slate Creeks. A limestone body more than 300 m long and 30 m thick and composed mainly of oyster shells is reportedly present in Waterman Creek (Cummings, 1960; Cummings and others, 1962). Smaller lenses of limestone crop out along Mindego Creek, along San Gregorio Creek near Redwood Terrace, and on the top of Mindego Hill (Touring, 1959; Cummings and others, 1962).

A fossiliferous limestone known as the "Burns sand" occurs in the subsurface of the South La Honda oilfield and has produced modest amounts of petroleum (Table 1). Electric log correlations indicate that the Burns sand is lenticular and about 800 m long, 200 m wide, and up to 50 m thick. This lens of limestone occurs at the stratigraphic top of the Mindego Basalt and is overlain by the Lambert Shale; thus, its stratigraphic context is identical to that of the limestone in Slate Creek. Available core descriptions are sketchy but indicate that the Burns sand contains numerous megafossil fragments. I speculate that the Burns sand represents a bank top accumulation of carbonate sand analogous to the limestone of Slate Creek, but I have not been able to obtain detailed lithologic and paleontologic evidence to support my claim.

SLATE CREEK SECTION

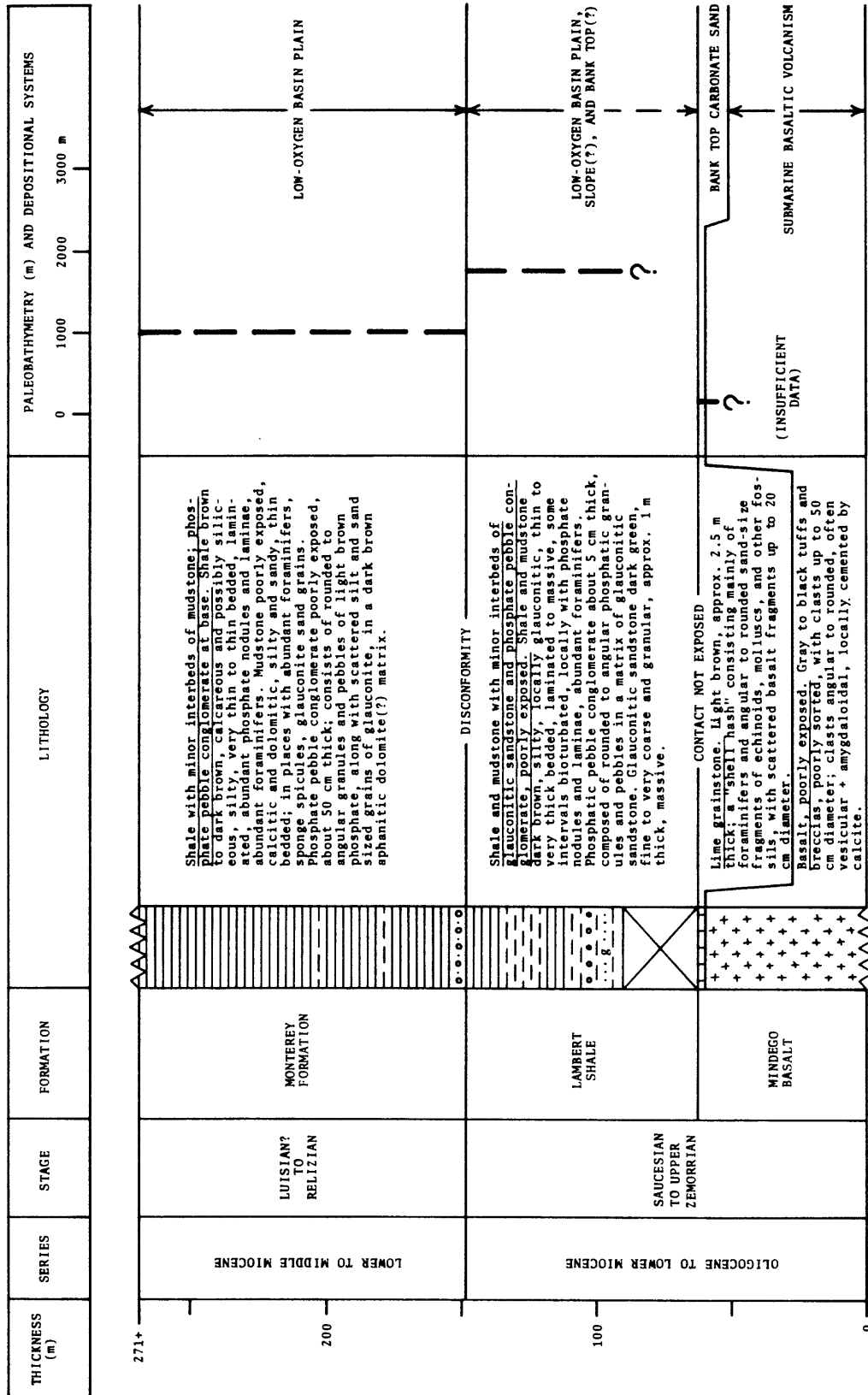


Figure 60. Inferred stratigraphy, paleobathymetry, and depositional systems of the Slate Creek section (see Figure 6 for location). Section measured with tape and Brunton compass in September 1982 by H. Gibbons and R. G. Stanley. Lithology shown schematically. Series, stage, and paleobathymetry based on paleontological samples Tla-10-24, Tla-10-25, Tm-10-8, and Tm-10-9 (Appendix 1); precise stratigraphic positions of these samples are unknown.

Summary

Most of the Mindego Basalt apparently erupted in a pull-apart setting from submarine vents in the vicinity of Mindego and Langley hills. Secondary eruptive centers not obviously related to the pull-apart were located in the Zayante area near the Zayante-Vergeles fault, and in the Woodside-Half Moon Bay area near the La Honda fault.

Most, if not all, of the extrusive rocks in the Mindego Basalt were erupted in submarine settings. Evidence for this interpretation includes: (1) the interstratification of the extrusive rocks with sandstones, limestones, and mudrocks containing marine fossils; and (2) the presence of pillow lavas, pillow fragments in some breccias, and autoclastic "jigsaw breccias," all of which indicate that hot lava was in contact with water.

Most of the Mindego Basalt consists of massive to crudely stratified basaltic tuff and breccia that probably formed initially by autoclastic and pyroclastic processes. The mechanisms of transport and deposition of this volcanoclastic material are unclear, but hot pyroclastic flows and cold sediment gravity flows such as debris flows and turbidity currents may have been important.

In places, the volcanic piles evidently built up above the sea floor to form submarine knolls. The tops of these knolls were colonized by barnacles, molluscs, and other shelly invertebrates whose skeletal remains accumulated to form richly fossiliferous limestones. Some of the volcanic piles may have reached above sea level to form islands, but no clear-cut evidence of emergence or subaerial volcanism has been found.

Lambert Shale

Introduction

The Lambert Shale consists of laminated shale and bioturbated mudstone with minor turbidite sandstone, glauconitic sandstone, and phosphatic pebble conglomerate. The formation was named by Dibblee (1966) who designated a type section along Lambert and Peters creeks in the Mindego Hill quadrangle (Figure 6).

Rocks assigned to the Lambert Shale by Brabb (1970) and by me include parts of the Monterey shale of Branner and others (1909); parts of the San Lorenzo, Vaqueros, Mindego, and Sandholdt formations of Touring (1959), Mack (1959), Cummings (1960), Cummings and others (1962), and Beaulieu (1970); the Slate Creek Shale of Lamb (1964); the "Brush Creek shale," "Vaqueros shale," and "Hester Creek shale" of various unpublished oil company reports; and "Formation X" of Burford (1961).

The Lambert Shale is widely distributed in outcrop and in the subsurface on the La Honda block, but is entirely missing from the Ben Lomond block (Figure 61). In some areas the Lambert Shale cannot be distinguished from the lithologically similar Twobar Shale and Rices Mudstone because of poor outcrops, complex structure, and sparse fossil control.

The Lambert Shale is generally poorly exposed. During the 1980-1982 field seasons, the best exposures were in the upper Zayante Creek, Soquel-Hinckley, and Slate Creek sections (Figures 23, 35, and 60) and in roadcuts along Highway 9 and Indian Trail Road near Saratoga Gap (Sec. 7-8S-2W).

Age

Benthic foraminifers are locally abundant and indicate that the Lambert Shale ranges in age from early Zemorrian to Relizian(?) but most of it is late Zemorrian to Saucian (Mack, 1959; McCollom, 1959; Cummings, 1960; Burford, 1961; Clark, 1966; Dibblee, 1966; Fairchild and others, 1969; Hector, 1976; K.

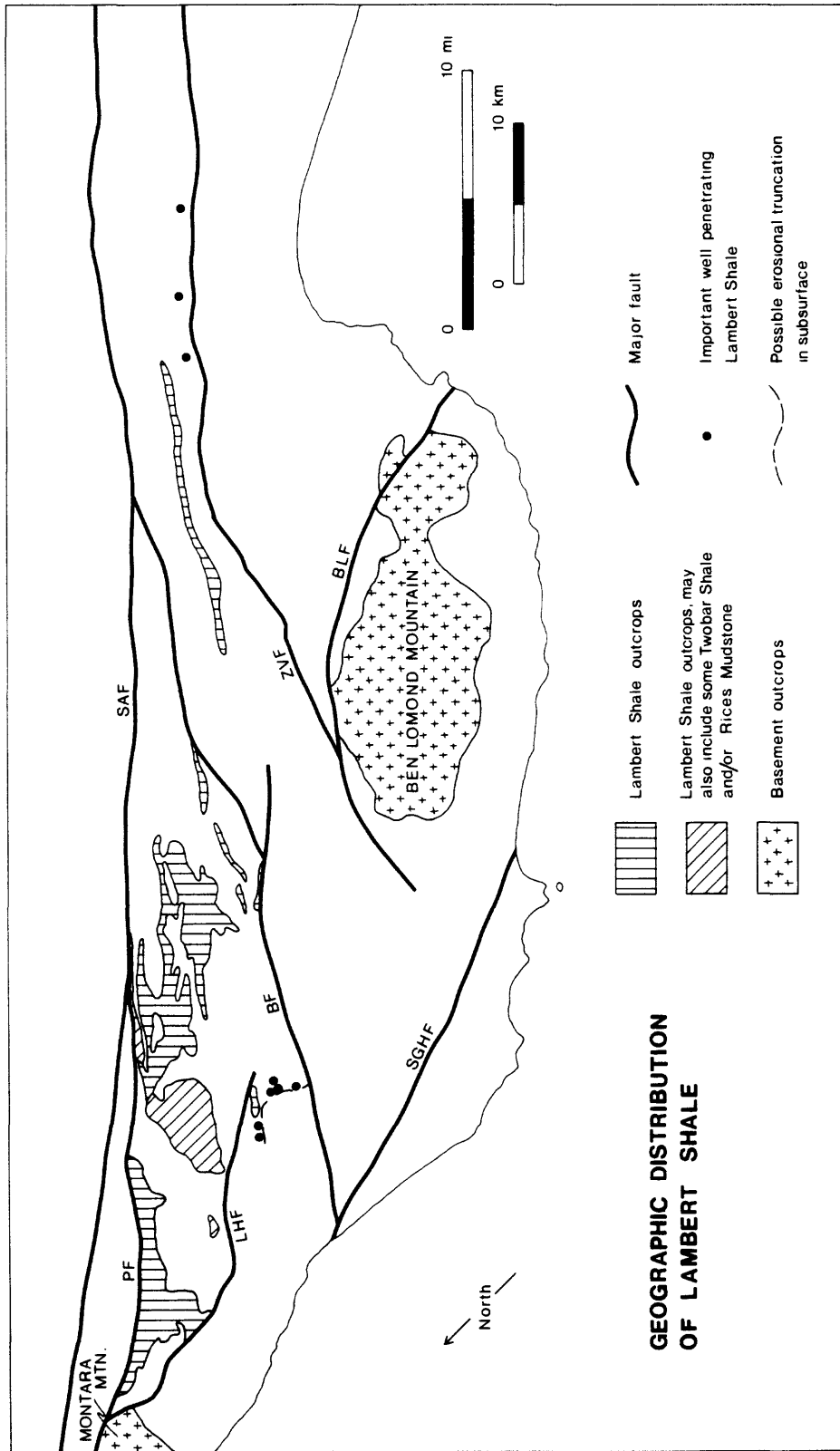


Figure 61. Map of geographic distribution of the Lambert Shale in the La Honda basin. BF = Butano fault, BLF = Ben Lomond fault, LHF = La Honda fault, PF = Pilarcitos fault, SAF = San Andreas fault, SGHF = San Gregorio-Hosgri fault, ZVF = Zayante-Verdege fault.

A. McDougall, unpublished report, 1979). An outcrop in the Woodside quadrangle that is questionably assigned to the Lambert Shale yielded a sparse and poorly preserved assemblage of planktic foraminifers of the lower to middle Miocene N7 to N12 zones (Poore, unpublished data, 1978). These paleontological results suggest that most of the Lambert Shale was deposited about 30(?) to 18 m.y. ago during the late Oligocene and early Miocene.

Stratigraphic Relations

The stratigraphic relations of the Lambert Shale are complex (Figure 14). In most of the La Honda basin, the Lambert Shale conformably overlies and interfingers with the Vaqueros Sandstone and the Mindego Basalt (Cummings, 1960; Dibblee, 1966; Clark, 1966, 1981; Beaulieu, 1970; Brabb, 1970). The lateral equivalence of the Lambert Shale and part of the Vaqueros Sandstone is clearly illustrated, for example, along Zayante Creek. In the upper Zayante Creek section, the Zemorrian-Saucesian stage boundary apparently coincides with the Lambert-Vaqueros contact; but about one km to the south in the lower Zayante Creek section, the same stage boundary falls well within the Vaqueros (Figures 35 and 44; Clark, 1966; Brabb and others, 1977).

In parts of the La Honda quadrangle, both the Vaqueros Sandstone and Mindego Basalt are missing and the Lambert Shale apparently overlies the Rices Mudstone. This contact is not exposed and its nature is unknown; it may be either conformable or unconformable (Beaulieu, 1970).

In the Big Basin and Mindego hill quadrangles the Lambert Shale is overlain by the Monterey Formation. The Lambert-Monterey contact is probably an unconformity, as discussed later in this report in the chapter on the Monterey Formation. Elsewhere in the Santa Cruz Mountains, the Lambert Shale is overlain in angular unconformity by the Santa Cruz Mudstone and by the Purisima Formation (Cummings, 1960; Clark, 1966, 1981).

Thickness

The original depositional thickness of the Lambert Shale is unknown because the upper surface of the formation is everywhere eroded. The limited thickness data in Appendices 3 and 4, combined with the wide geographic distribution and relatively uniform lithology of the formation, suggest that the Lambert Shale was deposited over the entire La Honda basin as a sheet that was more than 450 m thick in the Woodside and Felton quadrangles and perhaps as much as 1460 m thick in the Mindego Hill quadrangle. The original sheet of Lambert Shale was widespread but probably highly variable in thickness due to lateral interfingering with the Vaqueros Sandstone and Mindego Basalt.

Lithology

The major categories of rocks in the Lambert Shale are: (1) laminated shales, (2) bioturbated mudrocks, (3) turbidite sandstones, (4) olistostromes, (5) glauconitic sandstones, and (6) phosphatic pebble conglomerates. Laminated shale and bioturbated mudrocks together make up about 90% of the formation, while turbidite sandstones make up most of the remaining 10%. Olistostromes, glauconitic sandstones, and phosphatic pebble conglomerates together make up less than 1% of the formation.

Laminated shales and bioturbated mudrocks occur throughout the formation and in places are interbedded with each other. However, laminated shales become more abundant than bioturbated mudrocks higher in the formation, at least in the upper Zayante Creek section (Figure 35) and in the type section along Lambert and Peters creeks (Dibblee, 1966).

Laminated shales. --

The shales are generally dark brown on fresh surfaces and weather to light brown, light orangish brown, and nearly white. The shales weather in sheets that generally are parallel to stratification and range in thickness from less than one mm in some outcrops near Saratoga Gap to "plates" several mm thick in the Zayante Creek and Slate Creek areas. The shales are often highly fractured, and in some roadcuts and other hillside outcrops the fracture surfaces are covered by yellow jarosite(?) and small crystals of gypsum.

The shales are generally very thin to thin bedded and laminated (Figures 62, 63). The laminae range from less than one mm to several mm thick and are marked by minute variations in color and texture between adjacent laminae, as well as by the alignment of flattened or elongate particles such as fish scales, plant fragments, and foraminifers. Some of the laminae consist almost entirely of fossil foraminifers and are normally graded. Some other laminae are light brown to cream colored in reflected light, nearly isotropic in thin-section under cross-nicols, and probably are phosphatic. In many cases the individual laminae are laterally persistent and can be traced across the outcrop (generally less than 5 m to 10 m), but some laminae are not so persistent.

In the classification of Blatt (1982), most of these rocks are mud-shales, but clay-shales and silt-shales also occur. Examination of 14 thin-sections shows that the shales consist of microfossils and detrital grains of siliciclastic silt and sand scattered in a very fine grained matrix. The microfossils consist mainly of benthic foraminifers and fish fragments, with lesser amounts of sponge spicules, possible diatoms, and possible radiolarians. The siliciclastic grains consist mainly of quartz and feldspar with lesser amounts of biotite, detrital hematite, and detrital glauconite. The matrix of the shales is too fine grained to resolve clearly with the petrographic microscope, but its brown color and birefringence, combined with x-ray diffraction analyses and staining of thin-sections for carbonate minerals, suggest that the matrix of most of the shales is a complex mixture of clay minerals, phosphate, microcrystalline calcite, and finely disseminated organic matter. Some shales are dolomitic rather than calcitic. X-ray diffraction analyses also show that several samples from the upper Zayante Creek section contain substantial amounts of opal-CT in addition to calcite and dolomite.

Phosphatic material occurs in the shales not only as fish fragments but also as authigenic laminae and nodules. The phosphate nodules are generally cream-colored in reflected light and range in size from less than one mm to lenses up to 0.5 cm thick and several cm long (Figures 62 and 63). The margins of the nodules range from gradational (Figure 62) to sharp (Figure 63). In many cases, laminae bend around the nodules, suggesting that the nodules formed prior to compaction during early burial diagenesis.

Dolomitic concretions are common in most outcrops of shale and weather out in relief. The concretions are generally dark brown to dark gray on fresh surfaces and weather to various shades of orange. They range in size from lenses only a few mm thick to large tabular "beds" that in some cases are more than 100 cm thick. Lamination and phosphate nodules are commonly well-preserved in the concretions, but fossil foraminifers are generally recrystallized and poorly preserved.

Benthic foraminiferal assemblages from the shales and from the associated bioturbated mudrocks (described below) suggest deposition at middle to lower bathyal depths, or 500 m to more than 2000 m (Appendix 1; Figures 23, 35, and 60).

The laminated shales probably represent deposition in low-oxygen bottom waters, as suggested by the excellent preservation of laminae, the absence of megafossils, the dark color and apparently high organic content, and the abundance of phosphatic nodules and laminae. These features are common in low-oxygen muds in modern environments, and also in inferred anoxic shales in the rock record (Garrison, 1981; Pisciotto and Garrison, 1981; Soutar and others, 1981).

The shales are hemipelagic sediments composed of a mixture of terrigenous and biogenic components. By analogy with modern basins in the southern California borderland, much of the detrital silt and clay may have reached the sea floor as fecal pellets. However, the association of the shales with turbidite sandstones (described below) suggests that at least some of the terrigenous mud was transported

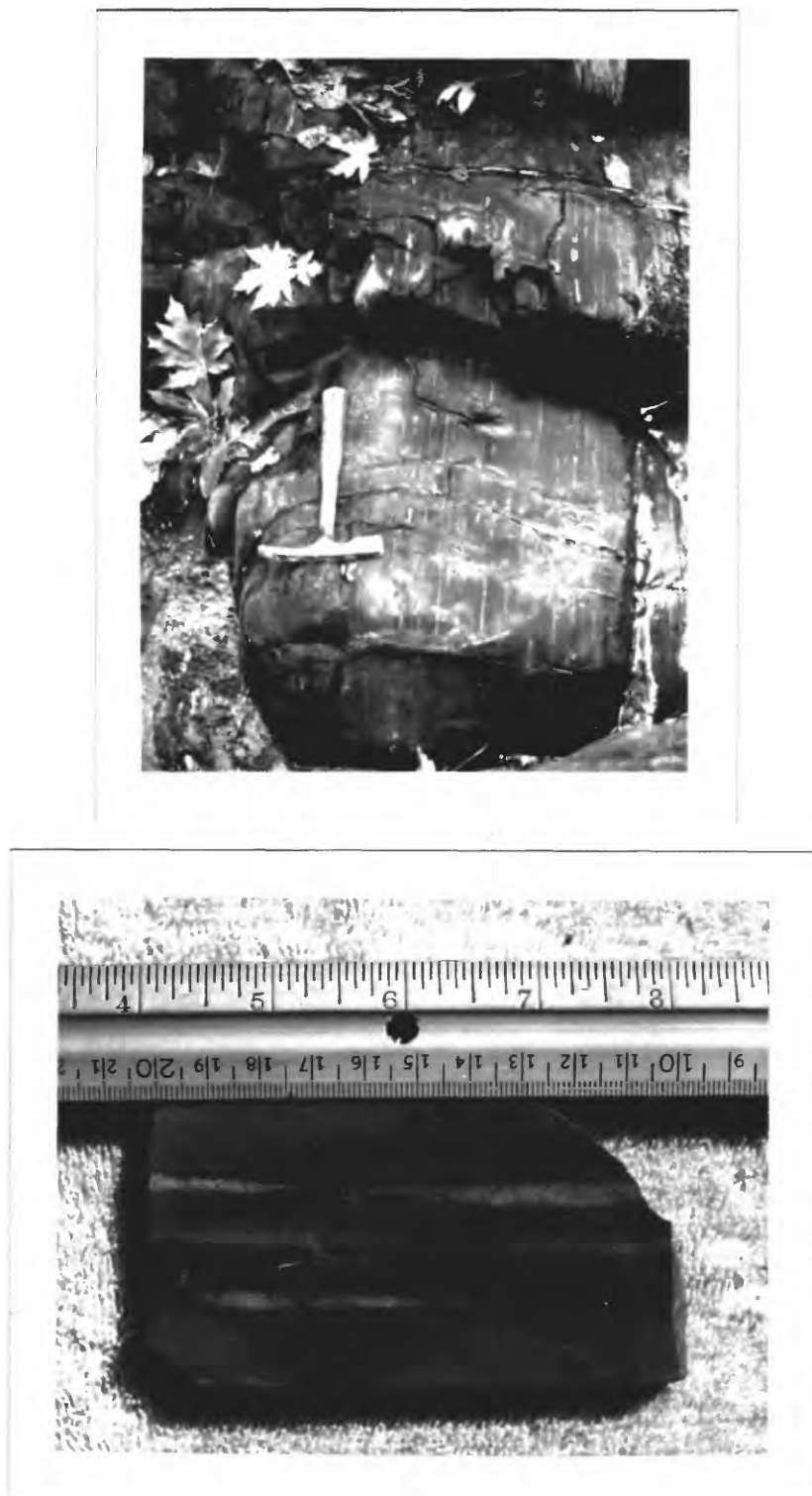


Figure 62. Rocks from the Lambert Shale. **Top:** Outcrop of weakly fissile dark-colored shale with light cream-colored phosphate nodules and laminae, upper Zayante Creek section. Bedding is vertical and faces to the right. Hammer handle is about 28 cm long. **Bottom:** Sawn slab from the same outcrop. Light-colored areas are phosphatic. Bedding is upside down. Scale is in inches and centimeters.

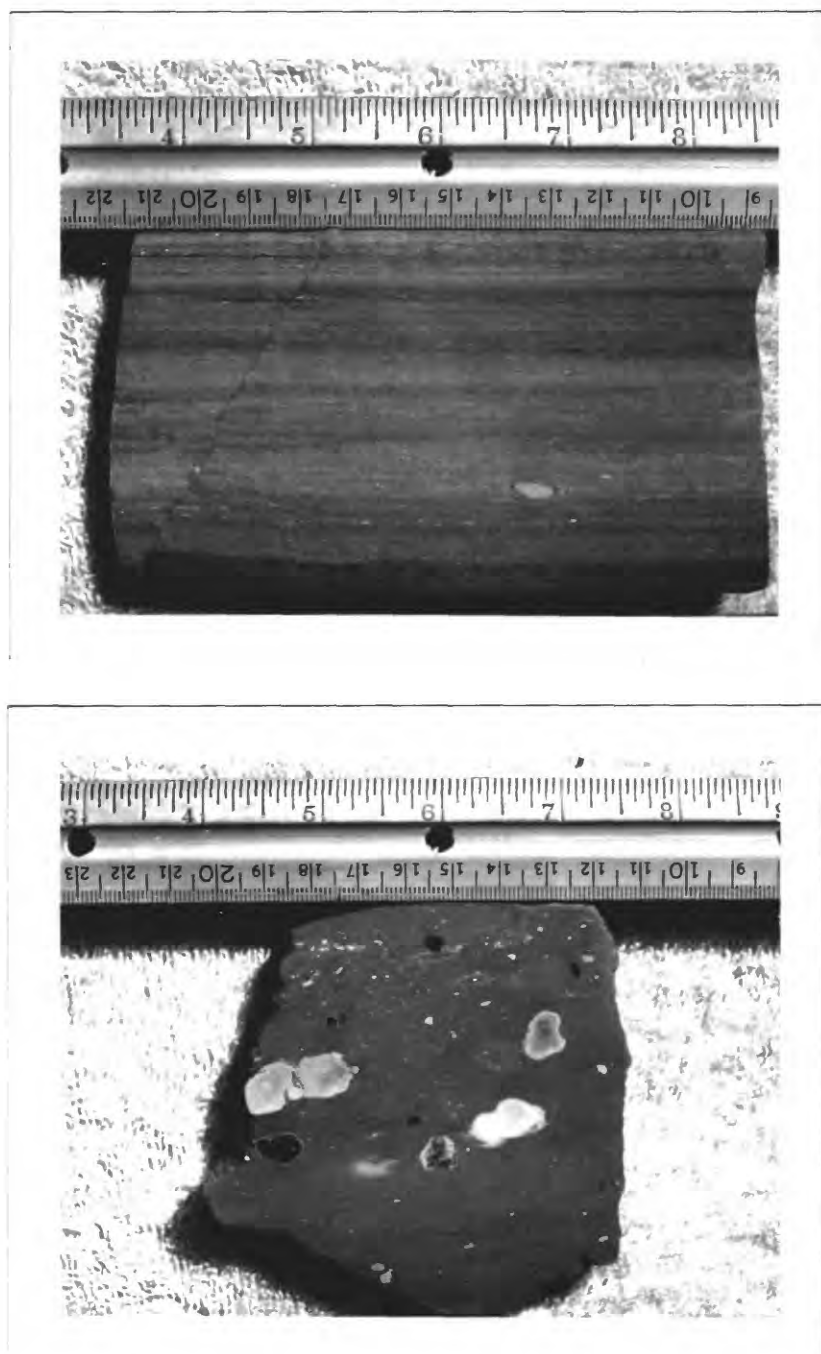


Figure 63. Sawn slabs of mudrocks from the Lambert Shale. Both slabs are shown with bedding right side up; scales are in inches and centimeters. **Top:** Siliceous and calcareous laminated shale with cream colored phosphate nodules and laminae; sample collected from the upper Zayante Creek section. **Bottom:** Bioturbated mudstone with scattered cream-colored phosphate nodules; sample collected from the Slate Creek section.

from shallower water by low-density turbidity currents. Many of the biogenic particles—including foraminifers, radiolarians, and diatoms—probably also arrived at the sea floor via fecal pellet packages. Some of the benthic foraminifers probably lived at or near the site of deposition. The thin graded beds and laminae composed of benthic foraminifers probably represent "hemipelagic turbidites," or hemipelagic sediments that were originally deposited higher on the slope and subsequently transported downslope and redeposited by turbidity currents. Such a process has been hypothesized for other formations, including the Sandholdt Unit of the Monterey Formation of the Salinas basin (Graham, 1976; Garrison and others, 1979).

The origin of the opal-CT and microcrystalline calcite and dolomite in the matrix of the shales is unclear. The opal-CT may be a recrystallization product of siliceous microfossils such as diatoms or radiolarians; such an origin has been suggested for the opal-CT in lithologically similar shales in the Sandholdt Unit of the Monterey Formation of the Salinas basin by Garrison and others (1979). Also by analogy with the Sandholdt, some of the microcrystalline calcite in the Lambert shales may consist of the skeletal remains of coccoliths, but this hypothesis should be tested by detailed observations with the electron microscope. Most of the calcite and dolomite in the Lambert shales occur as microcrystalline mosaics and are most likely of post-depositional origin, but the details of the diagenetic processes involved are unknown.

Bioturbated mudrocks.--

Bioturbated mudrocks occur as interbeds in the laminated shales discussed above and also occur in some places as intervals more than 60 m thick. The bioturbated mudrocks are gray, dark gray, or dark brown on fresh surfaces, and weather light brown and light orangish brown to nearly white. In roadcuts and hillside exposures they generally are soft and spheroidal- to chippy-weathering, but in places—for example, along Highway 9 about one km southwest of Saratoga Gap—they are hard, brittle, and exhibit conchoidal fracture.

In general, the bioturbated mudrocks are medium to very thick bedded, with some beds more than 2 m thick. In many outcrops, however, stratification is not visible or is very poorly defined by differential weathering or by the preferred orientation of tabular calcareous concretions.

The bioturbated mudrocks range in texture from claystone to siltstone, but mudstone and siltstone are the most common types. In places these mudrocks grade into bioturbated very fine sandstone, for example in the lower part of the formation in the lower Zayante Creek section (Figure 44).

Bioturbated mudrocks in the Lambert Shale are petrographically similar to those in the Rices Mudstone: they consist mainly of microfossils and detrital grains of siliciclastic sand and silt in a brown argillaceous matrix. The microfossils are mainly benthic foraminifers and fish scales and bones. Plant fragments are fairly common, but other macrofossils are exceedingly rare; I found a few small unidentified bivalves and an unidentified vertebrate bone in the upper Zayante Creek section. The siliciclastic grains are mainly quartz and silt, with lesser amounts of biotite, muscovite, chlorite, and glauconite.

Lenticular calcitic and dolomitic concretions are common in the bioturbated mudrocks in all areas except along Slate Creek, where they are noticeably few.

Bioturbation in the mudrocks is clearly defined by color and textural mottling visible on water-polished outcrops and on the sawn surfaces of rocks collected from apparently "massive" outcrops (Figure 64). Most of the burrows and other trace fossils are oriented parallel or subparallel to stratification, but oblique and vertical traces are also common.

Bioturbated mudrocks in the Lambert Shale probably represent periods during which bottom waters were well-oxygenated and supported an active sediment-churning infauna. The alternation of bioturbated mudrocks with laminated shales in some outcrops probably reflects fluctuating levels of oxygenation of the bottom waters, but the reasons for these fluctuations are unknown. The fluctuations may have been



Figure 64. Rocks from the Lambert Shale. **Top:** Outcrop of dark laminated shale and light gray sandstone in the upper Zayante Creek section. Bedding is vertical and faces to the right. Hammer head is about 17 cm across. Sandstone beds are interpreted as Mutti and Ricci Lucchi facies E turbidites. **Bottom:** Sawn slab of bioturbated siltstone; sample collected in the upper Zayante Creek section. Bedding is vertical, more or less parallel to flattened burrows and perpendicular to the ruler, and facing to the right. Scales in inches and centimeters.

caused by variations in the location of the bottom or top of the oxygen minimum zone relative to the sea floor. Alternatively, if the entire La Honda basin was at times a silled anoxic basin, as seems likely, the bioturbated beds may represent periodic but temporary episodes of oxygenation of the basin waters by overturn, as has been suggested for the Monterey Formation by Pisciotto and Garrison (1981).

In the Slate Creek section (Figure 60), some bioturbated mudrocks contain scattered phosphate nodules that are irregular in shape and up to 2 cm in diameter (Figure 63). The origin of such rocks is unclear. I speculate that they represent sediments that accumulated initially in anoxic conditions as laminated muds; phosphate nodules grew in these muds during very early diagenesis, and at very shallow burial depths. Subsequently, the bottom waters became temporarily better oxygenated, and the muds were reworked by sediment-churning organisms who destroyed the lamination but not the relatively coherent phosphate nodules.

Turbidite sandstones. --

Beds of feldspathic arenite and wacke, interpreted as the deposits of turbidity currents and possibly other kinds of sediment gravity flows, occur throughout the Lambert Shale but seem to be thicker and more numerous in the Felton, Laurel, and Castle Rock Ridge quadrangles than elsewhere in the La Honda basin. During the 1980-1982 field seasons the best exposures of these sandstones were in the upper Zayante Creek section (Figures 35 and 64) and in roadcuts along Indian Trail Road south of Saratoga Gap (Sec. 7-8S-2W).

The sandstones are generally light gray to light brown on fresh surfaces and weather light brown to white. Visual estimates of the compositions of 16 thin-sections show that the sandstones consist of about 40-60% quartz, 10-30% potassium feldspar, 10-20% plagioclase, 5-10% lithic fragments, and 0-15% biotite. Other detrital grains make up generally less than 2% of the rock and include glauconite, muscovite, detrital hematite, phosphatic pellets, and biogenic grains such as benthic foraminifers, echinoid spines, and fish fragments. The lithic fragments include chert, silicic volcanic rocks, granitic rocks, siltstone, quartzite, mica schist, and basalt. The composition of the sandstones in the Lambert Shale is very similar to that of the underlying Vaqueros Sandstone, suggesting that they were derived from the same source area.

Sandstones in the Lambert Shale range from strongly weathered and friable to hard and well-cemented. The most common cements are dolomite, calcite, and unidentified clay minerals. Phosphatic cement was noted in two samples collected from roadcuts along Aptos Creek Road in the Laurel Quadrangle. Calcitic concretions are common in some areas, particularly along Hinckley Creek.

Sandstones in the Lambert Shale can be divided very generally into two groups based on recurrent associations of bed thickness, grain size, and sedimentary structures. The two groups are: (1) thin bedded, fine grained sandstones that exhibit normal grading and partial Bouma sequences and are interbedded with roughly equal amounts of shale; and (2) thick to very thick bedded, coarse grained, massive to plane laminated sandstones that in some cases are amalgamated to form intervals up to 5 m thick. These two groups of sandstones probably represent interchannel and channel-fill deposits, respectively, and are discussed in further detail below.

(1) Thin bedded fine sandstones.

Intervals of thin-bedded fine sandstone and interbedded shale are common in the Lambert Shale in the upper Zayante Creek section (Figures 35 and 64) and along Hinckley Creek. The sandstones range in texture from very fine to coarse but most are very fine to fine and moderately to well sorted. Most beds are continuous across the outcrop (generally 5 to 10 m) but some become thinner and pinch out laterally. The lower contacts of the sandstone beds are always sharp, and often are scoured and clearly erosional. The upper contacts of the sandstones with the overlying shales range from sharp to gradational. Common sedimentary structures include normal grading, ripple and climbing ripple cross-lamination, and plane lamination; less common are starved ripples, convolute lamination, flame structures, and load casts.

Bouma Tce and Tbce sequences are common, but no "complete" Bouma Tabcde or Tabce sequences were noted. Plant fragments and mica flakes are commonly concentrated along laminae in the sandstones.

These sandstones strongly resemble the facies D and E turbidites of Mutti and Ricci Lucchi (1972) and are interpreted as the deposits of turbidity currents. Most of these thin bedded turbidites probably represent interchannel and channel-fill deposits, but no thinning-upward (or thickening-upward) vertical sequences were noted.

(2) Thick bedded coarse sandstones.

Thick to very thick bedded coarse sandstones occur sporadically in the Lambert Shale. Good outcrops occur in the upper Zayante Creek section, along Hinckley Creek, and along Indian Trail Road near Saratoga Gap. The sandstones range in texture from fine to very coarse grained, but most are medium to coarse and moderately to poorly sorted. The beds range from about 30 cm to more than 100 cm in thickness, and occur as single beds enclosed in shale, or as packets of amalgamated beds up to 5 m thick. The bases of the beds are usually sharp and often highly irregular and scoured with as much as 60 cm of erosional relief. The upper parts of the beds generally grade upward into the overlying shale, where shale is present.

Most of these thick to very thick coarse sandstones are massive or plane-laminated. Other common structures include rip-up clasts and flame structures. At the bases of two beds in the upper Zayante Creek section I found "sediment flaps" (terminology of Howell and Joyce, 1981, p. 67) in which part of the underlying mudrock was apparently pulled up as the sandstone bed was forcibly emplaced.

These thick bedded sandstones resemble the facies A and B turbidites of Mutti and Ricci Lucchi (1972). They are interpreted as submarine channel deposits that were emplaced by high-velocity turbidity currents, grain flows, or related kinds of sediment gravity flows.

Olistostromes.--

Olistostromes are uncommon in the Lambert Shale and are poorly exposed. Two olistostromal beds, one about 130 cm thick and the other between 50 and 250 cm thick, occur in the upper part of the formation in the upper Zayante Creek section. Both of these beds consist of jumbled blocks of contorted, thin-bedded sandstone and mudrock. Another olistostrome is exposed in Hinckley Creek, is about 60 cm thick, and consists of numerous angular clasts of dark brown mudrock in a matrix of medium sandstone. The mudrock clasts are similar in lithology to much of the Lambert Shale and are contorted as if they were soft and plastically deformed at the time of emplacement of the olistostrome.

These olistostromes correspond to facies F in the scheme of Mutti and Ricci Lucchi (1972) and probably represent soft-sediment slumps or debris flow deposits.

Glaucinitic sandstone.--

Only one bed of glauconitic sandstone was observed in the Lambert Shale. The bed is about one m thick and is very poorly exposed in the Slate Creek section about 30 m above the apparent base of the formation (Figure 60).

The base of the bed is sharp and marked by borings or burrows that extend downward for several cm into the underlying mudstone and are filled with glauconitic sand. The top of the sandstone bed grades upward into glauconitic sandy mudstone.

The glauconitic sandstone is dark green on fresh surfaces and weathers to various shades of orange and red on exposed surfaces and along fractures. The sandstone is fine to very coarse grained, poorly sorted, and contains scattered granules and pebbles of phosphate. The sandstone is apparently massive but may be bioturbated.

In thin-section the sandstone is composed of about 80-85% green glauconite, 5% phosphatic grains, and 10-15% detrital siliciclastic grains cemented by a brown, microcrystalline material that appears to be phosphatic. The grains of glauconite range from ovoid to irregular in shape and exhibit a wide variety of internal microstructures. Some of the glauconite grains appear to be aggregates of several smaller glauconite grains cemented together by glauconite; others have a faint lamellar structure, contain angular grains of quartz silt and "ghosts" of benthic foraminifers, and are interpreted as fragments of laminated mudrock that were entirely replaced by glauconite. The phosphatic grains include numerous fish fragments, a few phosphatic ooids, and many well-rounded, ovoid to irregularly-shaped grains that may represent fragments of phosphate nodules eroded from older phosphatic mudrocks. Fractures and small borings in some of the larger phosphatic grains are filled with glauconite. The detrital siliciclastic grains include quartz, feldspar, and biotite. Small euhedral blocks and framboids of pyrite are scattered throughout the rock, and appear to have partially replaced glauconitic and phosphatic grains as well as the phosphatic(?) cement.

This glauconitic sandstone, like the ones in the Rices Mudstone and Vaqueros Sandstone discussed earlier in this report, probably marks a disconformity and represents a period of erosion or very slow sedimentation. However, the disconformity in the Lambert Shale does not appear to correspond to any important biostratigraphic break, and is probably of local rather than regional extent because similar beds have not been observed in the Lambert Shale in other areas. I speculate that this glauconitic sandstone formed on the current-swept top or flank of a sediment-starved submarine topographic high in the Slate Creek area. The presence of such a submarine bank is supported by other evidence, including the occurrence of the fossiliferous limestone in the Slate Creek section described earlier in this report, and also by paleobathymetric maps based on an interpretation of benthic foraminiferal assemblages and presented later in this report (Figure 66).

Phosphatic pebble conglomerate.--

About 0.5 m stratigraphically above the just-described glauconitic sandstone is a bed of phosphatic pebble conglomerate. The bed is about 5 cm thick and poorly exposed but appears to be laterally continuous across the outcrop, which is about 3 m wide. The conglomerate consists of rounded to angular phosphatic granules and pebbles in a matrix of glauconitic sand. Thin-sections of two phosphatic pebbles show that they are oolitic phosphorites composed of sand-sized phosphatic pellets, phosphate-coated ooids, and minor detrital quartz and feldspar; these grains are cemented by microcrystalline phosphate. Most of the phosphate-coated ooids have nuclei of green glauconite.

Phosphatic pellets, glauconite, and detrital quartz and feldspar form veneers on the tops of some offshore banks in the modern southern California continental borderland (Pisciotta and Garrison, 1981). Perhaps similar phosphatic-glauconitic sands on the inferred submarine bank in the Slate Creek area were cemented by phosphate and then eroded and subsequently redeposited to form the phosphatic pebble conglomerate in the Lambert Shale.

Depositional Systems

The Lambert Shale represents deposition of organic-rich hemipelagic mud in bathyal environments where the bottom waters were generally anaerobic but occasionally well-oxygenated. The mud was deposited in a variety of settings including slope, basin plain, and bank top.

Along the southwestern margin of the La Honda block in the Felton, Laurel, and southeastern Castle Rock Ridge quadrangles, the Lambert Shale consists mainly of shale and mudstone (facies G of Mutti and Ricci Lucchi, 1972) with minor olistostromes (facies F) and turbidite sandstones (facies A, B, D, and E). This facies association is characteristic of slope deposits, according to Mutti and Ricci Lucchi (1972) and Howell and Normark (1982). Additional evidence for the presence of a slope in this area during the late Zemorrian and Saucian deposition of the Lambert Shale is provided by paleobathymetric data discussed later in this report and summarized in Figure 66.

Farther to the north, in the Mindego Hill and La Honda quadrangles, the Lambert Shale consists mainly of mudrocks with only minor turbidite sandstone, glauconitic sandstone, and phosphatic pebble conglomerate. Paleobathymetric reconstructions (Figure 66) suggest that the Lambert Shale in this area was deposited on a flat to gently sloping basin plain punctuated by submarine knolls.

Much of the Lambert Shale consists of laminated phosphatic shales that represent deposition in low-oxygen conditions. These anaerobic sediments occur in inferred slope, basin plain, and bank top settings, and their wide stratigraphic and geographic distribution suggests that low-oxygen conditions prevailed throughout the La Honda sea during much of late Zemorrian and Saucesian time. Thus, the Lambert shale apparently represents a basin-wide "anoxic event" similar to that recorded by the Eocene Twobar Shale and discussed earlier in this report. I speculate that both anoxic events occurred when circulation between the La Honda basin and the Pacific Ocean was partially blocked by sills whose tops occurred within the oxygen minimum zone. The locations and configurations of these hypothetical sills are unknown. Speculatively, the sills may have been caused by episodes of uplift of the San Gregorio high or other structural salients that are presently buried in the subsurface west of La Honda and east of the San Gregorio-Hosgri fault. Alternatively, the sills may have been formed by large-scale "shutter ridges," or large uplifted blocks of crust moving relatively northward along the west side of the San Gregorio-Hosgri fault; such large blocks may have temporarily blocked a deep, narrow channel or strait that connected the La Honda basin with the Pacific Ocean. A third possible explanation is that the La Honda-Pacific connection was partially blocked by construction of a volcanic edifice west of the La Honda area during the late Oligocene-early Miocene eruption of the Mindego Basalt.

The transition from the Vaqueros Sandstone and Mindego Basalt upward to the Lambert Shale represents a major marine transgression (Figures 23, 44; Clark, 1966, 1981). This transgression probably records a pulse of rapid subsidence during the late Oligocene and early Miocene, as discussed in the final section of this report.

LOWER TO MIDDLE MIOCENE SEQUENCE

The lower to middle Miocene sequence rests in angular unconformity on the older Paleocene and Eocene to lower Miocene sequences, and records a marine transgression of Relizian and Luisian age. The lower to middle Miocene sequence consists of a transgressive shallow-marine sheet sandstone, the Lompico Sandstone, and the overlying deeper-water Monterey Formation (also called the Monterey Shale by some authors).

Lompico Sandstone

The Lompico Sandstone consists chiefly of fossiliferous feldspathic sandstone with minor interbeds of mudstone and conglomerate. It was named by Clark (1966) for exposures in Lompico Creek. Its type section is along East Zayante Road, about one mile southeast of the town of Lompico (Figure 6; Clark, 1966, p.82). The Lompico Sandstone as recognized by Clark includes the lower sandstone unit of Brabb's (1960) "Formation A of the Monterey Group," as well as Relizian strata on Ben Lomond Mountain that were previously assigned to the Vaqueros Sandstone by Branner and others (1909), Page and Holmes (1945), and Brabb (1960).

As mapped by Brabb (1970), the Lompico Sandstone has a discontinuous geographic distribution. The Lompico is best developed on the Ben Lomond block. About 50 km to the north, on the southern flank of Montara Mountain, sandstones with similar lithology and stratigraphic position are also mapped as "Lompico Sandstone" by Brabb (1970). However, in the area between Montara Mountain and the Ben Lomond block, the Lompico is not present, and probably never was deposited there; its stratigraphic position is occupied by glauconitic and phosphatic strata at the base of the Monterey Formation. I infer that the two sandstone bodies called "Lompico" were deposited at about the same time but in geographically separate parts of the basin, and were never physically connected. Therefore, I suggest that

the name "Lompico" be applied only to the Ben Lomond exposures, and that the Relizian and Luisian sandstones on Montara Mountain be renamed.

On the Ben Lomond block, the Lompico Sandstone rests nonconformably on granitic and metamorphic basement, and in angular unconformity on the Locatelli Formation, the Butano Sandstone, and the Zayante (?) Sandstone of Majors Creek. A contact between the Lompico Sandstone and the Lambert Shale is nowhere exposed, but if it were it would probably be an unconformity, as implied by Figure 14. The Lompico is overlain conformably and gradationally by the Monterey Formation (Clark, 1966, 1981).

The Lompico Sandstone is about 150 m thick in its type section, and reaches a maximum thickness of 240 m along Majors Creek (Appendix 3). Shortly after its deposition, the Lompico Sandstone was probably a sheet about 100 m to 300 m thick that covered much of the northern Ben Lomond block.

The Lompico Sandstone, at least on the Ben Lomond block, is of early and perhaps middle Miocene age. Molluscs and echinoids of the Temblor Stage of Addicott (1972) are locally abundant. Benthic foraminifers suggest that the Lompico is of Relizian and possibly early Luisian age (Clark, 1966, 1981). Based on these data, and assuming that the Relizian Stage of the La Honda basin is the same age as the Relizian Stage of the Salinas basin (Poore and others, 1981), I conclude that most of the Lompico Sandstone was deposited between 18 m.y. and 17 m.y. ago.

The sedimentology of the Lompico Sandstone has not been studied in detail. On the Ben Lomond block, the Lompico Sandstone consists mainly of thick to very thick bedded, moderately to well sorted, fine to very fine feldspathic arenite. Fossils and fossil fragments are locally abundant and consist mainly of shallow-water marine molluscs, echinoids, and barnacles (Clark, 1981). Much of the sandstone is apparently massive, but some intervals are thoroughly bioturbated. Plane-laminated and tabular to trough cross-laminated sandstones are common and well-exposed in the Majors Creek area. Locally, individual tabular cross-laminated sets are more than 2 m thick and similar in appearance to the giant sand wave deposits described by Phillips (1981, 1983) from the overlying Santa Margarita Sandstone. The "echinoid reef" reported from Majors Creek by Page and Holmes (1945) consists of plane-laminated and cross-laminated coarse sandstone with abundant tests and fragments of an echinoid identified by Clark (1981) as *Vaquerosella coreyi*. Mudstone interbeds are few in the Lompico Sandstone, and yield benthic foraminifers indicative of outer shelf to upper bathyal depths (Appendix 1).

The Lompico Sandstone on the Ben Lomond block probably was deposited in shallow marine shelf environments, as suggested by: (1) locally abundant shallow-water marine megafossils and microfossils; (2) the predominance of "clean", moderately to well sorted sandstone with only a few mudstone interbeds, suggesting generally high-energy conditions that winnowed away most fine sediment; and (3) the common occurrence of trough and tabular cross-lamination indicating high-energy deposition by migrating bedforms such as dunes and sand waves. A granitic provenance for the sandstone is suggested by the abundance of quartz, feldspar, and biotite and by the presence of granitic clasts in the interbedded conglomerates. Much of the sediment may have been derived from erosion of the granitic core of Ben Lomond Mountain, which is believed to have been a topographic and structural high during early and middle Miocene time (Clark, 1981).

Little is known about the so-called Lompico Sandstone on the southern flank of Montara Mountain. These strata apparently rest nonconformably on granitic basement, are overlain conformably by the Monterey Formation, and are similar in lithology and fauna to the Lompico Sandstone of the Ben Lomond block (Clark, 1981, p.19-20). Elsewhere on the La Honda block--in particular, in the area between Montara Mountain and Ben Lomond Mountain--the fossiliferous feldspathic sandstone typical of the Lompico is missing. Instead, the stratigraphic position of the Lompico is occupied by a thin horizon of glauconitic siltstone, sandstone, or conglomerate (Figures 14 and 60; Cummings and others, 1962, p.194). This basal glauconitic horizon is mapped as part of the Monterey Formation by Brabb (1970) and by me, although it has been referred to the Lompico Sandstone by Beaulieu (1970). The lateral equivalence of the glauconitic horizon to the Lompico Sandstone is paleogeographically important because it suggests

that during Relizian time the shallow shelf areas on Montara and Ben Lomond mountains were separated by a deeper-water area in which glauconitic sand--rather than fossiliferous, cross-laminated and burrowed feldspathic sand--was deposited.

Monterey Formation

The Monterey Formation of the La Honda basin consists of siliceous and calcareous shale and mudstone, with locally abundant interbeds of sandstone and minor interbeds of bentonite. The Monterey Formation crops out extensively on the Ben Lomond block and is present in the subsurface beneath much of the onshore and offshore Monterey Bay area (Greene and Clark, 1979). On the La Honda block, however, the Monterey Formation is poorly exposed in small erosional remnants (see geologic map of Brabb, 1970) and is very poorly represented in the subsurface as well.

The name Monterey was borrowed from the Salinas Valley stratigraphic nomenclature and applied to strata in the Santa Cruz Mountains by Haebl and Arnold (1904) and by Branner and others (1909). Subsequent investigations have shown that strata mapped as Monterey by these early workers range in age from middle Eocene to upper Miocene and are now assigned to the Twobar Shale, Lambert Shale, Monterey Formation (or Monterey Shale) and Santa Cruz Mudstone. In this report, the name "Monterey" is restricted to strata of Relizian and Luisian age, following the procedure of Brabb (1970) and Clark (1966, 1981). The Monterey Formation so defined includes beds of the "Woodhams formation" of Touring (1959), the "Woodhams shale unit" of Cummings and others (1962), and the upper part of "Formation A" of Brabb (1960). The reader is warned that the "Monterey formation" of Touring (1959) and the "unnamed unit of the Monterey shale" of Cummings and others (1962) are of late Miocene age and are assigned to the Santa Cruz Mudstone by Brabb (1970) and by me.

On the Ben Lomond block and on the southern flank of Montara Mountain the Monterey Formation rests conformably and gradationally on the Lompico Sandstone. However, on the part of the La Honda block between Ben Lomond and Montara mountains, the Lompico Sandstone is absent, and the Monterey Formation rests directly on both the Mindego Basalt and the Lambert Shale. The Monterey-Mindego contact is marked by a glauconitic siltstone and is interpreted as an unconformity by Cummings and others (1962, p.194). The Monterey-Lambert contact is generally concordant but poorly exposed, and its interpretation is controversial. Clark (1966, p.74) and Beaulieu (1970) think that the contact is conformable and gradational. However, in Slate Creek, the Lambert Shale is sharply and concordantly overlain by a 50 cm-thick glauconitic and phosphatic pebble conglomerate at the base of the Monterey Formation (Figure 60). This contact is interpreted by Cummings and others (1962, p.194) and by me as a disconformity. The Monterey Formation is overlain in angular unconformity by the Santa Margarita Sandstone (Clark, 1966, 1981).

The original depositional thickness and geometry of the Monterey Formation are unknown due to extensive late Cenozoic erosion. The Monterey is at least 825 m thick on the Ben Lomond block and possibly 900 m or more thick on the La Honda block (Appendix 3). Erosional remnants of the Monterey Formation are widely scattered in the Santa Cruz Mountains, suggesting that the formation originally covered the entire area as a sheet that was several hundred meters thick.

The Monterey Formation of the La Honda basin is of early and middle Miocene age. Benthic foraminifers of the Relizian and Luisian stages are common throughout the basin (Appendix 1) and molds of molluscs of the Temblor Stage of Addicott (1972) have been reported from the Felton-Santa Cruz area by Clark (1966, 1981). Calcareous nannofossils found along Lompico Creek are tentatively referred to the lower or middle Miocene N5 Zone by Bukry and others (1977). These data suggest that the Monterey Formation in the La Honda basin was deposited between 18 m.y. and 14 m.y. ago, assuming that the Relizian and Luisian stages in the La Honda basin are the same ages as their type sections in the Salinas Valley area (Poore and others, 1981).

The sedimentology of the Monterey Formation of the La Honda basin has not been studied in detail. The available literature and my own limited field observations suggest, however, that there are significant lateral and vertical variations in the lithology of the Monterey.

On the Ben Lomond block in the Zayante-Lompico area, the Monterey Formation consists chiefly of shale and mudstone with numerous dolomitic concretions and interbeds of sandstone and bentonite. The lower half of the Monterey consists mainly of siliceous and calcareous shale. X-ray diffraction studies show that the shales contain opal-CT, quartz, and calcite (Grant, 1982). The opal-CT and some of the quartz may have formed by the diagenetic alteration of diatom-rich muds, while the calcite resides mainly in the tests of foraminifers and other calcareous microfossils. The shales typically are very thin to medium bedded, often laminated, contain abundant phosphatic nodules and laminae, and are dark-colored and rich in organic matter; these characteristics suggest that the shales were deposited in low-oxygen conditions. Molds of fossil bivalves are locally abundant and concentrated along bedding planes in the shales (Clark, 1966, 1981). It seems unlikely that the clams were able to live in low-oxygen conditions; instead they may have been transported and redeposited from shallower, more hospitable environments, or they may record intervals when the bottom waters were temporarily oxygenated. Benthic foraminifers from the shales suggest deposition at upper bathyal and possibly upper middle bathyal depths (Appendix 1).

Higher in the section in the Zayante-Lompico area, the low-oxygen shales are gradually replaced by massive, nonfissile, thick to very thick bedded, sandy and silty mudstones that are intensely bioturbated (Grant, 1982). The upward increase in bioturbation suggests increasingly more oxygenated bottom conditions.

Sandstone interbeds also become thicker and more numerous upsection in the Zayante-Lompico area. The sandstones are thin to thick bedded, very fine to medium feldspathic arenites and wackes that are similar in mineralogy to the underlying Lompico Sandstone (Clark, 1981). However, many of the sandstones in the Monterey are normally graded and exhibit partial to complete Bouma sequences, and therefore were probably deposited by turbidity currents. Limited paleocurrent data suggest that the turbidity currents flowed toward the northeast (Grant, 1982). The upward increase in thickness and frequency of the sandstone beds suggest that the upper part of the Monterey Formation is a regressive sequence and records progressive shallowing (Clark, 1981).

On the Ben Lomond block west of the Zayante-Lompico area, sandstone beds increase in thickness and frequency and the mudstones become siltier and sandier (Clark, 1966, 1981). On the southwestern flank of Ben Lomond Mountain the Monterey is poorly exposed but appears to consist mainly of siltstone and sandstone that reportedly contain "dwarfed" foraminiferal faunas. These rocks are inferred by Clark (1981) to record the persistence of shallow-water conditions in the Ben Lomond Mountain area following deposition of the Lompico Sandstone.

On the La Honda block in the Saratoga Gap and Portola Redwoods State Park areas, the Monterey Formation consists mainly of shale and mudstone (Figure 65). Dolomitic concretions and sandstone interbeds are also present but are less common than on the Ben Lomond block. The shales on the La Honda block are siliceous and calcareous, laminated, phosphatic, and rich in organic matter; like their counterparts on the Ben Lomond block, these shales probably were deposited in low-oxygen environments. However, the shales on the La Honda block are noticeably more fissile, more phosphatic, and less silty and sandy than correlative shales on the Ben Lomond block. In addition, thin interbeds of porcelanite, "opaline chert", and "impure diatomite" occur locally on the La Honda block, according to Cummings and others (1962); similar silica-rich rocks are present but less common on the Ben Lomond block. These observations show that in general the Monterey Formation of the La Honda block is finer grained and more siliceous than the Monterey of the Ben Lomond block. These differences suggest that the Monterey of the La Honda block accumulated in a more basinal setting and farther from sources of terrigenous sediment than the Monterey of the Ben Lomond block. In addition, benthic foraminifers from the La Honda block suggest deposition at middle bathyal depths, compared to upper bathyal and shelf depths on the Ben Lomond block (Appendix 1).

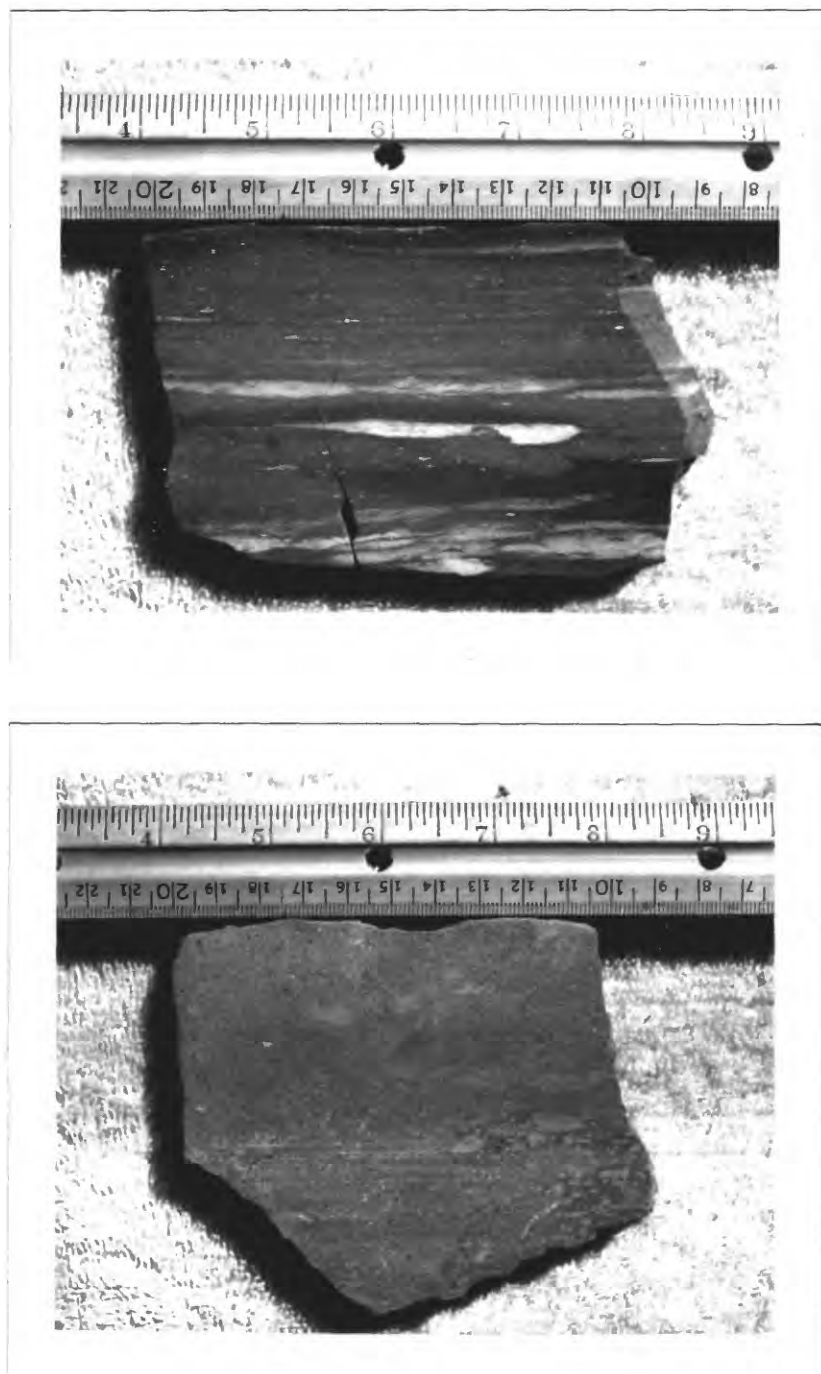


Figure 65. Sawn slabs of mudrocks from the Monterey Formation; samples collected from the Slate Creek section. Scales in centimeters and inches. Top: Laminated shale with light-colored phosphate nodules and laminae, and abundant benthic foraminifers. Stratigraphic top is toward the bottom of the page. Bottom: Bioturbated glauconitic sandy mudstone; bedding is more or less parallel to the ruler, and right side up.

Together, the Lompico Sandstone and Monterey Formation record a major marine transgression that followed an early Miocene (late Saucian to early Relizian) episode of extensive uplift and erosion. The transgression occurred during early to middle Miocene (Relizian and Luisian) time and was accompanied by subsidence and increasing water depth over much of the La Honda basin. On the basin margins, in both the Ben Lomond Mountain and Montara Mountain areas, the initial stages of deepening led to deposition of the Lompico Sandstone in high-energy shelf environments. In the deeper-water basin between these two shelf areas, however, the Lompico Sandstone was not deposited, and the initial subsidence and deepening are recorded by a disconformity and glauconitic bed at the base of the Monterey Formation. Continued subsidence led to deeper-water conditions and deposition of the Monterey Formation over much of the basin. The turbidite sandstones in the Monterey Formation of the Zayante-Lompico area were probably derived from a granitic source area to the southwest, as suggested by northeast-flowing paleocurrents, stratigraphic relationships, and the quartzofeldspathic mineralogy of the sandstones (Grant, 1982; Clark, 1966, p.115). The exact location of the granitic source area is unknown, but it may have been in the vicinity of the modern Ben Lomond Mountain (Clark, 1966) or Monterey Bay. On the northern margin of the La Honda basin, Montara Mountain may also have been a granitic high that shed sediment southward into the basin (Clark, 1966, p.115).

MIDDLE TO UPPER MIOCENE SEQUENCE

Deposition of the Monterey Formation was followed by a major episode of deformation, uplift, and erosion during middle Miocene time. Renewed subsidence and marine transgression began during the late middle Miocene and are recorded by strata of the middle to upper Miocene sequence. This sequence consists of two formations, the shallow marine Santa Margarita Sandstone and the deeper-water Santa Cruz Mudstone, which rest in angular unconformity on the Monterey Formation and all older rocks in the La Honda basin.

Santa Margarita Sandstone

The Santa Margarita Sandstone consists chiefly of fossiliferous feldspathic arenite and conglomerate. The name "Santa Margarita" was borrowed from the Salinas Valley stratigraphic nomenclature and applied to strata in the Santa Cruz Mountains by Branner and others (1909). As mapped by Brabb (1970), the Santa Margarita Sandstone includes strata formerly referred to as the basal sandstone of the "Monterey formation" by Touring (1959) and the basal sandstone of "Formation B" by Brabb (1960).

The Santa Margarita Sandstone is economically important. It is extensively quarried for sand and gravel in the Felton-Santa Cruz area and also is an important aquifer and source of domestic water. On the southwestern flank of Ben Lomond Mountain the Santa Margarita locally is saturated with heavy oil (Page and Holmes, 1945; Phillips, 1981). These bituminous sands were quarried for many years and used as road paving material (Huguenin and Castello, 1921). Attempts to extract the oil have been economically unsuccessful (Adams and Beatty, 1962; Hallmark, 1980).

Geographically, the Santa Margarita Sandstone is restricted to the central La Honda basin (see maps of Brabb, 1970, and Phillips, 1981, 1983). The Santa Margarita is thickest in the Felton-Scotts Valley area and thins generally northwestward to an apparent pinchout near Butano State Park (Phillips, 1981, Plate 1). East of the Felton-Scotts Valley area, the Santa Margarita is exposed in scattered outcrops as far east as Aptos Creek (Phillips, 1981) and probably is present in the subsurface as well. Geophysical evidence suggests that the Santa Margarita also is present in the Monterey Bay offshore area (Greene and Clark, 1979).

The Santa Margarita Sandstone rests nonconformably on granitic and metamorphic rocks. It also overlies, in angular unconformity, Tertiary strata as old as the Ynezian Locatelli Formation and as young as the Luisian Monterey Formation (Clark, 1981; Phillips, 1981). The Santa Margarita is conformably overlain by the Santa Cruz Mudstone. Depending on the locality, this upper contact is gradational,

interfingering, or abrupt; in places, this contact is associated with pebble beds, glauconitic sandstone, and local concentrations of mammal bones (Clark, 1966; Phillips, 1981).

An isopach map prepared by Phillips (1981) shows that the Santa Margarita reaches its maximum thickness of about 130 m in the Felton-Scotts Valley region. The area of greatest thickness is adjacent and parallel to the Ben Lomond fault, suggesting that the fault was active during deposition of the Santa Margarita (Phillips, 1983; Stanley and McCaffrey, 1983). Locally, the Santa Margarita thins and pinches out onto ancient structural and topographic highs, indicating that it was deposited by a sea that transgressed over an irregular, perhaps hilly erosional surface (Phillips, 1981, 1983).

Based on the occurrence of invertebrate fossils of the Margaritan and Jacalitos stages of Addicott (1972) and vertebrate fossils of the Clarendonian Stage, the Santa Margarita Sandstone was deposited during the late middle and early late Miocene about 9 m.y. to 12 m.y. ago (Phillips, 1981).

The sedimentology of the Santa Margarita Sandstone has been studied in detail by Phillips (1981, 1983). These investigations show that the Santa Margarita was deposited in a large tidal seaway—a kind of ancient Golden Gate—that connected the Pacific Ocean with an inland sea in the San Joaquin Valley. The tidal seaway was long and narrow, about 8 to 10 km wide, and oriented northeast-southwest or nearly perpendicular to the axis of Ben Lomond Mountain. In the center of the ancient seaway, extensive cross-stratified sandstones and conglomerates were deposited by large sand waves that migrated in response to strong tidal currents. On either side of the belt of cross-stratified sandstone and conglomerate, sandstones on the channel margins are intensely bioturbated and were deposited in relatively quiet-water environments. The paleocurrent pattern in this ancient tidal seaway, based on more than 1700 individual measurements, is bimodal and bipolar but assymetric; the dominant flow direction to the southwest represents flow during falling (ebb) tides, while weaker currents flowed to the northeast during rising (flood) tides (Phillips, 1983).

No benthic foraminiferal assemblages have been reported from the Santa Margarita Sandstone, so Ingle's (1980) method of paleobathymetric analysis cannot be applied. Phillips (1981, p.251) believes that the Santa Margarita was deposited in marine shelf environments, but probably below the zone of effective wave action at depths of 20 m or more. Deposition at shelf depths is suggested by the coarse texture of the sediment, the general lack of mudstone or shale interbeds, the presence of extensive large-scale cross-stratification, the bipolar paleocurrents indicating a strong tidal influence, and the locally abundant fossils of shallow-water molluscs, echinoids, barnacles, and other invertebrates.

The provenance of the Santa Margarita Sandstone has not been studied in detail. Analysis of 11 samples by Brabb (1960, p.72) shows that the modal mineralogy of the sandstone varies from 92% quartz to 90% plagioclase; thus, the Santa Margarita ranges from a quartz arenite to a feldspathic arenite. Clasts in the conglomerates include a wide variety of lithologies that suggest several different clastic sources, including Salinian and Franciscan basement rocks and older Tertiary sedimentary and volcanic rocks (Clark, 1981; Stanley, 1982).

The northeastern end of the Santa Margarita tidal seaway has apparently been truncated by 226 km of right-lateral strike-slip displacement along the San Andreas fault. Phillips (1983) believes that the missing fragment of seaway is represented on the east side of the fault by the Polonio Sandstone of northwestern Kern County.

The Santa Margarita Sandstone and the overlying Santa Cruz Mudstone are similar in lithology and stratigraphic relationships to the Laird Sandstone and Monterey Shale of the Point Reyes area, about 115 km to 120 km to the northwest of the La Honda basin and on the west side of the San Gregorio-Hosgri fault (Clark, 1968, 1981; Galloway, 1977). These similarities were cited by Graham and Dickinson (1978b) as evidence for 115 km to 120 km of right-lateral strike-slip displacement along the fault since late Miocene time.

Santa Cruz Mudstone

The Santa Cruz Mudstone consists chiefly of siliceous mudstone and porcelanite with locally abundant dolomitic and calcitic concretions. The formation was named by Clark (1966), who designated a type section in Moore Creek canyon and along the sea cliff in the city of Santa Cruz (Figure 6). The Santa Cruz Mudstone as recognized by Clark includes strata previously assigned to the "Monterey Formation" of Touring (1959), the unnamed upper unit of the "Monterey Formation" of Cummings and others (1962), and the upper part of "Formation B" of Brabb (1960).

The Santa Cruz Mudstone is thickest and best exposed along the coast northwest of Santa Cruz, and it can be traced in outcrop as far north as Pescadero Creek. Still farther north, it is present in the subsurface beneath much of the San Gregorio and western La Honda quadrangles (Touring, 1959, Plates 11 to 13). Away from the coastal area, the Santa Cruz Mudstone crops out in scattered small erosional remnants such as those near Riverside Grove and Scotts Valley (see map of Brabb, 1970). These remnants suggest that the Santa Cruz Mudstone once blanketed most of the central and northern Santa Cruz Mountains. East of the Felton and Santa Cruz quadrangles, the formation is not exposed in outcrop but is believed to be present, at least locally, in the subsurface. The Santa Cruz Mudstone probably thins to the southeast and pinches out in the subsurface somewhere between Santa Cruz and Moss Landing (Greene and Clark, 1979, p.281).

The stratigraphic relationships of the Santa Cruz Mudstone are complex. Over most of the La Honda basin, it rests conformably or possibly disconformably on the Santa Margarita Sandstone (Phillips, 1981). Locally, however, the Santa Margarita Sandstone is missing from the tops of old structural and topographic highs, and in these areas the Santa Cruz Mudstone lies nonconformably on granitic and metamorphic basement rocks (Clark, 1981) or unconformably on Tertiary strata as old as the Butano Sandstone and as young as the Monterey Formation (Phillips, 1981, p.50). The Santa Cruz Mudstone is overlain by the Purisima Formation. This upper contact is reportedly conformable in the La Honda quadrangle (Cummings and others, 1962) but it is an angular unconformity over most of the rest of the La Honda basin (Beaulieu, 1970).

Along the coast, the Santa Cruz Mudstone is at least 2700 m thick in the Texaco Poletti #1 well near Davenport, and at least 2400 m thick in the Texaco Steele #1 well near Pescadero (Clark and Brabb, 1978). In its type section, the formation is only 140 m thick (Clark, 1966, 1981) but stratigraphic and sedimentologic relationships suggest that at least 500 m of the Santa Cruz Mudstone were removed from the type section by erosion prior to deposition of the overlying Purisima Formation (Stuart and others, 1982). The Santa Cruz Mudstone is only about 60 m to 70 m thick in the Scotts Valley and Boulder Creek areas (Appendix 3), but much of the upper part of the formation in these areas may have been stripped off by pre-Purisima erosion.

The Santa Cruz Mudstone is sparsely fossiliferous and most of the formation is not well dated. The stratigraphic position of this formation between two well-dated upper Miocene units—the underlying Santa Margarita Sandstone and the overlying Purisima Formation—establishes the age of the Santa Cruz Mudstone as late Miocene. An assemblage of benthic foraminifers of the Delmontian Stage was found in the type section by Clark (1981). A diatom flora collected from a concretion in the type section just below the unconformable contact with the Purisima Formation is indicative of the upper Miocene North Pacific Diatom Zone XIa (R.M. Stuart, personal communication, 1980). These data suggest that the Santa Cruz Mudstone was deposited between 9 m.y. and 7 m.y. ago.

The sedimentology of the Santa Cruz Mudstone has not been studied in detail. The available literature and my own limited field observations indicate that the unit consists chiefly of thin to thick bedded siliceous mudstone and porcelanite. Both the mudstone and porcelanite are brown to dark brown in color, and rich in organic matter. Some beds are laminated, while others are massive and bioturbated. Glauconite is scattered throughout the formation (Clark, 1981) but no phosphatic nodules or laminae have been reported. Megafossils are rare, but a few ophiuroids, molluscs, and echinoids are reported by Clark (1981). Diatoms, sponge spicules, and fish fragments are common to abundant; locally, diatoms constitute

as much as 70% of the mudstone (Clark, 1981). Limited x-ray diffraction data from the type section show that most of the silica in the siliceous mudstones and porcelanites is opal-CT, but some is quartz. The opal-CT was probably derived from the diagenetic alteration and redistribution of silica from diatoms and sponge spicules (Clark, 1981). Some of the quartz may also be of diagenetic origin, but thin-sections show that much of the quartz occurs as detrital grains of silt.

The fine texture of the sediment suggests that the Santa Cruz Mudstone was deposited in quiet, deeper-water environments. Benthic foraminifers are rare in this formation, but a small assemblage from the type section suggests deposition at upper bathyal depths (Appendix 1). Clark (1966, 1981) believes that the Santa Cruz Mudstone was deposited at outer shelf depths, based on the occurrence of shallower-water benthic foraminifers and molluscs, but these fossils may have been transported into deeper water and redeposited.

The dark color, high organic content, common occurrence of laminations and glauconite, and scarcity of benthic fossils suggest that much of the Santa Cruz Mudstone was deposited in low-oxygen conditions. However, the bioturbated intervals probably formed in well-oxygenated environments that supported an active sediment-churning benthic megafauna. The occurrence of both laminated and bioturbated intervals suggests that there were fluctuations in the amount of dissolved oxygen in the bottom waters during deposition of the Santa Cruz Mudstone. However, the causes of these fluctuations are unknown.

The unusually high proportion of diatom tests in the Santa Cruz Mudstone indicates that rates of biogenic sedimentation were high relative to rates of terrigenous sedimentation. The absolute rates of diatom productivity may have been unusually high due to coastal upwelling and the resulting high fertility of surface waters; such an explanation has been proposed to explain the origin of other, lithologically similar siliceous mudrocks in the Miocene record of California (for examples, see Garrison, 1981; Pisciotto and Garrison, 1981). In addition, the supply of terrigenous sediment to the area may have been drastically reduced as local topographic highs that previously served as clastic sediment sources were submerged by the rapidly transgressing late Miocene sea. This interpretation is supported by the wide geographic distribution of the Santa Cruz Mudstone—including the presence of erosional remnants on the top of Ben Lomond Mountain—which suggests that the entire area of the central Santa Cruz Mountains was underwater during the late Miocene.

Together, the Santa Margarita Sandstone and Santa Cruz Mudstone record an extensive marine transgression during middle to late Miocene time. This transgression occurred immediately after an episode of deformation, uplift, and erosion; this deformation must have occurred during the middle Miocene, because the angular unconformity at the base of the Santa Margarita Sandstone truncates tilted strata of the Luisian Monterey Formation (Clark, 1966, 1981).

The initial stage of the middle to late Miocene transgression may have occurred at the same time as a eustatic rise in sea level (Phillips, 1981, p.47-48) but several observations suggest that the major cause of the transgression was rapid tectonic subsidence. Movement along the Ben Lomond fault resulted in differential subsidence and local thickening of the Santa Margarita Sandstone in the Felton-Santa Cruz area (Phillips, 1983; Stanley and McCaffrey, 1983). Profound and rapid subsidence occurred on the southwestern flank of Ben Lomond Mountain, where more than 2700 m of the Santa Cruz Mudstone were deposited in less than 5 m.y. Rapid subsidence, syn-sedimentary faulting, and marine transgression also occurred at about the same time in several other sedimentary basins in central and southern California. This episode of basin expansion may have been caused by regional extension associated with a change in relative motion between the Pacific and North American plates about 10 m.y. ago (Blake and others, 1978). Alternatively, the regional extension and basin formation may have occurred as the locus of strike-slip motion between the Pacific and North American plates shifted landward during the Miocene from offshore faults to the San Andreas and other onshore faults (Graham, 1978).

UPPER MIOCENE TO PLIOCENE SEQUENCE
Purisima Formation

The Purisima Formation embraces a wide variety of lithologies including quartzofeldspathic and volcanic sandstones, organic and terrigenous mudrocks, and conglomerate. The formation was named by Haehl and Arnold (1904) for exposures along Purisima Creek in the Half Moon Bay quadrangle (Figure 6).

Geographically, outcrops of the Purisima Formation are more widely distributed in the Santa Cruz Mountains than any other Tertiary formation. In the northern Santa Cruz Mountains, the Purisima is exposed in a roughly triangular area with apices at Half Moon Bay, Pescadero, and Portola State Park (Cummings and others, 1962; Beaulieu, 1970; see also the geologic map of Brabb, 1970). Also in this area, the formation has yielded modest amounts of petroleum from laterally discontinuous sandstones and fractured mudrocks in the Half Moon Bay and La Honda fields (Table 1; Figure 5). A second large area of Purisima exposures occurs in the central and southern Santa Cruz Mountains east of Ben Lomond Mountain and southwest of the San Andreas fault (see geologic map of Clark and Rietman, 1973). The Purisima is also well-exposed along the coast in the Año Nuevo and Santa Cruz-Capitola areas (Clark, 1981). Geophysical evidence and dredge hauls show that the Purisima is thick and widely distributed in the Monterey Bay and Santa Cruz-San Mateo county offshore areas (Greene, 1977; Greene and Clark, 1979; Nagel and Mullins, 1983).

The stratigraphic relations of the Purisima Formation are complex. Over most of the region, the lower contact of the formation is an unconformity, and the Purisima rests in angular discordance on rocks as old as the granitic-metamorphic basement and as young as the Santa Cruz Mudstone. In many places, this unconformity is immediately overlain by a glauconitic sandstone or conglomerate; excellent exposures of the basal glauconitic horizon occur along the seacliff in the city of Santa Cruz (Clark, 1966, 1981) and along Pescadero Creek south of Portola Redwoods State Park. However, in a few places the Purisima Formation is believed to rest concordantly and perhaps conformably on the Santa Cruz Mudstone, for example along Pescadero Creek near San Mateo County Memorial Park (Cummings and others, 1962, p.200).

Over most of the Santa Cruz Mountains the top of the Purisima Formation is eroded or unconformably overlain by Quaternary marine terrace, fluvial, and landslide deposits. In the Aptos-Watsonville area, the Purisima is overlain by the Aromas Sand; this contact appears to be conformable and gradational along the sea cliff (R.M. Stuart, personal communication, 1979) but locally may be unconformable (Greene and Clark, 1979).

The thickness of the Purisima Formation shows significant lateral variations (Appendix 3). In the Santa Cruz--Capitola area, the "true" stratigraphic thickness of the formation is about 300 m to 350 m, but over most of the rest of the La Honda basin the top of the formation is eroded and only minimum estimates of thickness can be made. The Purisima Formation is more than 670 m thick in the Monterey Bay offshore (Greene and Clark, 1979), at least 800 m thick in the Laurel quadrangle, and about 1700 m thick in the La Honda quadrangle. These large lateral variations in thickness suggest differential subsidence and at least mild tectonic deformation of the La Honda basin area during deposition of the Purisima Formation. In the Half Moon Bay area, the formation *may* be 2400 m or more thick, but this estimate is based on limited well control and may include strata more properly assigned to the Santa Cruz Mudstone.

The Purisima Formation ranges in age from late Miocene to late Pliocene, as indicated by radiometric, paleontologic, and paleomagnetic evidence. A potassium-argon date of 6.7 ± 0.6 m.y. was obtained from glauconite at the base of the formation in the city of Santa Cruz (Clark, 1981) but this date appears to be about 0.5 m.y. too old compared to the paleontologic and paleomagnetic evidence (R.M. Stuart, personal communication, 1982). Diatom floras collected from the lower part of the Purisima at various localities in the Santa Cruz and Point Año Nuevo areas are correlative with the upper Miocene and lower Pliocene North Pacific Diatom Zones X and IX (Addicott and others, 1978; Clark, 1981). A rich molluscan fauna of Pliocene age has been described from the Capitola area by Addicott and others

(1978), and vertebrate fossils from the same area suggest a late Hemphillian or Blancan mammalian age (Clark, 1981). Abundant Pliocene megafossils and rare Pliocene microfossils have also been found in the northern part of the La Honda basin in the Half Moon Bay, Woodside, San Gregorio, and La Honda quadrangles (Goodwin and Thompson, 1954; Bandy, 1955; Touring, 1959; Cummings and others, 1962). A water-lain rhyolitic tuff in the lower part of the Purisima Formation (Tahana unit of Cummings and others, 1962) exposed at San Gregorio beach is correlative with the 3.3 m.y. old Nomlaki Tuff of northern California, based on tephrochronological studies by A.M. Sarna-Wojcicki of the U.S. Geological Survey (Nilsen and Brabb, 1979, p.54). Magnetic polarity zonation of the coastal outcrops in the Santa Cruz-Capitola area shows that the Purisima and overlying Aromas formations contain a nearly complete sequence of magnetozones extending from uppermost Epoch 6 into the Matuyama Epoch (Stuart and others, 1982). Taken as a whole, the above data show that deposition of the Purisima Formation began about 6.1 m.y. to 6.2 m.y. ago during the late Miocene and continued through much of the Pliocene (Stuart and others, 1982).

The lithology of the Purisima Formation varies significantly both laterally and vertically, and as a result the internal stratigraphy and sedimentology of the formation are unresolved and controversial. In the northern Santa Cruz Mountains the Purisima Formation has been divided into five units, the Tahana, Pomponio, San Gregorio, Lobitos, and Tunitas units (Touring, 1959; Cummings and others, 1962). These units are composed chiefly of sandstone, mudstone, conglomerate, and tuff that were deposited in marine environments at bathyal to shelf depths (Goodwin and Thompson, 1954; Bandy, 1955; Cummings and others, 1962). The sedimentology of the Purisima Formation in this northern area has not been studied in detail except for a small area near Moss Beach where coarse sandstones and conglomerates were deposited on a wave-modified fan delta (Wiley and Moore, 1983).

In the Santa Cruz-Capitola area, the Purisima Formation has been investigated in detail by Clark (1981) and Stuart and others (1982). The lower part of the formation consists of a thin basal glauconitic sandstone overlain by 20 m to 30 m of laminated to intensely burrowed diatomaceous mudstone. The diatom-rich muds were probably deposited in quiet, deep water, possibly at middle bathyal depths (Greene and Clark, 1979, p.293). This lower part of the formation records a rapid marine transgression following uplift and erosion of at least 500 m of the underlying Santa Cruz Mudstone (Stuart and others, 1982).

The diatomaceous mudstone grades upward into a sequence of bioturbated and cross-laminated fossiliferous sandstones that were deposited in a variety of shallow-marine environments including storm-dominated shelves, protected embayments, high-energy shorelines, and possibly deltas (Addicott and others, 1978; Greene and Clark, 1979; Stuart and others, 1982). These sandstones constitute the upper nine-tenths of the thickness of the Purisima Formation and record progressive shallowing of water depths during Pliocene time. A disconformity marked by a distinctive phosphatic pebble bed indicates an abrupt change from storm-dominated to tide-dominated shelf sedimentation about 3.5 m.y. to 4.0 m.y. ago (Stuart and others, 1982). The cause of this sudden restructuring of the depositional basin is not known but may have been related to tectonic activity associated with movement along local faults such as the San Gregorio-Hosgri or Monterey Bay fault zone (R.M. Stuart, personal communications, 1981, 1982).

Clastic sediments in the Purisima Formation were derived from several different sources. Compositionally, the sandstones fall roughly into two groups, quartzofeldspathic and volcanic. The quartzofeldspathic sandstones probably were derived by erosion of granitic rocks and older Tertiary feldspathic sandstones from local topographic highs such as Ben Lomond Mountain. The volcanic sandstones include rhyolitic tuffs and andesitic "blue" sandstones that probably were derived from volcanos in the Sierra Nevada, the Cascades, and possibly the Coast Ranges (Lerbekmo, 1957; Cummings and others, 1962). Boulder conglomerates at Moss Beach were derived from nearby outcrops of granitic basement in the Montara Mountain area (Wiley and Moore, 1983). Other conglomerates in the Santa Cruz-Capitola area contain granitic and metamorphic clasts that probably were eroded from the Ben Lomond Mountain basement massif, and clasts of sandstone and mudstone eroded from older Tertiary formations (R.M. Stuart, personal communication, 1981). No clasts of obvious Franciscan provenance have been reported from conglomerates in the Santa Cruz-Capitola area (R.M. Stuart, personal

communication, 1981).

In summary, deposition of the Purisima Formation in the La Honda basin began after a major episode of regional deformation, uplift, and erosion during the late Miocene about 6 m.y. to 8 m.y. ago (Stuart and others, 1982). The Purisima records a rapid marine transgression during the late Miocene followed by a general regression and basin-filling during the Pliocene. The regression culminated in major regional uplift of the modern Santa Cruz Mountains during the late Pliocene and Quaternary. Clastic sediments were derived from granitic-metamorphic basement and older sedimentary rocks eroded from local topographic highs, and from distant rhyolitic and andesitic volcanos elsewhere in central and northern California. Deposition of the Purisima Formation took place in a tectonically active basin, as suggested by large lateral variations in thickness, rapid lateral and vertical variations in sedimentary facies, the presence of at least one major internal unconformity, and the occurrence—at least in the Santa Cruz-Capitola area—of sedimentary structures indicative of liquefaction during syn-sedimentary earthquakes (R.M. Stuart, personal communication, 1981). I believe that the most likely cause of this tectonic activity was right-lateral movement and wrenching along major strike-slip faults in the area, including the San Andreas, San Gregorio-Hosgri, and possibly the Monterey Bay fault zone.

LOWER TO MIDDLE TERTIARY STRATA OF THE NORTHERN GABILAN RANGE

Introduction

Sedimentary and volcanic rocks of Eocene to lower Miocene age are exposed in the northern Gabilan Range near San Juan Bautista, about 15 km southwest of Watsonville (Figure 12). These rocks are thought to represent the extreme southern end of the La Honda basin (Loel and Corey, 1932; Addicott, 1968; Clark and Rietman, 1973). Geophysical studies by Clark and Rietman (1973) show that the lower to middle Tertiary strata of the northern Gabilan Range are probably continuous in the subsurface with strata of similar age in the central and northern Santa Cruz Mountains. However, correlation of individual formations in the two areas is not straightforward. The lack of continuity of surface exposures, the limited well control, and probable lateral facies changes between the two areas have resulted in separate rock-stratigraphic nomenclatures (Clark and Rietman, 1973). The geologic histories of the two areas are similar in general but not in some details, as discussed below.

The lower to middle Tertiary section in the northern Gabilans is more than 2500 m thick, and is bounded on the northeast by the San Andreas fault and on the south and southwest by the Zayante-Vergeles fault. Eocene rocks at the base of the Tertiary section rest nonconformably on gabbro that has yielded a potassium-argon radiometric age of 156 ± 8 m.y. (Ross, 1970; Nilsen, 1984).

Owing to poor exposure and limited paleontologic control, the stratigraphy and structure of the Tertiary rocks in the northern Gabilans are unclear and controversial. At least nine different geologic maps of all or part of the area are available, including ones by Kerr and Schenck (1925), Allen (1946), Taliaferro (1948), McCroden (1949), Castro (1967), Walrond and others (1967), Clark and Rietman (1973), Dibblee and Rogers (1975), and Dibblee and others (1979). Some of these maps offer generally similar interpretations of stratigraphy and structure, but some are radically different; compare, for example, the map of Allen (1946) with that of Dibblee and others (1979). The stratigraphic scheme shown in Figure 12 and used below is generalized and slightly modified from that of Clark and Rietman (1973).

San Juan Bautista Formation

The San Juan Bautista Formation consists mainly of sandstone, siltstone, and shale, with minor amounts of conglomerate. The formation is 550 m to more than 1500 m thick, rests nonconformably on Jurassic gabbro, and is overlain by the Pinecate Formation (Clark and Rietman, 1973; Nilsen, 1984).

The San Juan Bautista Formation is mainly of Eocene age, based on the occurrence in outcrop samples of assemblages of benthic foraminifers of the Penutian, Ulatisian, Narizian, and Refugian stages (Waters, 1968; Nilsen, 1984), planktic foraminifers of the lower to middle Eocene P10 to P11 Zones (R. Z. Poore, 1975, unpublished data), and molluscs of the Refugian Stage (Schenck and Kleinpell, 1936; Allen, 1946; Addicott, 1968). Part of the formation may be of early Oligocene age, for McCroden (1949) reports the occurrence of the molluscan species *Spisula albaria* (Conrad) and *Tellina tenuilineata* Clark, which have their lowest stratigraphic occurrence in Addicott's (1972) unnamed Oligocene stage (Figure 9).

The Occidental Bingham #1 well (Monterey County, San Juan Bautista quadrangle, Sec. 34-12S-3E) penetrated strata yielding assemblages of Narizian and Refugian or lower Zemorrian benthic foraminifers in the drilled interval from 3503 feet to total depth at 7130 feet. Available electric logs, mudlogs, and dipmeter results suggest that this interval has a "true" stratigraphic thickness of about 850 m and consists of interbedded mudrocks and fine to coarse-grained and pebbly feldspathic sandstone. This interval is tentatively correlated with the San Juan Bautista Formation of outcrop sections based on its age, lithology, and stratigraphic position beneath a thick sequence of redbeds and shallow-marine sandstones. The well apparently bottomed in siltstone and shale without reaching the base of the San Juan Bautista Formation.

The stratigraphy and sedimentology of the San Juan Bautista Formation have been studied most recently by Nilsen (1984). The lower part of the formation, about 335 m thick, consists of a basal conglomerate about 15 m thick overlain by shale and siltstone with interbedded sandstone turbidites of facies D of Mutti and Ricci Lucchi (1972). Assemblages of benthic foraminifers from these rocks indicate deposition at lower middle bathyal to lower bathyal depths (Appendix 2). The facies D turbidites are laterally extensive and are not arranged in thickening- or thinning-upward sequences, suggesting that they were deposited on a basin plain (Nilsen, 1984). The mineralogy of the sandstones suggests a granitic provenance, and limited paleocurrent data indicate sediment transport from east to west with a vector mean of 272° (Nilsen, 1984).

The rest of the San Juan Bautista Formation reportedly consists of fossiliferous, bioturbated and cross-stratified sandstone, and poorly exposed siltstone and shale. These rocks are believed by Nilsen (1984) to represent deposition in shallow-marine environments.

Pinecate Formation

The Pinecate Formation consists of bioturbated and cross-laminated sandstone with interbeds of pebble to boulder conglomerate. The formation ranges from 200 m to more than 335 m thick (Clark and Rietman, 1973). The Pinecate Formation overlies the San Juan Bautista Formation; the contact is not clearly exposed but may be a disconformity (Kerr and Schenck, 1925; Castro, 1967). The Pinecate Formation is overlain by and laterally interfingers with a thick sequence of redbeds, described below.

The Pinecate Formation is sparsely fossiliferous, but reportedly contains a few "Vaqueros" molluscan fossils (McCroden, 1949). The Pinecate is assigned a Zemorrian age by Clark and Rietman (1973) and by Nilsen (1984), but these authors do not discuss the specific evidence for this age assignment.

The sedimentology of the Pinecate Formation has not been studied in detail, but the available literature and my own limited field observations suggest that it probably was deposited in shallow marine environments. The major categories of rocks in the Pinecate Formation are: (1) bioturbated sandstones; (2) plane-laminated to cross-laminated sandstones; and (3) pebble to boulder conglomerates. The sandstones range from fine to coarse grained, are commonly well-sorted, and in places contain shallow marine fossils including barnacles, bivalves and scaphopods. No paleocurrent studies have been done, but the cross-stratification in most outcrops is bi-directional, suggesting deposition by wave- or tidally-generated currents. The conglomerates generally are clast-supported, imbricated, consist mainly of well-rounded granitic and metamorphic rocks, and occur in laterally persistent beds; these are tentatively interpreted as storm or surf-zone deposits.

Redbeds

The Pinecate Formation is overlain by and interfingers laterally with a sequence of red sandstones, conglomerates, and mudrocks. The redbeds as yet have no formal status as a formation, but they have been given a number of informal names. Clark and Rietman (1973) and Nilsen (1984) refer to them as the "Red beds of Kerr and Schenck (1925)." The redbeds have also been mapped as part of the "Vaqueros group" by Allen (1946) and Bowen and Gray (1959); as part of the Vaqueros Formation by Castro (1967); and as the Zayante Sandstone by Dibblee and others (1979). The redbeds in the northern Gabilans, however, are not continuous in outcrop and are not known to be continuous in the subsurface with the Zayante Sandstone in its type area, about 45 km to the northwest.

The redbeds apparently are of late Oligocene to early Miocene age, based on the interfingering of the redbeds with the underlying Pinecate Formation of Zemorrian (?) age (Nilsen, 1984) and with the overlying volcanics of early Miocene age.

The thickness of the redbeds, according to Clark and Rietman (1973) is about 365 m. However, my tentative interpretations of electric logs, mudlogs, and dipmeter results from the Occidental Bingaman #1 well indicate that the redbeds are at least 725 m thick.

The sedimentology of the redbeds has not been studied in detail, but the available literature and my own limited field observations suggest that they were deposited in nonmarine environments, perhaps on an alluvial fan (Cloos and Apted, 1979, p. 121). The redbeds are poorly exposed, but seem to consist mainly of: (1) clast-supported, pebble to boulder conglomerates that resemble facies Gm of Miall (1977, 1978); (2) red, poorly-sorted, coarse sandstones that range from apparently massive to cross-stratified; and (3) red, laminated to bioturbated mudrocks that locally contain white calcitic nodules of possible pedogenic origin. In some outcrops along San Juan Grade, conglomerate, sandstone, and mudrocks are arranged in well-defined fining-upward sequences.

Some of the conglomerate beds are extremely coarse-grained and contain clasts up to 180 cm in diameter (McCroden, 1949), suggesting a nearby sediment source area. Limited paleocurrent data obtained by me from pebble and cobble imbrication in outcrops along San Juan Grade suggest that sediment transport was generally to the northeast and east. The conglomerates are composed mainly of granitic and metamorphic rocks that most likely were derived from a Salinian source terrane (Cloos and Apted, 1979). Conglomerates exposed along San Juan Grade contain abundant clasts of banded marble that are nearly identical to marble exposed in Salinian metamorphic roof pendants in the nearby Fremont Peak area, about 5 km to the southeast on the other side of the Zayante-Vergeles fault. If the marble clasts in the redbeds were in fact derived from the Fremont Peak area, as seems likely, then right-lateral strike-slip movement along the Zayante-Vergeles fault since late Oligocene or early Miocene time has been small, and probably less than 10 km.

Volcanic Rocks

The redbeds are overlain by and partly laterally equivalent to a sequence of poorly-exposed volcanic rocks. The volcanics are mainly andesitic and dacitic lavas, tuffs, and breccias, but minor basalt and rhyolite also occur (McCroden, 1949; Castro, 1967; Clark and Rietman, 1973). The volcanics are of early Miocene age, based on a single potassium-argon radiometric date of 21.6 ± 0.7 m.y. obtained by D.L. Turner and reported by Clark and Rietman (1973). The volcanics are about 300-425 m thick (Clark and Rietman, 1973) and reportedly thin to the northeast, away from the Zayante-Vergeles fault (Allen, 1946; Castro, 1967). The main volcanic vents evidently were near the Zayante-Vergeles fault, although other smaller vents may have existed farther to the north (McCroden, 1949).

Summary and Comparison with the Santa Cruz Mountains

The early to middle Tertiary histories of the Santa Cruz Mountains and northern Gabilan Range are similar in general but differ in some details.

Eocene deep-sea siliciclastic sedimentation is recorded in the northern Gabilans by the basin-plain deposits of the lower San Juan Bautista Formation, and in the Santa Cruz Mountains by the submarine fan and basin-plain deposits of the Butano Sandstone, Twobar Shale, and Rices Mudstone (Figure 12). The details of the paleogeographic relationship between the Butano submarine fan and the San Juan Bautista basin-plain are unclear, but one possible interpretation, proposed by Nilsen and Clarke, is shown in Figure 2. Sediments deposited on the Butano fan were derived from a Salinian granitic source to the south (Nilsen and Simoni, 1973), but turbidite sandstones on the San Juan Bautista basin-plain were apparently derived from a granitic source to the east (Nilsen, 1984)--possibly the Sierra Nevada or Mojave, according to the reconstruction in Figure 2.

The upper part of the San Juan Bautista Formation includes shallow-marine sandstones that are poorly dated but probably of Refugian to early Zemorrian age. In the Santa Cruz Mountains, strata of Refugian to early Zemorrian age include the Rices Mudstone and the Castle Rock unit of the Vaqueros Sandstone, which were deposited at lower middle bathyal to lower bathyal depths in basin-plain and submarine fan settings. These interpretations of age and depositional environments, if correct, suggest that during the late Eocene and early Oligocene the La Honda basin deepened to the northwest from a shallow-marine shelf in the San Juan Bautista area.

The unusually long interval of time represented by the San Juan Bautista Formation--perhaps 15-20 m.y., based on the paleontological evidence presented earlier--coupled with the occurrence of both basin-plain and shallow-marine deposits within the formation, suggest that there are one or more disconformities within the San Juan Bautista Formation that have not yet been identified. Recognition of these disconformities and their ages may help clarify the correlation of the San Juan Bautista Formation with coeval strata and disconformities in the Santa Cruz Mountains.

A major middle Oligocene regression is recorded in the Santa Cruz Mountains by the nonmarine, shallow-marine, and submarine fan deposits of the Zayante and Vaqueros sandstones, and also by a major unconformity within the Vaqueros that represents a minimum of 2000 m of shoaling due mainly to tectonic uplift. An Oligocene regression is also recorded in the northern Gabilan Range by the shallow-marine Pinecate Formation and the overlying nonmarine redbeds. Speculatively, the inferred disconformity at the base of the Pinecate Formation (Kerr and Schenck, 1925; Castro, 1967) may be correlative with the middle Oligocene unconformity in the Santa Cruz Mountains. The Oligocene regressions in both the Santa Cruz Mountains and northern Gabilan Range may have been associated with movement along the Zayante-Vergeles fault (Clark and Rietman, 1973).

Volcanism occurred in both the Santa Cruz Mountains and the northern Gabilan Range at about the same time, near the Oligocene-Miocene boundary. In the northern Gabilans, dacitic and andesitic volcanics were erupted about 21-22 m.y. ago from vents that apparently were associated with the Zayante-Vergeles fault. In the Santa Cruz Mountains, basaltic volcanics were erupted about 20-25 m.y. ago from minor vents along the Zayante-Vergeles and La Honda faults, and from major vents associated with a pull-apart in the Mindego Hill area.

An early Miocene marine transgression is recorded in the Santa Cruz Mountains by the gradual transition from the shallow-marine Laurel unit of the Vaqueros Sandstone upward into the overlying deeper-water slope deposits of the Lambert Shale. Whether a corresponding marine transgression also took place in the northern Gabilan Range is unknown, because rocks younger than the dacitic and andesitic volcanics and older than the upper Miocene(?) Purisima Formation are not preserved.

PALEOGEOGRAPHY, GEOLOGIC HISTORY, AND PALEOTECTONICS

Introduction

The preceding discussions of stratigraphy, sedimentation, structure, and paleoecology are summarized and evaluated below in terms of the paleogeographic and paleotectonic evolution of the La Honda Basin.

Table 4 summarizes my interpretations of the depositional systems represented by the Tertiary rock units of the central La Honda basin.

The maps in Figure 66 are reconstructions of paleobathymetry and paleogeography for 10 intervals of geologic time from Paleocene to middle Miocene. These maps are highly interpretive but were prepared using the methods outlined earlier in this report and the paleobathymetric data in Appendix 1. The time intervals are based on benthic foraminiferal stages and therefore are variable in length, ranging from about 2-3 m.y. for the Refugian to 8-10 m.y. for the late Zemorrian (Figure 9). Each paleobathymetric map probably represents an "average" paleogeography over a finite interval of geologic time, rather than a "snapshot" of an instant in time. I made no attempt to palinspastically restore the effects of crustal shortening or strike-slip faulting within the basin, because for the most part the amounts of these deformations are unknown.

Paleogeography and Geologic History

Paleocene

The oldest sedimentary unit in the area, the Ynezian Locatelli Formation, rests nonconformably on granitic basement. Because this unit is poorly exposed and has not been studied from a sedimentological point of view, little is known about the origin and earliest history of the La Honda basin. Figure 66A is a highly speculative interpretation of paleobathymetry and paleogeography during the Paleocene. It is based on available paleontological data and reconnaissance field work discussed earlier in this report in the section on the Locatelli Formation.

I infer that the Locatelli Formation was deposited on a north- to northeast-dipping paleoslope along the southern margin of a very deep and steep-sided marine basin. Depositional environments on this paleoslope ranged from a shallow-marine shelf at the southern end of what is now Ben Lomond Mountain, to a lower bathyal slope or submarine fan at the northern end of the mountain. The location and orientation of the Paleocene shoreline are unknown, but it probably was located near the southern end of Ben Lomond Mountain. The main source of sediment for the feldspathic sandstones of the Locatelli Formation probably was a granitic terrain to the south, perhaps the southern tip of Ben Lomond Mountain or an area that is now submerged beneath Monterey Bay.

The Paleocene basin must have continued northward across the Zayante-Vergeles fault, but the Locatelli Formation has not been found north of that fault. It is not known whether the Ben Lomond and La Honda blocks were in their present relative positions (Figure 12) during the Paleocene. Future deep drilling on the La Honda block should help clarify the Paleocene paleogeography of the area and the early history of the Zayante-Vergeles fault.

The tentative interpretation of Paleocene paleogeography shown in Figure 66A is consistent with the hypothesis of Nilsen and Yount (1981) that the La Honda basin was just one of several small steep-sided basins that formed on the Salinian block as a result of major tectonic activity during the early Tertiary. Other Paleocene basins in the area are represented by the Carmelo Formation of Point Lobos and by unnamed turbidites at Point San Pedro, northwest of Montara Mountain. Speculatively, these three Paleocene basins were separated from each other by uplifted ridges of granitic basement. The tectonic

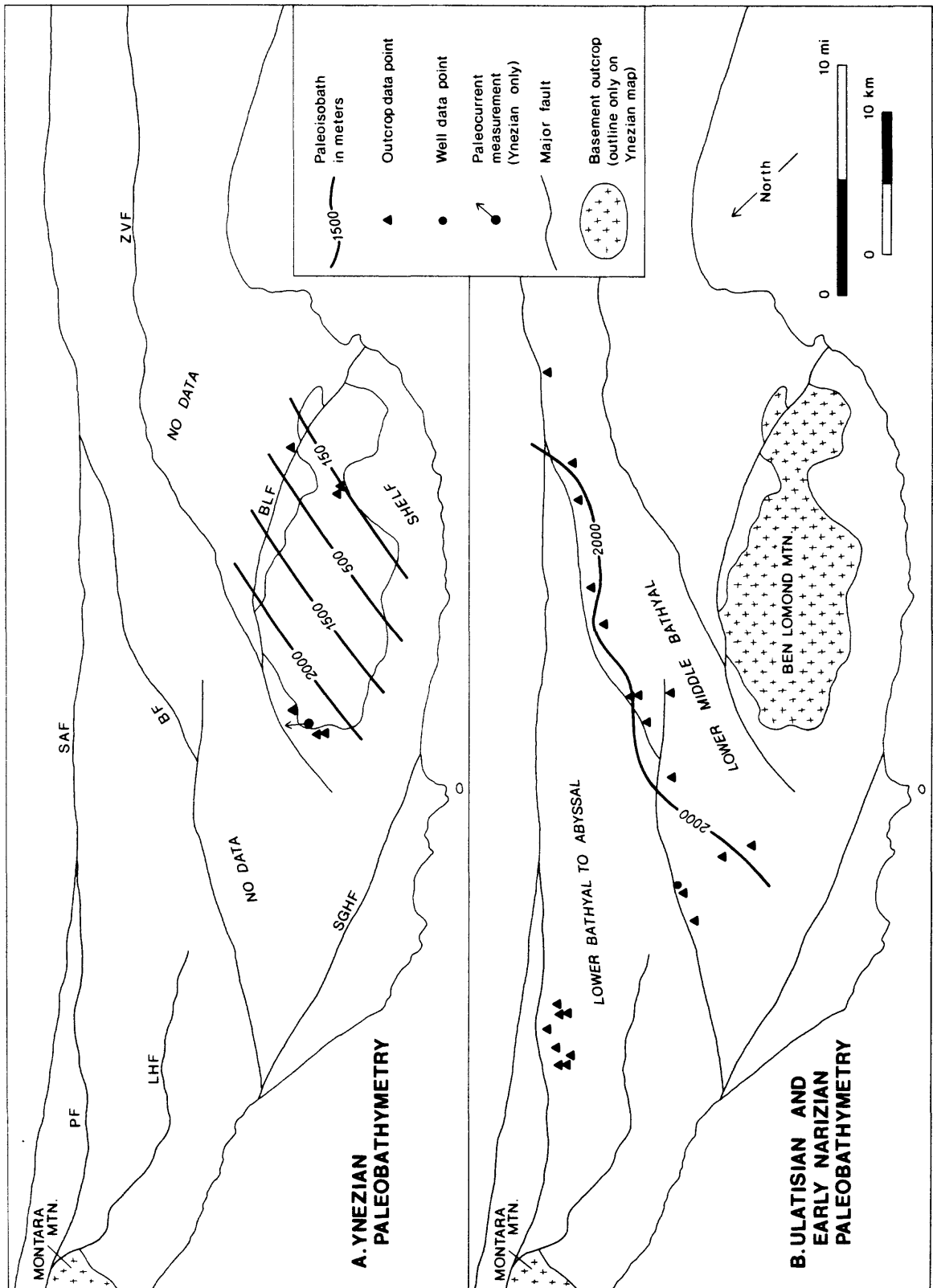
TABLE 4
DEPOSITIONAL SYSTEMS OF THE CENTRAL LA HONDA BASIN

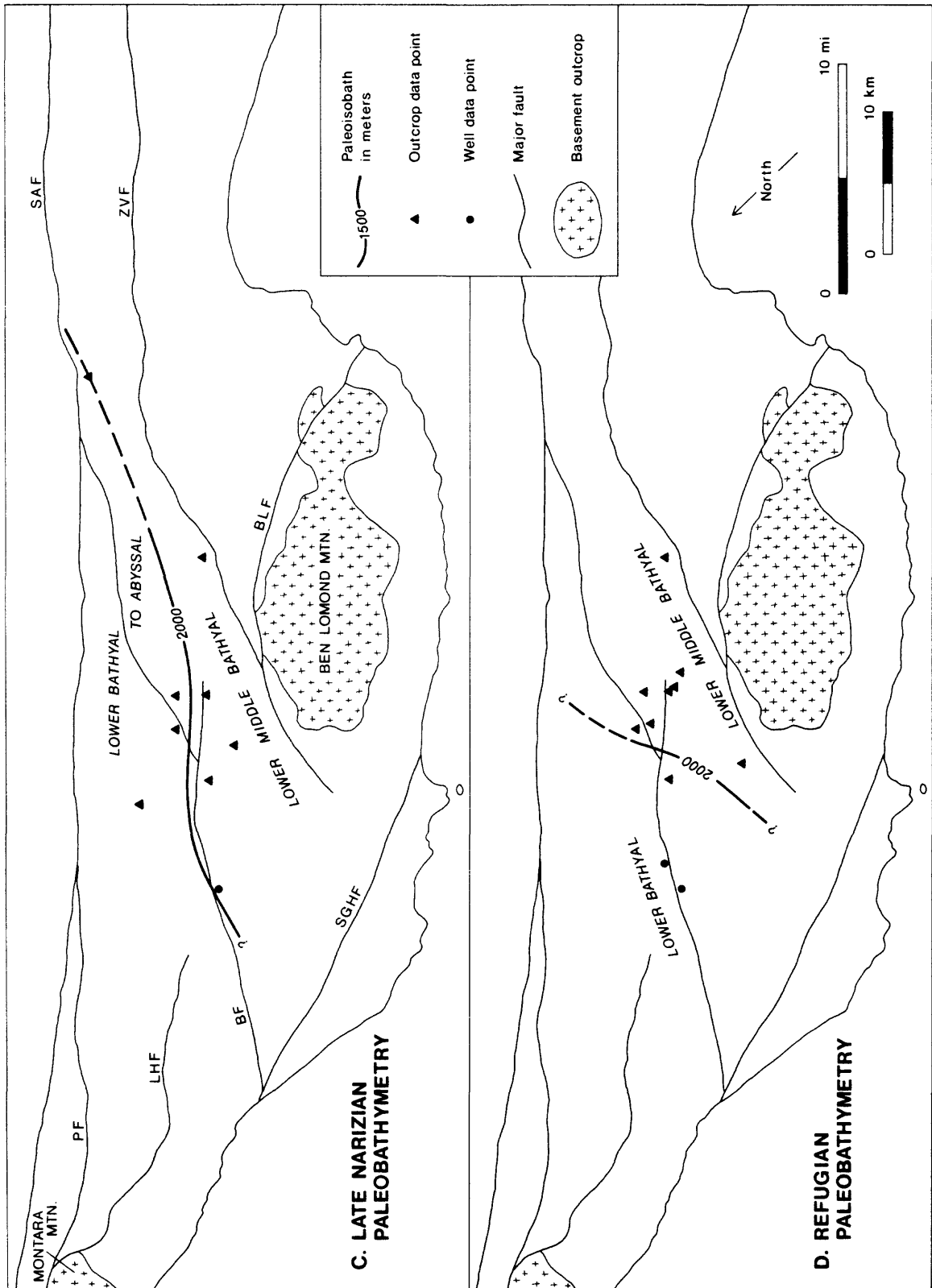
Depositional Sequence	Formation	Depositional Systems
Upper Miocene to Pliocene	Purisima Formation	Slope, shallow-marine shelf, and delta.
Middle to Upper Miocene	Santa Cruz Mudstone	Low-oxygen(?) upper slope and outer shelf.
	Santa Margarita Sandstone	Shallow-marine tidal seaway.
Lower to Middle Miocene	Monterey Formation	Low-oxygen slope and basin plain.
	Lompico Sandstone	Shallow marine shelf.
	Lambert Shale	Low-oxygen slope and basin plain.
	Mindego Basalt	Submarine basaltic volcanism.
	Zayante Sandstone	Fan-delta.
Eocene to Lower Miocene	Laurel unit of the Vaqueros Sandstone	Shallow-marine shelf.

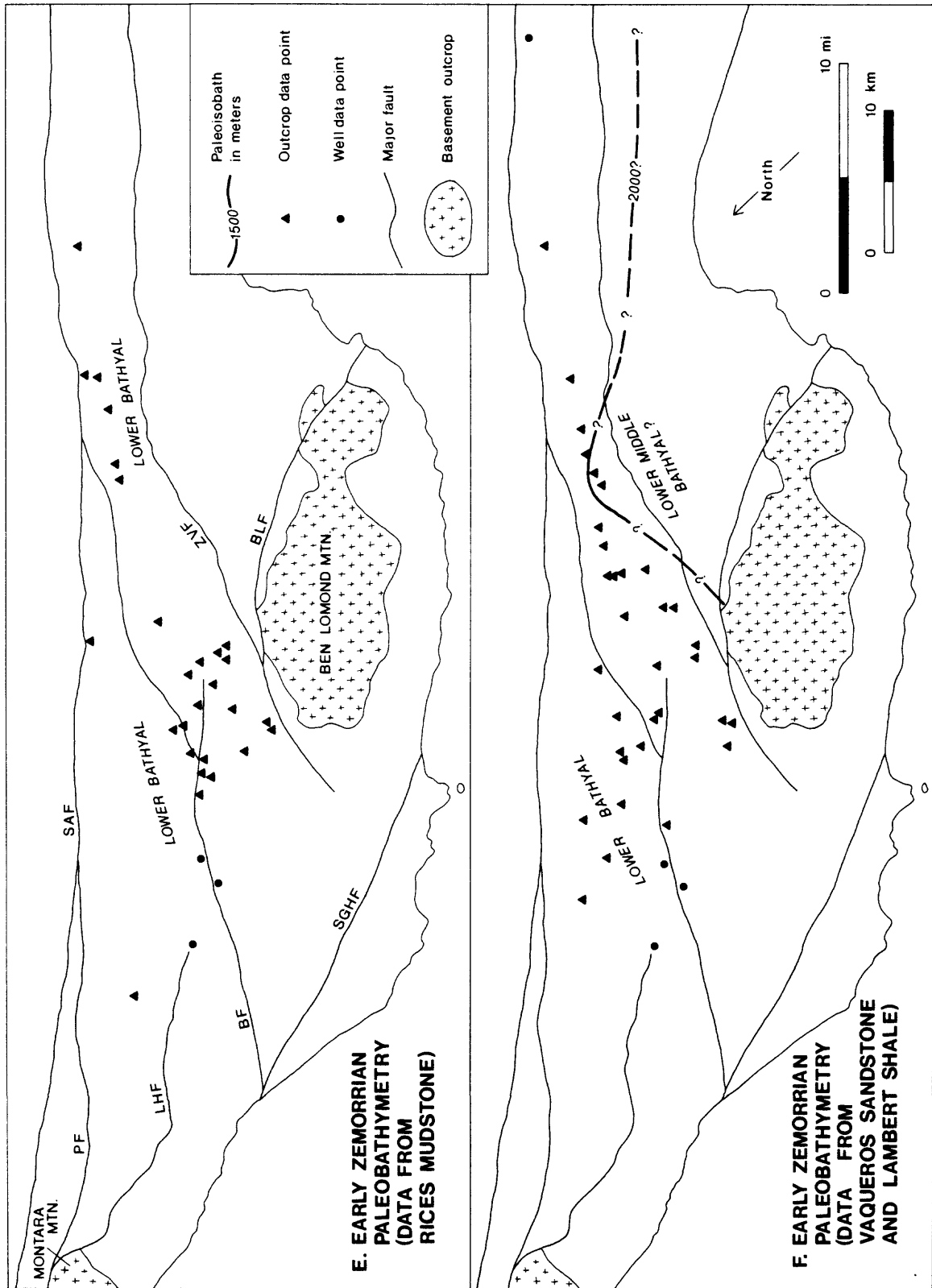
Table 4, continued

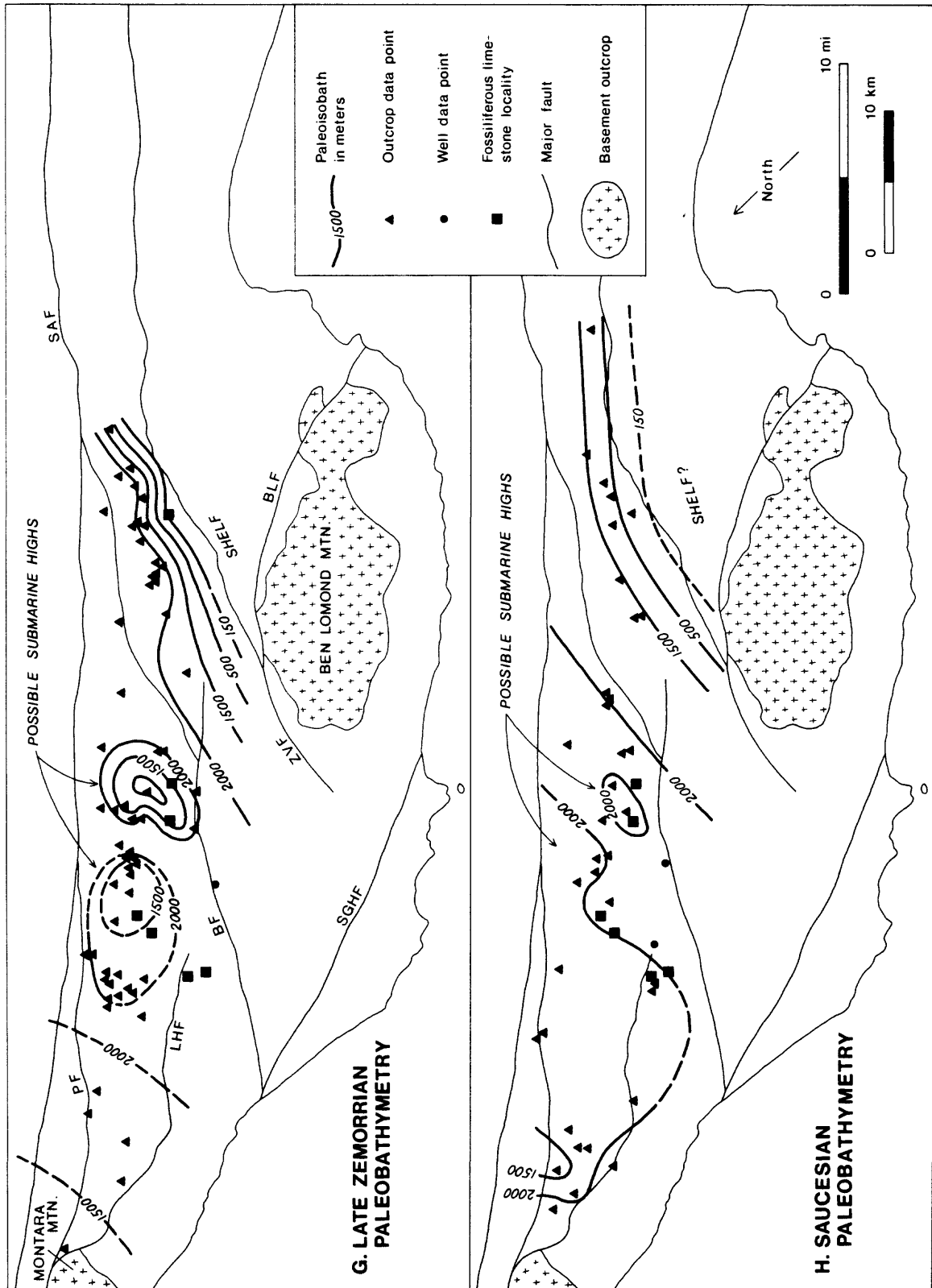
Depositional Sequence	Formation	Depositional Systems
Eocene to Lower Miocene (continued)	Castle Rock unit of the Vaqueros Sandstone	Submarine fan.
	Rices Mudstone	Well-oxygenated basin plain.
	Two-bar Shale	Low-oxygen basin plain.
	Butano Sandstone	Submarine fan.
Paleocene	Locatelli Formation	Shallow-marine shelf, and slope or submarine fan.

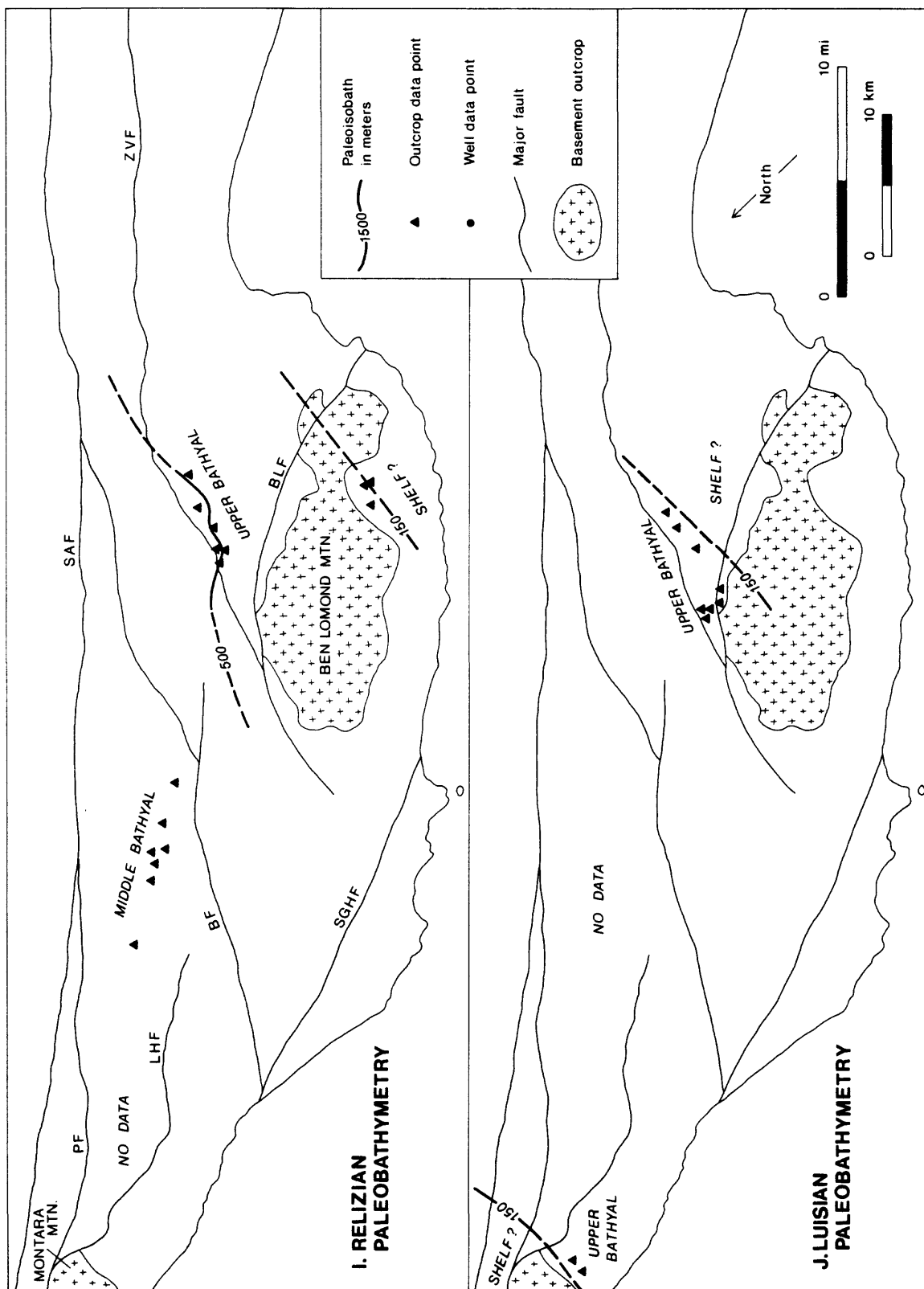
Figure 66. Maps of the paleobathymetry of the La Honda basin for 10 time intervals, based on data in Appendix 1 and methods described in the text. Time intervals and corresponding rock units are as follows: A, Ynezian Locatelli Formation. B, Ulatisian and Narizian Butano Sandstone. C, Narizian Twobar Shale. D, Refugian Rices Mudstone. E, early Zemorrian Rices Mudstone. F, early Zemorrian Vaqueros Sandstone and Lambert Shale. G, late Zemorrian Vaqueros Sandstone, Zayante Sandstone, Mindego Basalt, and Lambert Shale. H, Saucesian Vaqueros Sandstone, Mindego Basalt, and Lambert Shale. I, Relizian Lompico Sandstone and Monterey Formation. J, Luisian Monterey Formation. Faults are labeled as follows: BF = Butano fault, BLF = Ben Lomond fault, LHF = La Honda fault, PF = Pilarcitos fault, SAF = San Andreas fault, SGHF = San Gregorio-Hosgri fault, ZVF = Zayante-Vergeles fault.











origin of these small basins and intervening granitic islands or peninsulas is unknown. Several hypotheses are listed by Nilsen and Yount, including: (1) origin during an episode of rifting of the Salinian block away from an as-yet unidentified continental margin; (2) origin during a period in which subduction changed from normal to oblique; and (3) origin during an episode of right-slip and wrenching along a hypothetical proto-San Andreas fault or fault system. The latter hypothesis is consistent with plate-motion studies which suggest that oblique subduction and movement along a proto-San Andreas fault occurred along the California coast during the early Tertiary about 60(?)–42 m.y. ago (Carlson, 1982).

Uplift and erosion during the late Paleocene are recorded by the inferred unconformity between the Locatelli Formation and the overlying lower to middle Eocene Butano Sandstone (Clark, 1968). Uplift and erosion occurred at about the same time in the Salinas basin, suggesting a major regional tectonic event (Graham, 1976). The nature of this event is unknown, but it may have been related to: (1) an episode of wrench tectonism along the proto-San Andreas fault or fault system; (2) a major reorganization of plate motions in the Pacific basin about 55–56 m.y. ago (Carlson, 1982; Engebretson, 1982); or (3) the collision of the Salinian block with central California (J. G. Vedder and others, unpublished report, 1981).

Early to Middle Eocene

Subsidence and marine sedimentation resumed during the early Eocene with deposition of the Butano Sandstone on a submarine fan (Nilsen, 1979). The paleobathymetric map in Figure 66B suggests that during the Ulatisan and early Narizian the Butano fan accumulated mainly at lower middle bathyal to abyssal depths on a surface that sloped generally to the north and northeast. Paleocurrents and other sedimentological data presented by Nilsen and Simoni (1973) also indicate a north- to northeast-dipping paleoslope. Comparison of the map in Figure 66B with a map of Butano fan facies (Figure 13 of Nilsen, 1979) suggests that the inner-fan deposits accumulated at water depths shallower than 2000 m, the middle-fan deposits at depths of about 2000 m, and the outer-fan deposits at depths greater than 2000 m. Similar water depths probably prevailed on the Butano fan during Penutian and possibly Bulitian time, but no paleobathymetric maps were constructed for these time intervals because of the small number of available data points (Appendix 1).

The map in Figure 2, based on sedimentological studies by Nilsen and Clarke (1975), provides a clearer view of regional paleogeography than my paleobathymetric maps. Much as in the Paleocene, the La Honda basin during the early to middle Eocene was one of several small and very deep basins that were separated from each other by uplifted ridges of granitic basement. This borderland topography is thought to have been the result of wrench tectonism along the hypothetical proto-San Andreas fault or fault system. The Butano fan was deposited in the La Honda basin by northward-flowing turbidity currents that carried coarse sediment derived from a granitic island or peninsula located in the present position of Monterey Bay. Some of the turbidity currents spilled across the trace of the modern San Andreas fault into the San Joaquin basin, which was then contiguous with the La Honda basin. The shoreline must have been located several km or tens of km southwest of the modern Zayante-Vergeles fault; however, the exact location and orientation of this shoreline probably will never be known because Eocene strata have been largely removed from the Monterey Bay area by post-Eocene erosion (Greene, 1977).

Middle to Late Eocene

During the late middle Eocene, deposition of coarse sediment on the Butano submarine fan slowed considerably and was replaced by hemipelagic deposition of the Twobar Shale. Available paleobathymetric data (Appendix 1) suggest that during the late Narizian the Twobar Shale was deposited at lower middle bathyal to abyssal depths on a featureless basin-plan that sloped very gently to the northeast (Figure 66C). This peaceful deep-sea setting was occasionally disturbed by turbidity currents carrying sand from a granitic source area located to the southwest. This granitic source was probably the same island or peninsula that previously supplied sediment to the Butano submarine fan; however, the relatively small amounts of sandstone in the Twobar Shale suggest that during the late Narizian this granitic source was no longer being uplifted, and probably was eroded to a lowland or largely submerged.

The location of the shoreline is unknown, but it probably was located several km or tens of km southwest of the Zayante-Vergeles fault.

Sedimentological and stratigraphic data discussed earlier in this report suggest that the Twobar Shale was deposited in a silled anaerobic basin. The hypothetical sill may have been located in the San Gregorio area, as suggested earlier, but my paleobathymetric data in that area are insufficient to confirm or deny the existence of a sea-floor topographic high that could have functioned as a sill (Figure 66C).

Late Eocene to Early Oligocene

Hemipelagic deposition of the anoxic Twobar Shale ended abruptly at the Narizian-Refugian boundary about 39 m.y. ago with an episode of basin-wide erosion and deposition of glauconitic sand. Hemipelagic sedimentation resumed during the Refugian with deposition of the Rices Mudstone in well-oxygenated bottom waters. Available paleobathymetric evidence suggests that the Refugian muds accumulated at lower middle bathyal to lower bathyal depths on a basin-plain that sloped gently to the north and northwest (Figure 66D). Slight shallowing of the seafloor in the southern part of the basin from the Narizian to Refugian is suggested by comparison of the paleobathymetric maps (Figures 66C and 66D) and also by paleobathymetric data from the San Lorenzo River and Kings Creek sections (Figures 19 and 21). The cause of this shallowing is unknown; speculatively, it may have been the result of mild tectonic uplift and northward tilting of the basin.

A second episode of basin-wide erosion and deposition of glauconitic sand occurred at the Refugian-Zemorrian boundary about 37 m.y. ago. Shortly thereafter, hemipelagic deposition of the Rices Mudstone resumed during the early Zemorrian. Abundant paleobathymetric data from this stratigraphic interval indicate that the early Zemorrian muds accumulated on a basin-plain at water depths of 2000 m or more (Figure 66E). Feldspathic sand derived from a granitic source to the southwest was deposited as turbidites and bioturbated sandstones (including the Blooms Creek sandstone) at bathyal depths along the southwestern margin of the La Honda block.

The influx of sand increased abruptly near the end(?) of the early Zemorrian, and a submarine fan represented by the Castle Rock unit of the Vaqueros Sandstone prograded from southwest to northeast out over the basin-plain. Paleobathymetric data from these early Zemorrian fan deposits indicate that the fan was deposited at lower middle bathyal to lower bathyal depths on a surface that sloped to the north and northeast (Figure 66F). The increased supply of sand to the basin probably reflects uplift and erosion of a granitic source area located southwest of the Zayante-Vergeles fault, and marks the beginning of marine regression and major changes in the configuration of the La Honda basin during the middle Oligocene.

The location of the shoreline during the Refugian and early Zemorrian is unknown, but presumably it was located several km or tens of km southwest of the Zayante-Vergeles fault. The exact location of this shoreline probably will never be known because Refugian and Zemorrian deposits were removed from most of the Monterey Bay area prior to deposition of the Relizian Lompico Sandstone and Monterey Formation (Greene and Clark, 1979).

The San Gregorio and Tarwater Creek highs are recognizable in thickness maps of both the Rices Mudstone and the Vaqueros Sandstone, and therefore must have persisted at least until the early Zemorrian. My paleobathymetric data are insufficient to determine whether these inferred structural highs were also seafloor topographic highs during the Refugian and Zemorrian.

Late Oligocene to Early Miocene

Striking changes in the configuration of the La Honda basin occurred during the Zemorrian, suggesting that major tectonic events took place. Paleobathymetric data summarized in Figures 66G and 66H indicate that much of the basin remained at bathyal depths during the late Zemorrian and Saucian, but that a shallow-water shelf appeared along the southwestern margin of the La Honda block. The

development of this shelf resulted from a major episode of uplift and erosion that apparently was associated with movement along the Zayante-Vergeles fault. At least 2000 m of shoaling in this area is recorded by inferred unconformities in the Twobar Creek and Soquel-Hinckley sections. Uplift and erosion may also have occurred along the northwestern margin of the basin in the Woodside and Half Moon Bay quadrangles; in this area, the Twobar Shale and Rices Mudstone apparently were removed by erosion prior to deposition of the Vaqueros Sandstone unconformably on the Butano Sandstone.

Relatively abundant data permit a more detailed, though admittedly speculative, view of late Oligocene and early Miocene paleogeography shown in Figure 67. This map summarizes the interpretations of paleobathymetry, paleocurrents, provenance, and depositional systems presented earlier in this report. The reconstruction in Figure 67 also assumes that the La Honda and San Joaquin basins were joined at this time to form a single large inland sea that straddled the San Andreas fault.

The La Honda-San Joaquin sea during the late Oligocene and early Miocene probably was connected to the Pacific Ocean by a relatively narrow, east-west trending passage in which the deepest water depths were more than 2000 m. The "mouth" of this passage was roughly in the area of the present towns of San Gregorio and Pescadero.

The La Honda-San Joaquin sea was bounded on the southwest by an area of uplifted Salinian granitic and metamorphic rocks. This "granitic mountainous peninsula" (Figure 67) jutted out northwestward into the Pacific Ocean and occupied approximately the same position as two present-day topographic lows, Monterey Bay and the Salinas Valley. Speculatively, the peninsula may have extended northwestward across the San Gregorio-Hosgri fault; perhaps the northwestern tip of the peninsula was displaced far to the northwest by post-Saucesian right-lateral movement along the fault, and is now represented by granitic rocks in the area of Point Reyes and Bodega Head.

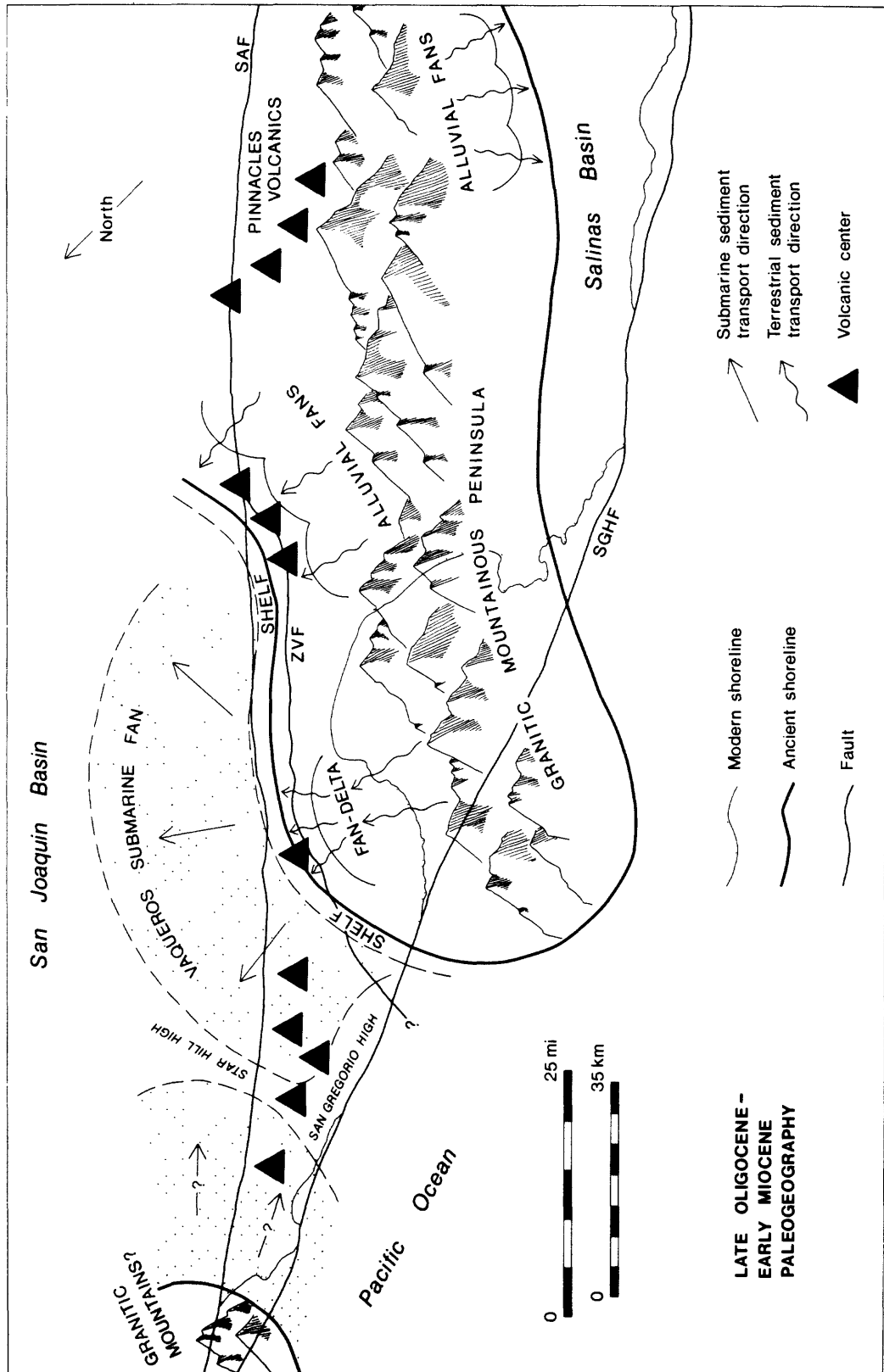
A major depocenter developed north of the Zayante-Vergeles fault, where a pile of sand, gravel, and mud more than a kilometer thick was deposited on a fan-delta and submarine fan complex represented by the Zayante and Vaqueros Sandstones. The lateral extent of the Vaqueros submarine fan to the northwest was apparently restricted by the San Gregorio and Star Hill highs, two structural positives that also may have been topographic highs on the seafloor. Speculatively, turbidity currents flowing down the Vaqueros submarine fan may have spilled eastward across the San Andreas fault (Figure 67). Thus, a large part of the Vaqueros fan may have been offset more than 300 km to the southeast by Neogene movement along the San Andreas fault; however, no such fan fragment has yet been identified in the San Joaquin basin.

At the southeastern end of the La Honda basin in the San Juan Bautista area, another thick pile of sediment was deposited in shallow-marine and alluvial fan environments represented by the Pinecate Formation and the overlying redbeds. Still farther to the south sediment shed southwestward from the granitic mountainous peninsula was deposited on alluvial fans and a nearby shallow-marine shelf represented by the Berry Conglomerate and the Vaqueros(?) Formation of the Indians Ranch area (Graham, 1976, 1978).

The northwestern margin of the La Honda-San Joaquin basin was apparently bounded by an uplifted area of Salinian granitic rocks located north of Half Moon Bay (Figure 67). Sediments eroded from this granitic uplift were transported southward into the La Honda-San Joaquin basin to form the Vaqueros Sandstone of the Woodside area. However, little is known about the depositional systems in this area, and the position of the shoreline shown in Figure 67 is entirely conjectural.

Volcanism was widespread in the area of Figure 67 during the late Oligocene and early Miocene. Most of the volcanic activity apparently took place shortly *after* the major Oligocene marine regression, for in most places the volcanic rocks overlie the Vaqueros Sandstone and its correlatives. Basaltic volcanic rocks were extruded from several vents in the central La Honda basin, including an apparent pull-apart in the Mindego Hill area. In at least two places, the volcanic piles in that pull-apart built up to form submarine topographic highs that persisted from the late Zemorrian to the Saucesian (Figures 66G and 66H). The tops and flanks of these and other volcanic piles were colonized by barnacles, molluscs,

Figure 67. Generalized paleogeography of part of central California during the late Oligocene and early Miocene (late Zemorrian and Saucesian), assuming restoration of post-Oligocene, right-lateral offsets of 305-330 km on the San Andreas fault and 105-160 km on the San Gregorio-Hosgri fault. This map is highly speculative but is based on interpretations of paleobathymetry, paleocurrents, depositional systems, and provenance presented earlier in this report. The ancient southwestern shoreline of the La Honda-San Joaquin basin is shown at its probable northeasternmost extent at the height of the Oligocene regression. The general locations of the alluvial fans and shoreline on the northeastern margin of the Salinas basin are slightly modified from paleogeographic maps by Graham (1976, 1978). Faults are labeled as follows: SAF, San Andreas fault; SGHF, San Gregorio-Hosgri fault; ZVF, Zayante-Vergeles fault. Present-day geographic reference is given by the modern shoreline in the area between the San Andreas and San Gregorio-Hosgri faults.



and other invertebrates whose skeletal remains accumulated to form fossiliferous limestones.

Minor centers of basaltic volcanic activity occurred along the La Honda fault in the Woodside-Half Moon Bay area, and along the Zayante-Vergeles fault in the Zayante area. Volcanic activity also occurred at the southern end of the La Honda basin in the San Juan Bautista area, where dacite and andesite were erupted from vents in nonmarine and possibly shallow-marine settings. Still farther to the southeast, andesite, dacite, and rhyolite were erupted from vents in the Pinnacles area about 23.5 m.y. ago (Matthews, 1976; Graham, 1976).

Along the southwestern margin of the La Honda basin near the Zayante-Vergeles fault, a major marine transgression began at about the same time as the volcanic activity. During the latest Zemorrian and Saucesian, the shoreline retreated to an unknown position southwest of the Zayante-Vergeles fault (Figures 66G and 66H). As the marine transgression continued, the shallow-marine shelf sands of the Laurel unit of the Vaqueros Sandstone were gradually overlapped by the deeper-water slope muds of the Lambert Shale. The influx of sand from the former "granitic mountainous peninsula" decreased, suggesting that uplift of this area slowed or ceased during Saucesian time, and that the mountains were eroded to low hills or a coastal plain.

The laminated, organic-rich mudrocks of the Lambert shale represent a return to silled-basin conditions and an "anoxic event" similar to that represented by the Eocene Twobar Shale. As discussed earlier in this report, the location of the hypothetical sill during late Oligocene-early Miocene time is unknown, but it may have been the San Gregorio high, a structural feature that apparently lay directly across the narrow connection between the Pacific Ocean and the La Honda-San Joaquin basin (Figure 67).

Early to Middle Miocene

Deposition of the Lambert Shale ended abruptly with an episode of uplift, deformation, and erosion that occurred over the entire basin during the late Saucesian or early Relizian. This major tectonic episode is recorded on the Ben Lomond block by an angular unconformity at the base of the Lompico Sandstone, and on the La Honda block by an inferred unconformity at the base of the Monterey Formation.

The amount of uplift that occurred during the late Saucesian and Relizian is unknown, but may have been substantial. On the Ben Lomond block, the entire Refugian to Saucesian section is missing (with the possible exception of the Zayante(?) Sandstone of the Majors Creek area); it probably was removed by erosion prior to deposition of the Relizian Lompico Sandstone in angular unconformity on the Butano Sandstone. On the La Honda block, the available paleobathymetric data suggest that about 500-1000 m of shoaling occurred between the Saucesian and the Relizian (Figure 60; also, compare Figures 66H and 66I). The magnitude of the shoaling and local thinning of the Lambert Shale (as in the Slate Creek section) suggest that most of the shoaling was due to tectonic uplift. However, some of the shoaling may have resulted from minor eustatic sea level drops reported at 19 and 16.5 m.y. ago by Vail and Hardenbol (1979).

Following this late Saucesian-early Relizian episode of uplift and erosion, renewed marine transgression during the Relizian and Luisian led to deposition of the shallow-marine Lompico Sandstone and the deeper-water deposits of the Monterey Formation. The paleogeography of the La Honda basin during the Relizian and Luisian is poorly understood because neither the Lompico Sandstone nor the Monterey Formation has been studied in detail. The available paleobathymetric data, however, suggest that the basin persisted as a deep-water trough bordered by wide, shallow-water shelves on both the northwest and southwest (Figures 66I and 66J). Maximum water depths of 1000 m or more occurred in the La Honda and Mindego Hill quadrangles. The La Honda basin probably was still connected with the Pacific Ocean to the west and the San Joaquin basin to the east. However, precise correlations of the Lompico Sandstone and Monterey Formation with their offset equivalents on the east side of the San Andreas fault have not yet been made.

Along the southwestern margin of the basin, a granitic landmass—perhaps including the southern end of Ben Lomond Mountain and part of northern Monterey Bay—was a major source of sediment for both the shallow-water Lompico Sandstone and the deeper-water turbidite sandstones of the Monterey Formation. Another granitic landmass in the Montara Mountain area was an important source of sediment for the northwestern part of the La Honda basin.

The Monterey Formation consists in part of laminated, organic-rich shales that probably represent deposition in anaerobic bottom waters. These anoxic shales are widely distributed in the La Honda basin, suggesting that the Monterey Formation, like the Eocene Twobar Shale and the upper Oligocene-lower Miocene Lambert Shale, represents deposition in silled-basin conditions and an "anoxic event" during the early to middle Miocene. As with the two earlier anoxic events, the location of the offending sill is unknown, but the San Gregorio high is a prime suspect. Alternatively, early to middle Miocene movement on the San Gregorio-Hosgri fault may have resulted in the temporary emplacement of a topographic high along the west side of the fault that for a time partly blocked the exchange of deep water between the La Honda basin and the Pacific Ocean. Such a giant "shutter ridge," if its top intersected the oxygen minimum zone, could have caused anaerobic silled-basin conditions in the La Honda basin until further displacement along the San Gregorio-Hosgri fault moved it to the north and out of the way.

Middle Miocene and Younger

A detailed account of the paleogeography and geologic history of the La Honda basin from the middle Miocene onward is beyond the scope of this report. Paleogeographic maps illustrating the Neogene evolution of parts of the area have been prepared by Greene (1977), Greene and Clark (1979), and Phillips (1981, 1983). Evidence mentioned earlier in this report shows that periods of subsidence and marine transgression occurred during the late Miocene (represented by the Santa Margarita Sandstone and Santa Cruz Mudstone) and the late Miocene to Pliocene (represented by the Purisima Formation). Major episodes of uplift, deformation, and erosion occurred during the middle Miocene, late Miocene, and late Pliocene to Quaternary, and are recorded by major unconformities.

Middle Tertiary Paleotectonics of the La Honda Basin

Introduction

The middle Tertiary paleotectonic history of the La Honda basin is summarized in the plots of total subsidence vs. time, or "qualitative geohistory diagrams" (van Hinte, 1978) shown in Figure 68. Three such diagrams were prepared, one for each of the following parts of the basin: (1) the presumed "basin center" in the La Honda area; (2) the inferred "basin margin" in the Zayante-Boulder Creek area, just northeast of the Zayante-Vergeles fault; and (3) the northeastern flank of Ben Lomond Mountain, just southwest of the Zayante-Vergeles fault.

The qualitative geohistory diagrams in Figure 68 were constructed using the data on age, paleobathymetry, and thickness shown in Table 5. A major uncertainty in this data stems from the difficulty of assigning precise numerical ages to some important lithologic boundaries, including the contact between the Rices Mudstone and the Vaqueros Sandstone; the middle Oligocene unconformity; and the upper and lower contacts of the Mindego Basalt. A further complication is the presence of several unconformities from which unknown thicknesses of strata are missing, including the disconformities within and at the base of the Rices Mudstone; the middle Oligocene unconformity; and the unconformities at the bases of the Lompico Sandstone and Monterey Formation. In addition, no attempt was made to correct for sediment compaction. These uncertainties and complications preclude a *quantitative* analysis of rates of subsidence and uplift in the La Honda basin, although such analysis has been successful in other Tertiary basins in California where better data are available (e.g., Graham, 1976; Ingle, 1980). Nevertheless, I believe that the data from the La Honda basin presented in Table 5 and Figure 68 are

QUALITATIVE GEOHISTORY DIAGRAMS:
MIDDLE TERTIARY,
LA HONDA BASIN

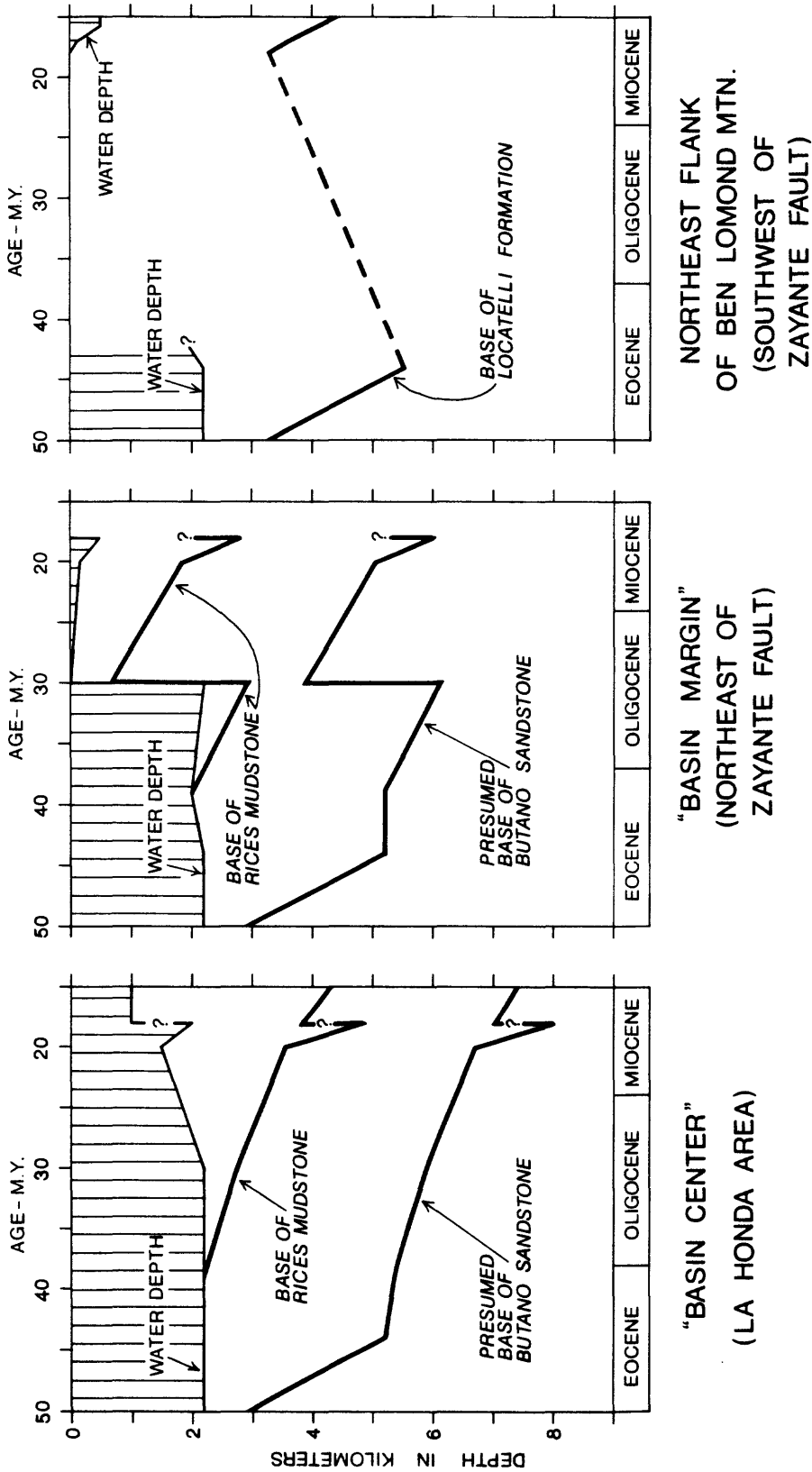


Figure 68. Qualitative geohistory diagrams showing the general history of subsidence, uplift, and paleobathymetry of three areas in the La Honda basin. These diagrams were prepared using the numerical data in Table 5. For simplicity, uplift along the basin margin about 30 m.y. ago is shown as being instantaneous, although it may have occurred over several million years.

TABLE 5
RAW DATA FOR QUALITATIVE GEOHISTORY DIAGRAMS

FORMATION	AGE OF BASE AND TOP (m.y.)	"BASIN CENTER"		"BASIN MARGIN"		NORTHEAST FLANK BEN LOMOND MTN.	
		WATER DEPTH(m)	THICKNESS (m)	WATER DEPTH(m)	THICKNESS (m)	WATER DEPTH(m)	THICKNESS (m)
Monterey Formation	18-14	1000	600+	-	-	150-500	800+
Lompico Sandstone	18-17	-	-	-	-	0-150	150
Lambert Shale	20-18	1500- 2000	800+	150-500	450+	-	-
Mindego Basalt	30-20	2200- 1500	1500+	-	-	-	-
Vaqueros Ss. (Laurel unit) +Zayante Ss.	30-20	-	-	0-150	1000	-	-
Vaqueros Ss. (Castle Rock unit)	37-30	2200	200	2200	400+	-	-
Rices Mudstone	39-30	2200	350	2000- 2200	300	-	-

Table 5, continued

FORMATION	AGE OF BASE AND TOP (m.y.)	"BASIN CENTER"		"BASIN MARGIN"		NORTHEAST FLANK BEN LOMOND MTN.	
		WATER DEPTH(m)	THICKNESS (m)	WATER DEPTH(m)	THICKNESS (m)	WATER DEPTH(m)	THICKNESS (m)
Two-bar Shale	44-39	2200	150	2200- 2000	200	-	-
Butano Sandstone	52-44	2200	3000?	2200	3000?	2200	3000?
Locatelli Formation	59-54	-	-	-	-	0-2200	300+

reliable enough to show in a *qualitative* way the timing and relative magnitudes of episodes of subsidence and uplift in different parts of the basin.

Figure 69 shows the approximate relative rates of accumulation for selected rock units in the La Honda basin. This figure was prepared using the data on age and thickness shown in Table 6. These data are subject to the same uncertainties as those used to construct the qualitative geohistory diagrams. Because no correction for compaction was made, the rates of accumulation in Table 6 and Figure 69 cannot be compared with actual rates of sedimentation in modern basins, but they can be used to identify important changes in *relative* rates of accumulation through time in the Tertiary La Honda basin.

The major events shown in Figures 68 and 69 include: (1) episodes of relatively rapid subsidence and accumulation during the early to middle Eocene, late Oligocene to early Miocene, and early to middle Miocene; (2) a period of relatively slow subsidence and accumulation during the late Eocene to early Oligocene; and (3) episodes of uplift during the middle Oligocene and early Miocene. These events can be interpreted in terms of plate motions and regional tectonics, as discussed below.

Early to Middle Eocene Rapid Subsidence

Relatively rapid rates of subsidence and sediment accumulation occurred in the La Honda basin about 52-44 m.y. ago (Figures 68 and 69). This interval is recorded by the Butano Sandstone, which was deposited in very deep water on a submarine fan that apparently covered the entire La Honda block and much of the Ben Lomond block as well. Sediment on the Butano fan was supplied by an uplifted granitic highland to the south. The rapid and deep subsidence of the La Honda basin and simultaneous uplift of the adjacent sediment source area probably were the result of wrench tectonism associated with strike-slip movement along the proto-San Andreas fault system. The La Honda and other basins in the early Tertiary continental borderland of California probably resulted from local crustal extension and downwarping or block-faulting of the crust, while the adjacent highlands were formed by local compression and uplift. This tectonic activity probably took place within a complex system of branching and braided strike-slip faults that may have been analogous to that of the modern southern California borderland (e.g., Crowell, 1974).

A major fault in the proto-San Andreas system may have followed the same trace as the modern San Andreas fault, but movement along this ancient fracture must have ceased prior to deposition of the Butano-Point of Rocks submarine fan (Nilsen and Clarke, 1975). Wrenching during deposition of this fan probably occurred along faults of the proto-San Andreas system located offshore; however, these faults have not yet been identified.

The inferred period of wrench tectonism during deposition of the Butano fan about 52-44 m.y. ago is consistent with the plate-motion studies of Carlson (1982) which indicate that oblique subduction and movement along the proto-San Andreas system occurred about 60(?)–42 m.y. ago. There is an apparent difference of 2 m.y. between the end of deposition of the Butano fan about 44 m.y. ago, inferred by me from available paleontologic data, and the end of oblique subduction about 42 m.y. ago inferred by Carlson (1982) from magnetic stripes. It is not clear that this 2 m.y. discrepancy is "real"; it may simply reflect errors and uncertainties in the methods of dating.

Late Eocene to Early Oligocene Slow Subsidence

Relatively slow rates of subsidence and slow rates of sediment accumulation occurred in the La Honda basin during the late Eocene and early Oligocene about 44-30(?) m.y. ago (Figures 68 and 69). This interval is recorded by the Twobar Shale and Rices Mudstone, both of which represent hemipelagic deposition of mud on a flat to gently-sloping basin-plain that apparently covered the entire preserved part of the La Honda basin. The uniform character of the muddy sediments over such a large area, the slow rates of subsidence, and the relatively low influx of coarse sediment suggest that this was a tectonically quiet time in the La Honda basin. The early Tertiary wrench tectonism that had created the basin and adjacent granitic highlands was no longer active, and the former highlands were reduced to lowlands by

Figure 69. Approximate relative accumulation rates for selected rock units in the La Honda basin, based on numerical data in Table 6. Accumulation rates are uncorrected for compaction. Horizontal bars show the maximum accumulation rates and age ranges of the rock units given in Table 6; filled circles and heavy line show the general trend over time. Abbreviations of rock units are as follows: Tl, Locatelli Formation. Tb, Butano Sandstone. Tst, Twobar Shale. Tsr, Rices Mudstone. Tvc, Castle Rock unit of the Vaqueros Sandstone. Tvl, Laurel unit of the Vaqueros Sandstone. Tz, Zayante Sandstone. Tmb, Mindego Basalt. Tla, Lambert Shale. Tlo, Lompico Sandstone. Tm, Monterey Formation. Tsm, Santa Margarita Sandstone. Tsc, Santa Cruz Mudstone. Tps, Purisima Formation of the Santa Cruz-Capitola area. Tpl, Purisima Formation of the La Honda area.

APPROXIMATE RELATIVE ACCUMULATION RATES,
LA HONDA BASIN

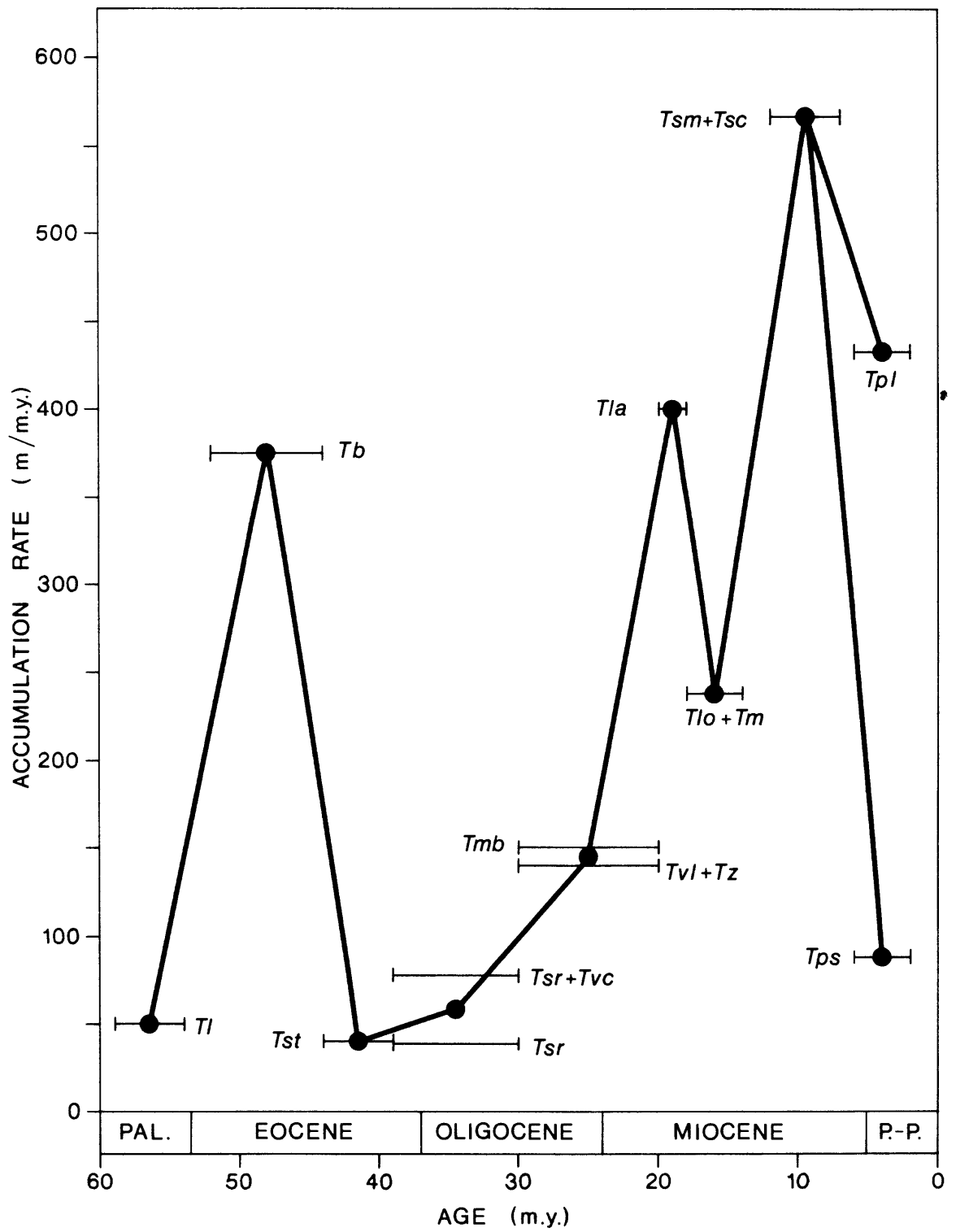


TABLE 6
 APPROXIMATE RELATIVE RATES OF ACCUMULATION FOR
 SELECTED ROCK UNITS IN THE LA HONDA BASIN
 (UNCORRECTED FOR COMPACTION)

ROCK UNIT	AGE OF BASE AND TOP (m.y.)	APPROX. THICKNESS (m)	ACCUMULA- TION RATE (m/m.y.)
Purissima Formation	6-2	350-1722	88-431
Santa Cruz Mudstone + Santa Margarita Ss.	12-7	2830	566
Monterey Formation + Lompico Sandstone	18-14	600-950	150-238
Lambert Shale	20-18	450-800	225-400
Mindego Basalt	30-20	1500	150
Zayante Sandstone + Laurel unit, Vaqueros Sandstone	30-20	1400	140
Rices Mudstone + Castle Rock unit, Vaqueros Sandstone	39-30	550-700	61-78
Rice Mudstone	39-30	300-350	33-39
Twobar Shale	44-39	150-200	30-40
Butano Sandstone	52-44	3000	375
Locatelli Formation	59-54	300	50

erosion or submerged.

According to the plate-motion studies of Carlson (1982), this tectonically quiet time corresponds to an interval of normal convergence along the California continental margin. Carlson's interpretation implies that from a regional point of view the La Honda basin was in a forearc (i.e., arc-trench gap) paleogeographic and paleotectonic setting. Such a setting is consistent with the apparently low rates of subsidence and sediment accumulation in the La Honda basin; according to data compiled by Howell and von Huene (1981), such rates in forearc areas are generally equal to or lower than the rates in areas of wrench tectonism.

Middle Oligocene Regression and Uplift

Major tectonic and eustatic events during the middle Oligocene resulted in a marine regression and uplift of the La Honda basin margins and adjacent sediment source areas. The regression began during the early Oligocene when the basin-plain represented by the Rices Mudstone was overlapped from the south to north by a prograding submarine fan represented by the Castle Rock unit of the Vaqueros Sandstone. The regression reached its peak during the late(?) Oligocene with deposition of a major fan-delta and submarine fan complex represented by the Zayante and Vaqueros Sandstones. I infer that this middle Oligocene regression records a dramatic increase in the supply of sediment to the La Honda basin from a granitic source area to the southwest—the inferred "granitic mountainous peninsula" shown in Figure 67. I also infer that the increased supply of sediment resulted from at least two causes acting in concert: (1) tectonic uplift and mountain-building in the granitic source area, with subsequent rapid erosion of granitic basement and the overlying cover of lower Tertiary (and Mesozoic?) sedimentary rocks; and (2) a major eustatic sea level fall about 29 m.y. ago (Vail and Hardenbol, 1979), which probably resulted in lowered base level and a subsequent increase in rates of erosion and sediment production.

Tectonic uplift also occurred *within* the La Honda basin along the southwestern basin margin (Figure 68), where about 2000 m of shoaling is recorded by inferred unconformities in the Twobar Creek and Soquel-Hinckley sections. However, the available data indicate that continued subsidence, and not uplift, occurred in the basin center (Figure 68). The apparent restriction of uplift to the basin margin suggests that the uplift was associated with deformation and movement along a nearby fault, most likely the Zayante-Vergeles fault. Oligocene movement along this fault was previously suggested by Clark and Rietman (1973) to explain, among other things, the coarsening of Oligocene deposits toward the fault, and the apparent restriction of Oligocene nonmarine and shallow-marine deposits to areas adjacent to the fault. The hypothesis of Oligocene activity along the fault is also supported by: (1) the orientation of the late Oligocene shoreline and paleobathymetric contours generally parallel to the fault (Figures 66G and 67); and (2) the very steep paleoslopes near the fault inferred from benthic foraminiferal paleobathymetry (Figure 66G). Thus, the configuration of the southwestern margin of the basin appears to have been controlled during the middle to late Oligocene by movement along the Zayante-Vergeles fault.

Tectonic uplift and erosion apparently also occurred along the northwestern margin of the basin during the middle Oligocene. In the Woodside-Half Moon Bay area, the Eocene Twobar Shale and Eocene to lower Oligocene Rices Mudstone were eroded away prior to deposition of the upper(?) Oligocene Vaqueros Sandstone on the Eocene Butano Sandstone. I infer that the source of sediment for the Vaqueros Sandstone in this area was a tectonically uplifted area of granitic rocks located in the Montara Mountain area or farther northwest. However, the available stratigraphic, sedimentologic, and paleobathymetric data from this area are too few to allow a detailed discussion of the tectonic events that occurred there.

In summary, major marine regression occurred in the La Honda basin during the middle Oligocene. The regression occurred at about the same time as a major eustatic drop in sea level, but the primary cause of the regression was tectonic uplift of the basin margins and adjacent granitic source areas. The middle Oligocene regression and uplift in the La Honda basin cannot be dated more precisely with presently available biostratigraphic and radiometric information. However, I suspect that these local tectonic events were associated with regional events that accompanied the change in tectonic regime from

normal convergence to right-slip during the middle Oligocene about 30 m.y. ago (Figure 4; Carlson, 1982). The Oligocene was a time of regionally extensive tectonism and uplift throughout central and southern California, and was marked by widespread erosion with the creation of unconformities, the formation of numerous fault-bounded basins, and the deposition of regressive sequences and extensive nonmarine deposits (Dibblee, 1977; Nilsen, 1982).

The cause of this regional tectonism is unclear. Nilsen (1982) has proposed that it was related to the approach and collision of the Farallon-Pacific spreading ridge with the California continental margin. This is an attractive hypothesis, but some important questions remain unanswered. For example, the plate-motion reconstructions by Atwater and Molnar (1973) and Engebretson (1982) show that the initial contact of the ridge with the continental margin occurred well to the south of the modern California-Mexico border, and at least 300 km southeast of the restored position of the La Honda-San Joaquin basin. It remains to be explained how a collision at least 300 km away caused movement along the Zayante-Vergeles fault and uplift of both the northwestern and southwestern margins of the basin, while the center of the basin continued to subside. Speculatively, perhaps the collision of the ridge with the trench caused movement on a conjugate system of faults in the adjacent continental margin. Horizontal and vertical movement of fault-bounded blocks in such a system could have resulted in the formation of local basins and adjacent uplifts, for example the La Honda basin and the granitic mountains on its northwestern and southwestern borders.

Late Oligocene to Early Miocene Extension

The late Oligocene to early Miocene was a time of volcanism, marine transgression, and increased rates of subsidence and sediment accumulation in the La Honda basin. After the middle Oligocene uplift, subsidence resumed along the southwestern basin margin (Figure 68). Rates of subsidence there and in the basin center increased abruptly and were apparently very high during the early Miocene about 20 m.y. ago (Figure 68). At about the same time, rates of sediment accumulation also increased (Figure 69). Along the southwestern basin margin, the Zayante Sandstone, Laurel unit of the Vaqueros Sandstone, and Lambert Shale were deposited on the relatively downthrown side of the Zayante-Vergeles fault, which apparently remained active through Saucian time. In the center of the basin, the Mindego Basalt and overlying Lambert Shale accumulated in a pull-apart.

The occurrence at about the same time of marine transgression, volcanism, and increased rates of subsidence suggests that extensional tectonics prevailed in the La Honda basin during the late Oligocene and early Miocene. A combination of extension and right-lateral shear, or "transtension" (Reading, 1980) may have resulted in the formation of a pull-apart in the Mindego Hill area.

Extensional tectonics associated with volcanism, marine transgression, and rapid subsidence of local areas occurred not just in the La Honda basin but also in the Salinas basin and much of the rest of central and southern California during the late Oligocene and early Miocene (Graham, 1976, 1978; Ingle, 1980). The cause of this regional episode of extension is unknown, but a number of hypotheses have been proposed. For example, Dickinson and Snyder (1979) suggested that local extension and volcanism accompanied the northward migration of the Mendocino triple junction along the California continental margin following the ridge-trench collision about 30 m.y. ago. Their geometric analysis predicts that the triple junction passed through the La Honda basin area about 20-22 m.y. ago. This predicted time agrees remarkably well with available information on the ages of the Mindego Basalt, the development of the Mindego pull-apart, and the pulse of rapid subsidence shown in Figure 68.

The hypothesis of Dickinson and Snyder also predicts that episodes of local extension and volcanism were *sequential* rather than *synchronous* along the California continental margin; in other words, pulses of subsidence and volcanic activity, if they were indeed due to the northward migrating triple junction, should have occurred earlier in the south than in the north. Unfortunately, the available data on the timing of important events are ambiguous and do not clearly support or refute the hypothesis of Dickinson and Snyder. For example, marine transgression and pulses of subsidence occurred in the Salinas and La Honda basins near the Oligocene-Miocene boundary (Graham, 1976, 1978), but the dating of these

events is neither accurate nor precise enough to show that rapid subsidence began earlier in one basin or the other. Moreover, the available radiometric dates on volcanic rocks in central California can be interpreted as showing either (1) an imperfect "younging" from south to north, or (2) essentially synchronous volcanism. The volcanic rocks in question, listed generally in order from southwest to northeast, include: (a) basalt flows in the Simmler Formation of the Caliente Range dated at 22.9-23.4 m.y. (Ballance and others, 1983); (b) dacitic volcanics and shallow intrusives of the Morro Rock-Islay Hill zone and the Cambria Felsite dated at 22.1-26.5 m.y. (Ernst and Hall, 1974); (c) undated and unnamed rhyolites and basalts in the Saucesian Sandholdt unit of the Monterey Formation in the southern Salinas Valley area (Graham, 1976, p. 121); (d) rhyolite, dacite, and andesite of the Pinnacles Volcanic Formation dated at about 23.5 m.y. (Matthews, 1976); (e) unnamed dacites and andesites near San Juan Bautista in the northern Gabilan Range dated at 21.6 m.y. (Clark and Rietman, 1973); (f) the Mindego Basalt, radiometrically dated at 19.7-23.1 m.y. (Turner, 1970); and (g) the Iversen Basalt of the Point Arena area, dated at 22.6-24.3 m.y. (Turner, 1970).

An alternative hypothesis that explains *synchronous* rather than sequential volcanism and rapid subsidence is that an episode of regional strike-slip motion with a component of extension, or "transtension" (Reading, 1980), took place in central California during the late Oligocene and early Miocene. Speculatively, such a transtensional episode may have occurred when the Salinian block became partially coupled to the northwest-moving Pacific plate, resulting in a short-lived episode of strike-slip faulting in central California. Some of this strike-slip motion may have occurred along the San Andreas fault, resulting in formation of a pull-apart basin in the Mindego Hill area. *Major* strike-slip movement along the San Andreas fault, however, did not begin until later in the Miocene (Blake and others, 1978; Graham, 1978).

The late Oligocene-early Miocene episode of extension (or transtension) in California occurred at about the same time as extensional tectonism and basin formation in many areas around the Pacific rim, including the Phillipine Islands, Japan, and Kamchatka (Ingle, 1980). This essentially synchronous tectonism over so wide an area may have been the product of an adjustment of plate motions and changes in the rates and azimuths of sea-floor spreading and subduction (Ingle, 1980).

Early Miocene Uplift

Extensional tectonics and volcanism in the La Honda basin ended with an episode of uplift and erosion during the late Saucesian or early Relizian. This episode is recorded by unconformities at the base of the Relizian Stage in the basin center and on Ben Lomond Mountain (Figures 12 and 68). Uplift probably occurred over the entire La Honda basin but cannot be documented in the Boulder Creek-Zayante area northeast of the Zayante-Vergeles fault (Figure 68) because Relizian strata are not preserved there.

This episode of uplift was accompanied by at least mild deformation and tilting of pre-Relizian strata, because relations shown on the geologic map of Brabb (1970) indicate that the Relizian to Luisian Monterey Formation rests with angular discordance on the Zemorrian to Saucesian Lambert Shale in the Saratoga Gap area (Secs. 11, 12, 13, 14-8S-3W, northeastern Big Basin quadrangle).

The early Miocene episode of uplift in the La Honda basin was most likely associated with a tectonic event of regional significance, because uplift and erosion are recorded by unconformities at the base of the Relizian Stage in the Santa Maria, Salinas Valley, San Joaquin Valley, Point Reyes, and offshore areas (Graham, 1976; Harding, 1976). The uplift and erosion occurred at about the same time as *en echelon* folding in the San Joaquin basin (Harding, 1976), and possibly at about the same time as the development of wrench-related small basins and uplifts within the Salinas basin (Graham, 1976). These events may have been related to the initiation of major right-lateral motion and wrench tectonism along the San Andreas fault and subsidiary strike-slip faults in the Salinian block (Graham and others, 1982). The widespread occurrence of uplift and deformation suggests that this early movement was "transpressional" (Reading, 1980)—in other words, consisted of right-lateral shear with a component of compression.

An alternative hypothesis proposed by Glazner (1981, 1982) suggests that uplift and erosion in the La Honda and other coastal basins may have been related to unusual subcrustal phenomena associated with passage of the Mendocino triple junction. Glazner believes that subduction of the Mendocino fracture zone, a 1000 m-high north-facing topographic scarp in the ancient Farallon plate, may have caused a northward-moving wave of uplift in the overlying North American plate as it followed in the wake of the migrating Mendocino triple junction. The amount of uplift predicted by this model--about 500-1000 m--and the timing are consistent with what is inferred from independent evidence for the La Honda basin (Figure 68). The Glazner model also predicts, however, that uplift was sequential from south to north along the California continental margin. The available data, based on benthic foraminiferal biostratigraphy, suggest that uplift of the California margin basins was synchronous rather than sequential (e.g., Graham, 1976). Nevertheless, this should be checked by using more refined dating tools such as planktic foraminifers or nannofossils.

Following this early Miocene episode of uplift, subsidence resumed in the La Honda basin and led to deposition of the Lompico Sandstone and Monterey Formation. This renewed subsidence and the subsequent late Tertiary and Quaternary paleotectonic history of the La Honda basin were most likely controlled by strike-slip tectonics along the San Andreas fault system. However, most of the details of this history remain to be worked out. Some aspects of late Tertiary and Quaternary paleotectonics in the area are discussed by Greene and Clark (1979), Weber and others (1979), Clark (1981), Stuart and others (1982), and Stanley and McCaffrey (1983).

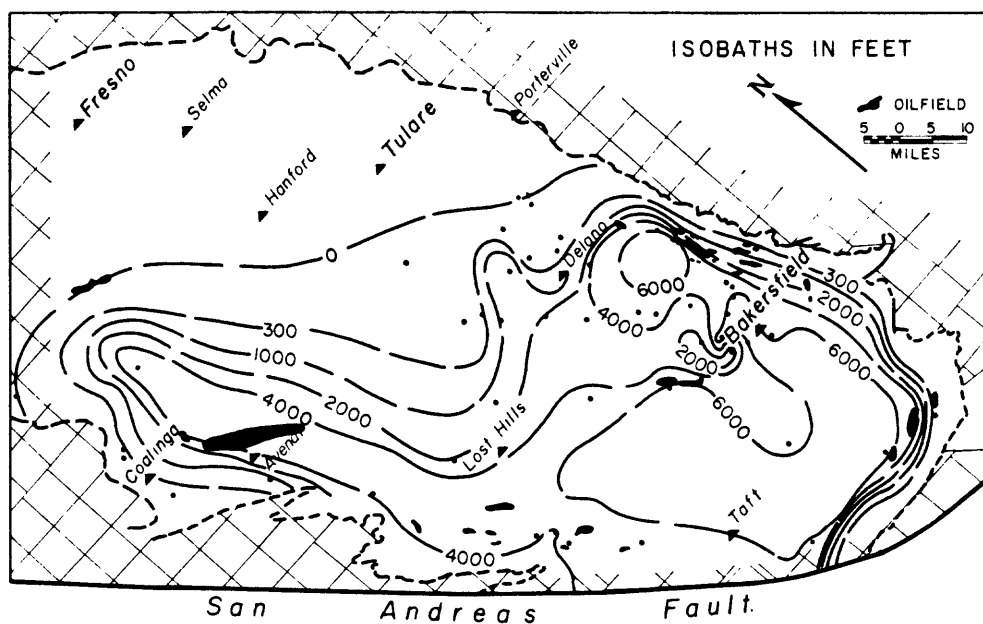
New Estimates of Offset Along the San Andreas Fault

Addicott (1968) and Bandy and Arnal (1969) suggested that the La Honda and San Joaquin basins were contiguous during the middle Tertiary and were later separated by large right-lateral movement along the San Andreas fault. This view is supported by evidence from benthic foraminiferal paleobathymetry. Comparison of late Zemorrian and Saucian paleobathymetric maps of the two basins (Figures 66G, 66H, and 70), shows that the maximum water depths in both basins were 2000 m or more, and that the deepest parts of the basins were adjacent to and truncated by the San Andreas fault.

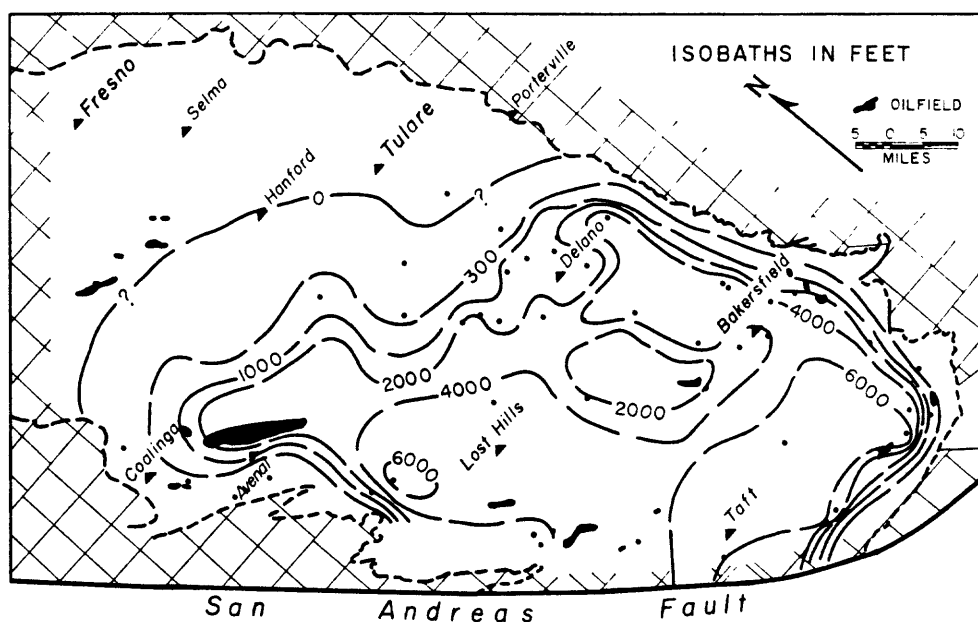
Using the deepest parts of the two basins as piercing points along the San Andreas fault, I estimate that post-late Zemorrian right-lateral displacement along the fault has been about 330 km, and post-Saucian displacement about 320 km. These figures agree well with previous estimates of the displacement along the fault of other middle Tertiary geologic features, including: (1) the 305-330 km offset of the Eocene Butano-Point of Rocks submarine fan (Clarke and Nilsen, 1973); (2) the 305-320 km offset of Eocene basin-plain and shallow-marine deposits in the northern Gabilan Range and San Emigdio Mountains (Nilsen, 1984); (3) the 315 km offset of the Pinnacles and Neenach volcanics, dated at about 23.5 m.y. (Matthews, 1976); and (4) the 280-305 km offset of an ancient shoreline and associated dacitic volcanic rocks dated at about 21.7 m.y. in the northern Gabilan Range and San Emigdio Mountains (Dickinson and others, 1972).

These estimates of offset are compatible with the hypothesis presented earlier in this report that a small amount of right-lateral displacement occurred along the San Andreas fault during the formation of a pull-apart in the Mindego Hill area during the late Oligocene and early Miocene. Of the estimated offsets listed above, those of the older geologic features are generally somewhat greater than the younger ones. Using the maximum and minimum figures listed above, offset of the Eocene features is 0-50 km more than the offset of the early Miocene shoreline and dacitic volcanic rocks. Thus, the amount of right-lateral displacement along the San Andreas fault during the late Oligocene and early Miocene, if it occurred at all, was probably in the range of 0-50 km.

A rough estimate of the amount of right-lateral displacement required to create the pull-apart in the Mindego Hill area can be calculated using relationships based on model studies of pull-apart basins by Rodgers (1980, p. 32). Rodgers's investigations show that the depth of an ideal pull-part basin is generally



Paleobathymetry at the end of the Zemorrian Stage, probably about 24.5 m.y. ago. Isobaths are given in feet and oil fields are indicated as black areas. The heavy broken line marks the approximate boundary of the San Joaquin Valley.



Paleobathymetry at the end of the Saucesian Stage, probably about 20.5 m.y. ago. Isobaths are given in feet and oil fields are indicated as black areas.

Figure 70. Maps of Zemorrian and Saucesian paleobathymetry of the San Joaquin basin (Bandy and Arnal, 1969), for comparison with Figure 66 of this report.

about 10-20% of the offset on the adjoining master faults. If the depth of the Mindego pull-apart is taken to be 1500 m--the approximate maximum thickness of the Mindego Basalt--then the calculated right-lateral offset on the master faults (one of which was presumably the San Andreas) is 7.5-15 km. If the depth of the Mindego pull-apart is taken as 3500 m--the thickness of the Mindego Basalt plus the maximum late Zemorrian to Saucesian water depths in the area, based on benthic foraminiferal paleobathymetry--the calculated offset on the master faults is 17.5-35 km.

These calculations suggest that the Mindego pull-apart could have formed as a result of 7.5-35 km of right-lateral displacement along the San Andreas fault during the late Oligocene and early Miocene. This estimate is well within the 0-50 km range allowed by available data on the offset of middle Tertiary geologic features and discussed earlier.

A third estimate of the amount of late Oligocene-early Miocene offset along the fault can be made by assuming that the dimensions of the crustal "hole" created by the pull-apart correspond roughly to the rhomb-shaped area of the Mindego Basalt seen on the distribution and thickness maps in Figures 55 and 56. The length of the pull-apart and therefore the amount of strike-slip displacement on the master faults can then be assumed to be roughly equal to the length, measured parallel to the master faults, of the thickest part of the Mindego Basalt. Using the thickness map in Figure 56 and measuring the distance, parallel to the San Andreas fault, between the two 200 m isopachs, I estimate that strike-slip offset along the fault during formation of the Mindego pull-apart was about 15-25 km.

Speculations on Offset Along the San Gregorio-Hosgri Fault

The paleobathymetric and paleogeographic maps in Figures 66 and 67 suggest that the deep-water trough of the La Honda basin extended westward across the San Gregorio-Hosgri fault during the late Oligocene and early Miocene. If this is correct, then the western continuation of the La Honda basin may have been truncated and transported relatively to the northwest by large-scale, late Cenozoic right-slip along the San Gregorio-Hosgri and San Andreas faults. Put another way, if the Tertiary strata on Ben Lomond Mountain are truly the offset equivalents of Tertiary strata in the Point Reyes area as suggested by Dickinson and Graham (1978b), then the Zemorrian strata north of Ben Lomond Mountain also should have offset equivalents in the area northwest of Point Reyes (Figure 1).

Unfortunately, no such offset of Zemorrian rocks has yet been documented. Zemorrian strata are present in outcrops along the coast south of Point Arena and include the Iversen Basalt, the Skooner Gulch Formation, and the Gallaway Formation (Addicott, 1967). The Iversen Basalt is about 22.6-24.3 m.y. old (Turner, 1970); it may be the offset correlative of the Mindego Basalt, but it may also have been erupted from volcanic vents that were along the same trend but separated by some distance from the Mindego vents (Graham and Peabody, 1981).

Zemorrian strata may also be present in parts of the offshore Bodega and Point Arena basins. These basins reportedly include locally thick sections of upper Eocene to lower Miocene sandstones and shales (Hoskins and Griffiths, 1971; McCulloch and others, 1977). However, correlation of these offshore strata with onshore sections in the Point Arena, Point Reyes, and Santa Cruz Mountains areas is not straightforward due to complex structure, numerous unconformities, questionable age control, and possible lateral facies changes.

The Zayante-Vergeles fault is a major linear geologic feature that may provide a piercing point to measure offset along the San Gregorio-Hosgri fault. In the western part of the La Honda basin, the Zayante-Vergeles fault trends east-west--nearly perpendicular to the San Gregorio-Hosgri fault--and has an estimated 2000-3000 m of down-to-the-north vertical separation. If the Zayante-Vergeles fault has been truncated by the San Gregorio-Hosgri fault and its western continuation moved relatively to the northwest, it should be fairly easy to identify in the offshore using geophysical methods such as seismic reflection and gravity.

The offset western extension of the La Honda basin--if it exists--may not include the Eocene Twobar Shale or the upper Oligocene-lower Miocene Lambert Shale. These anoxic shales probably formed during periods when the La Honda basin was separated from the Pacific Ocean by a shallow sill that intersected the base of the oxygen-minimum zone. If the sill was located over the San Gregorio high on the east side of the San Gregorio-Hosgri fault, as suggested earlier in this report, then these anoxic shales and potential source beds of petroleum probably were never deposited west of the fault. Similarly, if the late Oligocene-early Miocene Vaqueros submarine fan was bounded on the west by the San Gregorio high as shown in Figure 67, then no offset correlative of this fan--a potential petroleum reservoir--will be found west of the San Gregorio-Hosgri fault.

SUMMARY OF MAJOR CONCLUSIONS

(1) To a first approximation, major events in the middle Tertiary evolution of the La Honda basin can be correlated with regional events predicted by plate-motion reconstructions (e.g., Atwater, 1970; Atwater and Molnar, 1973; Carlson, 1982; Engebretson, 1982).

(2) Oblique convergence along the California continental margin prior to 42 m.y. ago (Carlson, 1982) probably drove right-lateral movement along the hypothetical proto-San Andreas fault system. During the Paleocene and again during the Eocene, wrench tectonism along this fault system apparently caused rapid subsidence of the La Honda basin and simultaneous uplift of adjacent granitic sediment source areas, resulting in deposition of the Locatelli Formation about 59-54 m.y. ago, and deposition of the Butano Sandstone about 52-44 m.y. ago.

(3) A period of normal convergence occurred along the California continental margin about 42-30 m.y. ago during the late Eocene to early Oligocene (Carlson, 1982). In the La Honda basin, this was a time of relatively slow rates of subsidence and slow hemipelagic deposition of the Twobar Shale and Rices Mudstone in lower bathyal basin-plain environments. Major basin-wide disconformities at about 39 m.y. and 37 m.y. ago represent episodes of sediment starvation and may reflect eustatic sea level changes, tectonic events, or episodes of intense bottom current activity.

(4) Major restructuring of the La Honda basin occurred during the middle Oligocene, apparently as a consequence of the approach and collision of the Farallon-Pacific spreading ridge with the North American continental margin about 30 m.y. ago. Local events included uplift and erosion of the basin margins, movement along the Zayante-Vergeles fault, and a major marine regression. A fan-delta and submarine fan complex represented by the Zayante and Vaqueros Sandstones was fed by northward-flowing braided streams carrying coarse sediment eroded from a nearby granitic highland that was undergoing tectonic uplift. Formation of the fan-delta and submarine fan complex may have been enhanced by a major eustatic fall in sea level about 29 m.y. ago (Vail and Hardenbol, 1979).

(5) A period of extensional tectonics marked by volcanism, marine transgression, rapid rates of subsidence, and formation of a pull-apart in the Mindego Hill area occurred near the Oligocene-Miocene boundary about 20-25 m.y. ago. The extension apparently was associated with a small amount (perhaps 15-25 km) of right-slip along the San Andreas fault. The extension may have been caused by passage of the northward-migrating Mendocino triple junction. Alternatively, the extension may have been caused by regional transtension along the San Andreas fault; the transtension may have been due to an adjustment of plate motions in the Pacific basin, or to partial coupling of the Salinian block to the northwest-moving Pacific plate.

(6) Basin-wide uplift, deformation, and erosion occurred near the Saucian-Relizian boundary about 18 m.y. ago and are recorded by unconformities at the bases of the Lompico Sandstone and the Monterey Formation. The uplift may have been a response to regional transpression and wrenching along the San Andreas fault or, alternatively, it may have been related to northward subcrustal migration of the subducted Mendocino fracture zone.

(7) Anoxic conditions occurred at least three times in the La Honda basin and resulted in deposition of laminated organic-rich shales, including the Eocene Twobar Shale, the upper Oligocene to lower Miocene Lamber Shale, and the lower to middle Miocene Monterey Formation. The exact causes of these basin-wide anoxic events are unclear, but they probably resulted from intermittent uplift of a sill in the San Gregorio area, perhaps in concert with episodes of expansion of the oxygen-minimum zone in the adjacent Pacific Ocean in response to climatic or oceanographic events.

(8) The La Honda and San Joaquin basins, and possibly parts of the Bodega and Point Arena basins of northern California, were probably joined together during the middle Tertiary. This ancient large basin was dissected during the Neogene by large right-lateral movements along the San Andreas and San Gregorio-Hosgri faults. Comparison of paleobathymetric maps of the La Honda and San Joaquin basins suggests that right-lateral displacement along the San Andreas fault has been about 330 km since the late Zemorrian and about 320 km since the Saucesian.

APPENDIX I

PALEONTOLOGIC DATA FROM THE
SANTA CRUZ MOUNTAINS

Listed below are the inferred ages and paleodepths of over 800 faunal lists compiled from more than 30 reports and well files. Each list is identified according to formation, quadrangle, and an arbitrary locality number; thus, "Tsr-14-22" refers to a sample from the Rices Mudstone (or "Tsr" - see Table 2) in the Big Basin quadrangle (or quadrangle number 14 - see Figure 7) at my locality number 22. For each list I have also given the original reference and sample number (if any), an age call, and a paleobathymetric interpretation. Age calls made by me are identified by the notation (RGS). All other age calls are from the original references. All paleobathymetric interpretations were made by me using the procedures outlined in the text under "Methods."

Abbreviations for the benthic foraminiferal stages of Schenck and Kleinpell (1936), Kleinpell (1938), and Mallory (1959) are listed below:

Del. = Delmontian
 Moh. = Mohnian
 Luis. = Luisian
 Rel. = Relizian
 Sauc. = Saucian
 Zem. = Zemorrian
 Ref. = Refugian
 Nar. = Narizian
 Ulat. = Ulatisian
 Pen. = Penutian
 Bul. = Bulitian
 Ynez. = Ynezian

Abbreviations for the paleobathymetric biofacies of Ingle (1980) are as follows:

IS = inner shelf (0-50 m)
 OS = outer shelf (50-150 m)
 UB = upper bathyal (150-500 m)
 UMB = upper middle bathyal (500-1500 m)
 LMB = lower middle bathyal (1500-2000 m)
 MB = middle bathyal, undivided (500-2000 m)
 LB = lower bathyal (2000 m and greater)

Other abbreviations are as follows:

ARF = Assemblage consisting entirely or almost entirely of arenaceous species. The paleoecologic significance of such assemblages is uncertain; see the text (under "Methods") for further discussion.

DW = "Deep water" assemblage. Denotes a microfossil assemblage in which the benthic foraminifers alone are insufficient to allow a paleobathymetric interpretation, but in which the presence of abundant radiolarians and/or planktic foraminifers suggests water depths at the shelf edge or deeper.

OMZ =
 Possible oxygen minimum zone assemblage. Denotes an assemblage containing

common to abundant individuals of at least one species thought by Ingle (1980), or Milam and Ingle (1982), to be indicative of anaerobic bottom conditions produced by water of low oxygen content.

NED =

Not enough data to make a paleobathymetric interpretation.

- Tl-14-1: (Brabb, 1960: EB 27) Ynez., ARF, DW.
- Tl-14-2: (Brabb, 1960: EB 144) Ynez., ARF.
- Tl-14-3: (Brabb, 1960: EB 145) Ynez., ARF.
- Tl-14-4: (Brabb, 1960: EB 242A) Ynez., ARF.
- Tl-14-5: (Brabb, 1960: EB 242B) Ynez., ARF.
- Tl-14-6: (Brabb, 1960: EB 242D) Ynez., ARF.
- Tl-14-7: (Brabb, 1960: EB 342G) Ynez., ARF.
- Tl-14-8: (Brabb, 1960: EB 83A) Ynez., ARF, DW.
- Tl-14-9: (Brabb, 1960: EB 337D) Ynez., ARF, DW.
- Tl-14-10: (Brabb, 1960: EB 337C) Ynez., ARF, DW.
- Tl-14-11: (Brabb, 1960: EB 337B) Ynez., MB to LB.
- Tl-14-12: (Brabb, 1960: EB 337A) Ynez., LB.
- Tl-14-13: (Brabb, 1960: EB 340) Ynez., LB.
- Tl-14-14: (Brabb, 1960: EB 307) Ynez., LB.
- Tl-14-15: (Brabb, 1960: EB 125) Ynez., ARF.
- Tl-14-16: (Brabb, 1960: EB 259) Ynez., ARF.
- Tl-14-17: (Brabb, 1960: EB 308) Ynez., ARF, DW.
- Tl-14-18: (Brabb, 1960: EB 25) Ynez., ARF.
- Tl-19-2: (Clark, 1966, and Clark and others, 1979: JC14, JC60-126, M4668, 76CB1511) Ynez., OS to UB.
- Tl-19-3: (Clark, 1966, and Clark and others, 1979: JC60-93, 76CB1511A) Ynez., ARF, possibly LB to abyssal.
- Tl-19-6: (Clark, 1966, and Clark and others, 1979: JC23, M4669, JC60-120) Ynez., UB.
- Tb-6-1: (Touring, 1959: F73) Nar., LB?
- Tb-6-2: (Touring, 1959: F74) Nar., LB.
- Tb-6-3: (Touring, 1959: F76) Nar., LMB?
- Tb-6-4: (Touring, 1959: F78) Nar., DW.
- Tb-6-5: (Touring, 1959: F109) Nar., LB?
- Tb-6-6: (Touring, 1959: F130) Bul., ARF.
- Tb-6-7: (Touring, 1959: F131) "Eocene", ARF.
- Tb-6-8: (Touring, 1959: F132) Nar., LMB?
- Tb-6-9: (Touring, 1959: F146) Bul, LB?
- Tb-6-10: (Touring, 1959: F154) "Eocene", LB?
- Tb-6-11: (Touring, 1959: F155) Nar. or Pen., LB?
- Tb-6-12: (Touring, 1959: F204) Nar., LB?
- Tb-6-13: (Poore, unpublished data, 1978: MF 2535) Eocene planktic foram. Zones P13-P14, DW.
- Tb-6-14: (Poore, unpublished data, 1978: MF 2536) Eocene planktic foram. Zones P12-P17, DW.
- Tb-6-15: (Poore, unpublished data, 1978: MF 2539A) Eocene planktic foram. Zones P10-P12, DW.
- Tb-6-16: (Poore, unpublished data, 1978: MF 2539B) Eocene planktic foram. Zones P11-P12, DW.
- Tb-6-17: (Poore, unpublished data, 1978: MF 2540) Eocene planktic foram. Zones P10-P12, DW.
- Tb-6-18: (Mack, 1959: JM-61m) Eocene, ARF.
- Tb-6-19: (Mack, 1959: JM-208m) Eocene, NED.
- Tb-6-20: (Mack, 1959: JM-232m) Eocene, NED.
- Tb-6-21: (Mack, 1959: RE-137m) Eocene to Paleocene, ARF.
- Tb-6-22: (Mack, 1959: RE-56m) Eocene?, ARF.
- Tb-6-23: (Mack, 1959: JM-59m) Eocene?, DW.
- Tb-6-24: (Mack, 1959: JM-70m) Eocene? (RGS), DW.
- Tb-6-25: (Mack, 1959: JM-378m) Eocene?, DW.

- Tb-9-1: (Cummings, 1960: 57-260) Upper Ulat. to Nar., LMB.
 Tb-9-2: (Touring, 1959: F187) Eocene, DW.
 Tb-9-3: (Touring, 1959: F189) Nar., LB?
 Tb-9-4: (Touring, 1959: F213) Eocene, LB?
 Tb-9-5: (Touring, 1959: F214) Eocene, DW.
 Tb-9-6: (Touring, 1959: F217) Nar., LMB.
 Tb-9-7: (Touring, 1959: F261) Nar., LB?
 Tb-9-8: (Touring, 1959: F263) Nar., LB.
 Tb-9-9: (Touring, 1959: F308) Eocene, DW.
 Tb-9-10: (Touring, 1959: F558) Eocene, NED.
 Tb-9-11: (Touring, 1959: F559) Nar., LB.
 Tb-9-12A: (Touring, 1959: F731-1) Nar., LMB?
 Tb-9-12B: (Touring, 1959: F731-2) Nar., LB.
 Tb-9-13: (Touring, 1959: F613-2) Nar., MB to LB.
 Tb-9-14: (Touring, 1959: F613-11) Nar., MB to LB.
 Tb-9-15: (Touring, 1959: F613-12) Nar., ARF.
 Tb-9-16: Humble Santa Cruz Lumber Co. #1 well, drilled interval 3560-4975 feet. Nar. (RGS), LB?
 Tb-10-1: (Cummings, 1960, 56-181) upper Ulat. to Nar., DW.
 Tb-10-2: Western Gulf Wells Fargo #1 well, drilled interval 4600-5410 feet. Pen. to Nar.? (RGS), DW.
 Tb-13-1: (Brabb, 1960: EB 486) Nar., ARF, DW.
 Tb-13-2: (Brabb, 1960: EB 164) Nar., ARF, DW.
 Tb-13-3: (Brabb, 1960: EB 474) Nar., ARF, DW.
 Tb-13-4: (Brabb, 1960: EB 477) Nar., DW.
 Tb-13-5: (Brabb, 1960: EB 170) Nar., LB.
 Tb-13-6: (Brabb, 1960: EB 139) Nar., ARF, DW.
 Tb-13-7: (Brabb, 1960: EB 455) Nar., NED.
 Tb-13-8: (Brabb, 1960: EB 167) Nar., LMB?
 Tb-13-9: (Brabb, 1960: EB 149) Nar., ARF, DW.
 Tb-13-10: (Brabb, 1960: EB 143) Nar., ARF, DW.
 Tb-13-11: (Brabb, 1960: EB 151) Nar., NED.
 Tb-14-1: (Sullivan, 1962: B-2228; Poore and Brabb, 1977: MF 3301) lower Nar., Eocene planktic foram. Zones P13-P14, LB.
 Tb-14-2: (Poore and Brabb, 1977: MF 3300) Eocene planktic foram. Zones P13-P14, DW.
 Tb-14-3: (Poore and Brabb, 1977: MF 3299) Eocene planktic foram. Zones P13-P14?, but could be as old as P-11, DW.
 Tb-14-4: (Sullivan, 1962: B-2229) lower Nar., OS to UB.
 Tb-14-5: (Sullivan, 1962: B-2230) lower Nar., UB.
 Tb-14-6: (Fairchild and others, 1969: B-4355), Nar., LMB.
 Tb-14-7: (Brabb, 1960: EB 330L) Nar., NED.
 Tb-14-8: (Brabb, 1960: EB 330H) Nar., DW.
 Tb-14-9: (Brabb, 1960: EB 330F) Nar., NED.
 Tb-14-10: (Brabb, 1960: EB 330E) Nar., NED.
 Tb-14-11: (Brabb, 1960: EB 330D) Nar., NED.
 Tb-14-12: (Brabb, 1960: EB 330B) Nar., DW.
 Tb-14-13: (Brabb, 1960: EB 202G) Nar., DW.
 Tb-14-14: (Brabb, 1960: EB 202A) Nar., DW.
 Tb-14-15: (Brabb, 1960: EB 202H) Nar., DW.
 Tb-14-16: (Brabb, 1960: EB 202B) Nar., LMB?
 Tb-14-19: (Cummings, 1960: 56-700) upper Ulat. to Nar., DW.
 Tb-14-20: (Cummings, 1960: 56-701) upper Ulat. to Nar., NED.
 Tb-14-21: (Cummings, 1960: 56-702) upper Ulat. to Nar., DW.
 Tb-14-22: (Brabb, 1960: EB 24) Nar., NED.
 Tb-14-23: (Brabb, 1960: EB 82) Nar., DW.
 Tb-14-24: (Brabb, 1960: EB 261) Nar., ARF.
 Tb-14-25: (Brabb, 1960: EB 444) lower Nar., DW.

- Tb-14-26: (Brabb, 1960: EB 220) Nar., DW.
 Tb-14-27: (Brabb, 1960: EB 182) Nar., DW.
 Tb-14-28: (Brabb, 1960: EB 121) Nar., DW.
 Tb-14-29: (Brabb, 1960: EB 120) Nar., DW.
 Tb-14-30: (Brabb, 1960: EB 445) Nar., DW.
 Tb-14-31: (Brabb, 1960: EB 166) Nar., ARF, DW.
 Tb-14-32: (Brabb, 1960: EB 165) Nar., ARF, DW.
 Tb-14-33: (Brabb, 1960: EB 169) Nar., ARF, DW.
 Tb-14-34: (Brabb, 1960: EB 188) Nar., ARF.
 Tb-14-35: (Brabb, 1960: EB 38) Nar., ARF, DW.
 Tb-14-38: (Brabb, 1960: EB 346) Nar., DW.
 Tb-14-39: (Brabb, 1960: EB 485) Nar., DW.
 Tb-14-40: (Brabb, 1960: EB 190) Nar., ARF, DW.
 Tb-14-41: (Brabb, 1960: EB 97) Nar., DW.
 Tb-14-42: (Brabb, 1960: EB 69) Nar., ARF, DW.
 Tb-14-43: (Brabb, 1960: EB 214) Nar., DW.
 Tb-15-1: (Fairchild and others, 1969: B-2280) upper Ulat., LB?
 Tb-15-2: (Fairchild and others, 1969: B-2281) upper Ulat., LB?
 Tb-15-3: (Fairchild and others, 1969: B-2282) upper Ulat., LB.
 Tb-15-4: (Fairchild and others, 1969: B-2283) upper Ulat., LB?
 Tb-15-5: (Fairchild and others, 1969: B-2284) upper Ulat., LB.
 Tb-15-6: (Fairchild and others, 1969: B-2285) upper Ulat., LB.
 Tb-15-7: (Fairchild and others, 1969: B-2286) upper Ulat., LB?
 Tb-15-8: (Fairchild and others, 1969: B-2287) upper Ulat., LB.
 Tb-15-9: (Fairchild and others, 1969: B-2288) upper Ulat., LB.
 Tb-15-10: (Fairchild and others, 1969: B-2289) upper Ulat., LB?
 Tb-15-11: (Fairchild and others, 1969: B-2290) upper Ulat., LMB?
 Tb-15-12: (Fairchild and others, 1969: B-2291) upper Ulat., LMB to LB.
 Tb-15-13: (Fairchild and others, 1969: B-2292) upper Ulat. to lower Nar., LB.
 Tb-15-14: (Fairchild and others, 1969: B-2293) upper Ulat. to lower Nar., LB.
 Tb-15-15: (Fairchild and others, 1969: B-4375) upper Ulat., NED.
 Tb-15-16: (Fairchild and others, 1969: B-2294) upper Ulat., LMB.
 Tb-15-17: (Fairchild and others, 1969: B-2295) upper Ulat., LMB?
 Tb-15-18: (Fairchild and others, 1969: B-2296) upper Ulat., LMB?
 Tb-15-19: (Fairchild and others, 1969: B-4376) upper Nar.?, NED.
 Tb-15-20: (Fairchild and others, 1969: B-4374) upper Nar.?, NED.
 Tb-15-21: (Brabb, 1960: EB 426B) Nar., ARF, DW.
 Tb-15-22: (Brabb, 1960: EB 425C) Nar., DW.
 Tb-15-23: (Brabb, 1960: EB 425A) Nar., LMB?
 Tb-15-24: (Brabb, 1960: EB 514) Nar., DW.
 Tb-15-25: (Brabb, 1960: EB 513) Nar., DW.
 Tb-15-26: (Brabb, 1960: EB 512) Nar., DW.
 Tb-15-27: (Brabb, 1960: EB 511) upper Nar., DW.
 Tb-15-28: (Brabb, 1960: EB 361) Nar., LB?
 Tb-15-29: (Brabb, 1960: EB 362) Nar., LB.
 Tb-15-30: (Hector, 1976: SH 637) upper Nar.? (RGS), ARF.
 Tb-15-31: (Hector, 1976: SH 706) upper Nar.? (RGS), ARF.
 Tb-16-1: (Fairchild and others, 1969: B-4384) upper Nar.?, NED.
 Tb-16-2: (Melendres, 1958: MM 22) Nar., LB.
 Tb-19-1: (Clark, 1966: JC60-20) Ulat., DW.
 Tb-19-2: (Clark, 1966: JC60-37) Pen., NED.
 Tb-19-3: (Clark, 1966: JC60-51) Ulat., NED.
 Tb-19-4: (Clark, 1966: JC60-74) Nar., NED.
 Tb-19-5: (Clark, 1966: JC60-75) Nar., NED.
 Tb-19-6: (Clark, 1966: JC60-90) upper Ulat. to lower Nar., NED.

- Tb-19-7: (Clark, 1966: JC60-113) Pen.?, NED.
 Tb-19-8: (Clark, 1966: JC60-115) upper Pen., LB?
 Tb-19-9: (Travers, 1959: WT-78) middle Eocene or older, DW.
 Tb-19-10: (Travers, 1959: WT-68) upper Eocene or older, DW, possibly LB.
 Tb-20-1: (Smith, 1971: B-7123) Nar. or Ref., DW.
 Tb-20-2: (Smith, 1971: B-7124) Nar. or Ref., ARF, LMB?
 Tb-20-3: (Smith, 1971: B-7125) Nar. or Ref., DW.
 Tb-20-4: (Smith, 1971: B-7126) Nar. or Ref., LMB.
 Tb-20-5: (Smith, 1971: B-7127) Nar. or Ref., DW.
 Tb-20-6: (Smith, 1971: B-7128) Nar. or Ref., ARF.
 Tb-20-7: (Smith, 1971: B-7129) Nar. or Ref., ARF.
 Tb-20-8: (Smith, 1971: B-7130) Nar. or Ref., LMB.
 Tb-20-10: (Fairchild and others, 1969: B-4385) upper Nar.? NED.
 Tb-20-11: (Burford, 1961: ROB 61-7 and ROB 61-2) Nar., NED.
 Tb-20-12: (Burford, 1961: ROB 61-3) Nar., DW.
 Tb?-26-1: (McDougall, unpublished data, 1977: MF 2984) Ulat. to lower Nar., LMB.
 Tsl-9-1: (Brabb, 1960: EB 501A) Ref. to Zem. (RGS), LMB.
 Tsl-9-2: (Brabb, 1960: EB 501C) Ref.? (RGS), LMB.
 Tsl?-9-5: Jergins YMCA #2 well, drilled interval 4411-4417 feet. lower Zem. (RGS), MB?
 Tsl?-9-6: Jergins YMCA #2 well, drilled interval 4548-4562 feet. lower Zem.? (RGS), MB to LB.
 Tsl?-9-7: Jergins YMCA #2 well, drilled interval 4535-4735 feet. lower Zem.? (RGS), NED.
 Tsl?-9-14: (Touring, 1959: F767) Nar., LMB.
 Tsl-10-1: (Graham and Drooger, 1952) upper Oligocene, NED.
 Tsl-10-2: (Cummings, 1960: 57-848) Nar. to Zem., DW.
 Tsl-10-3: (Cummings, 1960: 57-842) Nar., DW.
 Tsl-10-4: Western Gulf Wells Fargo #1 well, drilled interval 2560 to 3860 feet, reported by Strom (1956). Ref., LB.
 Tsl-14-1: (Fairchild and others, 1969: B-4363) lower Zem. (RGS), LB.
 Tsl-14-2: (Fairchild and others, 1969: B-4361) lower Zem. (RGS), LB.
 Tsl-14-3: (Fairchild and others, 1969: B-4360) lower Zem. (RGS), LB.
 Tsl-14-4: (Fairchild and others, 1969: B-4359) Ref., LMB.
 Tsl-14-5: (Fairchild and others, 1969: B-4356) Nar. or lower Ref.?, DW.
 Tsl-14-7: (Cummings, 1960: 57-374) lower Zem. (RGS), LB.
 Tsl-14-8: (Cummings, 1960: 56-601) lower Zem. (RGS), MB.
 Tsl-14-9: (Cummings, 1960: 57-422) Ref. to Sauc. (RGS), NED.
 Tsl-14-10: (Cummings, 1960: 56-698) upper Ulat. to Nar., LB.
 Tsl-14-11: (Cummings, 1960: 56-699) upper Ulat. to Nar., NED.
 Tsl-14-100: (Cummings, 1960: 57-6) upper Zem.? (RGS), LB.
 Tsl-15-2: (Kleinpell, 1938: K-32) lower Zem. (RGS), LB.
 Tsl-15-3: (Hector, 1976: SH 759) age indeterminate (RGS), ARF, DW.
 Tsl-20-100: (Burford, 1961: ROB 61-16, 17, and 18) upper Zem. to Sauc. (RGS), UMB.
 Tst-9-1: (Touring, 1959: F192) Eocene, ARF.
 Tst-9-2: (Touring, 1959: F219) Eocene, DW.
 Tst-9-3: Humble Santa Cruz Lumber Co. #1 well, drilled interval 3252-3580 feet. Nar. (RGS), MB to LB.
 Tst-14-1: (Sullivan, 1962: B-2231) Nar., DW.
 Tst-14-2: (Sullivan, 1962: B-2232) Nar., ARF.
 Tst-14-3: (Sullivan, 1962: B-2232; Poore and Brabb, 1977: MF 3304 and MF 1350; K. A. McDougall, unpublished data, 1979: MF 1350) Nar., Eocene planktic foram. Zone P14, LMB, OMZ?
 Tst-14-4: (Sullivan, 1962: B-2234; Poore and Brabb, 1977: MF 3305 and MF 1351; K. A. McDougall, unpublished data, 1979: MF 1351) Nar., Eocene planktic foram. Zones P15-P16, UMB, OMZ.
 Tst-14-5: (Sullivan, 1962: B-2235; Poore and Brabb, 1977: MF 3306 and MF 1352; K. A. McDougall, unpublished data, 1979, MF 1352) upper Narizian, Eocene planktic foram. Zone P16, DW.
 Tst-14-6: (Sullivan, 1962: B-2236) Nar., MB, OMZ.
 Tst-14-7: (Sullivan, 1962: B-2237) Nar., MB, OMZ.

- Tst-14-8: (Sullivan, 1962: B-2242) Nar., MB, OMZ.
 Tst-14-9: (Sullivan, 1962: B-2243) Nar., MB, OMZ.
 Tst-14-10: (Sullivan, 1962: B-2244) Nar., MB.
 Tst-14-11: (Sullivan, 1962: B-2246) Nar., MB.
 Tst-14-12: (Sullivan, 1962: B-2247) Nar., MB?
 Tst-14-13: (Sullivan, 1962: B-2248) Nar., MB.
 Tst-14-14: (Sullivan, 1962: B-2249) Nar., UMB?, OMZ.
 Tst-14-15: (Sullivan, 1962: B-2250) Nar., MB?, OMZ.
 Tst-14-16A: (Poore and Brabb, 1977: MF 3308) Nar., NED.
 Tst-14-16B: (K. A. McDougall, unpublished data, 1979: MF 1355) Nar., LMB?
 Tst-14-16C: (K. A. McDougall, unpublished data, 1979: MF 1356) Nar., LMB.
 Tst-14-16D: (K. A. McDougall, unpublished data, 1979: MF 1357) Nar., LMB.
 Tst-14-17: (Sullivan, 1962: B-2245) Nar., MB, OMZ.
 Tst-14-18: (Sullivan, 1962: B-2241) Nar., MB.
 Tst-14-19: (Sullivan, 1962: B-2240) Nar., MB.
 Tst-14-20: (Sullivan, 1962: B-2239) Nar., MB, OMZ.
 Tst-14-21: (Sullivan, 1962: B-2238) Nar., LB.
 Tst-14-22: (Fairchild and others, 1969: B-2297) Nar., LMB, OMZ.
 Tst-14-23: (Fairchild and others, 1969: B-2306) Nar., UMB?
 Tst-14-24: (Fairchild and others, 1969: B-2307) Nar., MB.
 Tst-14-25: (Fairchild and others, 1969: B-2305) Nar., MB, OMZ.
 Tst-14-26: (Fairchild and others, 1969: B-2304) Nar., UMB?, OMZ.
 Tst-14-27: (Fairchild and others, 1969: B-2303) Nar., UMB, OMZ.
 Tst-14-28: (Fairchild and others, 1969: B-2302) Nar., LMB, OMZ.
 Tst-14-29: (Fairchild and others, 1969: B-2301) Nar., UMB?, OMZ.
 Tst-14-30: (Brabb, 1960: EB 203B) Nar., DW.
 Tst-14-31: (Brabb, 1960: EB 203D) Nar., DW.
 Tst-14-32: (Brabb, 1960: EB 203C) Nar., LMB?
 Tst-14-33: (Brabb, 1960: EB 204C) Nar., DW.
 Tst-14-34: (Brabb, 1960: EB 204D) Nar., DW.
 Tst-14-35: (Brabb, 1960: EB 204A) Nar., LMB?
 Tst-14-36: (Brabb, 1960: EB 205A) Nar., MB?
 Tst-14-37: (Brabb, 1960: EB 205J) Nar., NED.
 Tst-14-38: (Brabb, 1960: EB 229D) Nar., DW.
 Tst-14-39: (Brabb, 1960: EB 273) Nar., DW.
 Tst-14-40: (Brabb, 1960: EB 450) Nar., DW.
 Tst-14-41: (Brabb, 1960: EB 256B) Nar., MB.
 Tst-14-42: (Brabb, 1960: EB 247) Nar., MB.
 Tst-14-43: (Brabb, 1960: EB 310A) Nar., DW.
 Tst-14-44: (Brabb, 1960: EB 453) Nar., NED.
 Tst-14-45: (Brabb, 1960: EB 347) Nar., DW.
 Tst-14-46: (Brabb, 1960: EB 132) Nar., DW.
 Tst-14-47: (Brabb, 1960: EB 12) Nar., DW.
 Tst-14-48: (Brabb, 1960: EB 5) Nar., DW.
 Tst-14-49: (Brabb, 1960: EB 99) Nar., DW.
 Tst-14-50: (Brabb, 1960: EB 130) Nar., ARF, DW.
 Tst-14-51: (Brabb, 1960: EB 71) Nar., ARF, DW.
 Tst-14-52: (Brabb, 1960: EB 105) Nar., MB.
 Tst-14-53: (Brabb, 1960: EB 495) Nar., ARF, DW.
 Tst-14-54: (Brabb, 1960: EB 494C) Nar., NED.
 Tst-14-55: (Brabb, 1960: EB 494B) Nar., LB?
 Tst-14-56: (Brabb, 1960: EB 494A) Nar., NED.
 Tst-14-57: (Brabb, 1960: EB 288) Nar., NED.
 Tst-14-59: (Sullivan, 1962: B-2251) Refugian according to Sullivan (1962) and Poore and Brabb (1977), but Narizian according to McDougall (unpublished data, 1979), LMB.

- Tst-15-1: (Fairchild and others, 1969: B-4357) Nar.?, DW.
 Tst-15-2: (Fairchild and others, 1969: B-4358) Nar.?, MB.
 Tst-15-3: (Brabb, 1960: EB 363B) Nar., DW.
 Tst-15-4: (Brabb, 1960: EB 363C) Nar., ARF.
 Tst-15-5: (Brabb, 1960: EB 419A) Nar., MB, OMZ.
 Tst-15-6: (Brabb, 1960: EB 419C) Nar., LMB?
 Tst-15-7: (Brabb, 1960: EB 366B) Nar., ARF.
 Tst-15-8: (Brabb, 1960: EB 366C) Nar., MB, OMZ.
 Tst-15-9: (Brabb, 1960: EB 366D) Nar., MB?
 Tst-15-10: (Brabb, 1960: EB 366E) Nar., DW.
 Tst-15-11: (Brabb, 1960: EB 367A) Nar., LB?
 Tst-15-12: (Brabb, 1960: EB 367B) Nar., LMB?
 Tst-15-13: (Brabb, 1960: EB 510) Nar., DW.
 Tst-19-1: (Brabb, 1960: EB 507) Nar.? MB.
 Tst-20-1: (Smith, 1971: B-7109) Nar., ARF.
 Tst-20-2: (Smith, 1971: B-7108) Nar., LMB to LB.
 Tst-20-3: (Smith, 1971: B-7107) Nar., ARF.
 Tst-20-4: (Smith, 1971: B-7106) Nar., ARF.
 Tst-20-5: (Smith, 1971: B-7105) Nar., LMB?
 Tst-20-6: (Smith, 1971: B-7110) Nar., ARF.
 Tst-20-7: (Smith, 1971: B-7111) Nar., LB?, OMZ.
 Tst-20-8: (Smith, 1971: B-7112) Nar., LB?
 Tst-20-9: (Smith, 1971: B-7113) Nar., NED.
 Tst-20-10: (Smith, 1971: B-7114) Nar., DW.
 Tst-20-11: (Smith, 1971: B-7115) Nar., ARF.
 Tst-20-12: (Burford, 1961: ROB 61-6) Ref.? near Refugian-Narizian boundary, DW.
 Tsr-9-1: Humble Santa Cruz Lumber Co. #1 well, drilled interval 1940-2210 feet. lower Zem. (RGS), LB.
 Tsr-9-2: Humble Santa Cruz Lumber Co. #1 well, drilled interval 2240-2270 feet. lower Zem. (RGS), LB?
 Tsr-9-3: Humble Santa Cruz Lumber Co. #1 well, drilled interval 2270-2300 feet. lower Zem. (RGS), LB?
 Tsr-9-4: Humble Santa Cruz Lumber Co. #1 well, drilled interval 2810-2840 feet. lower Zem. (RGS), MB.
 Tsr-9-5: Humble Santa Cruz Lumber Co. #1 well, drilled interval 2930-2960 feet. Ref. (RGS), NED, possibly LB.
 Tsr-10-1: (Cummings, 1960: 57-505) Nar. to Zem., NED.
 Tsr-10-2: Western Gulf Wells Fargo #1 well, drilled interval 2060-3140 feet. Ref.? to lower Zem. (RGS), LB.
 Tsr-14-1: (Sullivan, 1962: B-2252) Ref., LMB.
 Tsr-14-2: (Sullivan, 1962: B-2253) Ref., LMB.
 Tsr-14-3: (Sullivan, 1962: B-2254) Ref., LMB.
 Tsr-14-4: (Sullivan, 1962: B-2255) Refugian according to Sullivan (1962) and Poore and Brabb (1977), but lower Zemorrian according to McDougall (unpublished data, 1979), LMB.
 Tsr-14-5: (Sullivan, 1962: B-2256) Refugian according to Sullivan (1962) and Poore and Brabb (1977), but could be lower Zemorrian (RGS), LMB?
 Tsr-14-6: (Poore and Brabb, 1977: MF 1366; K. A. McDougall, unpublished data, 1979: MF 1366) lower Zemorrian, Oligocene planktic foram. Zones P19-P20, Oligocene nannofossil Zones NP23-NP25, DW.
 Tsr-14-7: (Poore and Brabb, 1977: MF 2700; K. A. McDougall, unpublished data, 1979: MF 2700) lower Zemorrian, Oligocene planktic foram. Zones P19-P20, LMB.
 Tsr-14-8: (Sullivan, 1962: B-2257) lower Zem., LMB?
 Tsr-14-9: (Poore and Brabb, 1977: MF 2701; K. A. McDougall, unpublished data, 1979: MF 2701) lower Zem., Oligocene planktic foram. Zones P19-P20, DW.
 Tsr-14-10A: (Sullivan, 1962: B-2258; Poore and Brabb, 1977: MF 3310) lower Zem., Oligocene planktic

- foram. Zones P19-P20, Oligocene nannofossil Zones NP23-NP25, LMB.
- Tsr-14-10C: (K. A. McDougall, unpublished data, 1979: MF 1368) lower Zem., NED.
- Tsr-14-11: (Sullivan, 1962: B-2259) lower Zem., LMB.
- Tsr-14-12: (Sullivan, 1962: B-2260) lower Zem., LMB.
- Tsr-14-14: (Sullivan, 1962: B-2261) lower Zem., LB.
- Tsr-14-15: (Sullivan, 1962: B-2262) lower Zem., LB.
- Tsr-14-16: (Sullivan, 1962: B-2263) lower Zem., LB.
- Tsr-14-17: (Sullivan, 1962: B-2264) lower Zem., LB.
- Tsr-14-18: (Sullivan, 1962: B-2265) lower Zem., LB.
- Tsr-14-19: (Sullivan, 1962: B-2266) lower Zem., LB.
- Tsr-14-20: (Sullivan, 1962: B-2267) lower Zem., LB.
- Tsr-14-21: (Sullivan, 1962: B-2268) lower Zem., LMB.
- Tsr-14-22: (Sullivan, 1962: B-2269) lower Zem., LMB.
- Tsr-14-23: (Sullivan, 1962: B-2270) lower Zem., LB.
- Tsr-14-24: (Sullivan, 1962: B-2271) lower Zem., LB.
- Tsr-14-25: (Sullivan, 1962: B-2272) lower Zem., LMB.
- Tsr-14-26: (Sullivan, 1962: B-2273) lower Zem., LMB.
- Tsr-14-27: (Sullivan, 1962: B-2274) lower Zem., LMB?
- Tsr-14-28: (Sullivan, 1962: B-2275) lower Zem., LB?
- Tsr-14-29: (Sullivan, 1962: B-2276) lower Zem., LMB.
- Tsr-14-30: (Fairchild and others, 1969: B-2300) lower Zem?, LB.
- Tsr-14-31: (Fairchild and others, 1969: B-2299) lower Zem.?, LB.
- Tsr-14-32: (Fairchild and others, 1969: B-2298) lower Zem.?, LB?
- Tsr-14-33: (Fairchild and others, 1969: B-4362) Ref. to lower Zem. (RGS), LMB?
- Tsr-14-34: (K. A. McDougall, unpublished data, 1979: MF 1360) lower Ref., LMB.
- Tsr-14-35: (K. A. McDougall, unpublished data, 1979: MF 1361) lower Ref., LMB?
- Tsr-14-36: (K. A. McDougall, unpublished data, 1979: MF 1362) lower Ref., NED.
- Tsr-14-37: (K. A. McDougall, unpublished data, 1979: MF 1364) upper Ref., NED.
- Tsr-14-38: (K. A. McDougall, unpublished data, 1979: MF 1365) upper Ref., NED.
- Tsr-14-39: (K. A. McDougall, unpublished data, 1979: MF 1367) lower Zem., NED.
- Tsr-14-40: (Brabb, 1960: EB 205C) Ref., LMB?
- Tsr-14-41: (Brabb, 1960: EB 205H) Ref., LB.
- Tsr-14-42: (Brabb, 1960: EB 205D) Ref., LB.
- Tsr-14-43: (Brabb, 1960: EB 205F) Ref., LMB.
- Tsr-14-44: (Brabb, 1960: EB 205M) lower Zem. (RGS), NED.
- Tsr-14-45: (Brabb, 1960: EB 206) lower Zem. (RGS), LB.
- Tsr-14-46: (Brabb, 1960: EB 223A) lower Zem. (RGS), LB.
- Tsr-14-47: (Brabb, 1960: EB 37) Ref. or lower Zem. (RGS), LB.
- Tsr-14-48: (Brabb, 1960: EB 197) Ref. or lower Zem. (RGS), LB.
- Tsr-14-49: (Brabb, 1960: EB 93) Ref. or lower Zem. (RGS), NED.
- Tsr-14-50: (Brabb, 1960: EB 216) lower Zem. (RGS), LB.
- Tsr-14-51: (Brabb, 1960: EB 222) Ref. or lower Zem. (RGS), NED.
- Tsr-14-52: (Brabb, 1960: EB 95) lower Zem. (RGS), LB.
- Tsr-14-53: (Brabb, 1960: EB 394) Ref. or lower Zem. (RGS), LMB?
- Tsr-14-54: (Brabb, 1960: EB 391) Ref. or lower Zem. (RGS), NED.
- Tsr-14-55: (Brabb, 1960: EB 254) lower Zem.? (RGS), LB.
- Tsr-14-56: (Brabb, 1960: EB 389) Ref. or lower Zem. (RGS), LB.
- Tsr-14-57: (Brabb, 1960: EB 332) lower Zem.? (RGS), LB?
- Tsr-14-58: (Brabb, 1960: EB 451) Ref. or lower Zem. (RGS), NED.
- Tsr-14-59: (Brabb, 1960: EB 393) lower Zem. (RGS), LB.
- Tsr-14-60: (Brabb, 1960: EB 392) Ref. or lower Zem. (RGS), LB.
- Tsr-14-61: (Brabb, 1960: EB 380) lower Zem. (RGS), LB.
- Tsr-14-62: (Brabb, 1960: EB 416) Ref. or lower Zem. (RGS), LMB?
- Tsr-14-63: (Brabb, 1960: EB 207) lower Zem. (RGS), LB?
- Tsr-14-64: (Brabb, 1960: EB 287) Zem., NED.

- Tsr-14-65: (Brabb, 1960: EB 211) lower Zem. (RGS), LMB.
 Tsr-14-66: (Brabb, 1960: EB 478) lower Zem. (RGS), LMB.
 Tsr-14-67: (Brabb, 1960: EB 496) Zem., NED.
 Tsr-14-68: (Brabb, 1960: EB 493B) lower Zem. (RGS), LB.
 Tsr-14-69: (Brabb, 1960: EB 493A) lower Zem. (RGS), LB.
 Tsr-14-70: (Brabb, 1960: EB 178) Ref. or lower Zem. (RGS), LB.
 Tsr-14-71: (Brabb, 1960: EB 276) Ref. or lower Zem. (RGS), LMB?
 Tsr-14-72: (Brabb, 1960: EB 395C) Ref. or lower Zem. (RGS), NED.
 Tsr-14-73: (Brabb, 1960: EB 246) Ref. or lower Zem. (RGS), LB.
 Tsr-14-74: (Brabb, 1960: EB 409) Ref. or lower Zem. (RGS), NED.
 Tsr-14-75: (Brabb, 1960: EB 410) lower Zem. (RGS), NED.
 Tsr-14-76: (Brabb, 1960: EB 378) Ref. or lower Zem. (RGS), LB.
 Tsr-14-77: (Brabb, 1960: EB 386) Ref.-lower Zem. boundary (RGS), NED.
 Tsr-14-78: (Brabb, 1960: EB 385) lower Zem. (RGS), NED.
 Tsr-14-79: (Brabb, 1960: EB 383) Ref. or lower Zem. (RGS), LMB.
 Tsr-14-80: (Brabb, 1960: EB 312) Ref. or lower Zem. (RGS), NED.
 Tsr-14-81: (Brabb, 1960: EB 60) Ref. or lower Zem. (RGS), LB.
 Tsr-14-82: (Brabb, 1960: EB 179) Ref. or lower Zem. (RGS), LB.
 Tsr-14-83: (Brabb, 1960: EB 395A) Ref., UB.
 Tsr-14-84: (Brabb, 1960: EB 384) Ref., LMB.
 Tsr-14-85: (Brabb, 1960: EB 279) Ref., MB.
 Tsr-14-86: (Brabb, 1960: EB 277) Ref. to lower Zem. (RGS), LMB.
 Tsr-14-87: (Brabb, 1960: EB 275) Ref. to lower Zem. (RGS), LMB.
 Tsr-14-88: (Brabb, 1960: EB 282) Ref., LMB.
 Tsr-14-89: (Brabb, 1960: EB 256A) Ref., MB.
 Tsr?-14-105: (Kleinpell, 1938: LSJU 363) lower Zem. (RGS), LMB.
 Tsr-14-106: (Kleinpell, 1938: LSJU 363B) lower Zem. (RGS), LB.
 Tsr-14-107: (Kleinpell, 1938: LSJU 363C) lower Zem. (RGS), LB?
 Tsr-14-107X: (Kleinpell, 1938: LSJU 1163) lower Zem. (RGS), LB.
 Tsr-14-118: (Cummings, 1960: 57-419) Nar. to Zem., NED.
 Tsr-14-119: (Cummings, 1960: 57-285) Zem. (RGS), LMB?
 Tsr-14-120: (Cummings, 1960: 56-586) Zem. (RGS), LB.
 Tsr-14-121: (Cummings, 1960: 56-584) Nar. to Zem., NED.
 Tsr-14-123: (Cummings, 1960: 57-341) Nar. to Zem., NED.
 Tsr-14-127: (Kleinpell, 1938: LSJU 1103) lower Zem. (RGS), LB.
 Tsr-15-1: (Fairchild and others, 1969: B-4377) lower Zem., LB.
 Tsr-15-2: (Brabb, 1960: EB 367D) Ref., LMB.
 Tsr-15-3: (Brabb, 1960: EB 367F) Re., LMB.
 Tsr-15-4: (Brabb, 1960: EB 365A) Ref., NED.
 Tsr-15-5: (Brabb, 1960: EB 365B) Ref., LMB?
 Tsr-15-6: (Brabb, 1960: EB 364B) Zem., LB?
 Tsr-15-7: (Brabb, 1960: EB 420D) lower Zem. (RGS), LB.
 Tsr-15-8: (Brabb, 1960: EB 420B) lower Zem. (RGS), LB?
 Tsr-15-9: (Brabb, 1960: EB 421A) lower Zem. (RGS), LMB.
 Tsr-15-10: (Brabb, 1960: EB 422B) lower Zem. (RGS), LB.
 Tsr-15-11: (Brabb, 1960: EB 468) Ref. or lower Zem. (RGS), NED.
 Tsr-15-12: (Brabb, 1960: EB 313) lower Zem. (RGS), LB.
 Tsr-15-13: (Brabb, 1960: EB 469) Ref., NED.
 Tsr-15-22: (McCollom, 1959: LSJU M-4) Zem., NED, possibly LB.
 Tsr-15-24: (Burchfiel, 1958: LSJU M-5) lower Zem., NED.
 Tsr-15-25: (Burchfiel, 1958: LSJU 1767) lower Zem., NED.
 Tsr-15-27: (Burchfiel, 1958: C7) Zem., LB?
 Tsr-15-33: (Hector, 1976: SH 399) lower Zem.? (RGS), ARF, DW.
 Tsr-15-34: (Hector, 1976: SH 485) lower Zem.? (RGS), ARF, LMB?
 Tsr-15-35: (Hector, 1976: SH 491) lower Zem.? (RGS), LB.

- Tsr-16-1: (Fairchild and others, 1969: B-4386) Zem. to lower Sauc., LMB-LB boundary.
 Tsr-16-2: (Melendres, 1958: MM17) Ref. or Zem. (RGS), ARF, LMB or deeper.
 Tsr-16-3: (Melendres, 1958: MM18) upper Eocene, ARF.
 Tsr-19-1: (Brabb, 1960: EB 508) lower Zem. (RGS), UMB?
 Tsr-19-2: (Travers, 1959: WT 64) Ref.?, NED, possibly LMB.
 Tsr-20-1: (Smith, 1971: B-7103) lower Zem., LB, OMZ?
 Tsr-20-2: (Smith, 1971: B-7102) lower Zem., LB.
 Tsr-20-3: (Smith, 1971: B-7101) lower Zem., LB.
 Tsr-20-4: (Smith, 1971: B-7100) lower Zem., ARF.
 Tsr-20-5: (Smith, 1971: B-7099) lower Zem., LB, OMZ?
 Tsr-20-6: (Smith, 1971: B-7098) lower Zem., LB.
 Tsr-20-7: (Smith, 1971: B-7097) lower Zem., LB.
 Tsr-20-8: (Smith, 1971: B-7096) lower Zem., LB, OMZ?
 Tsr-20-9: (Smith, 1971: B-7095) lower Zem., ARF, OMZ?
 Tsr-20-10: (Smith, 1971: B-7117) lower Zem., LB.
 Tsr-20-11: (Smith, 1971: B-7118) lower Zem., LB.
 Tsr-20-12: (Smith, 1971: B-7119) lower Zem., LB.
 Tsr-20-13: (Smith, 1971: B-7120) lower Zem., LB.
 Tsr-20-14: (Smith, 1971: B-7121) lower Zem., LB.
 Tsr-20-15: (Smith, 1971: B-7122) lower Zem., LB.
 Tsr-20-16: (Fairchild and others, 1969, B-4388) lower Zem., (RGS), LB.
 Tsr-20-17: (Fairchild and others, 1969, B-4387) lower Zem., (RGS), LB?
 Tsr?-20-19: (Burford, 1961: ROB 61-22) lower Zem., NED.
 Tsr-20-20: (Burford, 1961: ROB 61-27) lower Zem., LB.
 Tsr-20-21: (Burford, 1961: ROB 61-38) lower Zem., LB?
 Tsr-20-22: (Burford, 1961: ROB 61-10) lower Zem., MB?
 Tsr-20-23: (Burford, 1961: ROB 61-14) lower Zem., DW.
 Tsr-20-24: (Burford, 1961: ROB 61-9) lower Zem., LB?
 Tsr-20-25: (Burford, 1961: ROB 61-8 and EB 574) Ref., DW.
 Tsr-20-26: (Burford, 1961: ROB 61-1) Ref.?, DW.
 Tsr-20-27: (Melendres, 1958: MM25) lower Zem. (RGS), LB.
 Tsr-20-28: (Smith, 1971: B-7104) Ref., NED.
 Tsr-20-29: (Smith, 1971: B-7116) Ref., NED.
 Tsr-20-31: (McCollom, 1959: EB 412) lower Miocene, ARF.
 Tsr-21-1: (reference withheld by request) lower Zem. (RGS), LB.
 Tos-6-1: (Poore, unpublished data, 1978: MF 2534) middle Eocene planktic foram. Zones P12-P14, DW.
 Tos-9-1: (Cummings, 1960: 57-750) upper Zem. to Sauc. (RGS), LMB?
 Tos-9-2: (Cummings, 1960: 57-265) upper Zem. (RGS), UB?, OMZ?
 Tos-9-3: (Cummings, 1960: 57-813) upper Zem. (RGS), UB?
 Tos-9-5: (Touring, 1959: F198) Oligocene, NED.
 Tos-9-6: (Touring, 1959: F200) Oligocene, NED.
 Tos-9-7: (Touring, 1959: F223) Oligocene, NED.
 Tos-9-8: (Touring, 1959: F225) upper Zem. (RGS), LMB.
 Tos-9-9: (Touring, 1959: F226) Zem.?, MB.
 Tos-9-10: (Touring, 1959: F227) Zem. to Sauc. (RGS), LMB?
 Tos-9-11: (Touring, 1959: F228) Zem.?, LMB?
 Tos-9-12: (Touring, 1959: F231) upper Zem.? (RGS), LMB?
 Tos-9-13: (Touring, 1959: F232) age indeterminate, LMB?
 Tos-9-14: (Touring, 1959: F233) upper Zem.? (RGS), LB.
 Tos-9-15: (Touring, 1959: F234) upper Zem.? (RGS), LMB.
 Tos-9-16: (Touring, 1959: F236) Zem.? DW.
 Tos-9-17: (Touring, 1959: F241M) upper Zem.? (RGS), LMB.
 Tos-9-18: (Touring, 1959: F270) Zem. to Sauc. (RGS), LMB.
 Tos-9-19: (Touring, 1959: F272) Zem., LMB.
 Tos-9-20: (Touring, 1959: F274) lower Zem.? (RGS), LB.

- Tos-9-21: (Touring, 1959: F275) Zem. to Sauc. (RGS), LMB.
 Tos-9-22: (Touring, 1959: F278) Zem. to Sauc. (RGS), UMB?, OMZ.
 Tos-9-23: (Touring, 1959: F279) Zem. to Sauc. (RGS), LMB, OMZ.
 Tos-9-24: (Touring, 1959: F281) Zem. to Sauc. (RGS), MB, OMZ.
 Tos-9-25: (Touring, 1959: F282) Oligocene, UB, OMZ.
 Tos-9-26: (Touring, 1959: F284) upper Zem.? (RGS), LB.
 Tos-9-27: (Touring, 1959: F285) upper Zem. (RGS), LB.
 Tos-9-28: (Touring, 1959: F310) Oligocene, NED.
 Tos-9-29: (Touring, 1959: F315) Oligocene, NED.
 Tos-9-30: (Touring, 1959: F323) Oligocene, ARF.
 Tos-9-31: (Touring, 1959: F330) Oligocene, DW.
 Tos-9-32: (Touring, 1959: F331M) upper Zem.? (RGS), LB, OMZ?,
 Tos-9-33: (Touring, 1959: F335) Nar., NED.
 Tos-9-34: (Touring, 1959: F753) Zem. to Sauc. (RGS), NED.
 Tos-9-35: (Touring, 1959: F769) Zem. to Sauc. (RGS), MB, OMZ?
 Tos-9-36: (Touring, 1959: F798) Zem., UB, OMZ.
 Tos-9-37: (Touring, 1959: F804) Oligocene, LMB?
 Tos-9-38: (Touring, 1959: F797) upper Zem. (RGS), MB.
 Tos-10-1: (Cummings, 1960: 57-747) upper Zem. (RGS), LB.
 Tos-10-2: (Cummings, 1960: 57-808) upper Zem. (RGS), LB?
 Tos-10-3: (Cummings, 1960: 57-922) Nar. to Zem., NED.
 Tos-10-4: (Cummings, 1960: 57-756) Zem. to lower Sauc., DW.
 Tos-10-4X: (Cummings, 1960: 56-172) upper Pen. to lower Ulat., LMB.
 Tvw-6-1: (Mack, 1959: RE-219m) Zem. or younger, possibly upper Zem. (RGS), ARF.
 Tvw-6-2: (Mack, 1959: JM-225m) Zem., possibly upper Zem. (RGS), DW.
 Tvw-6-3: (Mack, 1959: JM-226m) Zem., possibly upper Zem. (RGS), ARF.
 Tvw-6-4: (Mack, 1959: JM-99m) Zem., possibly upper Zem. (RGS), ARF.
 Tvw-6-5: (Mack, 1959: JM101m) Zem., possibly upper Zem. (RGS), LMB.
 Tvw-6-6: (Classen, 1959: C-100) upper Zem.? (RGS), LMB.
 Tvw-6-7: (Classen, 1959: 14-59) Zem., possibly upper Zem. (RGS), ARF.
 Tvc-9-1: Humble Santa Cruz Lumber Co. #1 well, drilled interval 1880-1910 feet. lower Zem. (RGS), LMB to LB.
 Tvc-9-2: Jergins YMCA #2 well, drilled interval 3004-3035 feet. lower Zem.? (RGS), LMB to LB?
 Tvc-9-3: Jergins YMCA #2 well, drilled interval 3035-3040 feet. lower Zem.? (RGS), NED.
 Tvc-9-4: Jergins YMCA #1 well, drilled interval 2324-2327 feet. lower Zem.? (RGS), LB.
 Tvc-10-1: (Cummings, 1960: 56-238) upper Zem. to Sauc. (RGS), UMB?
 Tvc-10-2: (Cummings, 1960: 57-222) lower Zem. (RGS), UMB?
 Tvc-10-4: (Cummings, 1960: 57-885) upper Zem.? (RGS), NED.
 Tvc-10-8: Western Gulf Wells Fargo #1 well, drilled interval 1440-1727 feet. upper Zem.? to Sauce. (RGS), LB.
 Tvc-10-9: Western Gulf Wells Fargo #1 well, drilled interval 2020-2040 feet. lower Zem. (RGS), LB.
 Tvc-14-1: (Sullivan, 1962: B-2277) lower Zem., LB.
 Tvc-14-2: (Fairchild and others, 1969: B-4370) lower Zem., LMB to LB?
 Tvc-14-3: (Fairchild and others, 1969: B-2312) lower Zem., LMB to LB.
 Tvc-14-4: (Fairchild and others, 1969: B-4364) lower Zem., LB.
 Tvc-14-5: (Fairchild and others, 1969: B-4368) lower Zem. (RGS), LMB-LB boundary.
 Tvc-14-6: (Fairchild and others, 1969: B-4366) lower Zem. (RGS), LB.
 Tvc-14-7: (Fairchild and others, 1969: B-4365) lower Zem. (RGS), LMB-LB boundary.
 Tvc-14-8: (Fairchild and others, 1969: B-4367) lower Zem. (RGS), LB.
 Tvc-14-9: (Brabb, 1960: EB 236) lower Zem. (RGS), UB?
 Tvc-14-10: (Brabb, 1960: EB 491) lower Zem. (RGS), NED.
 Tvc-14-11: (Brabb, 1960: EB 36) Zem., LB.
 Tvc-14-12: (Brabb, 1960: EB 459B) lower Zem. (RGS), LB.
 Tvc-14-13: (Brabb, 1960: EB 377) Zem., LB.
 Tvc-14-14: (Brabb, 1960: EB 223H) lower Zem. (RGS), LB.

- Tvc-14-15: (Brabb, 1960: EB 223F) lower Zem. (RGS), LB.
 Tvc-14-16: (Brabb, 1960: EB 302) lower Zem. (RGS), LB.
 Tvc-14-17: (Brabb, 1960: EB 280) lower Zem. (RGS), LB.
 Tvc-14-18: (Brabb, 1960: EB 55) Zem., LMB?
 Tvc-14-19: (Brabb, 1960: EB 223C) lower Zem. (RGS), LB.
 Tvc-14-20: (Brabb, 1960: EB 181) Zem., LMB.
 Tvc-14-21: (Brabb, 1960: EB 126) Zem., ARF.
 Tvc-14-22: (Brabb, 1960: EB 186) Zem., ARF, DW.
 Tvc-14-23: (Brabb, 1960: EB 194) Zem., ARF.
 Tvc-14-30: (Brabb, 1960: EB 315) upper Zem., LMB to LB.
 Tvc-14-31: (Brabb, 1960: EB 316) upper Zem., LMB to LB.
 Tvc-14-32: (Brabb, 1960: EB 319) upper Zem., LMB to LB.
 Tvc-14-33: (Kleinpell, 1938: LSJU 1162) lower Zem. (RGS) LB.
 Tvc-14-34: (Kleinpell, 1938: LSJU 364) Zem.? (RGS), LMB.
 Tvc-14-36: (Cummings, 1960: 57-297) upper Zem. to Sauc. (RGS), NED.
 Tvc-14-37: (Cummings, 1960: 57-27) Zem. to lower Sauc. (RGS), NED.
 Tvc-14-38: (Cummings, 1960: 57-1) upper Zem.? (RGS), UMB, OMZ?
 Tvc-14-39: (Cummings, 1960: 56-536) upper Zem. to Sauc. (RGS), LMB.
 Tvc-14-40: (Cummings, 1960: 57-289) upper Zem. to Sauc.? (RGS), UB.
 Tvc-14-41: (Cummings, 1960: 57-227) lower Zem.? (RGS), NED.
 Tvc-14-42: (Cummings, 1960: 57-426) Zem. (RGS), NED.
 Tvc-14-43: (Cummings, 1960: 57-318) Zem. to lower Sauc., UB.
 Tvc-14-47: (McCollom, 1959: EB 267) Zem.?, ARF, possibly LMB.
 Tvc-14-48: (McCollom, 1959: F5) age indeterminate, NED, possibly LB.
 Tvc-14-49: (Barrow, 1980) upper Zem.? (RGS), UB to UMB.
 Tvc-14-50: (Leon, 1958: 39) Zem. (RGS), MB.
 Tvc-15-1: (Fairchild and others, 1969: B-4369) upper Zem.? (RGS), LMB.
 Tvc-15-2: (Fairchild and others, 1969: B-4378) lower Zem., LB.
 Tvc-15-3: (Fairchild and others, 1969: B-4379) upper Zem., MB to LB.
 Tvc-15-4: (Fairchild and others, 1969: B-4380) upper Zem., LMB to LB.
 Tvc-15-5: (Fairchild and others, 1969: B-4381) upper Zem., LB.
 Tvc-15-6: (Fairchild and others, 1969: B-4382) upper Zem., LMB to LB.
 Tvc-15-7: (Fairchild and others, 1969: B-4383) upper Zem., LMB.
 Tvc-15-8: (K. A. McDougall, unpublished data, 1979: MF 4683) lower Zem., LMB.
 Tvc-15-9: (K. A. McDougall, unpublished data, 1979: MF 4681) upper Zem., LB.
 Tvc-15-10: (K. A. McDougall, unpublished data, 1979: MF 4679) upper Zem., LMB to LB.
 Tvc-15-11: (K. A. McDougall, unpublished data, 1979: MF 4677) upper Zem., LMB, near UMB-LMB boundary, OMZ?
 Tvc-15-12: (K. A. McDougall, unpublished data, 1979: MF 4682) lower Zem., LB. OMZ?
 Tvc-15-13: (Brabb, 1960: EB 423C) lower Zem.? (RGS), LB.
 Tvc-15-14: (Brabb, 1960: EB 424C) lower Zem. (RGS), LMB.
 Tvc-15-15: (Brabb, 1960: EB 427B) lower Zem. (RGS), LB?
 Tvc-15-16: (Brabb, 1960: EB 427C) lower Zem. (RGS), LB.
 Tvc-15-17: (Brabb, 1960: EB 428B) lower Zem. (RGS), LB.
 Tvc-15-18: (Brabb, 1960: EB 368B) lower Zem.? (RGS), LB?
 Tvc-15-21: (Kleinpell, 1938: LSJU 1744) Sauc. (RGS), LMB.
 Tvc-15-29: (McCollom, 1959: LSJU M-1 and LF 157A) lower Sauc.?, LMB.
 Tvc-15-30: (Burchfiel, 1958: LSJU M-2 and LF 163A) lower Zem., LMB.
 Tvc-15-40: (Kleinpell, 1938: LSJU 987) lower Zem. (RGS), LB.
 Tvc-15-41: (Kleinpell, 1938: LSJU 1102) lower Zem. (RGS), LB.
 Tvc-15-44: (Travers, 1959: WT 54) lower Zem.? (RGS), LB.
 Tvc-15-45: (Travers, 1959: WT 52) lower Zem.? (RGS), LB.
 Tvc-15-46: (Travers, 1959: WT 49) Zem.? (RGS), ARF.
 Tvc-15-47: (Travers, 1959: WT 44) upper Zem., LB.
 Tvc-15-48: (Travers, 1959: WT 43) upper Zem., LMB.

- Tvc-15-49: (Travers, 1959: WT 35) Zem.? (RGS), NED.
 Tvc-15-50: (Travers, 1959: WT 30) upper Zem., LB.
 Tvc-15-51: (Travers, 1959: WT 29) upper Zem., MB.
 Tvc-15-52: (Travers, 1959: WT 26) upper Zem., UMB.
 Tvc-15-53: (Travers, 1959: WT 25) upper Zem., UMB.
 Tvc-15-54: (Travers, 1959: WT 24) Zem.? (RGS), NED.
 Tvc-15-55: (McCollom, 1959: RM 2) Zem.-Sauc. boundary (RGS), UMB?
 Tvc-15-56: (McCollom, 1959: RM 5) lower Zem., NED, possibly UB.
 Tvc-15-57: (McCollom, 1959: RM 6) lower Zem., LMB to LB.
 Tvc-15-58: (McCollom, 1959: RM 7) lower Zem., LB?
 Tvc-15-59: (McCollom, 1959: RM 8) lower Zem., LMB to LB.
 Tvc-15-60: (McCollom, 1959: RM 9) lower Zem., LB?
 Tvc-15-61: (McCollom, 1959: RM 10) upper Zem. (RGS), MB.
 Tvc-15-62: (McCollom, 1959: RM 11) Zem., NED, possibly LB.
 Tvc-15-63: (McCollom, 1959: RM 12) Zem., NED, possibly LB.
 Tvc-15-64: (McCollom, 1959: RM 13) upper Zem.? (RGS), UMB?
 Tvc-15-65: (McCollom, 1959: RM 14) Zem., MB.
 Tvc-15-66: (Hector, 1976: SH 177) Zem.? (RGS), ARF, LMB to LB?
 Tvc-15-67: (Hector, 1976: SH 317) Zem.? (RGS), ARF.
 Tvc-15-68: (Hector, 1976: SH 342) Zem.? (RGS), ARF, LMB?
 Tvc-15-69: (Hector, 1976: SH 500) Zem.? (RGS), NED.
 Tvc-15-70: (Hector, 1976: SH 708) lower Zem.? (RGS), ARF, DW.
 Tvc-15-71: (Hector, 1976: SH 709) lower Zem.? (RGS), DW.
 Tvc-15-72: (Hector, 1976: SH 713) Zem. (RGS), LMB to LB?
 Tvc-15-73: (Hector, 1976: UO 12) Zem. or younger (RGS), DW.
 Tvc-15-74: (Hector, 1976: UO 15) Zem.? (RGS), ARF.
 Tvc-15-75: (Hector, 1976: UO 34) Zem., possibly upper Zem. (RGS), NED.
 Tvc-15-76: (Hector, 1976: UO 18) Zem. or younger? (RGS), DW.
 Tvc-15-77: (Hector, 1976: UO 196) Zem.? (RGS), ARF.
 Tvc-15-78: (Hector, 1976: UO 218) Zem.? (RGS), NED.
 Tvc-15-79: (Hector, 1976: UO 271) upper Zem.? (RGS), UMB.
 Tvc-15-80: (Hector, 1976: UO 287A) lower Zem., LB?
 Tvc-15-81: (Hector, 1976: UO 287B) lower Zem., NED.
 Tvc-15-82: (Hector, 1976: UO 288) lower Sauc., NED.
 Tvc-15-83: (Hector, 1976: UO 319) lower Miocene, DW.
 Tvc-15-84: (Hector, 1976: UO 700) lower Zem., LB.
 Tvc-16-1: (Brabb, 1960: EB 414) upper Zem. (RGS), LB?
 Tvl-19-1: (Clark, 1966: JC7B) upper Zem., IS.
 Tvl-19-2: (Clark, 1966: JC7C) upper Zem., IS.
 Tvl-19-4: (Clark, 1966: JC60-42) Sauc., NED.
 Tvl-19-5: (Clark, 1966: JC61-2) lower Sauc., UB?
 Tvl-19-6: (Clark, 1966: JC61-14) lower Sauc., NED.
 Tvc-20-1: (Clark, 1966: JC61-7) upper Zem., LMB.
 Tvc-20-2: (Smith, 1971: B-7094) lower Zem., LB.
 Tvc-20-3: (Smith, 1971: B-7093) lower Zem., LB.
 Tvc-20-4: (Smith, 1971: B-7092) lower Zem., LMB.
 Tvc-20-5: (Fairchild and others, 1969: B-4390) lower Sauc., MB?
 Tvc-20-6: (Fairchild and others, 1969: B-4395) lower Zem., LMB.
 Tvc-20-7: (Fairchild and others, 1969: B-4394) lower Zem., LMB.
 Tvc-20-8: (Fairchild and others, 1969: B-4393) lower Zem., LMB.
 Tvc-20-9: (Fairchild and others, 1969: B-4392) lower Zem., LMB.
 Tvc-20-10: (Fairchild and others, 1969: B-4389) Zem.? (RGS), LMB.
 Tvc-20-11: (Fairchild and others, 1969: B-4391) lower Zem., LMB.
 Tvc-20-12: (Brabb, 1960: EB 413) upper Zem. (RGS), LMB.
 Tvc-20-13: (Burford, 1961: ROB 61-13) Zem. (RGS), UMB?

- Tvc-20-14: (Burford, 1961: ROB 1014L and ROB 1014C) lower Zem., NED.
 Tvc-20-15: (Burford, 1961: ROB 61-19) lower Zem., LB.
 Tvc-20-16: (Burford, 1961: ROB 1012) lower Zem., LB.
 Tvc-20-17: (Burford, 1961: ROB 61-12) lower Zem., LB.
 Tvc-20-18: (Burford, 1961: ROB 61-11) Zem. (RGS), LMB?
 Tvc-20-21: (McCullom, 1959: HM 23) upper Zem. (RGS), LB.
 Tvc-20-22: (Melendres, 1958: MM27) upper Zem.? (RGS), ARF.
 Tvc-20-23: (McCullom, 1959: HM 16) upper Zem. (RGS), LMB.
 Tvc-20-24: (Melendres, 1958: MM4) upper Zem. (RGS), LMB.
 Tvc-20-25: (Melendres, 1958: MM28) upper Zem. (RGS), LB?
 Tvc-20-26: (Melendres, 1958: HM 16a) upper Zem.? (RGS), MB.
 Tvc-21-1: (reference withheld by request) lower Zem. (RGS), LB.
 Tvc-26-1: Monterey Oil Co. Porter #2 well, drilled interval 1869-1885 feet. lower Zem.? (RGS), LB.
 Tvc-26-2: Monterey Oil Co. Porter #2 well, drilled interval 2286-2294 feet. lower Zem. (RGS), LB.
 Tvc-26-3: Monterey Oil Co. Porter #2 well, drilled interval 2641-2646 feet. lower Zem. (RGS), LB.
 Tvc-26-4: Monterey Oil Co. Porter #2 well, drilled interval 3545-3560 feet. lower Zem.? (RGS), LB?
 Tmb-5-1: (Touring, 1959: F698) upper Zem. to Sauc. (RGS), UB?
 Tmb-5-2: (Mack, 1959: JM-174m) upper Zem., UMB, OMZ?
 Tmb-6-1: (Mack, 1959: JM-8m) Sauc., MB, OMZ?
 Tmb-6-2: (Mack, 1959: JM-21m) Sauc., DW.
 Tmb-6-3: (Mack, 1959: JM-25m) Sauc., ARF, DW.
 Tmb-6-4: (Mack, 1959: JM-68m) Zem. to Sauc. (RGS), DW.
 Tmb-9-1: (Touring, 1959: F763) Zem. to Sauc. (RGS), UMB.
 Tmb-9-2: (Touring, 1959: F796) Sauc.? (RGS), UB?
 Tmb-9-3: (Jergins YMCA #1 well, drilled interval 1271- 1274 feet. lower Zem.? (RGS), NED.
 Tmb-9-4: Jergins YMCA #1 well, drilled interval 1310- 1350 feet. lower Zem.? (RGS), LMB to LB.
 Tmb-10-1: (Turner, 1970: 28aF5) upper Zem., MB.
 Tmb-10-2: (Turner, 1970: 28bF2) upper Zem., MB.
 Tmb-10-4: (Cummings, 1960: 57-169) upper Zem. to lower Sauc. (RGS), LMB.
 Tmb-10-5: (Cummings, 1960: 56-345) upper Zem. (RGS), LB.
 Tmb-10-6: (Touring, 1959: F774) Zem. (RGS), MB?
 Tla-5-1: (Mack, 1959: JM-370m) Sauc., LB?
 Tla-5-2: (Mack, 1959: JM-383m) Sauc., LB?
 Tla?-6-3: (Poore, unpublished data, 1978: MF 2568) Miocene planktic foram. Zones N7-N12, DW.
 Tla-6-4: (Mack, 1959: RE-76m) upper Zem., LMB.
 Tla-6-5: (Mack, 1959: RE-124m) Zem. to Sauc.? (RGS), NED.
 Tla-6-6: (Mack, 1959: RE-128m) upper Zem., LMB.
 Tla?-6-7: (Mack, 1959: RE-132m) Zem. or younger (RGS), NED.
 Tla-6-8: (Mack, 1959: JM-109m) Sauc., LMB.
 Tla-6-9: (Mack, 1959: JM-115m) Sauc., LMB.
 Tla-6-10: (Mack, 1959: JM-137m) Zem. or younger (RGS), ARF.
 Tla-6-11: (Mack, 1959: JM-159m) Zem. or younger (RGS), ARF.
 Tla-6-12: (Mack, 1959: JM-256m) Zem. (RGS), NED.
 Tla-6-13: (Mack, 1959: JM-280m) Zem. or younger (RGS), NED.
 Tla-6-14: (Mack, 1959: JM-299m) Zem. or younger (RGS), LB.
 Tla-6-15: (Mack, 1959: JM-302m) Zem. to Sauc. (RGS), UMB?
 Tla-6-16: (Mack, 1959: JM-304m) Zem. to Sauc. (RGS), ARF, MB?
 Tla-6-17: (Mack, 1959: JM-324m) upper Zem. to Sauc. (RGS), UMB?
 Tla-6-18: (Mack, 1959: JM-344m) Sauc., LMB.
 Tla-6-19: (Mack, 1959: JM-408m) Sauc., LB.
 Tla-6-20: (Mack, 1959: JM-410m) Sauc., LMB?
 Tla-6-21: (Mack, 1959: RE-36m) age indeterminate, ARF, DW.
 Tla-6-22: (Mack, 1959: RE-38Am) Sauc., MB.
 Tla-6-23: (Mack, 1959: RE-40m) Sauc., LB?
 Tla-6-24: (Mack, 1959: RE-49m) Zem. to Sauc. (RGS), ARF.

- Tla-6-25: (Mack, 1959: RE-273m) Zem. or younger (RGS), NED.
 Tla-6-26: (Mack, 1959: JM-211m) Zem. or younger (RGS), (RGS), ARF, LMB?
 Tla-6-27: (Classen, 1959: 15-59) age indeterminate, NED.
 Tla-9-1: (Touring, 1959: F347M) Zem. or Sauc. (RGS), LMB?
 Tla-9-2: (Touring, 1959: F354) Sauc. (RGS), MB.
 Tla-9-3: (Touring, 1959: F357) Sauc. (RGS), LMB.
 Tla-9-4: (Touring, 1959: F360M) Sauc. (RGS), MB.
 Tla-9-5: (Touring, 1959: F706) Sauc. (RGS), LMB.
 Tla-9-6: (Touring, 1959: F794) Sauc. (RGS), LMB.
 Tla-9-7: (Touring, 1959: F795) Sauc. (RGS), UB?
 Tla-10-1: (Cummings, 1960: 57-203) lower Sauc. (RGS), LB.
 Tla-10-2: (Cummings, 1960: 57-45) upper Zem. to lower Sauc. (RGS), LB.
 Tla-10-3: (Cummings, 1960: 57-44) upper Zem. (RGS), LB.
 Tla-10-4: (Cummings, 1960: 57-43) Zem. to lower Sauc., NED.
 Tla-10-5: (Cummings, 1960: 57-152) Zem. to lower Sauc., NED, OMZ?
 Tla-10-6: (Cummings, 1960: 57-199) Zem. to lower Sauc., NED.
 Tla-10-7: (Cummings, 1960: 57-181) upper Zem. (RGS), UB?
 Tla-10-8: (Cummings, 1960: 57-693) Zem. to Sauc. (RGS), OS?
 Tla-10-9: (Cummings, 1960: 57-692) Zem. to lower Sauc., UB?
 Tla-10-10: (Cummings, 1960: 56-254) Zem. to lower Sauc., ARF.
 Tla-10-11: (Cummings, 1960: 57-188) upper Zem. to Sauc. (RGS), LMB.
 Tla-10-12: (Cummings, 1960: 56-511) Zem. to lower Sauc., DW.
 Tla-10-13: (Cummings, 1960: 57-918) upper Zem. (RGS), UMB, OMZ?
 Tla-10-14: (Cummings, 1960: 57-66) Zem. to lower Sauc., DW.
 Tla-10-15: (Cummings, 1960: 57-48) upper Zem. (RGS), MB, OMZ.
 Tla-10-16: (Cummings, 1960: 56-469) upper Zem. (RGS), UMB, OMZ?
 Tla-10-17: (Cummings, 1960: 56-303) upper Zem. (RGS), UB to UMB, OMZ?
 Tla-10-18: (Cummings, 1960: 57-41) Zem. to lower Sauc., NED.
 Tla-10-19: (Cummings, 1960: 57-206) Zem. to lower Sauc., MB?
 Tla-10-20: (Cummings, 1960: 57-69) Sauc.? (RGS), LMB to LB. Sauc.? (RGS), LMB to LB
 Tla-10-21: (Cummings, 1960: 57-71) lower Zem. (RGS), LB.
 Tla-10-23: (Cummings, 1960: 57-207) upper Zem. (RGS), UMB.
 Tla-10-24: (Cummings, 1960: 57-31b) upper Zem. to lower Sauc. (RGS), LMB.
 Tla-10-25: (Cummings, 1960: 57-31c) upper Zem. to lower Sauc. (RGS), LMB?, OMZ?
 Tla-10-26: (Cummings, 1960: 57-219) Zem. (RGS), UB?
 Tla-10-27: (Cummings, 1960: 57-221) Zem. (RGS), UB?
 Tla-10-28: (Cummings, 1960: 56-462) upper Zem. (RGS), LMB, OMZ?
 Tla-10-29: (Cummings, 1960: 57-50) Zem. to lower Sauc. (RGS), UMB to UB, OMZ.
 Tla-10-30: (Cummings, 1960: 57-58) lower Zem. (RGS), UMB?
 Tla-10-31: (Cummings, 1960: 57-647) upper Zem.? (RGS), UMB.
 Tla-10-32: (Cummings, 1960: 57-902) upper Zem.-Sauc. boundary (RGS), UB.
 Tla-10-33: (Cummings, 1960: 57-78a) upper Zem. (RGS), MB?
 Tla-10-34: (Cummings, 1960: 57-79) upper Zem.? (RGS), UB, OMZ?
 Tla-10-35: (Cummings, 1960: 57-79c) upper Zem. to Sauc. (RGS), LMB?
 Tla-10-36: (Cummings, 1960: 57-79b) upper Zem. (RGS), UB.
 Tla-10-37: (Cummings, 1960: 57-79a) upper Zem.? (RGS), NED.
 Tla-10-38: (Cummings, 1960: 57-861) Zem. to lower Sauc., NED.
 Tla-10-39: (Cummings, 1960: 56-300) lower Sauc. (RGS), UB to UMB, OMZ?
 Tla-10-40: (Cummings, 1960: 56-293) upper Zem. (RGS), UMB, OMZ?
 Tla-10-41: (Cummings, 1960: 56-250) Zem. to lower Sauc. (RGS), ARF.
 Tla-10-42: (Cummings, 1960: 56-328) Zem. to lower Sauc., ARF.
 Tla-10-43: (Cummings, 1960: 57-167) upper Zem.? (RGS), MB.
 Tla-10-44: (Cummings, 1960: 57-168) Zem. to lower Sauc., NED.
 Tla-10-45: (Cummings, 1960: 57-170) Zem. to lower Sauc., (RGS), MB.
 Tla-10-46: (Cummings, 1960: 57-924) lower Zem. (RGS), LMB?

- Tla-10-47: (Cummings, 1960: 57-926) Zem. to lower Sauc., NED.
 Tla-10-48: (Cummings, 1960: 57-664) Zem. (RGS), MB?
 Tla-10-49: (Cummings, 1960: 56-357) upper Zem.? (RGS), UMB.
 Tla-10-50: (Cummings, 1960: 57-115) Zem.? (RGS), UB?
 Tla-10-51: (Cummings, 1960: 57-114) Zem.? (RGS), UB, OMZ?
 Tla-10-52: (Cummings, 1960: 57-110) Sauc.? (RGS), UB.
 Tla-10-53: (Cummings, 1960: 57-666) upper Zem. (RGS), MB?
 Tla-10-56: (Cummings, 1960: 57-335) Zem. to Sauc. (RGS), UB, OMZ?
 Tla-10-58: (McCollom, 1959: 6H) upper Zem. (RGS), LMB.
 Tla-10-59: (McCollom, 1959: 6G) upper Zem. (RGS), LMB.
 Tla-10-60: (McCollom, 1959: 6E) upper Zem. (RGS), UMB, OMZ?
 Tla-10-61: (McCollom, 1959: 5) upper Zem. (RGS), LMB.
 Tla-10-62: (McCollom, 1959: 4B) Zem. (RGS), MB.
 Tla-10-63: (McCollom, 1959: RM 15) upper Zem., NED. possibly LB.
 Tla-10-64: (McCollom, 1959: RM 16) upper Zem., NED, possibly LB.
 Tla?-10-65: (Cummings, 1960: 57-916) upper Zem. (RGS), LB.
 Tla?-10-66: (Cummings, 1960: 56-489) Zem. to lower Sauc., NED, OMZ?
 Tla-10-500: (Cummings, 1960: 57-730) Zem. to lower Sauc., NED.
 Tla-11-1: (Cummings, 1960: 56-500) upper Zem.? (RGS), LB, OMZ.
 Tla-11-2: (Cummings, 1960: 56-494) Zem. to lower Sauc., NED, possibly OMZ.
 Tla-14-1: (Fairchild and others, 1969: B-4373) lower Sauc., UMB?
 Tla-14-2: (Fairchild and others, 1969: B-2311) lower Sauc., LMB.
 Tla-14-3: (Fairchild and others, 1969: B-4372) lower Sauc., LB.
 Tla-14-4: (Fairchild and others, 1969: B-2310) upper Zem., LB.
 Tla-14-5: (Fairchild and others, 1969: B-2309) upper Zem., LMB.
 Tla-14-6: (Fairchild and others, 1969: B-4371) Zem.-Sauc. boundary (RGS), LMB.
 Tla-14-7: (Fairchild and others, 1969: B-2308) lower Zem., UMB?
 Tla-14-8: (Cummings, 1960: 57-173) Sauc.? (RGS), MB?
 Tla-14-9: (Cummings, 1960: 57-471) Zem.-Sauc. boundary (RGS), LMB.
 Tla-14-10: (Cummings, 1960: 57-2) upper Zem. to Sauc. (RGS), MB.
 Tla-14-11: (Cummings, 1960: 57-276) upper Zem. (RGS), NED, OMZ?
 Tla-14-13: (Cummings, 1960: 57-322) Zem.? (RGS), UB.
 Tla-14-14: (Leon, 1958: 36) upper Zem.? (RGS), NED.
 Tla-15-1: (K. A. McDougall, unpublished data, 1979: MF 4671) lower Sauc., UMB?
 Tla-15-2: (Travers, 1959: WT 38) upper Zem., UMB.
 Tla-15-3: (McCollom, 1959: RM 3) upper Zem., UMB?
 Tla-15-4: (McCollom, 1959: RM4) upper Zem., UMB?
 Tla-15-5: (Hector, 1976: SH 53) upper Zem. to Sauc.? (RGS), LMB.
 Tla-15-6: (Hector, 1976: SH 276) upper Zem. to Sauc.? (RGS), ARF, LB?
 Tla-15-7: (Hector, 1976: SH 307) upper Zem. to Sauc.? (RGS), ARF, LMB to LB?
 Tla-15-8: (Hector, 1976: SH 367) upper Zem. to Sauc.? (RGS), ARF.
 Tla-15-9: (Hector, 1976: UO 51A) lower Miocene, DW.
 Tla-15-10: (Hector, 1976: UO 51B) upper Zem., DW.
 Tla-15-11: (Hector, 1976: UO 275A) upper Zem. to Sauc., MB.
 Tla-15-12: (Hector, 1976: UO 305A) Sauc., ARF.
 Tla-15-13: (Hector, 1976: UO 305B) Sauc., ARF.
 Tla-15-14: (Hector, 1976: UO 305C) Sauc., ARF.
 Tla-15-15: (Hector, 1976: UO 306) lower Miocene, DW.
 Tla-15-16: (Hector, 1976: UO 310) lower Miocene, DW.
 Tla-15-17: (Hector, 1976: UO 701) upper Zem., DW.
 Tla-15-18: (Hector, 1976: UO 702) upper Zem., DW.
 Tla-20-1: (Clark, 1966: JC61-4) Sauc.?, NED.
 Tla-20-2: (Clark, 1966: JC61-5) Sauc., UB.
 Tla-20-3: (Clark, 1966: JC61-6) Sauc., UB.
 Tla-20-4: (Fairchild and others, 1969: B-4396; Clark, 1966: JC61-6) lower to middle Sauc., MB?

- Tla-20-5: (Burford, 1961: ROB 60-1) lower Sauc.? (RGS), UMB.
 Tla-20-6: (Burford, 1961: ROB 61-33, ROB 61-34, ROB 61-35) upper Zem. to lower Sauc.?, MB?
 Tla?-20-7: (reference withheld by request) Sauc.? (RGS), UMB, OMZ.
 Tlo-19-5: (Clark, 1966: JC62-17) Rel., UB, shelf edge.
 Tlo-19-6: (Clark, 1966: JC62-18) Rel., OS?
 Tlo-23-6: (Clark, 1966: JC62-23) Rel., NED.
 Tm-5-1: (Poore, unpublished data, 1978: MF 2557) Rel. to Luis., DW.
 Tm-5-2: (Classen, 1959: 4-58) Luis., UB.
 Tm-5-3: (Classen, 1959: 10-58) Luis.?, DW.
 Tm-10-1: (Cummings, 1960: 56-390) Rel. (RGS), MB.
 Tm-10-2: (Cummings, 1960: 56-271) Rel. (RGS), MB.
 Tm-10-3: (Cummings, 1960: 56-343) Rel. (RGS), MB.
 Tm-10-4: (Cummings, 1960: 57-700) Rel. (RGS), MB.
 Tm-10-6: (Cummings, 1960: 56-423) Rel. (RGS), MB.
 Tm-10-7: (Cummings, 1960: 57-202) Rel.? (RGS), NED.
 Tm-10-8: (Cummings, 1960: 57-30) Rel. (RGS), MB.
 Tm-10-9: (Cummings, 1960: 57-31a) Rel. or Luis., UMB.
 Tm-14-1: (Cummings, 1960: 57-5) Rel. or Luis., NED.
 Tm-14-2: (Cummings, 1960: 57-486) Rel. or Luis., NED.
 Tm-14-3: (Cummings, 1960: 57-392) Rel. (RGS), MB.
 Tm-14-4: (Cummings, 1960: 57-484) Rel. or Luis., UB, OMZ?
 Tm-14-5: (Cummings, 1960: 57-255) Rel. or Luis., NED.
 Tm-18-4: (Clark, 1966: JC62-15) Rel., UB.
 Tm-19-1: (Clark, 1966: JC25, JC61-1) Rel., UMB.
 Tm-19-2: (Clark, 1966: JC60-2) Rel., UB, shelf edge.
 Tm-19-3: (Clark, 1966: JC60-19) Luis., UB, shelf edge.
 Tm-19-4: (Clark, 1966: JC60-22) Rel., UB.
 Tm-19-5: (Clark, 1966: JC60-30) Luis., UB?, shelf edge?
 Tm-19-6: (Clark, 1966: JC60-49) Rel., IS.
 Tm-19-7: (Clark, 1966: JC60-62) Luis., UB.
 Tm-19-8: (Clark, 1966: JC60-69) Rel., UMB.
 Tm-19-9: (Clark, 1966: JC60-109) Rel., UB.
 Tm-19-10: (Clark, 1966: JC61-32) Rel. or Luis.? (RGS), UB?
 Tm-19-11: (Clark, 1966: JC62-9) Luis., OS.
 Tm-19-12: (Clark, 1966: JC62-12) Luis., OS to UB?
 Tm-19-13: (Brabb, 1960: EB 439) Luis., UB?
 Tm-19-14: (Brabb, 1960: EB 437) Luis., UB?
 Tm-19-15: (Brabb, 1960: EB 435C) Luis., UB?
 Tm-19-16: (Brabb, 1960: EB 435H) Luis., UB?
 Tm-19-17: (Brabb, 1960: EB 432) Luis., UB?
 Tm-19-18: (Brabb, 1960: EB 440) Luis., UB?
 Tm-19-19: (Brabb, 1960: EB 123) Luis., UB, OMZ?
 Tm-19-20: (Kleinpell, 1938: LSJU 367) upper Rel. or Luis. (RGS), UB?
 Tm-19-21: (Kleinpell, 1938: LSJU 367A) Luis. (RGS), NED.
 Tm-19-22: (Travers, 1959: WT 13) Rel., DW.
 Tm-19-23: (Travers, 1959: WT 75) possibly Rel., UB.
 Tm-19-24: (Travers, 1959: WT 74) Rel., UB, shelf edge.
 Tm-19-25: (Travers, 1959: WT 73) Rel., UB, shelf edge.
 Tsc-19-1: (Clark, 1981: Mf 2187) Del., UB.

APPENDIX 2

PALEONTOLOGIC DATA FROM THE NORTHERN GABILAN RANGE

Listed below are the inferred ages and paleodepths for 10 faunal lists compiled from reports and well files on the San Juan Bautista Formation of the San Juan Bautista Quadrangle in the northern Gabilan Range. The organization and abbreviations used below are the same as for Appendix 1.

- Tsj-30-1: (Waters, 1968: D-515)
Pen. or Ulat., NED, possibly LB.
- Tsj-30-2: (Nilsen, unpublished data, 1983: MF 2549)
Ulat., Eocene planktic foram. Zones P10-P11, LMB.
- Tsj-30-3: (Nilsen, unpublished data, 1983: MF 2550)
Ulat., MB.
- Tsj-30-4: (Nilsen, unpublished data, 1983: MF 2551)
lower Nar., Eocene planktic foram. Zone P11, LMB.
- Tsj-30-5: (Nilsen, unpublished data, 1983: MF 2552)
upper Nar., LMB?, OMZ?
- Tsj-30-6: (Nilsen, unpublished data, 1983: MF 2553)
upper Nar., LMB, OMZ?
- Tsj-30-8: (Nilsen, unpublished data, 1983: MF 2555)
upper Nar., LB, OMZ?
- Tsj-30-9: (Nilsen, unpublished data, 1983: MF 2556)
upper Nar., LB, OMZ?
- Tsj?-30-17: Occidental Bingaman #1 well, drilled
interval 3635-4543 feet: upper Ref. (RGS), LMB to LB.
- Tsj?-30-18: Occidental Bingaman #1 well, drilled
interval 6040-7130 feet: Nar. (RGS), LMB to LB?

APPENDIX 3

THICKNESS ESTIMATES FROM OUTCROPS AND CROSS-SECTIONS

The estimates of stratigraphic thickness tabulated below were compiled from over 25 published and unpublished reports and from my own field work. The list is not exhaustive, but includes only those data useful in constructing the thickness maps and other diagrams in this report. Most of the thicknesses were originally measured in feet, often only to the nearest 100 feet. I've converted these to meters without further rounding; this may give a false impression of precision, but avoids the problem of over-rounding. Formation abbreviations are given in Table 2.

Notes:

- (A) Estimated by me from stratigraphic column or cross-section.
- (B) Estimated by me from map.
- (C) The "Middle San Lorenzo Sandstone" of Smith (1971) is here included as part of the Rices Mudstone.
- (D) Thickness of combined Vaqueros Sandstone and Zayante Sandstone interval.
- (E) Thickness includes some of the lower Aromas Sand.

THICKNESS ESTIMATES FROM OUTCROPS

LOCATION	STRATIGRAPHIC INTERVAL	STRATIGRAPHIC THICKNESS (meters)	REFERENCE (if any)
Jamison Rd., 15-9S-3W	T1	244+	Brabb, 1960, p.15
Tuck's Creek, 17-9S-3W	T1	82+	Brabb, 1960, p.15
Smith Grade - Empire Grade area	T1	270+	Clark, 1981, p.8
Smith Grade - Empire Grade area	T1	305+	Clark, 1966, p.20
Sky Londa - La Honda Cr. area	Tb	3048+	Touring, 1959, p.32
Big Basin quad. (composite)	Tb	2743	Brabb, 1960, p.31
Butano Ridge	Tb	1829+	Brabb, 1960, p.31
Jamison Road	Tb	914+	Brabb, 1960, p.31
northern Felton and Laurel quads.	Tb	2730+	Clark, 1981, p.11
northern Felton and Laurel quads.	Tb	3658+	Beaulieu, 1970 p.129
La Honda Cr. 36-6S-4W	Tst	110	Cummings, 1960, pl.5 (A)
La Honda Cr. 35-6S-4W	Tst	170-220	Brabb, 1980 (B)
La Honda quad.	Tst	240	Brabb, 1980
Langley Hill area 1,2, 13-7S-4W	Tst	190	Cummings, 1960, pl.5 (A)
Little Boulder Cr. 21,22,28-8S-2W	Tst	229	Brabb, 1960, p.29

LOCATION	STRATIGRAPHIC INTERVAL	STRATIGRAPHIC THICKNESS (meters)	REFERENCE (if any)
Little Boulder Cr. 21,22,28-8S-2W	Tst	198	Brabb, 1960, p.40
San Lorenzo R. 1-9S-3W	Tst	260	Brabb and others, 1977, p.30-31 (A)
San Lorenzo R. 1-9S-3W	Tst	229	Brabb, 1964, p.671
San Lorenzo R. 1-9S-3W	Tst	223	Sullivan, 1962, p.247
Kings Cr. 31-8S-2W	Tst	241	Brabb, 1960, p.40
Bear Cr.	Tst	198	Brabb, 1960, p.40
Bear Cr. 3-9S-2W	Tst	172	Brabb and others, 1977, p.56 (A)
Bear Cr. area 4?-9S-2W	Tst	244-275	Hector, 1976, p.34
Newell Cr. 27?-9S-2W	Tst	183	Travers, 1959, p.12
Newell Cr. 27-9S-2W	Tst	193	Brabb, 1960, p.40
Newell Cr. 27-9S-2W	Tst	60	Clark, 1981, p.13
Laurel area	Tst	107	Burford, 1961, pl.7 (A)
Soquel Cr.	Tst	122+	Smith, 1971, p.9
Little Boulder Cr. 22-8S-2W	Tsr	85+	Brabb, 1960, p.29
San Lorenzo R. 1, 12-9S-3W	Tsr	296+	Brabb, 1960, p.47
San Lorenzo R. 1, 12-9S-3W	Tsr	435	Sullivan, 1962, p.248

LOCATION	STRATIGRAPHIC INTERVAL	STRATIGRAPHIC THICKNESS (meters)	REFERENCE (if any)
Kings Cr. 31-8S-2W, and 6-9S-2W	Tsr	314	Brabb, 1960, p.45
upper Zayante Cr. 18-9S-1W	Tsr	309	Brabb and others, 1977, p.65 (A)
Castle Rock Ridge quad.	Tsr	457-549	Hector, 1976, p.36
Bear Cr. 3, 10-9S-2W	Tsr	518	Brabb, 1960, p.47
Bear Cr. 3, 10-9S-2W	Tsr	482	Brabb and others, 1977, p.55-56 (A)
Twobar Cr. 18-9S-2W	Tsr	98+	Brabb, 1960, p.62
Newell Cr. 27-9S-2W	Tsr	275	Clark, 1981, p.13
Newell Cr. 27-9S-2W	Tsr	259	Travers, 1959, p.13
Love Cr. 29-9S-2W	Tsr	240+	Clark, 1981, p.13
Laurel quad.	Tsr	533	Burford, 1961, pl.4 (A)
Soquel Cr.	Tsr	671	Smith, 1971, p.9-10 (C)
Woodside quad.	Tvw	671+	Esser, 1958
Half Moon Bay quad.	Tvw	762+	Classen, 1959 (A)
Corte Madera Cr. 16-7S-3W	Tv	152	Cummings, 1960, p.71
Peters Cr. 28-7S-3W	Tv	270-380	Cummings, 1960, pl.5 (A)

LOCATION	STRATIGRAPHIC INTERVAL	STRATIGRAPHIC THICKNESS (meters)	REFERENCE (if any)
Slate Cr. area 9, 16-8S-3W	Tv	330	Cummings, 1960, pl.5 (A)
Skyline Blvd. 36-7S-3W	Tv	276+	McCollom, 1959, p.12
Skyline Blvd.	Tv	292	Brabb, 1970 (B)
Skyline Blvd. 36-7S-3W, 1-8S-3W	Tv	483	Dibblee, 1966 (A)
Long Ridge 34-7S-3W	Tv	335	Cummings, 1960, p.71
Table Mt. 31-7S-2W	Tv	805+	Dibblee, 1966 (A)
Table Mt. 36-7S-3W	Tv	380	Cummings, 1960, pl.5 (A)
Saratoga Gap	Tv	732	Cummings and others, 1962,p.189
Saratoga Gap 8-8S-2W	Tv	760	Cummings, 1960, pl.5 (A)
Saratoga Gap 5, 8-8S-2W	Tv	1219	Dibblee, 1966 (A)
Oil Cr. 10-8S-3W	Tv	354	Dibblee, 1966, (A)
Oil Cr. 12-8S-3W	Tv	724	Dibblee, 1966, (A)
Waterman Cr. 14, 15-8S-3W	Tv	335	Cummings, 1960, p.71
Waterman Cr. 10, 11, 14, 15-8S-3W	Tv	300	Cummings, 1960, pl.5 (A)
San Lorenzo R. 24-8S-3W	Tv	457	Cummings, 1960, p.71

LOCATION	STRATIGRAPHIC INTERVAL	STRATIGRAPHIC THICKNESS (meters)	REFERENCE (if any)
upper Zayante Cr. 19-9S-1W	Tv	1072	Brabb and others, 1977, p.63-65
upper Zayante Cr. 19-9S-1W	Tv	920	Clark, 1981, p.15
lower Zayante Cr.	Tv	515	Brabb and others, 1977, p.68
lower Zayante Cr. 30-9S-1W	Tv	350-440	Clark, 1981, p.15
Kings Cr. 6-9S-2W	Tvc	284+	Burchfiel, 1958, p.47-50
Kings Cr. 6-9S-2W	Tvc	357+	Brabb, 1960, p.45
Kings Cr. 6,7-9S-2W	Tvc	373+	Burchfiel, 1958, pl.2 (A)
Twobar Cr. 18, 19-9S-2W	Tv	730+	Brabb, 1960, p.62
Twobar Cr. 18, 19-9S-2W	Tvc	364+	Brabb, 1960, p.62 (A)
Twobar Cr. 18, 19-9S-2W	Tv1	366+	Brabb, 1960, p.62 (A)
Twobar Cr. 8-9S-2W	Tv	675+	Burchfiel, 1958, pl.2 (A)
Twobar Cr. 8-9S-2W	Tv	680+	McCollom, 1959, p.18
Twobar Cr. 5,8-9S-2W	Tv	762+	Burchfiel, 1958, pl.4 (A)
Bear Cr. 9, 16-9S-2W	Tv	839+	Burchfiel, 1958, p.51-55
Bear Cr. 9, 10-9S-2W	Tv	717+	Brabb and others, 1977, p.54-55 (A)

LOCATION	STRATIGRAPHIC INTERVAL	STRATIGRAPHIC THICKNESS (meters)	REFERENCE (if any)
Bear Cr. 16,20,21-9S-2W	Tv	1372+	Burchfiel, 1958, p.11
Union Cr. 4-9S-3W	Tvc	175+	McCollom, 1959, p.8
Kelly Cr. 7-9S-3W	Tv	244+	McCollom, 1959, p.10
Blooms Cr. 9, 10-9S-3W	Tvc	274+	McCollom, 1959, p.6
Mt.Charlie - Glenwood area	Tv	823	Clark, 1966, p.58
Inspiration Point 28-9S-1W	Tv	953	McCollom, 1959, p.24
Laurel quad., Glenwood Basin area	Tv	762+	Burford, 1961, pl.4 (A)
Soquel Cr.	Tv(D)	974	(RGS field work)
Hinckley Cr.	Tv(D)	853?	Dibblee and others, 1978 (B)
lower Zayante Cr. 30,31-9S-1W	Tz	500+	Clark, 1981, p.14
lower Zayante Cr. 30,31-9S-1W	Tz	384+	(RGS field work)
Lompico Creek 26,35-9S-2W	Tz	550	Clark, 1981, p.14
Soquel Cr.	Tz	90	(RGS field work)
Half Moon Bay area	Tmb	366+	Classen, 1959, (A)
Langley and Mindego Hills area	Tmb	1524	Cummings, 1960, p.95
Langley and Mindego Hills area	Tmb	1829	Beaulieu, 1970, p.144

LOCATION	STRATIGRAPHIC INTERVAL	STRATIGRAPHIC THICKNESS (meters)	REFERENCE (if any)
La Honda Cr. 11, 14-7S-3W	Tmb	610+	Cummings, 1960, p.95
Peters Cr. 28?-7S-3W	Tmb	329+	Cummings, 1960, p.95
Tarwater Cr. 31-7S-3W	Tmb	850+	Cummings, 1960, pl.5 (A)
Table Mt. area 36-7S-3W	Tmb	350+	Cummings, 1960, pl.5 (A)
Slate and Oil Crs.	Tmb	610+	Cummings and others, 1962, p.193
Saratoga Gap 5,8-8S-2W	Tmb	150	Cummings, 1960, pl.5 (A)
Saratoga Gap 5-8S-2W	Tmb	129	Dibblee, 1966 (A)
Oak Ridge 26,27-8S-2W	Tmb	152	Hector, 1976, p.52
Castle Rock Park 18?-8S-2W	Tmb	91	Hector, 1976, p.52
Waterman Cr. 10, 11, 14, 15-8S-3W	Tmb	50	Cummings, 1960, pl.5 (A)
lower Zayante Cr. 30-9S-1W	Tmb	60	Clark, 1981, p.15
Woodside quad.	Tla	457+	Esser, 1958, p.32
Purisima and Harkins Crs.	Tla	457+	Mack, 1959, p.43
Lambert and Peters Crs., 27,28,33-7S-3W	Tla	1463	Dibblee, 1966
Peters Cr. 28-7S-3W	Tla	600	Cummings, 1960, pl.5 (A)

LOCATION	STRATIGRAPHIC INTERVAL	STRATIGRAPHIC THICKNESS (meters)	REFERENCE (if any)
Table Mt. area 36-7S-3W	T1a	870+	Cummings, 1960, pl.5 (A)
Slate Cr. area 3-8S-3W	T1a	792+	Cummings, 1960, p.111
Saratoga Gap 12-8S-3W	T1a	644+	Dibblee, 1966 (A)
Saratoga Gap 5,8-8S-2W	T1a	540+	Cummings, 1960, pl.5
Waterman Cr. 10, 11, 14, 15-8S-3W	T1a	220+	Cummings, 1960, pl.5
Kings Cr. 19-8S-2W	T1a	457-488+	Hector, 1976, p.45
McDonald Ridge 19,29,30-8S-2W	T1a	488+	Hector, 1976, p.46
Deer Cr. 28,29?-8S-2W	T1a	244+	Hector, 1976, p.48
Newell Cr. 24-9S-2W	T1a	152+	Travers, 1959, p.24
upper Zayante Cr. 19-9S-1W	T1a	397+	Brabb and others, p.62-63 (A)
lower Zayante Cr. 30-9S-1W	T1a	196+	Brabb and others, p.68 (A)
lower Zayante Cr. 30-9S-1W	T1a	185+	Clark, 1981, p.16
Mt. Charlie Gulch 29-9S-1W	T1a	450+	Clark, 1981, p.16
Laurel quad.	T1a	274+	Burford, 1961, p.12
Soquel Cr.	T1a	396+	(RGS field work)
Half Moon Bay quad.	T1o	91?	Classen, 1959 (A)

LOCATION	STRATIGRAPHIC INTERVAL	STRATIGRAPHIC THICKNESS (meters)	REFERENCE (if any)
San Lorenzo R. 32-9S-2W	Tlo	60	Brabb, 1960, p.73
Ben Lomond	Tlo	100	Clark, 1981, p.18
Lompico Cr.	Tlo	150	Clark, 1981, p.18
Zayante Cr.	Tlo	150	Clark, 1981, p.18
Newell Cr.	Tlo	150	Clark, 1981, p.18
Majors Cr.	Tlo	240	Clark, 1981, p.18
San Vicente Cr. 34-10S-3W	Tlo	135?	Clark, 1981, p.18
Vine Hill Rd. 16-10S-1W	Tlo	76+	Clark, 1966, p.95
Half Moon Bay quad.	Tm	914+	Classen, 1959 (A)
La Honda area 13-7S-4W	Tm	152+	Touring, 1959, p.78
Woodhams Cr.	Tm	152+	Cummings and others, 1962, p.195
Langley Hill 7, 18?-7S-3W	Tm	549+	Cummings, 1960, p.123
Mindogo Hill quad.	Tm	610+	Dibblee, 1966
Peters Cr.	Tm	549+	Cummings, 1960, p.123
Peters Cr. 5,6,7,8-8S-3W	Tm	160+	Cummings, 1960, pl.5 (A)
Peters Cr.	Tm	457+	Cummings and others, 1962,p.195
Slate Cr. 5,6,7,8-8S-3W	Tm	220+	Cummings, 1960, pl.5 (A)

LOCATION	STRATIGRAPHIC INTERVAL	STRATIGRAPHIC THICKNESS (meters)	REFERENCE (if any)
Slate Cr. 9-8S-3W	Tm	122+	(RGS field work)
Waterman Cr. 10, 11, 14, 15-8S-3W	Tm	430+	Cummings, 1960, pl.5 (A)
Zayante and Lompico Cr.	Tm	825+	Clark and others, 1979,p.7
Newell Cr. 34-9S-2W and 3-10S-2W	Tm	1036+	Brabb, 1960, p.73
Laguna Cr.	Tm	370+	Clark, 1981, p.21
Santa Cruz - Scotts Valley area	Tsm	130+	Phillips, 1981, p.50
near Riverside Grove 11?-9S-3W	Tsc	76+	Brabb, 1960, p.75
Zayante Cr. area 3-10S-2W	Tsc	74+	Clark, 1981, p.31
well: Texaco Poletti #1	Tsc	2700+	Clark, 1981, p.31
Santa Cruz 15,22,23-11S-2W	Tsc	140+	Clark, 1981, p.30
Scotts Valley area	Tsc	61+	Clark and others, 1979, p.10 (A)
Woodside quad.	Tp	610+	Beaulieu, 1970, p.159
Half Moon Bay area	Tp	2438+	Musser and Murray-Aaron, 1962, p.274
La Honda quad.	Tp	1722	Touring, 1959, p.119
Scotts Valley area	Tp	61-152+	Clark, 1966, p.140

LOCATION	STRATIGRAPHIC INTERVAL	STRATIGRAPHIC THICKNESS (meters)	REFERENCE (if any)
Laurel quad.	Tp	823+	Burford, 1961, p.17
northern Monterey Bay coastline	Tp	350 (E)	Stuart and others, 1982
La Honda area	R-S	2900+	Cummings, 1960, pl.5 (A)
Langley Hill area	R-S	2760+	Cummings, 1960, pl.5 (A)
Mindego Hill area	R-S	2250+	Dibblee, 1966 (A)
Peters Cr. area	R-S	2030+	Cummings, 1960, pl.5 (A)
Alpine Rd. area	R-S	2575+	Dibblee, 1966 (A)
Saratoga Gap area	R-S	2060+	Cummings, 1960, pl.5 (A)
Bear Cr. area	R-S	1890+	(combined Tsr + Tv)
Zayante Cr. area	R-S	1780+	(combined Tsr + Tv + Tla)
Soquel Cr. area	R-S	2163+	(combined Tsr +Tv + Tz + Tla)
Ben Lomond Mtn.	Ynez.	305+	Clark, 1966, p.20
Lompico area	Pen.	771+	Brabb and others, 1977, p.72 (A)
Lompico area	Ulat.	509	Brabb and others, 1977, p.72 (A)
La Honda basin	Nar.	3100+?	(combined Teb + Tst)
Little Boulder Cr. 22-8S-2W	Ref.	12	Brabb, 1960, p.29
San Lorenzo R. 1, 12-9S-3W	Ref.	69	Sullivan, 1962, p.248

LOCATION	STRATIGRAPHIC INTERVAL	STRATIGRAPHIC THICKNESS (meters)	REFERENCE (if any)
San Lorenzo R. 1, 12-9S-3W	Ref.	67	Brabb, 1964, p.675
San Lorenzo R. 1, 12-9S-3W	Ref.	63	Brabb and others, 1977, p.29-30 (A)
Zayante Cr. 18-9S-1W	Ref.	47	Brabb and others, 1977, p.65 (A)
Kings Cr. 31-8S-2W, and 6-9S-2W	Ref.	61	Brabb, 1960, p.45
Bear Cr. 3, 10-9S-2W	Ref.	137	Brabb, 1960, p.47
Bear Cr. 3, 10-9S-2W	Ref.	108	Brabb and others, 1977, p.55-56 (A)
Soquel Cr.	Ref.	61-76	Smith, 1971, p.9
upper Zayante Cr.	Zem.	1335	Brabb and others, 1977, p.63-65 (A)
upper Zayante Cr.	lower Zem.	457	Brabb and others, 1977, p.64-65 (A)
Kings Cr.	lower Zem.	610+	Brabb, 1960
upper Zayante Cr.	upper Zem.	878	Brabb and others, 1977, p.63-64 (A)
lower Zayante Cr.	upper Zem.	1065?	(combined Tz + Tv)
upper Zayante Cr.	Sauc.	397+	Brabb and others, 1977, p.62 (A)
lower Zayante Cr.	Sauc.	594+	Brabb and others, 1977, p.68 (A)
Mt. Charlie Gulch	Sauc.	513+	Brabb and others, 1977, p.78 (A)
Scotts Valley area	Rel. +Luis.	1180+	(combined Tlo + Tm)

LOCATION	STRATIGRAPHIC INTERVAL	STRATIGRAPHIC THICKNESS (meters)	REFERENCE (if any)
La Honda area	Ynez. to Luis.	7100+	(combined max. thickness of all stages)
Zayante - Scotts Valley area	Ynez. to Luis.	6400+	(combined max. thickness of all stages)
La Honda area	Tertiary	8800+	(best guess)
Zayante - Scotts Valley area	Tertiary	9500+	(best guess)

APPENDIX 4 DATA FROM EXPLORATORY WELLS

The subsurface stratigraphic data in the following table were obtained from the literature and from files on more than 75 wells drilled in the search for oil and gas in the La Honda basin. *Total depths and drilled formation tops are given in feet*, as read directly from electric logs, but *stratigraphic thicknesses are given in meters* to allow direct comparison with the outcrop data in Appendix 3. Stratigraphic thicknesses were calculated using dip data from dipmeter surveys or core descriptions, where such data were available. Formation abbreviations are explained in Table 2:

Notes:

- (A) "Redbeds" are reported from below a drilled depth of 3000 feet in this well (Christensen and Knight, 1964a).
- (B) Formation tops and dip data from Christensen and Knight (1964a).
- (C) Dip data from Christensen and Knight (1964a).
- (D) Thickness of combined Twobar Shale and Rices Mudstone interval.
- (E) Thickness of combined Twobar Shale, Rices Mudstone, and Mindego Basalt interval.
- (F) Cut out by fault?
- (G) Thickness of combined Mindego Basalt and Lambert Shale interval.
- (H) This well spudded in the Santa Cruz Mudstone and encountered Santa Margarita Sandstone at a drilled depth of 3333 feet. The estimated stratigraphic thickness of the Santa Cruz Mudstone is 1000+ m, and of the Santa Margarita Sandstone is 144 m.
- (J) This well encountered "granodiorite" at a drilled depth of 1920 feet (California Division of Oil and Gas, 1964, 1982a).
- (K) The "Tp" interval in this well may also include the following formations: Lompico Sandstone, Monterey Formation, Santa Margarita Sandstone, and Santa Cruz Mudstone.
- (L) Thickness of combined Vaqueros Sandstone and Lambert Shale interval. Dip data from Christensen and Knight (1964b).
- (M) Thickness of combined Vaqueros Sandstone and Zayante Sandstone interval.
- (N) This well encountered "granite" at a drilled depth of 3183 feet.
- (P) The identify of the formations below a drilled depth of 1753 feet is unknown, and could conceivably include the Butano Sandstone, Vaqueros Sandstone, or other units composed of interbedded sandstone and mudstone.

DATA FROM EXPLORATORY WELLS

LOCATION
(SECTION,
TOWNSHIP
RANGE)
TOTAL
DEPTH
(FEET)
DRILLED TOP OF FORMATION (FEET), AND
STRATIGRAPHIC THICKNESS OF FORMATION (METERS)

WELL NAME	Teb	Tst	Tsr	Tv	Tmb	Tla	Tm	Tp	R-S	Ref
1. Westates Beffa #1	3545?						0 - (A)			
2. Standard Cafferata and Pimental #1	3250 1381+							0 1374+ (B)		
3. Conoco Bianchi #1	0 1092+ (C)									
4. Wilshire Cowell #3							0	-		
5. Wilshire Cowell #1								0 -		
6. Wilshire Cowell #2								0 -		
7. Neaves Neaves-Leib #1	2050 64+	1789 57	1005 172		0 220+				0 392+	1353 96
8. Texaco C.H. Leib #1	2428 118+		1360 209+ (D)		100 247+			0 31+	100 -	2000 78

WELL NAME	LOCATION (SECTION, TOWNSHIP RANGE)	TOTAL DEPTH (FEET)	DRILLED TOP OF FORMATION (FEET), AND STRATIGRAPHIC THICKNESS OF FORMATION (METERS)									
			Teb	Tst	Tsr	Tv	Tmb	Tla	Tm	Tp	R-S	Ref
9. Union E.L. Moore #1	31-7S-3W	6027	4346 387+	4247 20	3688 138	2962 186	500? 656+		0 132+	500? 980+		
10. Neaves N.T. Ross #1	5-7S-4W	3286	3060 67+	2795 78	1678 335		100 474+		0 30+	100 809+	2369 128	
11. Texaco Ford #1	5-7S-4W	4104	2950 288+	2760 54+	1781 258+		400 365+		0 122+	400 632+	2440 83	
12. Carlsberg Wool #1	9-7S-4W	3400	2900? 98+		1491 352+ (D)	1288 54	0 340+			0 -		
13. Union Guerra #1	11-7S-4W	3551			2380 -	2260	0 -					
14. Richfield Isenberg #1	12-7S-4W	4699	2253 701+				0 687+ (E)			0 576+	1303 -	
15. Neaves N. Stanton #1	16-7S-4W	2657	2440 37+	2070 63+	775 302+				0 223+	775 302+		
16. Neaves N.U.O.L. #1	16-7S-4W	4271	3620 181+	3270 98	2530 201	2290 69	830 315+		0 191+	830 585+		
17. Neaves N.U.O.L. #6	16-7S-4W	3458	3315 40+	3010 92	2145 260	1845 87	1425 126	1215? 64+	0 350+	1215? 538+		

DRILLED TOP OF FORMATION (FEET), AND
STRATIGRAPHIC THICKNESS OF FORMATION (METERS)

LOCATION
(SECTION,
TOWNSHIP
RANGE)

TOTAL
DEPTH
(FEET)

WELL NAME

Ref

R-S

Tp

Tm

Tla

Tmb

Tv

Tsr

Tst

Teb

Tsb

Tsc

Tsd

Tse

Tsf

Tsg

Tsh

Tsi

Tsj

Tsk

Tsl

Tsm

Tsn

Tso

Tsp

Tsq

Tst

Tsu

Tsv

Tsw

Tsx

Tsy

Tsz

Tta

Ttb

Ttc

Ttd

Tte

Ttf

Ttg

Tth

Tti

Ttj

Ttk

Ttl

Ttm

Ttn

Tto

Ttp

Ttq

Tts

Ttu

Ttv

Ttw

Ttx

Tty

Ttz

Tta

Ttb

Ttc

Ttd

Tte

Ttf

Ttg

Tth

Tti

Ttj

Ttk

Ttl

Ttm

Ttn

Tto

Ttp

Ttq

Tts

Ttu

Ttv

Ttw

Ttx

Tty

Ttz

Tta

Ttb

Ttc

Ttd

Tte

Ttf

Ttg

Tth

Tti

Ttj

Ttk

Ttl

Ttm

Ttn

Tto

Ttp

Ttq

Tts

Ttu

Ttv

Ttw

Ttx

Tty

Ttz

Tta

Ttb

Ttc

Ttd

Tte

Ttf

Ttg

Tth

Tti

Ttj

Ttk

Ttl

Ttm

Ttn

Tto

Ttp

Ttq

Tts

Ttu

Ttv

Ttw

Ttx

Tty

Ttz

Tta

Ttb

Ttc

Ttd

Tte

Ttf

Ttg

Tth

Tti

Ttj

Ttk

Ttl

Ttm

Ttn

Tto

Ttp

Ttq

Tts

Ttu

Ttv

Ttw

Ttx

Tty

Ttz

Tta

Ttb

Ttc

Ttd

Tte

Ttf

Ttg

Tth

Tti

Ttj

Ttk

Ttl

Ttm

Ttn

Tto

Ttp

Ttq

Tts

Ttu

Ttv

Ttw

Ttx

Tty

Ttz

Tta

Ttb

Ttc

Ttd

Tte

Ttf

Ttg

Tth

Tti

Ttj

Ttk

Ttl

Ttm

Ttn

Tto

Ttp

Ttq

Tts

Ttu

Ttv

Ttw

Ttx

Tty

Ttz

Tta

Ttb

Ttc

Ttd

Tte

Ttf

Ttg

Tth

Tti

Ttj

Ttk

Ttl

Ttm

Ttn

Tto

Ttp

Ttq

Tts

Ttu

Ttv

Ttw

Ttx

Tty

Ttz

Tta

Ttb

Ttc

Ttd

Tte

Ttf

Ttg

Tth

Tti

Ttj

Ttk

Ttl

Ttm

Ttn

Tto

Ttp

Ttq

Tts

Ttu

Ttv

Ttw

Ttx

Tty

Ttz

Tta

Ttb

Ttc

Ttd

Tte

Ttf

Ttg

Tth

Tti

Ttj

Ttk

Ttl

Ttm

Ttn

Tto

Ttp

Ttq

Tts

Ttu

Ttv

Ttw

Ttx

Tty

Ttz

Tta

Ttb

Ttc

Ttd

Tte

Ttf

Ttg

Tth

Tti

Ttj

Ttk

Ttl

Ttm

Ttn

Tto

Ttp

Ttq

Tts

Ttu

WELL NAME	LOCATION (SECTION, TOWNSHIP RANGE)	TOTAL DEPTH (FEET)	DRILLED TOP OF FORMATION (FEET), AND STRATIGRAPHIC THICKNESS OF FORMATION (METERS)									
			Teb	Tst	Tsr	Tv	Tmb	Tla	Tm	Tp	R-S	Ref
29. Neaves N.U.B. #5	21-7S-4W	1435					1293 -		0	1293 -		
30. Neaves N.U.B. #6	21-7S-4W	1478					1357 32+	1202? 40+	0	1202? 361+ 72+		
31. Neaves N.U.B. #7	21-7S-4W	1711					1516 -	1360? -	0	1360? -		
32. Neaves N.U.B. #8	21-7S-4W	1474					1360 -	1190? -	0	1190 -		
33. Neaves N.U.B. #9	21-7S-4W	1365					1200 -		0	1200 -		
34. Neaves N.U.B. #10	21-7S-4W	2962	2746 60+	2567 44	1640 256	1393 59+			0	1393 396+ 315+		
35. Neaves N.U.B. #12	21-7S-4W	3318	3170 40+	3055 28	2410 169+	(F)	1450 176+	1325? 26+	0	1325 360+ 371+		
36. Neaves N.U.B. #14	21-7S-4W	2731	2486 43+	2455 8	2286 50+	(F)	1868 124+		0	1868 524+ 174+		
37. Neaves N.U.B. #15	21-7S-4W	2500	2342 47+	2165 54	1765 110+				0	1765 533+ 110+		
38. Neaves N.U. Callan #1	21-7S-4W	3076	2828 68+	2725 30	2153 155		1465 187+		0	1465 405+ 342+		

WELL NAME	LOCATION (SECTION, TOWNSHIP RANGE)	TOTAL DEPTH (FEET)	DRILLED TOP OF FORMATION (FEET), AND STRATIGRAPHIC THICKNESS OF FORMATION (METERS)									
			Teb	Tst	Tsr	Tv	Tmb	Tla	Tm	Tp	R-S	Ref
39. Neaves N.U. Callan #2	21-7S-4W	3123	2663 139+	2631 10	2313 97		1704 186+			0 513+	1704 283+	
40. Pacific Western Burns #1	21-7S-4W	1767				1467 73+	1418 12+			0 413+	1418 85+	
41. Texaco Tichenor	21-7S-4W	1907			1275 81+	1105 22	544 72+			0 166+	544 176+	
42. Neaves N.U.T.B. #1	22-7S-4W	4015	3730 82+	3480 62	2624 214	1870 148	1275 139	1204? 19+		0 354+	1204 519+	
43. Neaves N.T.B. #2	22-7S-4W	1530					1383? -	1140? -		0 -	1140? -	
44. Jergins YMCA #1	26-7S-4W	2510				2150 76+	770 336+			0 226+	770 412+	
45. Jergins YMCA #2	26-7S-4W	4735			4380 72+	2160 220	768 -			0 -	768 -	
46. Neaves N.K. Burns #1	27-7S-4W	2691					1955 212+	1880? 22+	1570? 89+	0 410+	1880? 234+	
47. Neaves N. Turnbow #1	28-7S-4W	3441						3138 86+ (G)		0 915+	3138 -	
48. Neaves N.U.H. Turnbow #1	29-7S-4W	3445	3158 46+		3008 26+ (D)					0 862+		

WELL NAME	LOCATION (SECTION, TOWNSHIP RANGE)	TOTAL DEPTH (FEET)	DRILLED TOP OF FORMATION (FEET), AND STRATIGRAPHIC THICKNESS OF FORMATION (METERS)									
			Teb	Tst	Tsr	Tv	Tmb	Tla	Tm	Tp	R-S	Ref
49. Union Towne #1	36-7S-4W	4345	4038 88+	3861 50	3092 216	2380 204	995 397+			0 281+	995 816+	
50. Neaves N.T. Con. Farms #1	1-7S-5W	3517		3510 -	2736 -		2096 -			0 -	2096 -	3020? -
51. Texaco Con. Farms #1	11-7S-5W	6738	4403 563+		4230 47+					0 1117+	4230 47+	
52. Texaco Hayward #1	5-8S-2W	4313	3853 -			0 653+					0 653+	
53. Grober Janette #1	27-8S-2W	3008	2090 -	1738? -	952? -	0 -					0 -	
54. Western Gulf Clement #1	29-8S-2W	4005	1597 367+		0 243+ (D)						0 -	
55. Union E.L. Moore #2 (O.H.)	6-8S-3W	3958	3542 124+	3367 53	2594 230	1675 265	510 336+			0 135+	510 831+	
56. Union E.L. Moore #2 (R.D.)	6-8S-3W	4429	3766 169+	3530 54	2643 210	1681 249	510 303+			0 135+	510 761+	
57. Western Gulf Wells Fargo #1	7-8S-3W	6054	3848 610+	3458 108	2540 254	1396 302	956 95+			0 -	956 650+	

WELL NAME	LOCATION (SECTION, TOWNSHIP RANGE)	TOTAL DEPTH (FEET)	DRILLED TOP OF FORMATION (FEET), AND STRATIGRAPHIC THICKNESS OF FORMATION (METERS)									
			Teb	Tst	Tsr	Tv	Tmb	Tla	Tm	Tp	R-S	Ref
58. Western Gulf Wells Fargo #2	7-8S-3W	930							0	265+		
59. Union Rich.-Eaton #1	10-8S-3W	3733	2985?		0						0	
			-		-						-	
60. Union Rich.-Costa #1	14-8S-3W	3804	1592		0						0	
			337+		366+						-	
					(D)							
65. Union Rich.-Costa #4 (O.H.)	14-8S-3W	5112	3628	2950	0						0	
			240+	87	436+						436+	
67. Western Gulf Western Shores #1	16-8S-3W	5020	3683	3300?	1764	1131			0	1131		
			387+	112	448	139			183+	-		
68. Humble S.C. Lumber #1	1-8S-4W	4975	3523	3247	1978	1318	958		0	958	2868?	
			439	81	345	189	106+		292+	640+	107	
69. M+H Oil Carter #1	10-9S-2W	4333	1553		318	0					0	
			-		-	-					-	
70. Honolulu Hinman #1	17-9S-2W	5820	1285		0						0	
			1242+		349+						-	
					(D)							
71. British Am. Gairaud #1	18-9S-2W	1113	992		0						0	
			36+		298+						-	
					(D)							

WELL NAME	LOCATION (SECTION, TOWNSHIP RANGE)	TOTAL DEPTH (FEET)	DRILLED TOP OF FORMATION (FEET), AND STRATIGRAPHIC THICKNESS OF FORMATION (METERS)									
			Teb	Tst	Tsr	Tv	Tmb	Tla	Tm	Tp	R-S	Ref
72. Snyder Gairaud #1	18-9S-2W		1163 13+		0 272+ (D)						0 -	
73. Western Gulf Vosti #1A	4-9S-4W	5133	3880 230+							(H)		
74. B.J. Marks Marks #2	6-10S-1E	2223	1610 -		0 -						0 -	
75. B.J. Marks Marks #1	16-10S-1E	3537	1919? 247+		0 507+ (D)						0 -	
76. Union Loma Prieta #1	19-10S-1E	1928						(J)	0 - (K)			
77. Union Loma Prieta #2	20-10S-1E	4570						3100? 273+ (L)	0 794+ (K)		3100? 273+	
78. Bean Hill Ltd. Hihn #1A	34-10S-1E	2575						2278? 78+	0 601+		2278? 78+	
79. Union T. Hihn #1	34-10S-1E	7747				3698 793+ (M)		3280? 64+	0 643+		3280? 857+	

WELL NAME	LOCATION (SECTION, TOWNSHIP RANGE)	TOTAL DEPTH (FEET)	DRILLED TOP OF FORMATION (FEET), AND STRATIGRAPHIC THICKNESS OF FORMATION (METERS)									
			Tst	Tsr	Tv	Tmb	Tla	Tm	Tp	R-S	Ref	
80. Union T. Hihn #2	34-10S-1E	3507						(N)	0			
81. Texaco J.H. Blake #1	12-11S-1E	7522			5373 421+ (M)	5097 49+			0 1371+ (K)	5097 470+		
82. Monterey Porter #1	25-11S-2E	2958			1753 (P)				0	1753	-	
83. Monterey Porter #2	30-11S-3E	3973			1715 414+				0	1715	414+	

APPENDIX 5 PALEOCURRENT DATA

In the following table, paleocurrent data are given as the vector mean of all measurements on a given type of sedimentary structure (e.g., flute casts, or cobble imbrication) at a single location. A "location" usually consists of one outcrop, but in some cases consists of two or more closely spaced outcrops. For certain kinds of sedimentary structures, such as groove casts or parting lineation, the vector mean is only one of the two possible azimuths of the *line* of current movement. For other structures, such as flute casts of cross-stratification, the vector mean is the azimuth of the true *direction* of movement, and this fact is specified in the table, as in the notation "295 to the NW." Formation abbreviations are given in Table 2.

FORMATION	LOCATION, SECTION, TOWNSHIP, AND RANGE	VECTOR MEAN	VECTOR STRENGTH (r/n)	NUMBER OF MEASUREMENTS (n)	INDICATOR
Tsr	Kings Cr. 6-9S-2W	53 to NE	1.0	1	flute cast
Tsr	Soquel Cr.	298	1.0	1	weak parting lineation
Tvc	Fall Creek 8-8S-3W	100 to SE	.35	4	ripple cross-lamination
Tvc	Fall Creek 8-8S-3W	30 to NE	1.0	1	flute cast
Tvc	Skyline Blvd. 21-8S-2W	41 to NE	1.0	1	flute cast
Tvc	Skyline Blvd. 21-8S-2W	13	.90	2	groove casts
Tvc	Skyline Blvd. 21-8S-2W	88	.75	6	groove casts
Tvc	Skyline Blvd. 22-8S-2W	27	.38	3	groove casts
Tvc	Skyline Blvd. 26-8S-2W	129	1.0	1	groove cast
Tvc	Skyline Blvd. 26-8S-2W	164 to SE	.73	3	flute casts

FORMATION	LOCATION; SECTION, TOWNSHIP, AND RANGE	VECTOR MEAN	VECTOR STRENGTH (r/n)	NUMBER OF MEASUREMENTS (n)	INDICATOR
TVC	Skyline Blvd. 27-8S-2W	303	.99	2	groove casts
TVC	Skyline Blvd. 1-9S-2W	49 to NE	1.0	1	possible flute cast
TVC	Highway 9 24-8S-3W	258	1.0	1	parting lineation
TVC	Zayante Cr. 19-9S-1W	95 to E	.24	19	ripple cross-lamination
TVC	Bear Cr. 10-9S-2W	34 to NE	.99	2	flute casts
TVC	Bear Cr. 10-9S-2W	44	1.0	1	groove cast
TVC	Kings Cr. 6-9S-2W	21 to NE	1.0	1	flute cast
TVC	Kings Cr. 7-9S-2W	24	.91	3	groove casts
TVC	Twobar Cr. 18-9S-2W	19 to NE	.99	2	flute casts
TVC	Twobar Cr. 18-9S-2W	1	.95	7	groove casts

FORMATION	LOCATION; SECTION, TOWNSHIP, AND RANGE	VECTOR MEAN	VECTOR STRENGTH (r/n)	NUMBER OF MEASUREMENTS (n)	INDICATOR
Tvc	Twohar Cr. 18-9S-2W	75 to NE	1.0	1	ripple cross-lamination
Tvc	San Lorenzo R. 36-8S-2W	18	.99	2	groove casts
Tvc	Union Creek 4-9S-3W	14 to NE	1.0	1	ripple cross-lamination
Tvc	Blooms Creek 10-9S-3W	42 to NE	.74	10	ripple cross-lamination
Tvc	Corralitos Cr. 26-10S-1E	82	.99	4	possible groove casts
Tvc	Corralitos Cr. 26-10S-1E	98	.99	4	oriented rip-up(?) clasts
Tvs	Corralitos Cr. 26-10S-1E	95 to E	.96	6	giant flute casts
Tvl	Mtn. Charlie Gulch 32-9S-1W	347 to NW	1.0	1	cross-lamination
Tvl	Twohar Cr. 18-9S-2W	135 to SE	.87	6	tabular cross-lamination
Tz	Mtn. Charlie Gulch 32-9S-1W	73 to NE	.42	5	cobble imbrication

FORMATION	LOCATION, SECTION, TOWNSHIP, AND RANGE	VECTOR MEAN	VECTOR STRENGTH (r/n)	NUMBER OF MEASUREMENTS (n)	INDICATOR
Tz	Mtn. Charlie Gulch, 32-9S-1W	64 to NE	1.0	1	cobble imbrication
Tz	Mtn. Charlie Gulch 32-9S-1W	32 to NE	.98	2	cobble imbrication
Tz	Mtn. Charlie Gulch 32-9S-1W	73 to NE	.97	2	pebble imbrication
Tz	Mtn. Charlie Gulch 32-9S-1W	323 to NW	1.0	1	cross-lamination
Tz	Mtn. Charlie Gulch 31-9S-1W	59 to NE	.78	6	cobble and pebble imbrication
Tz	Mtn. Charlie Gulch 31-9S-1W	349 to N	.95	3	cobble imbrication
Tz	Mtn. Charlie Gulch 31-9S-1W	264 to W	1.0	1	cobble imbrication
Tz	Mtn. Charlie Gulch 31-9S-1W	309 to NW	.64	5	cross-lamination
Tz	Mtn. Charlie Gulch 31-9S-1W	87 to E	1.0	1	cross-lamination
Tz	Zayante Cr.	90 to E	1.0	2	cobble imbrication

FORMATION	LOCATION; SECTION, TOWNSHIP, AND RANGE	VECTOR MEAN	VECTOR STRENGTH (\bar{x}/n)	NUMBER OF MEASUREMENTS (n)	INDICATOR
Tz	Mtn. Charlie Gulch, 32-9S-1W	64 to NE	1.0	1	cobble imbrication
Tz	Mtn. Charlie Gulch 32-9S-1W	32 to NE	.98	2	cobble imbrication
Tz	Mtn. Charlie Gulch 32-9S-1W	73 to NE	.97	2	pebble imbrication
Tz	Mtn. Charlie Gulch 32-9S-1W	323 to NW	1.0	1	cross-lamination
Tz	Mtn. Charlie Gulch 31-9S-1W	59 to NE	.78	6	cobble and pebble imbrication
Tz	Mtn. Charlie Gulch 31-9S-1W	349 to N	.95	3	cobble imbrication
Tz	Mtn. Charlie Gulch 31-9S-1W	264 to W	1.0	1	cobble imbrication
Tz	Mtn. Charlie Gulch 31-9S-1W	309 to NW	.64	5	cross-lamination
Tz	Mtn. Charlie Gulch 31-9S-1W	87 to E	1.0	1	cross-lamination
Tz	Zayante Cr.	90 to E	1.0	2	cobble imbrication

FORMATION	LOCATION; SECTION, TOWNSHIP, AND RANGE	VECTOR MEAN	VECTOR STRENGTH (r/n)	NUMBER OF MEASUREMENTS (n)	INDICATOR
Tz	Lompico 35-9S-2W	6 to N	.76	6	cobble imbrication
Tla	Zayante Cr. 30-9S-1W	245 to SW	.39	7	ripple cross-lamination

REFERENCES CITED

- Adams, E. W., and Beatty, W. B., 1962, Bituminous rocks in California: Mineral Information Service, California Division of Mines and Geology, v. 15, p. 1-9.
- Addicott, W. O., 1967, Age of the Skooner Gulch Formation, Mendocino county, California: U.S. Geological Survey Professional Paper 1254-C, p. C1-C11.
- , 1968, Mid-Tertiary zoogeographic and paleogeographic discontinuities across the San Andreas fault, California, *in* Dickinson, W. R., and Grantz, A., eds., Proceedings of Conference on Geologic Problems of San Andreas Fault System: Stanford University Publications in Geological Sciences, v. 11, p. 145-165.
- , 1970, Tertiary paleoclimatic trends in the San Joaquin basin, California: U.S. Geological Survey Professional Paper 644-D, 19 p.
- , 1972, Provincial middle and late Tertiary molluscan stages, Temblor Range, California, *in* Proceedings of the Pacific Coast Miocene Biostratigraphic Symposium: Bakersfield, California, Society of Economic Paleontologists and Mineralogists, Pacific Section, p. 1-26.
- , 1978, Pectinids as biochronologic indices in the Neogene of the eastern North Pacific, *in* Proceedings of the Second Working Group Meeting, Biostratigraphic Datum-planes of the Pacific Neogene: Republic of Indonesia, Ministry of Mines and Energy, Geological Research and Development Centre Special Publication 1, p. 11-23.
- , 1980, Highlights in the 130-year history of marine Cenozoic stratigraphic paleontology on the Pacific Coast of North America: Professor Saburo Kanno Memorial Volume, p. 1-19.
- , Barron, J. A., and Miller, J. W., 1978, Marine late Neogene sequence near Santa Cruz, California, *in* Addicott, W. O., ed., Neogene biostratigraphy of selected areas in the California Coast Ranges: U.S. Geological Survey Open-File Report 78-446, p. 97-109.
- Allen, J. E., 1946, Geology of the San Juan Bautista quadrangle, California: California Division of Mines Bulletin 133, p. 9-75.
- Angstadt, D. M., Austin, J. A., Jr., and Buffler, R. T., 1983, Deep-sea erosional unconformity in the southeastern Gulf of Mexico: *Geology*, v. 11, p. 215-218.
- Arnal, R. E., 1980, Comment *on* "Comparison of Miocene provincial foraminiferal stages to coccolith zones in the California continental borderland": *Geology*, v. 8, p. 2-4.
- Arnold, R. A., 1908, Descriptions of new Cretaceous and Tertiary fossils from the Santa Cruz Mountains, California: U.S. National Museum Proceedings, v. 34, no. 1617, p. 345-390.
- Atwater, T., 1970, Implications of plate tectonics for the Cenozoic tectonic evolution of western North America: *Geological Society of America Bulletin*, v. 81, p. 3513-3536.
- , and Molnar, P., 1973, Relative motion of the Pacific and North American plates deduced from sea-floor spreading in the Atlantic, Indian, and South Pacific oceans, *in* Kovach, R. L., and Nur, A., eds., Proceedings of the Conference on Tectonic Problems of the San Andreas Fault System: Stanford University Publications in Geological Sciences, v. 13, p. 136-148.

- Ballance, P. F., Howell, D. G., and Ort, K., 1983, Late Cenozoic wrench tectonics along the Nacimiento, South Cuyama, and La Panza faults, California, indicated by depositional history of the Simmler Formation, in Anderson, D. W., and Rymer, M. J., eds., Tectonics and sedimentation along faults of the San Andreas system: Society of Economic Paleontologists and Mineralogists, Pacific Section, p. 1-9.
- Bandy, O. L., 1955, Evidence of displaced foraminifera in the Purisima Formation of the Halfmoon Bay area, California: Contributions from the Cushman Foundation for Foraminiferal Research, v. 6, part 2, p. 77-79.
- , 1961, Distribution of foraminifera, radiolaria, and diatoms in sediments of the Gulf of California: Micropaleontology, v. 7, p. 1-26.
- , 1967, Geologic history of a Tertiary basin, paleotectonism, and paleobathymetry: American Geological Institute, Short Course Lecture Notes, Paleoecology, New Orleans, Louisiana, p. OB-1--OB-24C.
- , and Arnal, R. E., 1960, Concepts of foraminiferal paleoecology: American Association of Petroleum Geologists Bulletin, v. 44, p. 1921-1932.
- , and ———, 1969, Middle Tertiary basin development, San Joaquin Valley, California: Geological Society of America Bulletin, v. 80, p. 783-820.
- Barrow, S., 1980, Application of the turbidite facies model to a roadcut in the Santa Cruz Mountains [unpublished student report]: Stanford University, 19 p.
- Bathurst, R. G. C., 1975, Carbonate sediments and their diagenesis (second edition): Amsterdam, Elsevier, 658 p.
- Beaulieu, J. D., 1970, Cenozoic stratigraphy of the Santa Cruz Mountains, California, and inferred displacement along the San Andreas fault [Ph.D. thesis]: Stanford University, 202 p.
- Berggren, W. A., and Aubert, J., 1977, Paleogene benthic foraminiferal biostratigraphy and paleobathymetry of the central Coast Ranges of California: Abstracts for field conference on the Paleogene of California and Mexico, Menlo Park, California, p. 1-3.
- Beveridge, A. J., 1958, Heavy minerals in lower Tertiary formations in the Santa Cruz Mountains, California [Ph.D. thesis]: Stanford University, 109 p.
- , 1960, Heavy minerals in lower Tertiary formations in the Santa Cruz Mountains, California: Journal of Sedimentary Petrology, v. 30, p. 513-537.
- Blake, G. H., and Douglas, R. G., 1980, Pleistocene occurrence of *Melonis pompilioiodes* in the California borderland and its implication for foraminiferal paleoecology: Cushman Foundation Special Publication 19, Memorial to Orville L. Bandy, p. 59-67.
- Blake, M. C., Campbell, R. H., Dibblee, T. W., Jr., Howell, D. G., Nilsen, T. H., Normark, W. R., Vedder, J. C., and Silver, E. A., 1978, Neogene basin formation in relation to plate-tectonic evolution of San Andreas fault system, California: American Association of Petroleum Geologists, v. 62, p. 344-372.
- Blatt, H., 1982, Sedimentary petrology: San Francisco, W. H. Freeman and Co., 564 p.

- Bowen, O. E., Jr., and Gray, C. H., 1959, Geology and economic possibilities of the limestone and dolomite deposits of the northern Gabilan Range, California: California Division of Mines and Geology Special Report 56, 40 p.
- Brabb, E. E., 1960, Geology of the Big Basin area, Santa Cruz Mountains, California [Ph.D. thesis]: Stanford University, 197 p.
- _____, 1964, Subdivision of the San Lorenzo Formation (Eocene-Oligocene), west-central California: American Association of Petroleum Geologists Bulletin, v. 48, p. 670-679.
- _____, 1970, Preliminary geologic map of the central Santa Cruz Mountains, California: U.S. Geological Survey Open-File Map, scale 1:62,500.
- _____, 1980, Preliminary geologic map of the La Honda and San Gregorio quadrangles, San Mateo county, California: U.S. Geological Survey Open-File Report 80-245, scale 1:24,000.
- _____, Clark, J. C., and Throckmorton, C. B., 1977, Measured sections of Paleogene rocks from the California Coast Ranges: U.S. Geological Survey Open-File Report 77-714, 114 p.
- _____, and Dibblee, T. W., Jr., 1979, Preliminary geologic map of the Castle Rock Ridge quadrangle, Santa Cruz and Santa Clara counties, California: U.S. Geological Survey Open-File Report 79-659, scale 1:24,000.
- _____, and Pampeyan, E. H., 1972, Preliminary geologic map of San Mateo county, California: U.S. Geological Survey Miscellaneous Field Studies Map MF-328, scale 1:125,000.
- Branner, J. C., Newsom, J. F., and Arnold, R., 1909, Description of the Santa Cruz quadrangle, California: U.S. Geological Survey Geologic Atlas Folio 163, 12 p.
- Bukry, D., Brabb, E. E., and Vedder, J. G., 1977, Correlation of Tertiary nannoplankton assemblages from the Coast and Peninsular Ranges of California, in Mem. Segundo Cong. Latinoamericano de Geologia, t. 3; Venezuela Bol. de Geologia, publ. especial no. 7, p. 1461-1483.
- Burchfiel, B. C., 1958, Geology of the Two Bar Creek area, Boulder Creek, California [M.S. thesis]: Stanford University, 57 p.
- _____, 1964, Stratigraphic reassignment of four species in the lower Miocene rocks of the Bear Creek area, Santa Cruz county, California: Journal of Paleontology, v. 38, p. 401-405.
- Burford, R. O., 1961, Geology of the Glenwood basin area, Santa Cruz Mountains, California [M.S. thesis]: Stanford University, 30 p.
- California Division of Oil and Gas, 1964, Exploratory wells drilled outside of oil and gas fields in California to December 31, 1963, 320 p.
- _____, 1973, California oil and gas fields, v. 1, north and east central California.
- _____, 1982a, Oil and gas prospect wells drilled in California through 1980, 258 p.
- _____, 1982b, 67th annual report of the state oil and gas supervisor [production figures for 1981], 137 p.

- Campbell, C. V., 1967, Lamina, laminaset, bed, and bedset: *Sedimentology*, v. 8, p. 7-26.
- Carlson, R. L., 1976, Cenozoic plate convergence in the vicinity of the Pacific northwest: a synthesis and assessment of plate tectonics in the northeastern Pacific [Ph.D. thesis]: Seattle, University of Washington, 129 p.
- , 1982, Cenozoic convergence along the California coast: a qualitative test of the hot-spot approximation: *Geology*, v. 10, p. 191-196.
- , 1983, Reply to Comment on "Cenozoic convergence along the California coast: a qualitative test of the hot-spot approximation": *Geology*, v. 11, p. 674.
- Castro, M. J., 1967, Geology and oil potential of the area westerly of San Juan Bautista, California, in Gabilan Range and adjacent San Andreas fault: Pacific Sections, American Association of Petroleum Geologists and Society of Economic Paleontologists and Mineralogists, Field Trip Guidebook, p. 81-86.
- Chamberlain, C. K., 1978, Recognition of trace fossils in cores, in Basan, P. B., ed., Trace fossil concepts: Society of Economic Paleontologists and Mineralogists, Short Course Notes No. 5, p. 119-166.
- Champion, D. E., Gromme, C. S., and Howell, D. G., 1981, Paleomagnetic study of the Upper Cretaceous Pigeon Point Formation, in Frizzell, V., ed., Upper Cretaceous and Paleocene turbidites, central California coast: Society of Economic Paleontologists and Mineralogists, Pacific Section, Annual Meeting Field Trip 6, Guidebook, p. 53-55.
- Christensen, E. W., and Knight, R. L., 1964a, San Andreas fault cross-section from the Gulf of the Farallones to Bielawski Mountain, California: American Association of Petroleum Geologists, Pacific Section, Committee for the Study of Lateral Faulting in California, Cross-section No. 2.
- , and ———, 1964b, San Andreas fault cross-section from Bielawski Mountain to Hollister, California: American Association of Petroleum Geologists, Pacific Section, Committee for the Study of Lateral Faulting in California, Cross-section No. 3.
- Cifelli, R., 1969, Radiation of Cenozoic planktonic foraminifera: *Systematic Zoology*, v. 18, p. 154-168.
- Clark, J. C., 1966, Tertiary stratigraphy of the Felton-Santa Cruz area, Santa Cruz Mountains, California [Ph.D. thesis]: Stanford University, 184 p.
- , 1968, Correlation of the Santa Cruz Mountains Tertiary—implications for San Andreas history, in Dickinson, W. R., and Grantz, A., eds., Proceedings of Conference on Geologic Problems of San Andreas Fault System: Stanford University Publications in Geological Sciences, v. 11, p. 166-180.
- , 1970, Geologic map of the southwestern Santa Cruz Mountains between Año Nuevo Point and Davenport, California: U.S. Geological Survey Open-File Map, scale 1:24,000.
- , 1981, Stratigraphy, paleontology, and geology of the central Santa Cruz Mountains, California Coast Ranges: U.S. Geological Survey Professional Paper 1168, 51 p.
- , and Brabb, E. E., 1978, Stratigraphic contrasts across the San Gregorio fault, Santa Cruz Mountains, west central California, in Silver, E. A., and Normark, W. R., eds., San Gregorio-Hosgri fault zone, California: California Division of Mines and Geology Special Report 137, p. 3-12.

- _____, _____, and Addicott, W. O., 1979, Tertiary paleontology and stratigraphy of the central Santa Cruz Mountains, California Coast Ranges: Geological Society of America, Cordilleran Section, Field Trip Guidebook, 23 p.
- _____, _____, Greene, H. G., and Ross, D. C., 1984, Geology of Point Reyes peninsula and implications for San Gregorio fault history, in Crouch, J. K., and Bachman, S. B., eds., Tectonics and sedimentation along the California margin: Society of Economic Paleontologists and Mineralogists, Pacific Section, p. 67-86.
- _____, and Rietman, J. D., 1973, Oligocene stratigraphy, tectonics, and paleogeography southwest of the San Andreas fault, Santa Cruz Mountains and Gabilan Range, California Coast Ranges: U.S. Geological Survey Professional Paper 783, 18 p.
- Clarke, S. H., Jr., and Nilsen, T. H., 1973, Displacement of Eocene strata and implications for the history of offset along the San Andreas fault, central and northern California, in Kovach, R. L., and Nur, A., eds., Proceedings of the Conference on Tectonic Problems of the San Andreas Fault System: Stanford University Publications in Geological Sciences, v. 13, p. 358-367.
- Classen, J. S., 1959, The geology of a portion of the Half Moon Bay quadrangle, San Mateo County, California [M.S. thesis]: Stanford University, 57 p.
- Cloos, M., and Apted, M., 1979, Guidebook to the southern Coast Ranges geology and plate tectonics: Los Angeles, University of California, Department of Earth and Space Sciences, 149 p.
- Coppersmith, K. J., 1979, Activity assessment of the Zayante-Vergeles fault, central San Andreas fault system, California [Ph.D. thesis]: Santa Cruz, University of California, 333 p.
- Crandall, R. R., 1943, Half Moon Bay district, in Jenkins, O. P., ed., Geologic formations and economic development of the oil and gas fields of California: California Division of Mines Bulletin 118, p. 478-480.
- Crouch, J. K., and Bukry, D., 1979, Comparison of Miocene provincial foraminiferal stages to coccolith zones in the California continental borderland: *Geology*, v. 7, p. 211-215.
- Crowell, J. C., 1974, Origin of late Cenozoic basins in southern California, in Dickinson, W. R., ed., Tectonics and sedimentation: Society of Economic Paleontologists and Mineralogists Special Publication 22, p. 190-204.
- Cummings, J. C., 1960, Geology of the Langley Hill-Waterman Gap area, Santa Cruz Mountains, California [Ph.D. thesis]: Stanford University, 233 p.
- _____, Touring, R. M., and Brabb, E. E., 1962, Geology of the northern Santa Cruz Mountains, California, in Bowen, O. E., Jr., ed., Geologic guide to the gas and oil fields of northern California: California Division of Mines and Geology Bulletin 181, p. 179-220.
- Dibblee, T. W., Jr., 1966, Geology of the Palo Alto quadrangle, Santa Clara and San Mateo counties, California: California Division of Mines and Geology Map Sheet 8, scale 1:62,500.
- _____, 1977, Sedimentology and diastrophism during Oligocene time relative to the San Andreas fault system, in Nilsen, T. H., ed., Late Mesozoic and Cenozoic sedimentation and tectonics in California: San Joaquin Geological Society, Short Course, Bakersfield, California, p. 99-108.

- _____, and Brabb, E. E., 1978a, Preliminary geologic map of the Chittenden quadrangle, Santa Clara, Santa Cruz, and San Benito counties, California: U.S. Geological Survey Open-File Report 78-453, scale 1:24,000.
- _____, and _____, 1978b, Preliminary geologic map of the Los Gatos quadrangle, Santa Clara and Santa Cruz counties, California: U.S. Geological Survey Open-File Report 78-453, scale 1:24,000.
- _____, and _____, 1978c, Preliminary geologic map of the Watsonville East quadrangle, Santa Cruz, Santa Clara, and Monterey counties, California: U.S. Geological Survey Open-File Report 78-453, scale 1:24,000.
- _____, and _____, 1980, Preliminary geologic map of the Loma Prieta quadrangle, Santa Cruz and Santa Clara counties, California: U.S. Geological Survey Open-File Report 80-944, scale 1:24,000.
- _____, _____, and Clark, J. C., 1978, Preliminary geologic map of the Laurel quadrangle, Santa Cruz and Santa Clara counties, California: U.S. Geological Survey Open-File Report 78-84, scale 1:24,000.
- _____, Nilsen, T. H., and Brabb, E. E., 1979, Preliminary geologic map of the San Juan Bautista quadrangle, San Benito and Monterey Counties, California: U.S. Geological Survey Open-File Report 79-375, scale 1:24,000.
- _____, and Rogers, T. H., 1975, Geologic map of the Hollister quadrangle, California: U.S. Geological Survey Open-File Map 75-394, scale 1:62,500.
- Dickinson, W. R., 1970, Interpreting detrital modes of graywacke and arkose: *Journal of Sedimentary Petrology*, v. 40, p. 695-707.
- _____, 1983, Cretaceous sinistral strike slip along Nacimiento fault in coastal California: *American Association of Petroleum Geologists Bulletin*, v. 67, p. 624-645.
- _____, Cowan, D. S., and Schweikert, R. A., 1972, Test of new global tectonics: Discussion: *American Association of Petroleum Geologists Bulletin*, v. 56, p. 375-384.
- _____, and Graham, S. A., 1975, Sedimentary environments, depositional systems, and stratigraphic cycles, in Dickinson, W. R., ed., *Current concepts of depositional systems with applications for petroleum geology*: San Joaquin Geological Society, Short Course, Bakersfield, California, p. 0-1--0-10.
- _____, Ingersoll, R. V., and Graham, S. A., 1979, Paleogene sediment dispersal and paleotectonics in northern California: *Geological Society of America Bulletin*, Part I, v. 90, p. 897-898; Part II, v. 90, p. 1458-1528.
- _____, and Snyder, W. S., 1979, Geometry of triple junctions related to San Andreas transform: *Journal of Geophysical Research*, v. 84, no. B2, p. 561-571.
- _____, and Suczek, C. A., 1979, Plate tectonics and sandstone composition: *American Association of Petroleum Geologists Bulletin*, v. 63, p. 2164-2182.
- Donovan, D. T., and E. J. W. Jones, 1979, Causes of world-wide changes in sea level: *Journal of the Geological Society of London*, v. 136, p. 187-192.

- Dott, R. H., Jr., 1964, Wacke, graywacke, and matrix--what approach to immature sandstone classification?: *Journal of Sedimentary Petrology*, v. 34, p. 625-632.
- Dunham, R. J., 1962, Classification of carbonate rocks according to their depositional texture, in Ham, W. E., ed., *Classification of carbonate rocks--a symposium: American Association of Petroleum Geologists Memoir 1*, p. 108-121.
- Dupre, W. R., Clifton, H. E., and Hunter, R. E., 1980, Modern sedimentary facies of the open Pacific coast and Pleistocene analogs from Monterey Bay, California, in Field, M. E., Bouma, A. H., Colburn, I. P., Douglas, R. G., and Ingle, J. C., Jr., eds., *Quaternary depositional environments of the Pacific coast: Society of Economic Paleontologists and Mineralogists, Pacific Section, Pacific Coast Paleogeography Symposium 4*, p. 105-120.
- Engebretson, D. C., 1982, Relative motions between oceanic and continental plates in the Pacific basin [Ph.D. thesis]: Stanford University, 211 p.
- Ernst, W. G., and Hall, C. A., Jr., 1974, Geology and petrology of the Cambria Felsite, a new Oligocene formation, west-central California Coast Ranges: *Geological Society of America Bulletin*, v. 85, p. 523-532.
- Esser, R. W., 1958, The reconnaissance geology of a part of the Woodside quadrangle, northeast of Skyline Boulevard, San Mateo county, California [M.S. thesis]: Stanford University, 78 p.
- Fairchild, W. W., Wesendunk, P. R., and Weaver, D. W., 1969, Eocene and Oligocene foraminifera from the Santa Cruz Mountains, California: *University of California Publications in Geological Sciences*, v. 81, p. 1-145.
- Fischer, A. G., and Arthur, M. A., 1977, Secular variations in the pelagic realm, in Cook, H. E., and Enos, P., eds., *Deep-water carbonate environments: Society of Economic Paleontologists and Mineralogists Special Publication 25*, p. 19-50.
- Fothergill, H. L., 1962a, La Honda oil field, California, in Bowen, O. E., Jr., ed., *Geologic guide to the gas and oil fields of northern California: California Division of Mines and Geology Bulletin 181*, p. 221-222.
- _____, 1962b, Oil Creek oil field, California: *ibid.*, p. 223-224.
- Francis, P., 1976, *Volcanoes*: New York, Penguin Books, 368 p.
- Friedman, G. M., 1971, Staining, in Carver, R. E., ed., *Procedures in sedimentary petrology*: John Wiley and Sons, Inc., p. 511-530.
- Galehouse, J. S., 1968, Anisotropy of magnetic susceptibility as a paleocurrent indicator: a test of the method: *Geological Society of America Bulletin*, v. 79, p. 387-390.
- Galliher, E. W., 1935, Geology of glauconite: *American Association of Petroleum Geologists Bulletin*, v. 19, p. 1569-1601.
- Galloway, A. J., 1977, Geology of the Point Reyes peninsula, Marin county, California: *California Division of Mines and Geology Bulletin 202*, 72 p.
- Garfunkel, Z., 1973, History of the San Andreas fault as a plate boundary: *Geological Society of America Bulletin*, v. 84, p. 2035-2042.

- Garrison, R. E., 1981, Pelagic and hemipelagic sedimentation in active margin basins, in Douglas, R. G., Colburn, I. P., and Gorsline, D. S., eds., *Depositional systems of active continental margin basins*: Society of Economic Paleontologists and Mineralogists, Pacific Section, Short Course Notes, San Francisco, p. 15-38.
- _____, Stanley, R. G., and Horan, L. J., 1979, Middle Miocene sedimentation on the southwestern edge of the Lockwood High, Monterey county, California, in Graham, S. A., ed., *Tertiary and Quaternary geology of the Salinas Valley and Santa Lucia Range, Monterey County, California*: Society of Economic Paleontologists and Mineralogists, Pacific Section, Pacific Coast Paleogeography Field Guide 4, p. 51-65.
- Glazner, A. F., 1981, Detachment faulting, volcanism, and the passage of the Mendocino fracture zone under the southwestern United States: Geological Society of America Abstracts with Programs, v. 13, p. 460.
- _____, 1982, Effect of subduction of the Mendocino fracture zone on Tertiary sedimentation in the southwestern United States: Geological Society of America Abstracts with Programs, v. 14, p. 167.
- Goodwin, J. C., and Thompson, J. N., 1954, Purisima Pliocene foraminifera of the Halfmoon Bay area, San Mateo county, California: Contributions from the Cushman Foundation for Foraminiferal Research, v. 5, part 4, p. 170-178.
- Graham, J. J., and Drooger, C. W., 1952, An occurrence of *Miogyopsina* in California: Contributions from the Cushman Foundation for Foraminiferal Research, v. 3, part 1, p. 21-22.
- Graham, S. A., 1976, Tertiary sedimentary tectonics of the central Salinian block of California [Ph.D. thesis]: Stanford University, 510 p.
- _____, 1978, Role of Salinian block in evolution of San Andreas fault system, California: American Association of Petroleum Geologists Bulletin, v. 62, p. 2214-2231.
- _____, and Dickinson, W. R., 1978a, Evidence for 115 kilometers of right slip on the San Gregorio-Hosgri fault trend: Science, v. 199, p. 179-181.
- _____, and _____, 1978b, Apparent offsets of on-land geologic features across the San Gregorio-Hosgri fault trend, in Silver, E. A., and Normark, W. R., eds., *San Gregorio-Hosgri fault zone, California*: California Division of Mines and Geology Special Report 137, p. 13-23.
- _____, and Peabody C. E., 1981, New evidence for major strike-slip along the San Gregorio-Hosgri fault of the San Andreas transform system: Geological Society of America Abstracts with Programs, v. 13, p. 463.
- _____, Williams, L. A., Bate, M., and Weber, L. S., 1982, Stratigraphic and depositional framework of the Monterey Formation and associated coarse clastics of the central San Joaquin basin, in Williams, L. A., and Graham, S. A., eds., *Monterey Formation and associated coarse clastic rocks, central San Joaquin basin, California*: Society of Economic Paleontologists and Mineralogists, Pacific Section, Guidebook, p. 3-16.
- Grant, M. J., 1982, Stratigraphy of the Monterey Formation as exposed in Lompico and Zayante Creeks near Santa Cruz, California [unpublished student report]: Santa Cruz, University of California, 38 p.

- Greene, H. G., 1977, Geology of the Monterey Bay region: U.S. Geological Survey Open-File Report 77-718, 347 p.
- , and Clark, J. C., 1979, Neogene paleogeography of the Monterey Bay area, California, in Armentrout, J. M., Cole, M. R., and TerBest, H., Jr., eds., *Cenozoic paleogeography of the western United States*: Society of Economic Paleontologists and Mineralogists, Pacific Section, Pacific Coast Paleogeography Symposium 3, p. 277-296.
- Gribi, E. A., Jr., 1957, Santa Cruz basin holds important promise: *Oil and Gas Journal*, v. 55, no. 13, p. 113-116.
- Haehl, H. L., and Arnold, R., 1904, The Miocene diabase of the Santa Cruz Mountains in San Mateo county, California: *Proceedings of the American Philosophical Society*, v. 43, no. 175, p. 15-53.
- Hallmark, F. O., 1980, Unconventional petroleum resources in California: California Division of Oil and Gas, 17 p.
- Hamlin, H., 1904, Water resources of the Salinas Valley, California: U.S. Geological Survey Water-Supply and Irrigation Paper 89, 91 p.
- Hanna, W. F., Brown, R. D., Ross, D. C., and Griscom, A., 1972, Aeromagnetic reconnaissance along the San Andreas fault between San Francisco and San Bernardino, California: U.S. Geological Survey Geophysical Investigations Map GP-815, scale 1:250,000.
- Haq, B. U., 1977, Calcareous nannofossil biostratigraphy of the Paleogene of Santa Cruz Mountains, California: Abstracts for field conference on the Paleogene of California and Mexico, Menlo Park, California, p. 5-6.
- Harding, T. P., 1976, Tectonic significance and hydrocarbon trapping consequences of sequential folding synchronous with San Andreas faulting, San Joaquin valley, California: *American Association of Petroleum Geologists Bulletin*, v. 60, p. 356-378.
- Harms, J. C., Southard, J. B., and Walker, R. G., 1982, Structures and sequences in clastic rocks: Society of Economic Paleontologists and Mineralogists, Short Course Notes No. 9.
- Heckel, P. H., 1972, Recognition of ancient shallow marine environments, in Rigby, J. K., and Hamblin, W. K., eds., *Recognition of ancient sedimentary environments*: Society of Economic Paleontologists and Mineralogists Special Publication 16, p. 226-286.
- Hector, S. T., 1976, Environmental geology of the Castle Rock Ridge area, Santa Cruz and Santa Clara counties [M.S. thesis]: Davis, University of California, 98 p.
- Heller, P. L., and Flessa, K. W., 1981, Comment on "Late Oligocene transgression of middle Atlantic coastal plain": *Geology*, v. 9, p. 290.
- Horn, A. J., 1983, The resurrection of the Half Moon Bay oil field [abs.]: Pacific Sections, American Association of Petroleum Geologists, Society of Exploration Geophysicists, and Society of Economic Paleontologists and Mineralogists, Annual Meeting, Sacramento, California, Program and Abstracts, p. 44-45.
- Hoskins, E. G., and Griffiths, J. R., 1971, Hydrocarbon potential of northern and central California offshore, in Cram, I. H., ed., *Future petroleum provinces of the United States--their geology and potential*: American Association of Petroleum Geologists Memoir 15, v. 1, p. 212-228.

- Howell, D. G., Crouch, J. K., Greene, H. G., McCulloch, D. S., and Vedder, J. G., 1980, Basin development along the late Mesozoic and Cainozoic California margin: a plate tectonic margin of subduction, oblique subduction, and transform tectonics, *in* Ballance, P. F., and Reading, H. G., eds., *Sedimentation in oblique-slip mobile zones: International Association of Sedimentologists Special Publication 4*, p. 43-62.
- _____, and Joyce, J. E., 1981, Field guide to the Upper Cretaceous Pigeon Point Formation, *in* Frizzell, V., ed., *Upper Cretaceous and Paleocene turbidites, central California coast: Society of Economic Paleontologists and Mineralogists, Pacific Section, Annual Meeting Field Trip 6, Guidebook*, p. 61-70.
- _____, and Normark, W. R., 1982, Submarine fans, *in* Scholle, P. A., and Spearing, D., eds., *Sandstone depositional environments: American Association of Petroleum Geologists Memoir 31*, p. 365-404.
- _____, and Vedder, J. G., 1978, Late Cretaceous paleogeography of the Salinian block, California, *in* Howell, D. G., and McDougall, K. A., eds., *Mesozoic paleogeography of the western United States: Society of Economic Paleontologists and Mineralogists, Pacific Section, Pacific Coast Paleogeography Symposium 2*, p. 523-534.
- _____, and von Huene, R., 1981, Tectonics and sediment, along active continental margins, *in* Douglas, R. G., Colburn, I. P., and Gorsline, D. S., eds., *Depositional systems of active continental margin basins: Society of Economic Paleontologists and Mineralogists, Pacific Section, Short Course Notes*, San Francisco, p. 1-13.
- Huguenin, E., and Castello, W. O., 1921, Santa Cruz county: California State Mining Bureau, Report 13 of the State Mineralogist, p. 228-241.
- Hyndman, D. W., 1972, *Petrology of igneous and metamorphic rocks*: New York, McGraw-Hill Book Company, 533 p.
- Ingle, J. C., Jr., 1967, Modern biofacies and lithofacies as empirical geological models: American Geological Institute, Short Course Lecture Notes, Paleocology, New Orleans, Louisiana, p. JI-A-1--JI-A-21.
- _____, 1973, Summary comments on Neogene biostratigraphy, physical stratigraphy, and paleo-oceanography in the marginal northeastern Pacific Ocean, *in* Kulm, L. D., von Huene, R., and others, eds., *Initial Reports of the Deep Sea Drilling Project, v. 18: U.S. Government Printing Office*, p. 949-960.
- _____, 1975a, Paleocologic indicators and trace fossils, *in* Dickinson, W. R., ed., *Current concepts of depositional systems with applications for petroleum geology: San Joaquin Geological Society, Short Course*, Bakersfield, California, p. 8-1--8-11.
- _____, 1975b, Paleobathymetric analyses of sedimentary basins: *ibid.*, p. 11-1--11-12.
- _____, 1979, Global late Paleogene climatic and eustatic events and the Oligocene hiatus; evidence from passive and active margins [abs.]: Lamont-Doherty Geological Observatory of Columbia University, Ancient Sea Level Changes Symposium.
- _____, 1980, Cenozoic paleobathymetry and depositional history of selected sequences within the southern California continental borderland: Cushman Foundation Special Publication 19, Memorial to Orville L. Bandy, p. 163-195.

- _____, Graham, S. A., and Dickinson, W. R., 1976, Evidence and implications of worldwide late Paleogene climatic and eustatic events: Geological Society of America Abstracts with Programs, v. 8, p. 934-935.
- _____, and Keller, G., 1980, Benthic foraminiferal biofacies of the eastern Pacific margin between 40°S and 32°N, in Field, M. E., Bouma, A. H., Colburn, I. P., Douglas, R. G., and Ingle, J. C., Jr., eds., Quaternary depositional environments of the Pacific coast: Society of Economic Paleontologists and Mineralogists, Pacific Section, Pacific Coast Paleogeography Symposium 4, p. 341-355.
- James, O. B., 1964, A petrographic study of Miocene basalts on either side of the San Andreas fault zone south of Palo Alto, California [unpublished student report]: Stanford University, 45 p.
- Johnson, H. D. 1978, Shallow siliciclastic seas, in Reading, H. G., ed., Sedimentary environments and facies: New York, Elsevier, p. 207-258.
- Kennedy, W. J., and Garrison, R. E., 1975a, Morphology and genesis of nodular chalks and hardgrounds in the Upper Cretaceous of southern England: Sedimentology, v. 22, p. 311-386.
- _____, and _____, 1975b, Morphology and diagenesis of nodular phosphates in the Cenomanian Glauconitic Marl of south-east England: Lethaia, v. 8, p. 339-360.
- Kennett, J. P., 1977, Cenozoic evolution of Antarctic glaciation, the circum-Antarctic ocean, and their impact on global paleoceanography: Journal of Geophysical Research, v. 82, p. 3843-3860.
- Kerr, P. F., and Schenck, H. G., 1925, Active thrust-faults in San Benito county, California: Geological Society of America Bulletin, v. 36, p. 465-494.
- Kerr, R. A., 1980, Changing global sea levels as a geologic index: Science, v. 209, p. 483-486.
- Kleinpell, R. M., 1938, Miocene stratigraphy of California: Tulsa, Oklahoma, American Association of Petroleum Geologists, 450 p.
- _____, 1980, The Miocene stratigraphy of California revisited: American Association of Petroleum Geologists Studies in Geology 11, p. 1-53.
- Krueger, M. L., 1943, Moody Gulch oil field, in Jenkins, O. P., ed., Geologic formations and economic development of the oil and gas fields of California: California Division of Mines Bulletin 118, p. 477.
- Kurten, B., 1971, The age of mammals: New York, Columbia University Press, 250 p.
- Lagoe, M. B., 1982, Stratigraphy and paleoenvironments of the Monterey Formation and associated rocks, Cuyama basin, California [Ph.D. thesis]: Stanford University, 216 p.
- _____, 1984, Paleogeography of Monterey Formation, Cuyama basin, California: American Association of Petroleum Geologists Bulletin, v. 68, p. 610-627.
- Lajoie, J., 1979, Volcaniclastic rocks, in Walker, R. G., ed., Facies models: Waterloo, Ontario, Geological Association of Canada, p. 191-200.
- Lamb, J. L., 1964, The stratigraphic occurrences and relationships of some mid-Tertiary Uvigerinas and Siphogenerinas: Micropaleontology, v. 10, p. 457-476.

- Leckie, R. M., and Webb, P. N., 1983, Late Oligocene-early Miocene glacial record of the Ross Sea, Antarctica: evidence from DSDP Site 270: *Geology*, v. 11, p. 578-582.
- Leon, H. J., 1958, Observations on the stratigraphy and structure of the Saratoga Gap area, California [unpublished student report]: Stanford University, 31 p.
- Lerbekmo, J. F., 1957, Authigenic montmorillonoid cement in andesitic sandstones of central California: *Journal of Sedimentary Petrology*, v. 27, p. 298-305.
- Loel, W., and Corey, W. H., 1932, The Vaqueros formation, lower Miocene of California. I. Paleontology: University of California Publications, Bulletin of the Department of Geological Sciences, v. 22, no. 3, p. 31-40.
- Mack, J. E., 1959, Reconnaissance geology of the Woodside quadrangle, San Mateo county, California [M.S. thesis]: Stanford University, 79 p.
- MacKinnon, T., 1980, Sedimentary petrology and tectonic aspects of Torless and related rocks, South Island, New Zealand [Ph.D. thesis]: Dunedin, New Zealand, University of Otago.
- Madsen, B. M., and Murata, K. J., 1970, Occurrence of laumontite in Tertiary sandstones of the central Coast Ranges, California: U.S. Geological Survey Professional Paper 700-D, p. D188-D195.
- Majewske, O. P., 1969, Recognition of invertebrate fossil fragments in rocks and thin sections: Leiden, E. J. Brill, 101 p.
- Mallory, V. S., 1959, Lower Tertiary biostratigraphy of the California Coast Ranges: Tulsa, Oklahoma, American Association of Petroleum Geologists, 416 p.
- Mann, P., Hempton, M. R., Bradley, D. C., and Burke, K., 1983, Development of pull-apart basins: *Journal of Geology*, v. 91, p. 529-554.
- Mathews, R. K., and Poore, R. Z., 1980, Tertiary δO^{18} record and glacio-eustatic sea-level fluctuations: *Geology*, v. 8, p. 501-504.
- Matthews, V., III, 1976, Correlation of Pinnacles and Neenach volcanic formations and their bearing on San Andreas fault problem: American Association of Petroleum Geologists Bulletin, v. 60, p. 2128-2141.
- McCollom, R. L., Jr., 1959, Lithofacies study of the Vaqueros formation, Santa Cruz Mountains, California [M.S. thesis]: Stanford University, 48 p.
- McCroden, T. J., 1949, Geology of a portion of the Gabilan Range, California [M.S. thesis]: Stanford University, 81 p.
- McCulloch, D. S., Clarke, S. H., Jr., Field, M. E., Scott, E. W., and Utter, P. M., 1977, A summary report on the regional geology, petroleum potential, and environmental geology of the southern proposed lease sale 53, central and northern California outer continental shelf: U.S. Geological Survey Open-File Report 77-593, 57 p.
- McKenzie, D. P., and Morgan, W. J., 1969, Evolution of triple junctions: *Nature*, v. 224, p. 125-133.
- McRae, S. G., 1972, Glauconite: *Earth-Science Reviews*, v. 8, p. 397-440.

- Melendres, M. M., 1958, Geology of the Inspiration Point area, Santa Cruz county, California [unpublished student report]: Stanford University.
- Miall, A. D., 1977, A review of the braided-river depositional environment: *Earth-Science Reviews*, v. 13, p. 1-62.
- , 1978, Lithofacies types and vertical profile models in braided river deposits: a summary, in Miall, A. D., ed., *Fluvial sedimentology: Canadian Society of Petroleum Geologists Memoir 5*, p. 597-604.
- Middleton, G. V., and Hampton, M. A., 1976, Subaqueous sediment transport and deposition by sediment gravity flows, in Stanley, D. J., and Swift, D. J. P., eds., *Marine sediment transport and environmental management: New York, Wiley Interscience*, p. 197-218.
- Milam, R., and Ingle, J. C., Jr., 1982, Paleo-oceanographic significance of Eocene diatomites in Kreyenhagen Formation of California [abs.]: *American Association of Petroleum Geologists Bulletin*, v. 66, p. 1695.
- Miller, K. G. and Olsson, R. K., 1981, Reply to Comment on "Late Oligocene transgression of middle Atlantic coastal plain": *Geology*, v. 9, p. 291-292.
- Milliman, J. D., 1974, *Marine carbonates: New York, Springer-Verlag*, 375 p.
- Mitchum, R. M., Jr., Vail, P. R., and Thompson, S., III, 1977, The depositional sequence as a basic unit for stratigraphic analysis, in Payton, C. E., ed., *Seismic stratigraphy--applications to hydrocarbon exploration: American Association of Petroleum Geologists Memoir 26*, p. 53-62.
- Molnar, P., and Stock, J. W., 1981, Relative positions among the Pacific, Farallon, and North American plates in the Tertiary: *Geological Society of America Abstracts with Programs*, v. 13, p. 97.
- Moore, J. G., 1975, Mechanism of formation of pillow lava: *American Scientist*, v. 63, p. 269-277.
- Moore, T. C., Jr., and Romine, K., 1981, In search of biostratigraphic resolution, in Warne, J. E., Douglas, R. G., and Winterer, E. L., eds., *The Deep Sea Drilling Project: a decade of progress: Society of Economic Paleontologists and Mineralogists Special Publication 32*, p. 317-334.
- Musser, E. H., and Murray-Aaron, E. R., 1962, Maps and data sheets for the oil and gas fields of northern San Joaquin valley, Sacramento valley, and north coastal region, in Bowen, O. E., Jr., ed., *Geological guide to the gas and oil fields of northern California: California Division of Mines and Geology Bulletin 181*, p. 227-365.
- Mutti, E., and Ricci Lucchi, F., 1972, Le torbiditi dell' Appennino settentrionale: introduzione all' analisi di facies: *Memorie della Societa Geologica Italiana*, p. 161-199. (English translation by Nilsen, T. H., 1978, Turbidites of the northern Appennines: introduction to facies analysis: *International Geology Review*, v. 20, no. 2, p. 125-166.)
- Nagel, D. K., and Mullins, H. T., 1983, Late Cenozoic offset and uplift along the San Gregorio fault zone: central California continental margin, in Andersen, D. W., and Rymer, M. J., eds., *Tectonics and sedimentation along faults of the San Andreas system: Society of Economic Paleontologists and Mineralogists, Pacific Section*, p. 91-103.
- Nelson, C. H., and Nilsen, T. H., 1974, Depositional trends of modern and ancient deep-sea fans, in Dott, R. H., Jr., and Shaver, R. H., eds., *Modern and ancient geosynclinal sedimentation: Society of Economic Paleontologists and Mineralogists Special Publication 19*, p. 69-91.

- Nilsen, T. H., 1979, Sedimentology of the Butano Sandstone, Santa Cruz Mountains, California, *in* Nilsen, T. H., and Brabb, E. E., eds., *Geology of the Santa Cruz Mountains, California: Geological Society of America, Cordilleran Section, Annual Meeting, Guidebook*, p. 30-39.
- _____, 1982, Oligocene synorogenic fluvial sedimentation, California: *Geological Society of America Abstracts with Programs*, v. 14, p. 220.
- _____, 1983, Comment *on* "Cenozoic convergence along the California coast: a qualitative test of the hot-spot approximation": *Geology*, v. 11, p. 673-674.
- _____, 1984, Offset along the San Andreas fault of Eocene strata from the San Juan Bautista area and western San Emigdio Mountains, California: *Geological Society of America Bulletin*, v. 95, p. 599-609.
- _____, and Brabb, E. E., eds., 1979, *Geology of the Santa Cruz Mountains, California: Geological Society of America, Cordilleran Section, Annual Meeting, Guidebook*, 97 p.
- _____, and Clarke, S. H., Jr., 1975, Sedimentation and tectonics in the early Tertiary continental borderland of central California: *U.S. Geological Survey Professional Paper* 925, 64 p.
- _____, and Link, M. H., 1975, Stratigraphy, sedimentology, and offset along the San Andreas fault of Eocene to lower Miocene strata of the northern Santa Lucia Range and the San Emigdio Mountains, Coast Ranges, central California, *in* Weaver, D. W., Hornaday, G. R., and Tipton, A., eds., *Paleogene symposium and selected technical papers, conference on future energy horizons of the Pacific coast: Pacific Sections, American Association of Petroleum Geologists, Society of Economic Paleontologists and Mineralogists, and Society of Exploration Geophysicists*, p. 367-400.
- _____, and McKee, E. H., 1979, Paleogene paleogeography of the western United States, *in* Armentrout, J. M., Cole, M. R., and TerBest, H., Jr., eds., *Cenozoic paleogeography of the western United States: Society of Economic Paleontologists and Mineralogists, Pacific Section, Pacific Coast Paleogeography Symposium* 3, p. 257-276.
- _____, and Simoni, T. R., 1973, Deep-sea fan paleocurrent patterns of the Eocene Butano Sandstone, Santa Cruz Mountains, California: *U.S. Geological Survey Journal of Research*, v. 1, p. 439-452.
- _____, and Yount, J. C., 1981, Sedimentology of the Paleocene strata of Point San Pedro, California, *in* Frizzell, V., ed., *Upper Cretaceous and Paleocene turbidites, central California coast: Society of Economic Paleontologists and Mineralogists, Pacific Section, Annual Meeting Field Trip 6, Guidebook*, p. 21-29.
- Odin, G. S., and Matter, A., 1981, De glauconarium origine: *Sedimentology*, v. 28, p. 611-641.
- Olson, J. A., Lindh, A. G., and Ellsworth, W. L., 1980, Seismicity and crustal structure of the Santa Cruz Mountains, California [abs.]: *EOS (American Geophysical Union Transactions)*, v. 61, p. 1042.
- Olsson, R. K., Miller, K. G., and Ungrady, T. E., 1980, Late Oligocene transgression of middle Atlantic coastal plain: *Geology*, v. 8, p. 549-554.
- Page, B. M., 1981, The southern Coast Ranges, *in* Ernst, W. G., ed., *The geotectonic development of California: Englewood Cliffs, New Jersey, Prentice-Hall, Inc., Rubey Volume I*, p. 329-417.

- , 1982, Migration of Salinian composite block, California, and disappearance of fragments: *American Journal of Science*, v. 282, p. 1694-1734.
- , and Holmes, C. N., 1945, Bituminous sandstone deposits near Santa Cruz, Santa Cruz county, California: U.S. Geological Survey Oil and Gas Investigations Preliminary Map 27.
- Pampeyan, E. H., 1981, Geologic map of the Montara Mountain quadrangle, San Mateo county, California: U.S. Geological Survey Open-File Report 81-451, scale 1:12,000.
- Parsons, W. H., 1969, Criteria for the recognition of volcanic breccias: a review, in Larsen, L., Manson, V., and Priur, M., eds., *Igneous and metamorphic geology*: Geological Society of America Memoir 115, p. 263-304.
- Phillips, R. L., 1981, Depositional environments of the Santa Margarita Formation in the Santa Cruz Mountains, California [Ph.D. thesis]: Santa Cruz, University of California, 358 p.
- , 1983, Late Miocene tidal shelf sedimentation Santa Cruz Mountains, California, in Larue, D. K., and Steel, R. J., eds., *Cenozoic marine sedimentation Pacific margin, U.S.A.*: Society of Economic Paleontologists and Mineralogists, Pacific Section, p. 45-61.
- Pisciotta, K. A., and Garrison, R. E., 1981, Lithofacies and depositional environments of the Monterey Formation, California, in Garrison, R. E., ed., *The Monterey Formation and related siliceous rocks of California*: Society of Economic Paleontologists and Mineralogists, Pacific Section, p. 97-122.
- Pitman, W. C., 1978, Relationship between eustasy and stratigraphic sequences of passive margins: *Geological Society of America*, v. 89, p. 1389-1403.
- Poore, R. Z., 1977, Paleogene planktonic foraminifers from the Santa Cruz Mountains and northern Santa Lucia range, California: Abstracts for field conference on the Paleogene of California and Mexico, Menlo Park, California, p. 7-8.
- , 1980, Age and correlation of California Paleogene benthic foraminiferal stages: U.S. Geological Survey Professional Paper 1162-C, p. C1-C8.
- , and Brabb, E. E., 1977, Eocene and Oligocene planktonic foraminifera from the upper Butano Sandstone and type San Lorenzo Formation, Santa Cruz Mountains, California: *Journal of Foraminiferal Research*, v. 7, p. 249-272.
- , and Bukry, D., 1977, Eocene to Miocene calcareous nannofossils from the Santa Cruz Mountains, California: Abstracts for field conference on the Paleogene of California and Mexico, Menlo Park, California, p. 10.
- , McDougall, K. A., Barron, J. A., Brabb, E. E., and Kling, S. A., 1981, Microfossil biostratigraphy and biochronology of the type Relizian and Luisian stages of California, in Garrison, R. E., ed., *The Monterey Formation and related siliceous rocks of California*: Society of Economic Paleontologists and Mineralogists, Pacific Section, p. 15-41.
- Potter, P. E., and Pettijohn, F. J., 1977, *Paleocurrents and basin analysis* (second edition): Berlin, Springer-Verlag, 425 p.
- Price, W. A., 1968, Oyster reefs, in Fairbridge, R. W., ed., *The encyclopedia of geomorphology*: New York, Reinhold Book Corporation, p. 799-803.

- Reading, H. G., 1980, Characteristics and recognition of strike-slip fault systems, in Ballance, P. F., and Reading, H. G., eds., Sedimentation in oblique-slip mobile zones: International Association of Sedimentologists Special Publication 4, p. 7-26.
- Rodgers, D. A., 1980, Analysis of pull-apart basin development produced by *en echelon* strike-slip faults: *ibid.*, p. 27-41.
- Rona, P. A., 1973, Worldwide unconformities in marine sediments related to eustatic changes of sea level: *Nature Physical Science*, v. 244, p. 25-26.
- Ross, D. C., 1970, Quartz gabbro and anorthositic gabbro: markers of offset along San Andreas fault in California Coast Ranges: *Geological Society of America Bulletin*, v. 81, p. 3647-3662.
- , 1977, Pre-intrusive metasedimentary rocks of the Salinian block, California—a paleotectonic dilemma, in Stewart, J. H., Stevens, C. H., and Fritsche, A. E., eds., Paleozoic paleogeography of the western United States: Society of Economic Paleontologists and Mineralogists, Pacific Section, Pacific Coast Paleogeography Symposium 1, p. 371-380.
- , 1978, The Salinian block—a Mesozoic granitic orphan in the California Coast Ranges, in Howell, D. G., and McDougall, K. A., eds., Mesozoic paleogeography of the western United States: Society of Economic Paleontologists and Mineralogists, Pacific Section, Pacific Coast Paleogeography Symposium 2, p. 509-522.
- , and Brabb, E. E., 1973, Petrography and structural relations of basement rocks in the Monterey Bay area, California: *U.S. Geological Survey Journal of Research*, v. 1, p. 273-282.
- Rupke, N. A., 1978, Deep clastic seas, in Reading, H. G., ed., Sedimentary environments and facies: New York, Elsevier, p. 372-415.
- Savin, S. M., 1977, The history of the earth's surface temperature during the past 100 million years: *Annual Review of Earth and Planetary Sciences*, v. 5, p. 319-355.
- Schenck, H. G., and Kleinpell, R. M., 1936, Refugian Stage of Pacific coast Tertiary: *American Association of Petroleum Geologists Bulletin*, v. 20, p. 215-225.
- Shackleton, N. J., and Kennett, J. P., 1975, Paleotemperature history of the Cenozoic and the initiation of Antarctic glaciation: oxygen and carbon isotope analyses in DSDP sites 277, 279, and 281, in Kennett, J. P., Houtz, R. E., and others, eds., Initial Reports of the Deep Sea Drilling Project, v. 29: U.S. Government Printing Office, p. 743-755.
- Smith, R. K., 1971, Foraminiferal studies in the lower and middle Tertiary of Soquel Creek, Santa Cruz county, California: *University of California Publications in Geological Sciences*, v. 91, p. 1-111.
- Snyder, S. W., Müller, C., and Miller, K. G., 1984, Eocene-Oligocene boundary: biostratigraphic recognition and gradual paleoceanographic change at DSDP Site 549: *Geology*, v. 12, p. 112-115.
- Soutar, A., Johnson, S. R., and Baumgartner, T. R., 1981, In search of modern depositional analogs to the Monterey Formation, in Garrison, R. E., ed., The Monterey Formation and related siliceous rocks of California: Society of Economic Paleontologists and Mineralogists, Pacific Section, p. 123-147.

- Stanley, R. G., 1973, Paleocology of a shell bank in the Vaqueros Sandstone (lower Miocene) near Zayante, Santa Cruz county, California [Senior thesis]: Santa Cruz, University of California, 59 p.
- , 1982, Rocks and landforms, *in* Warrick, S. F., ed., The natural history of the U.C. Santa Cruz campus: Santa Cruz, University of California, Environmental Field Program Publication 11, p. 35-103.
- , and McCaffrey, R., 1983, Extent and offset history of the Ben Lomond fault, Santa Cruz county, California, *in* Andersen, D. W., and Rymer, M. J., eds., Tectonics and sedimentation along faults of the San Andreas system: Society of Economic Paleontologists and Mineralogists, Pacific Section, p. 79-90.
- Strom, R. G., 1956, Stratigraphy of the southwestern part of the Mindego Hill quadrangle, California [M.S. thesis]: Stanford University, 58 p.
- Stuart, R. M., Madrid, V. M., and Versosub, K. L., 1982, Late Neogene tectonics and sedimentation, Santa Cruz Mountains, California: Geological Society of America Abstracts with Programs, v. 14, p. 237-238.
- Sullivan, F. R., 1962, Foraminifera from the type section of the San Lorenzo Formation, Santa Cruz county, California: University of California Publications in Geological Sciences, v. 37, p. 233-352.
- Taliaferro, N. L., 1948, Geologic map of the Hollister quadrangle, California: California Division of Mines Bulletin 143, scale 1:62,500.
- Thorup, R. R., 1943, Type locality of the Vaqueros Formation, *in* Jenkins, O. P., ed., Geologic formations and economic development of the oil and gas fields of California: California Division of Mines Bulletin 118, p. 463-466.
- Touring, R. M., 1959, Structure and stratigraphy of the La Honda and San Gregorio quadrangles, San Mateo county, California [Ph.D. thesis]: Stanford University, 228 p.
- Travers, W. B., 1959, Geology of the Newell Creek area, Boulder Creek, California [M.S. thesis]: Stanford University, 44 p.
- Turner, D. L., 1970, Potassium-argon dating of Pacific coast Miocene foraminiferal stages, *in* Bandy, O. L., ed., Radiometric dating and paleontologic zonation: Geological Society of American Special Paper 124, p. 91-129.
- Turner, P., 1980, Continental red beds: Amsterdam, Elsevier, Developments in Sedimentology 29, 562 p.
- Vail, P. R., and Hardenbol, J., 1979, Sea-level changes during the Tertiary: *Oceanus*, v. 22, p. 71-79.
- , ———, and Todd, R. G., 1981, Jurassic unconformities, chronostratigraphy, and sea-level changes from seismic and biostratigraphy: Proceedings of the Joint United States Society of Exploration Geophysicists and the China Geophysical Society Meeting, Beijing, typewritten manuscript (preprint), 30 p.
- , Mitchum, R. M., Jr., Shipley, T. H., and Buffler, P. T., 1980, Unconformities of the North Atlantic: *Philosophical Transactions of the Royal Society of London*, series A, v. 294, p. 137-155.

- _____, _____, and Thompson, S., III, 1977, Global cycles of relative changes of sea level, *in* Payton, C. E., ed., Seismic stratigraphy—applications to hydrocarbon exploration: American Association of Petroleum Geologists Memoir 26, p. 83-97.
- _____, _____, Todd, R. G., Widmier, J. M., Thompson, S., III, Sangree, J. B., Bubbs, J. N., and Hatlelid, W. G., 1977, Seismic stratigraphy and global changes of sea level: *ibid.*, p. 49-212.
- van Hinte, J. E., 1978, Geohistory analysis—application of micropaleontology in exploration geology: American Association of Petroleum Geologists Bulletin, v. 62, p. 201-222.
- Walker, R. G., 1978, Deep-water sandstone facies and ancient submarine fans: models for exploration for stratigraphic traps: American Association of Petroleum Geologists Bulletin, v. 62, p. 932-966.
- _____, 1979, Turbidites and associated coarse clastic deposits, *in* Walker, R. G., ed., Facies models: Waterloo, Ontario, Geological Association of Canada, p. 91-103.
- Walrond, H., Thorup, R. R., Gribi, E. A., Jr., and Rogers, T. H., 1967, Geologic map of the Gabilan uplift and adjacent areas, *in* Gabilan Range and adjacent San Andreas fault: Pacific Sections, American Association of Petroleum Geologists and Society of Economic Paleontologists and Mineralogists, Field Trip Guidebook, scale 1:125,000.
- Warren, A. D., and Newell, J. H., 1980, Plankton biostratigraphy of the Refugian and adjoining stages of the Pacific coast Tertiary: Cushman Foundation Special Publication 19, Memorial to Orville L. Bandy, p. 233-251.
- Waters, J. N., 1968, Eocene faunule from the basal San Juan Bautista Formation of California: Contributions from the Cushman Foundation for Foraminiferal Research, v. 19, part 1, p. 18-20.
- Weber, G. E., and Lajoie, K. R., 1980, Map of Quaternary faulting along the San Gregorio-Hosgri fault zone, San Mateo and Santa Cruz counties, California: U.S. Geological Survey Open-File Report 80-907, scale 1:24,000.
- _____, _____, and Griggs, G. B., eds., 1979, Coastal tectonics and coastal geologic hazards in Santa Cruz and San Mateo counties, California: Geological Society of America, Cordilleran Section, Annual Meeting, Guidebook, 187 p.
- Wescott, W. A., and Ethridge, F. G., 1980, Fan-delta sedimentology and tectonic setting—Yallahs fan delta, southeast Jamaica: American Association of Petroleum Geologists Bulletin, v. 64, p. 374-399.
- _____, and _____, 1983, Eocene fan delta-submarine fan deposition in the Wagwater Trough, east-central Jamaica: Sedimentology, v. 30, p. 235-247.
- Wiley, T. J., and Moore, E. J., 1983, Pliocene shallow-water sediment gravity flows at Moss Beach, San Mateo county, California, *in* Larue, D. K., and Steel, R. J., 1983, Cenozoic marine sedimentation Pacific margin, U.S.A.: Society of Economic Paleontologists and Mineralogists, Pacific Section, p. 29-43.